

Energy, Environment, and Sustainability  
Series Editor: Avinash Kumar Agarwal

Jitendra Kumar Katiyar  
Shantanu Bhattacharya  
Vinay Kumar Patel  
Vikram Kumar *Editors*

# Automotive Tribology



 Springer

# **Energy, Environment, and Sustainability**

## **Series Editor**

Avinash Kumar Agarwal, Department of Mechanical Engineering, Indian Institute of Technology Kanpur, Kanpur, Uttar Pradesh, India

This books series publishes cutting edge monographs and professional books focused on all aspects of energy and environmental sustainability, especially as it relates to energy concerns. The Series is published in partnership with the International Society for Energy, Environment, and Sustainability. The books in these series are edited or authored by top researchers and professional across the globe. The series aims at publishing state-of-the-art research and development in areas including, but not limited to:

- Renewable Energy
- Alternative Fuels
- Engines and Locomotives
- Combustion and Propulsion
- Fossil Fuels
- Carbon Capture
- Control and Automation for Energy
- Environmental Pollution
- Waste Management
- Transportation Sustainability

More information about this series at <http://www.springer.com/series/15901>

Jitendra Kumar Katiyar · Shantanu Bhattacharya ·  
Vinay Kumar Patel · Vikram Kumar  
Editors


# Automotive Tribology

 Springer

*Editors*

Jitendra Kumar Katiyar  
SRM Institute of Science and Technology  
Chennai, India

Vinay Kumar Patel  
Govind Ballabh Pant Institute  
of Engineering & Technology  
Pauri, Garhwal, India

Shantanu Bhattacharya   
Department of Mechanical Engineering  
Indian Institute of Technology Kanpur  
Kanpur, India

Vikram Kumar  
Indian Institute of Technology Kanpur  
Kanpur, India

ISSN 2522-8366

ISSN 2522-8374 (electronic)

Energy, Environment, and Sustainability

ISBN 978-981-15-0433-4

ISBN 978-981-15-0434-1 (eBook)

<https://doi.org/10.1007/978-981-15-0434-1>

© Springer Nature Singapore Pte Ltd. 2019

This work is subject to copyright. All rights are reserved by the Publisher, whether the whole or part of the material is concerned, specifically the rights of translation, reprinting, reuse of illustrations, recitation, broadcasting, reproduction on microfilms or in any other physical way, and transmission or information storage and retrieval, electronic adaptation, computer software, or by similar or dissimilar methodology now known or hereafter developed.

The use of general descriptive names, registered names, trademarks, service marks, etc. in this publication does not imply, even in the absence of a specific statement, that such names are exempt from the relevant protective laws and regulations and therefore free for general use.

The publisher, the authors and the editors are safe to assume that the advice and information in this book are believed to be true and accurate at the date of publication. Neither the publisher nor the authors or the editors give a warranty, expressed or implied, with respect to the material contained herein or for any errors or omissions that may have been made. The publisher remains neutral with regard to jurisdictional claims in published maps and institutional affiliations.

This Springer imprint is published by the registered company Springer Nature Singapore Pte Ltd. The registered company address is: 152 Beach Road, #21-01/04 Gateway East, Singapore 189721, Singapore

# Preface

Energy demand has been rising remarkably due to increasing population and urbanization. Global economy and society are significantly dependent on the energy availability because it touches every facet of human life and activities. Transportation and power generation are two major examples. Without the transportation by millions of personalized and mass transport vehicles and availability of 24 × 7 power, human civilization would not have reached contemporary living standards.

The International Society for Energy, Environment and Sustainability (ISEES) was founded at Indian Institute of Technology Kanpur (IIT Kanpur), India, in January 2014 with an aim to spread knowledge/awareness and catalyze research activities in the fields of energy, environment, sustainability, and combustion. The society's goal is to contribute to the development of clean, affordable, and secure energy resources and a sustainable environment for the society and to spread knowledge in the above-mentioned areas and create awareness about the environmental challenges, which the world is facing today. The unique way adopted by the society was to break the conventional silos of specializations (engineering, science, environment, agriculture, biotechnology, materials, fuels, etc.) to tackle the problems related to energy, environment, and sustainability in a holistic manner. This is quite evident by the participation of experts from all fields to resolve these issues. The ISEES is involved in various activities such as conducting workshops, seminars, and conferences in the domains of its interests. The society also recognizes the outstanding works done by the young scientists and engineers for their contributions in these fields by conferring them awards under various categories.

Third International Conference on 'Sustainable Energy and Environmental Challenges' (III-SEEC) was organized under the auspices of ISEES from December 18–21, 2018, at Indian Institute of Technology Roorkee. This conference provided a platform for discussions between eminent scientists and engineers from various countries including India, USA, Norway, Finland, Sweden, Malaysia, Austria, Hong-Kong, Bangladesh, and Australia. In this conference, eminent speakers from all over the world presented their views related to different aspects of energy, combustion, emissions, and alternative energy resource for sustainable development

and cleaner environment. The conference presented five high-voltage plenary talks from globally renowned experts on topical themes namely “The Evolution of Laser Ignition Over more than Four Decades” by Prof. Ernst Wintner, Technical University of Vienna, Austria; “Transition to Low Carbon Energy Mix for India” by Dr. Bharat Bhargava, ONGC Energy Center; “Energy Future of India” by Dr. Vijay Kumar Saraswat, Honorable Member (S&T) NITI Aayog, Government of India; “Air Quality Monitoring and Assessment in India” by Dr. Gufran Beig, SAFAR; and “Managing Large Technical Institutions and Assessment Criterion for Talent Recruitment and Retention” by Prof. Ajit Chaturvedi, Director, IIT Roorkee.

The conference included 24 technical sessions on topics related to energy and environmental sustainability including 5 plenary talks, 27 keynote talks, and 15 invited talks from prominent scientists, in addition to 84 contributed talks and 50 poster presentations by students and researchers. The technical sessions in the conference included advances in IC engines, solar energy, environmental biotechnology, combustion, environmental sustainability, coal and biomass combustion/gasification, air and water pollution, biomass to fuels/chemicals, combustion/gas turbines/fluid flow/sprays, energy and environmental sustainability, atomization and sprays, sustainable transportation and environmental issues, new concepts in energy conservation, waste to wealth. One of the highlights of the conference was the rapid-fire poster sessions in (i) engine/fuels/emissions, (ii) renewable and sustainable energy, and (iii) biotechnology, where 50 students participated with great enthusiasm and won many prizes in a fiercely competitive environment. Two hundred plus participants and speakers attended this four days of conference, which also hosted Dr. Vijay Kumar Saraswat, Honorable Member (S&T) NITI Aayog, Government of India, as the chief guest for the book release ceremony, where 14 ISEES books published by Springer, Singapore, under a special dedicated series “Energy, environment and sustainability” were released. This was the second time in a row that such significant and high-quality outcome has been achieved by any society in India. The conference concluded with a panel discussion on “Challenges, Opportunities and Directions for National Energy Security,” where the panelists were Prof. Ernst Wintner, Technical University of Vienna; Prof. Vinod Garg, Central University of Punjab, Bathinda; Prof. Avinash Kumar Agarwal, IIT Kanpur; and Dr. Michael Sauer, Boku University of Natural resources, Austria. The panel discussion was moderated by Prof. Ashok Pandey, Chairman, ISEES. This conference laid out the roadmap for technology development, opportunities, and challenges in energy, environment, and sustainability domain. All these topics are very relevant for the country and the world in present context. We acknowledge the support received from various funding agencies and organizations for the successful conduct of the Third ISEES conference III-SEEC, where these books germinated. We would therefore like to acknowledge NIT Srinagar, Uttarakhand (TEQIP) (Special thanks to Prof. S. Soni, Director, NIT, UK), SERB, Government of India (Special thanks to Dr. Rajeev Sharma, Secretary); UP Bioenergy Development Board, Lucknow (Special thanks to Sh. P. S. Ojha), CSIR, and our publishing partner Springer (Special thanks to Swati Meherishi).

The editors would like to express their sincere gratitude to large number of authors from all over the world for submitting their high-quality work in a timely manner and revising it appropriately at a short notice. We would like express our special thanks to Dr. Vinay Kumar Patel, Dr. Rajesh Shukla, Dr. Ranjeet Kumar Sahu, Dr. Vikram Kumar, Dr. Jayant Singh, Dr. Jagadeesha T, Dr. R. K. Upadhyay, Dr. Brijesh Gangil, Dr. Anuj Kumar Sharma, Dr. T. V. V. L. N. Rao, Dr. Shubrajit Bhaumik, Dr. Pankaj Kumar, Dr. Manoj Gupta, and Er. Sandeep Kumar, who reviewed various chapters of this monograph and provided their valuable suggestions to improve the manuscripts.

The editors sincerely hope that the present monograph gives the comprehensive study of current trends adopted by automobile sectors in the development of new technologies and materials for reduction of friction and wear because the customer satisfaction and environmental protection are very important factors in governing the development of automotive technology. Furthermore, the present monograph is intended for all level of students (UG, PG as well as doctorate), research scientist, and industry persons.

Chennai, India  
Kanpur, India  
Pauri, Garhwal, India  
Kanpur, India

Jitendra Kumar Katiyar  
Shantanu Bhattacharya  
Vinay Kumar Patel  
Vikram Kumar



# Contents

## Part I General

- 1 Introduction of Automotive Tribology** ..... 3  
Jitendra Kumar Katiyar, Shantanu Bhattacharya, Vinay Kumar Patel  
and Vikram Kumar

## Part II New Materials for Automotive Applications

- 2 Tribological Aspects of Automotive Engines** ..... 17  
Vikram Kumar and Avinash Kumar Agarwal
- 3 The Potential of Natural Fibers for Automotive Sector** ..... 31  
Shashi Kant Verma, Ashutosh Gupta, Vinay Kumar Patel,  
Brijesh Gangil and Lalit Ranikoti
- 4 Future of Metal Foam Materials in Automotive Industry** ..... 51  
Ankur Bisht, Vinay Kumar Patel and Brijesh Gangil
- 5 Study of Tribo-Performance and Application of Polymer  
Composite** ..... 65  
Hemalata Jena
- 6 Mechanical and Erosion Characteristics of Natural Fiber  
Reinforced Polymer Composite: Effect of Filler Size** ..... 101  
Ankush Sharma, Vishal Bhojak, Vikas Kukshal, S. K. Biswas,  
Amar Patnaik and Tapan Kumar Patnaik
- 7 Erosive Wear Behaviour of Carbon Fiber/Silicon Nitride Polymer  
Composite for Automotive Application** ..... 117  
Vikas Kukshal, Ankush Sharma, Vinayaka R. Kiragi, Amar Patnaik  
and Tapan Kumar Patnaik
- 8 Effects of Reinforcement on Tribological Behaviour  
of Aluminium Matrix Composites** ..... 131  
Manoj Kumar Gupta, Lalit Ranakoti and Pawan Kumar Rakesh

### **Part III New Lubricants for Automotive Applications**

- 9 Current and Future Trends in Grease Lubrication** . . . . . 147  
Sooraj Singh Rawat and A. P. Harsha
- 10 Lubrication Effectiveness and Sustainability of Solid/Liquid Additives in Automotive Tribology** . . . . . 183  
R. K. Upadhyay
- 11 Potential of Bio-lubricants in Automotive Tribology** . . . . . 197  
Manoj Kumar Pathak, Amit Joshi, K. K. S. Mer, Jitendra K. Katiyar and Vinay Kumar Patel

### **Part IV Surface Morphologies for Automotive Applications**

- 12 Influence of Surface Texturing on Friction and Wear** . . . . . 217  
Shubrajit Bhaumik, Chiradeep Ghosh, Basudev Bhattacharya, Viorel Paleu, Rajeev Kumar Naik, Prayag Gopinath, A. Adithya and Ankur Dhanwant
- 13 Magneto Rheological Fluid Based Smart Automobile Brake and Clutch Systems** . . . . . 237  
Rakesh Jinaga, Shreedhar Kolekar and T. Jagadeesha
- 14 Shot Peening Effects on Abrasive Wear Behavior of Medium Carbon Steel** . . . . . 269  
Neeraj Kumar and Jayant Singh
- 15 Tribological Performance of Surface Textured Automotive Components: A Review** . . . . . 287  
Nilesh D. Hingawe and Skylab P. Bhore
- 16 Applications of Tribology on Engine Performance** . . . . . 307  
Sangeeta Das and Shubhajit Das
- 17 Asbestos Free Braking Pads by Using Organic Fiber Based Reinforced Composites for Automotive Industries** . . . . . 327  
Sandeep Kumar, Brijesh Gangil, K. K. S. Mer, Don Biswas and Vinay Kumar Patel

## About the Editors



**Dr. Jitendra Kumar Katiyar** is Research Assistant Professor in the Department of Mechanical Engineering, SRM Institute of Science and Technology, Kattankulathur, Tamil Nadu, India. His research interests include tribology of carbon materials, polymer composites, self-lubricating polymers, lubrication tribology and coatings for advanced technologies. He obtained his Ph.D., from the Indian Institute of Technology Kanpur in 2017 and masters from the same institution in 2010. He obtained his bachelor degree from UPTU Lucknow with Honors in 2007. He has several professional memberships such as Tribology Society of India, Malaysian Society of Tribology, and The Indian Society for Technical Education (ISTE). He has published more than two dozen papers in reputed journals and international conferences. He is also a reviewer in many reputed journals such as Tribology International, Friction, Materials Research Express, and Inderscience Journals.



**Prof. Shantanu Bhattacharya** (Ph.D.) is Professor of Mechanical Engineering and Head of Design Program at Indian Institute of Technology Kanpur. Prior to this, he completed his MS in Mechanical Engineering from Texas Tech University, Lubbock, Texas, and a Ph.D. in bioengineering from the University of Missouri, Columbia, USA. He also completed a postdoctoral training at the Birck Nanotechnology Center at the Purdue University. His main research interests are design and development of micro- and nano-sensors and actuation platforms, nanoenergetic materials, micro- and nano-fabrication technologies, and water remediation using visible-light photocatalysis, and product design and development. He has won many awards and accolades to his credit which includes the Institute of Engineers Young Engineer Award, the Institute for Smart Structures and Systems Young Scientist Award, the Best Mechanical Engineering Design Award (National Design Research Forum, IEI), and Fellowship from the high energetic materials institute at Australia, Fellowship of the Institution of Engineers (India). He has guided many Ph.D. and masters students and has many international journal publication, patents, books, and conference proceedings.



**Dr. Vinay Kumar Patel** is Assistant Professor in the Department of Mechanical Engineering, Govind Ballabh Pant Institute of Engineering and Technology, Pauri, Garhwal, Uttarakhand, India. He completed his Ph.D. from Indian Institute of Technology Kanpur in 2015, specializing in nano-energetic materials. His research interests include nano-energetic materials, MEMS, welding, and tribology. He has published 25 peer-reviewed journal articles, 7 conference papers, 8 chapters, and edited 1 book on nano-energetic materials.



**Dr. Vikram Kumar** is Postdoctoral Fellow in Department of Mechanical Engineering, IIT Kanpur, funded by CSIR “Scientist Pool” scheme. He completed his doctoral thesis in the area of engine tribology from Department of Mechanical Engineering, IIT Kanpur. He completed his masters Heat and Power Engineering from UIT, RGPV Bhopal and Bachelors in Mechanical Engineering from COE, BVU Pune. He taught heat and mass transfer, fluid mechanics, thermodynamics, and IC engine subjects in UIT RGPV Bhopal from 2010 to 2012. He published 7 peer-reviewed journal papers and 2 chapters. His doctoral thesis awarded “Best Ph.D. Thesis Award” by International Society for Energy, Environment, and Sustainability. He also received “Best Paper Oral Presentation Award” at SEEC-2017 and CSIR Senior Research Associateship to do research at IIT Kanpur. Currently, he is working on methanol-fueled vehicle development.

# **Part I**

## **General**

# Chapter 1

## Introduction of Automotive Tribology



**Jitendra Kumar Katiyar, Shantanu Bhattacharya, Vinay Kumar Patel and Vikram Kumar**

**Abstract** Tribology is existed at the interface of two materials which are in relative motion and this causes friction at the interface. Due to friction, heat is generated between two mating surfaces which causes wear on surfaces either one or both the materials. To reduce friction and wear at interface, a lubricant is supplied. This lubricant may be either solid lubricant such as graphite, graphene etc. or liquid lubricant such as base oil, mineral oil etc. or semisolid lubricant such as grease. In this chapter, the detailed description of friction, wear and lubrication is given. Furthermore, a number of examples are also presented where tribology is very important such as bearings, gears, engines, orthopaedic joints and micro-machines. At last, the brief introduction of important applications are also discussed along with brief prescription about book chapters.

**Keywords** Friction · Wear · Lubrication · Automobile · Bearing · Gears etc.

### 1.1 Introduction

The word “Tribology” has been taken from the Greek word “Tribos” which means “rubbing” or to rub and suffix “Ology” means “the study of”. Thus, tribology means “the study of rubbing of two materials” (Duncan 1997). Therefore, Tribology is existed at the interface of two materials which are in relative motion and this causes friction at the interface. Due to friction, heat is generated between two mating surfaces which causes wear on surfaces either one or both the materials. To reduce friction

---

J. K. Katiyar (✉)

Department of Mechanical Engineering, SRM Institute of Science and Technology,  
Kattankulathur, Tamil Nadu 603203, India  
e-mail: [jitendrv@srmist.edu.in](mailto:jitendrv@srmist.edu.in)

S. Bhattacharya · V. Kumar

Department of Mechanical Engineering, Indian Institute of Technology Kanpur, Kanpur,  
Uttar Pradesh 208016, India

V. K. Patel

Department of Mechanical Engineering, Govind Ballabh Pant Institute of Engineering and  
Technology Ghurdauri, Pauri, Garhwal, Uttarakhand 246194, India

© Springer Nature Singapore Pte Ltd. 2019

J. K. Katiyar et al. (eds.), *Automotive Tribology*, Energy, Environment, and Sustainability,  
[https://doi.org/10.1007/978-981-15-0434-1\\_1](https://doi.org/10.1007/978-981-15-0434-1_1)

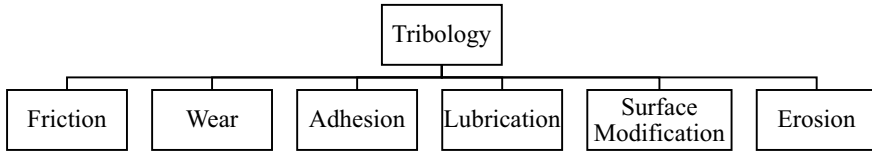
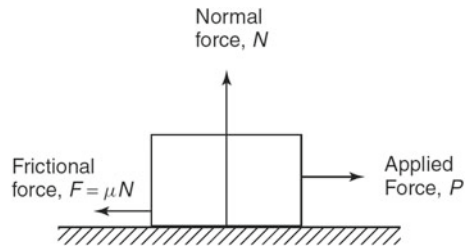


**Fig. 1.1** Different aspects of tribology

**Fig. 1.2** Schematic representation of friction



and wear at interface, a lubricant is supplied. Tribology involves the study and the applications of the principles of friction, wear, lubrication and surface modification which is diagrammatically shown in Fig. 1.1.

### **1.1.1 Friction**

The resistance force experienced in relative motion of solid surfaces, fluid layers, and/or material elements sliding against each other is known as friction which is shown in Fig. 1.2. There are two types of friction, dry friction and fluid film friction (Rabinowicz 1995). When there are two solid surfaces sliding against each other and energy is entirely dissipated between the surfaces then it is known as dry friction. This dry friction is again subdivided into two parts; static friction and kinetic friction.

### **1.1.2 Wear**

The degradation of material or removal of material is known as wear. Wear occurs due to the friction between two surfaces. There are different types of wear which is shown in Fig. 1.3.

When a hard material rubs against a soft or hard material in direct contact than abrasion wear occurs. It may also happen that hard particles are present at the interface as contamination or as “third body”. The third body is defined as the wear debris or oxidized particles that is trapped at the interface (Williams 2005).



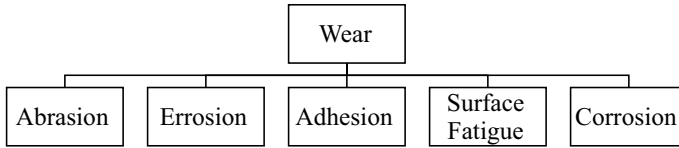


**Fig. 1.3** Classification of wear processes

When a small solid or liquid particle impacts a solid surface, deformation may take place on the solid surface. If such impacts are repeated over and over again with continuous impact of particles, there will be removal of the material locally. This mechanism of wear is known as erosive wear.

When the surfaces are soft and plastically deforming than adhesive wear occurs. Large adhesive forces between materials lead to plastic deformation and material removal in the form of highly deformed flakes. Very large adhesive forces can also lead to what is known as cold welding at localized contact points. The cold-welded part can also tear-off the material locally. The best example of adhesion is joining of slip gauges. They are joined because of applied pressure through hands.

Surface fatigue occurs because of repeated forces applied on the surfaces. Due to which cracks are propagated on subsurface which further grows and generated the wear debris on surface.

Corrosion is widely occurs in hydro turbines. This occurs because of the moisture present in surrounding and universe.

### ***1.1.3 Lubrication***

To overcome the effect of friction and wear at interface, the lubrication is provided. It is either in the form of solid lubricant such as graphite, graphene etc. or liquid lubricant such as base oil, mineral oil etc. or semisolid lubricant such as grease. The basic principle of lubricants are control friction, control wear, control interfacial temperature, control corrosion, remove contaminants, form a seal (grease) etc. (Stribeck 1902). The performance of a lubricant depends on its chemical, physical and rheological properties. It also depends on the external parameters imposed such as contact pressure, relative speed, and temperature. Based on the nature of the fluid film formation, different lubrication regimes are defined and they are, Boundary lubrication, Mixed Lubrication, Elasto-hydrodynamic lubrication and Hydrodynamic Lubrication (Dowson 1993). These lubrication regime are shown in Fig. 1.4.

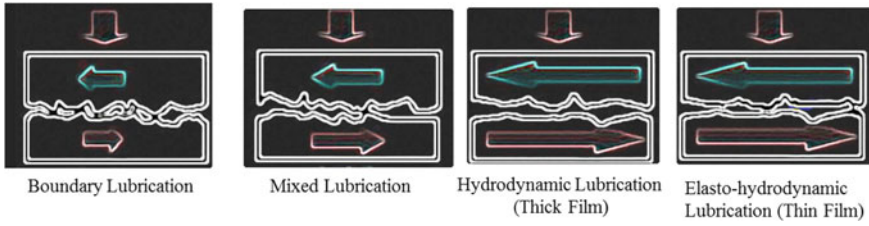


Fig. 1.4 Different regimes of lubrication

### 1.1.4 Factors Which Affect the Tribological Performance

There are various factors which affect the tribological performance of any system (Briscoe and Sinha 2002; Spikes 2001; Rathaur et al. 2018). These factors are shown in the Fig. 1.5.

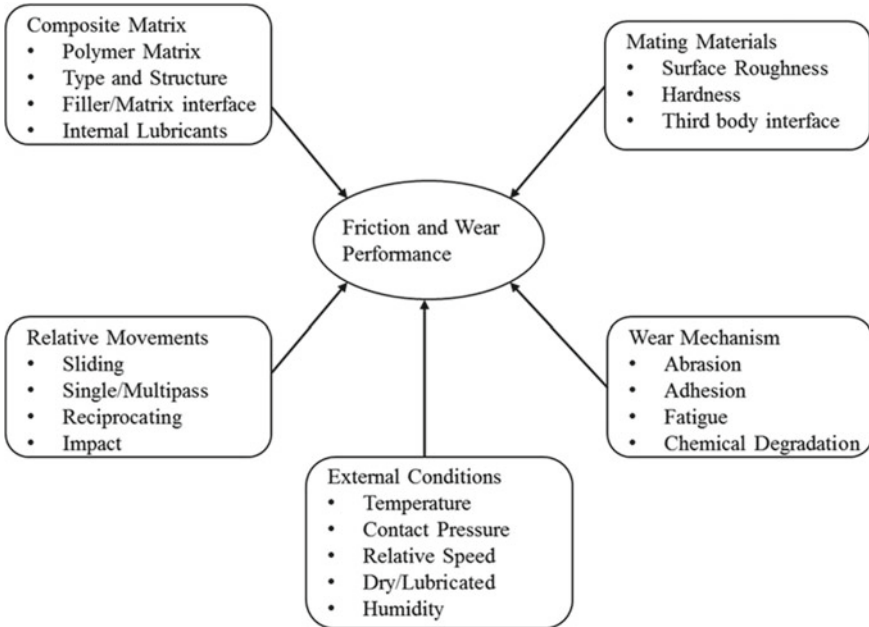
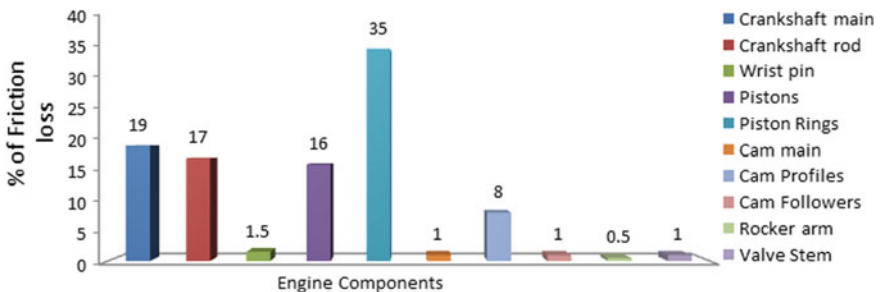


Fig. 1.5 Factors influenced the tribological performance of any system

### 1.1.5 Application of Tribology

It is very important to note that the tribological performance of any system, whether nano, micro or macro-scale, depends upon a large member of external parameters and important among them are temperature, contact pressure and relative speed. A number of examples, where tribology is very important. These are different kinds of bearings, gears, engines, orthopaedic joints and micro-machines etc. Among all these applications, tribological issues in automobile is discussed briefly in this chapter and detailed development in further chapters.

In automobile, there are various parts which are in a relative motion when vehicle moves. Among all parts, engine is most important part in automobile. This is also known as heart of automobile (Taylor 1998). The engine consists piston and piston ring, piston cylinder, connecting rod, gudgeon pin and cam-follower assembly. The lubrication is very important in all parts of engines. Now a days, customer satisfaction and environmental protection are very important factors in governing the development of automotive technology. There are various components present in automobile which affect the efficiency of engine largely such as bearing, piston ring, valve train and crank shaft etc. The researchers had tried various methods such as surface texturing, surface coating, modification in lubricant etc. for improving the efficiency of engine. The efficiency of any engine is largely affected by friction. The percentage of various friction losses with respect to engine components have been shown in Fig. 1.6. Therefore, in further sections, the various types of energy losses are described in brief.



**Fig. 1.6** Friction losses with respect to engine components (Taylor 1998; Nakasa 1995; Akiyama et al. 1987)

### 1.1.5.1 Energy Losses in a Vehicle

#### Engine Losses

The internal combustion engines (ICE) are very incompetent in converting the chemical energy of fuels into mechanical energy by movement of piston from top dead centre to bottom dead centre. Because of this movement, the friction occurs at interface which generates the frictional heat. In one survey, it is reported that approximately 62% of the fuel's energy is vanished in the ICE. For reduction of these losses, the advanced engine technologies are adopted. These are variable valve timing and lift, turbocharging, direct fuel injection, and cylinder deactivation. In addition, diesels are ~30 to 35% more competent than gasoline engines. This is because of the development in technologies and fuels which makes diesel vehicle more attractive.

#### Accessories

There are various types of accessories used in automobile such as air conditioning, power steering, windshield wipers, and other accessories. These accessories are used around 2% energy generated from the engine. Therefore, the improvement in fuel economy around 1% may be attainable with more efficient alternator systems and power steering pumps.

#### Driveline Losses

There are other losses of energy around 5% due to the transmission and other parts of the driveline. For reducing these losses in driveline various technologies developed which are automated manual transmission and continuously variable transmission.

#### Aerodynamic Drag

Drag is directly related to shape of the vehicle. Around 2–3% of energy is lost as aerodynamic drag in automobiles. The drag is significantly reduced by using smoother vehicle, but further reductions of 20–30% are possible.

#### Rolling Resistance

For forward movement of tire, a force is required which is known as rolling resistance force, which is directly proportional to the weight of the load supported by the tire. There are various technologies developed nowadays to overcome the rolling resistance such as improvement in designs of shoulder and tire tread as well as improvement in materials which is used in the tire belt and traction surfaces. For

passenger cars, the fuel efficiency is increased by 1% by reducing of rolling resistance by 5–7%. However, the balancing in these improvements are required against traction, durability, and noise.

### Overcoming Inertia; Braking Losses

For moving forward a vehicle, it is required to overcome the vehicle’s inertia, which is directly related to its weight. This is carried out by using drivetrains which provides the enough energy. If the vehicle weight is less than less energy is required for moving a vehicle. This can be achieved by using lightweight materials and lighter-weight technologies (e.g., automated manual transmissions weigh less than conventional automatics).

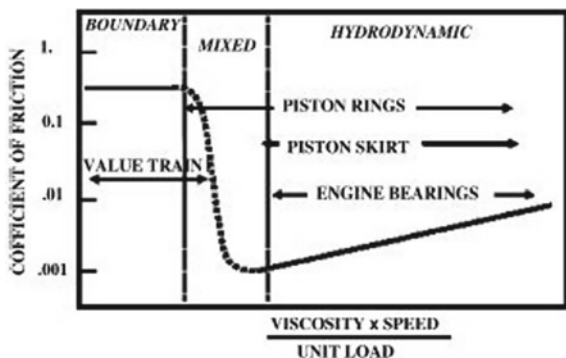
### 1.1.5.2 Energy Losses in Engine

More than 60% of losses in an automobile occur in the engine. These losses are exhaust gas losses (23.40%), in-cylinder heat losses (20.50%), and friction losses (7.70%), after cooler (7.30%) etc. Due to these losses, currently from an engine only 40% net power can be extracted. The net power is in engine can be improved by 10% by reducing exhaust gas losses, in-cylinder heat losses and frictional losses. Friction losses contribute to around 8% of total energy loss in an engine. The major subsystems of engine contributing to mechanical friction in an automobile engine are piston and ring pack, bearing and crank shaft system and auxiliary valve drives.

### 1.1.5.3 Systems in Engine Causing Friction

Figure 1.7 shows the stribeck curve of different components in engine and the lubrication regime they undergo during operation.

**Fig. 1.7** Different engine parts and corresponding lubrication regime (Tung and McMillan 2004)



## Piston Assembly System

The piston assembly system consists of piston, piston rings, piston pin, connecting rods and bearings. There are three main friction and lubrication groups contributing to friction in piston assembly system: piston skirt sliding up and down against liner, ring pack reciprocating against liner, and bearings in connecting rod and wrist pins.

The piston ring is one of the most intricate tribological elements in an engine which subjected to large variations in load, temperature, velocity and lubricant accessibility. Early studies show that the hydrodynamic lubrication theory is applicable to the interface of piston assembly and cylinder liner throughout most of the piston middle stroke. However, when the piston motion ceases near top dead centre (TDC) or bottom dead centre (BDC) of the stroke, the piston velocity is not adequate to establish a hydrodynamic lubrication action. Lubricating films become very thin and contact between the surface asperities on the ring and the liner will support part of the piston ring restoring force. Therefore, wear on the cylinder liner surface may occur in the vicinity of TDC and BDC. Severe surface wear could affect the liner-ring sealing performance and result in excessive gas blow-by and fuel consumption.

## The Crankshaft and Connecting-Rod Bearing Systems

The main bearings in crank shaft, connecting rod and piston pin, connecting rod and crank shaft interface are falls in the category of journal bearing lubrication. Most of the friction in crank shaft originate from the main bearings supporting crank shaft in its rotational motion. Lubrication regime in main bearings is primarily hydrodynamic. Oil is supplied to the bearing surfaces through oil feeds along the crank shaft.

If the bearings are adequately lubricated, wear on bearing will be lower after an initial stage of running in period. However, shaft misalignment or particulate contamination of the lubricant supply can lead to excessive wear. Corrosion is also reported as an additional failure mechanism.

## Valve Train System

This system consists of a series of mechanical parts that are used to control the intake and exhaust valves. The lubrication in valve train system ranges from hydrodynamic to boundary lubrication. Most of the friction in valve train system is contributed by camshaft bearings, cam/cam follower interface, rocker arm pivot/shaft and linear oscillatory components such as valves, guides, valve lifter, valve seal etc. The cam-follower interface is mostly under boundary lubrication, where the role of chemical reactions in thin films is vital. The action of lubricant additives especially extreme pressure additives is very important in this interface. Also, surface interactions takes place in cam and follower, thus surface topography of these parts is a critical parameter.

#### 1.1.5.4 Lubricants

Engine runs smoothly if correct engine oil is chosen. The lubricant creates a thin film between two mating surfaces of automobile which prevent them from rubbing against each other and becoming worn or damaged. Oil also prevents corrosion, cools the engine and helps to keep the engine clean and protected.

Generally, 80% base oil and 20% additives were presented in engine oil. These additives include anti-wear additives, antioxidants, dispersants and detergents that keep the engine clean, and viscosity index improvers that ensure the oil maintains an optimum viscosity throughout the engine's operating temperature range. The base oil carries these additives to where they are needed, and provides vital cooling to engine components, by drawing away heat. Base oils can be either mineral or synthetic, and engine oils can contain all mineral base oil, all synthetic base oil, or a mixture of the two. Engine oils containing a mixture are typically described as part-synthetic.

#### Causes of Lubricant Degradation

The life of lubricant is finite in operation. After that, the degradation of lubricant is started or sometimes it becomes contaminated which indicates the lubricant change. There are various factors which are responsible in degradation of oil in an engine. Among all factors, the most common factors are oxidation, thermal breakdown of the lubricant oil, micro-dieseling, additive depletion and contamination. The brief description of the factors are given below:

##### **Oxidation:**

In this process the oil molecules reacts with oxygen molecule. Due to which the viscosity of lubricant is increased, causes the formation of sludge and sediment. It is also responsible for chemical depletion and breakdown. After starting of oxidation, the increment in acid number is started. In addition, rust and corrosion in the equipment is because of oxidation of lubricant.

##### **Thermal Stability:**

The thermal stability of lubricant is inversely proposal to the temperature means an increase in temperature of lubricant will result in a decrease in thermal stability. In research, it has been shown that, if the oil operating temperature is increased by 10 °C than the rate of the oil oxidation is doubled. This statement stated that the life of the oil is halved. This situation is not quite as calamitous because it reflect that the oils naturally have quite a long life time. Temperature is only a significant issue if it reaches above 65 °C. The mostly lubricants which are used in high temperature for certain period of time, blended with additives which prevents the oxidation in lube oil.

### **Additives:**

The performance additives are twenty or more chemicals that is combined with the base stock to improve or impart different properties. Most of the additives are sacrificial in nature which means that they get used up during the lifetime of the oil. But, when the oil is using for lubricate a machinery components, the additives present inside the lube oil start depletion. Which causes wear at the interface of meeting surfaces. This indicates the change of lube oil inside the machinery.

Furthermore, the rate of degradation of lubricant is widely influenced by contamination such as soot, water, air, etc. Because of depletion, wear occurs at the meeting parts which contains the fine metal particles. The fine particles start the catalyst process which start sparks and speeds up the degradation process of lubricant. Air and water also provides the source of oxygen. This oxygen is reacts with the oil, causes the oxidation of the lubricant. Because of this reason, the oil analysis sometimes can be helpful in monitoring your lubricant's contamination levels.

The present monograph provides the current and emerging research in the field of automobile which is very useful for readers in enhancing their knowledge in the various dimensions of research. The present book is summarized some of the novel materials, lubrication and surface morphology used for automotive application into three different sections.

1. New Materials for Automotive Applications
2. New Lubricants for Automotive Applications
3. Surface Morphologies for Automotive Applications.

The editors sincerely hope that the present monograph gives the comprehensive study of current trends adopted by automobile sectors in the development of new technologies and materials for reduction of friction and wear because the customer satisfaction and environmental protection are very important factors in governing the development of automotive technology. Furthermore, the present monograph is intended for all level of students (UG, PG as well as Doctorate), research scientist and industry persons.

### **References**

- Akiyama K, Manunaga K, Kado K, Yoshioka T (1987) Cylinder wear mechanism in an EGR equipped diesel engine and wear protection by engine oil. SAE paper 872158
- Briscoe BJ, Sinha SK (2002) Wear of polymers. Proc Inst Mech Eng Part J: J Eng Tribol 216:401–413
- Dowson D (1993) Piston assemblies; background and lubrication analysis. In: Taylor CM (ed) Engine tribology. Tribology series, vol 26. Elsevier, Amsterdam, pp 213–240 (Chap. 9)
- Duncan D (1997) History of tribology, 2nd edn. Professional Engineering Publishing. ISBN 1-86058-070-X
- Nakasa M (1995) Engine friction overview. In: Proceedings of International Tribology Conference, Yokohama, Japan
- Rabinowicz E (1995) Friction and wear of materials. Wiley, New York. ISBN 10: 0471830844



- Rathaur AS, Katiyar JK, Patel VK, Bhaumik S, Sharma AK (2018) A comparative study of tribological and mechanical properties of composite polymer coatings on bearing steel. *Int J Surf Sci Eng* 12(5/6):379–401
- Spikes H (2001) Tribology research in the twenty-first century. *Tribol Int* 34:789–799
- Stribeck R (1902) Die wesentlichen Eigenschaften der Gleit- und Rollenlager (Characteristics of plain and roller bearings). *Zeit des VDI* 46
- Taylor CM (1998) Automobile engine tribology—design considerations for efficiency and durability. *Wear* 221(1):1–8
- Tung SC, McMillan ML (2004) Automotive tribology overview of current advances and challenges for the future. *Tribol Int* 37:517–536
- Williams JA (2005) Wear and wear particles—some fundamentals. *Tribol Int* 38(10):863–870

**Part II**  
**New Materials for Automotive Applications**

# Chapter 2

## Tribological Aspects of Automotive Engines



Vikram Kumar and Avinash Kumar Agarwal

**Abstract** There is tremendous requirement for development of compact and fuel efficient automotive engines with reduced emissions. From tribological point of view, automotive engine components such as piston assembly, bearings and valve trains are lubricated and their surface behaviors have been extensively studied. In this chapter, current and future trends of automotive lubrication and requirements from automotive lubricants are discussed in detail. American Society for Testing and Materials (ASTM) standards are used for selection of automotive lubricants. The lubrication of light weight materials (Al, Mg) was studied, which was used to replace heavier cast iron blocks used presently. In this chapter, future trends of light weighted tribological materials to be used in near future as well as nano tribology are discussed. New trends of tribology in automotive engines were explained and also selections of new lubricant used in advance engines were discussed. The overall studies of tribology of engines components enhance the engine performance.

**Keywords** Tribology · Light weighted materials · Automotive lubricants · Surface finish

### 2.1 Introduction

Study of surfaces of automotive engine components under relative motion is essential to understand their mechanical and tribological behaviour. Solid surfaces give complex responses due to many external variables such as temperature, strain rate, gaseous environment, humidity etc. When the surface interacts with external environment, physical and chemical changes occur in the solid surfaces. When surfaces are in relative motion under contact, shear stress develops which wears out both mating surfaces by plastic deformation, fracture and fatigue. Wear of material also leads to noise, vibrations and ultimately failure of machine elements. Understanding wear phenomenon requires knowledge of friction between materials. Friction is defined

---

V. Kumar (✉) · A. K. Agarwal (✉)  
Department of Mechanical Engineering, Indian Institute of Technology Kanpur, Kanpur,  
Uttar Pradesh 208016, India  
e-mail: [akag@iitk.ac.in](mailto:akag@iitk.ac.in)

as the force resisting the motion, when there is a relative motion between the two mating surfaces. Friction occurs due to surface morphology i.e. physical and chemical nature of the surfaces. Friction and wear of contacting surfaces can be reduced by providing interfacial lubrication. Lubrication is needed to separate the contact between surfaces by forming a liquid film or a boundary film, which adheres to the metallic surfaces. This liquid or boundary film by virtue of its physical or chemical nature provides low shear stress and bears load mechanically.

The word “Tribology” originates from the Greek word “Tribos”. The meaning of tribos is rubbing (Jost 1966). Nobel Prize winner physicist Wolfgang Pauli had quoted that, “God made solids, but the surfaces were the work of devil” (Jamtveit and Meakin 1999). This quote signifies the challenges and importance of tribology at any scale (micro- to nano-scale). Friction and wear are not always undesirable. Sometimes friction is necessary, such as for holding, walking, braking, rolling etc.

The use of rubbing is in existence since ancient ages (~0.2 million years ago), when humans generated fire by rubbing two (wood) surfaces against each other. After that, around 3500 B.C., wheels were invented. Egyptians were first recorded tribologists (nearly 2400 B.C.). They used sticky, greasy substances, and water as lubricant in transportation of objects by sliding. In modern era, Leonardo da Vinci (1452–1519) showed some friction experiments through his sketches. Amonton (1689) independently gave two laws of friction, which surmised:

- Frictional force (F) is proportional to the applied normal load (N). This law provides the relation, where  $\mu$  is the coefficient of friction.
- Friction force is independent of the (apparent) area of contact.

Leonhard Euler (1778) (Euler 1778) explained that coefficient of friction is due for interlocking of asperities and is equal to the tangent angle of interlocking asperities ( $\mu = \tan\theta$ ). He also proposed two types of coefficients of friction (static and kinematic).

The thermal and mechanical efficiencies of IC engines are low and this is their main drawback. 4–15% of total fuel energy is lost due to friction alone in the engine. Major part of the fuel energy is wasted in the form of heat (Taylor 1998). Apart from this, IC engines cause air pollution by generating particulates and harmful gases. There is tremendous effort underway for development of fuel efficient and compact automotive engines with lower environment impact, required for the 21st century. Engine efficiency can be also improved by adequate application of tribology. Friction and wear of engine components such as bearings, piston assembly and valve trains can be reduced by developing new lubrication technique. These techniques must be durable at high loads, speeds and temperatures. Overall ~15% fuel energy is lost due to friction from these components and based on the data, ~10% reduction in frictional losses would lead to ~1.5% lower specific fuel consumption. Piston ring assembly, bearings and valve trains are the main contributors to frictional losses in an IC engine (Andersson 1991). Engine components such as engine bearings, piston-rings systems, and valves trains are loaded to very fast and broad variations in speeds, loads, temperatures and lubricant availability (Dowson et al. 1983).

## 2.2 Automotive Engine Tribology

### 2.2.1 Engine

IC engines are very popular because of their reliability, versatility and performance. However major drawback of IC engine is lower thermal and mechanical efficiency due to dissipation of energy into heat and frictional losses. IC engines also contribute to the environmental pollution by emitting unburned hydrocarbons, particulates, oxides of nitrogen (NO<sub>x</sub>), carbon monoxide and carbon dioxide.

Tribological studies are required to reduce the wear and friction by adequate lubrication of all engine components, which are under relative motion. This study is done in the large set of working conditions of varying loads, speeds and temperatures. Better tribological performances of IC engine have advantages of lower fuel consumption, higher power output, lower oil consumption, lower harmful emissions, superior reliability, longer durability and engine life, and reduced engine maintenance and longer service intervals. A small improvement of engine durability, efficiency and emission levels have large impact on the global environment and economy. Energy produced from the combustion of fuel is dispersed into engine and powertrain. 12% of total energy is used to drive the automotive wheels and 15% of mechanical energy is lost in frictional heat. Engine frictional losses due to piston rings, piston skirts and bearings are ~66% of total frictional losses and ~34% losses are due to crankshaft, valvetrain, gears and transmission lines (Nakasa 1995). Largest friction loss is due to sliding of piston rings and piston skirts against the cylinder wall. Next higher frictional losses are due to engine bearings, followed by valvetrains.

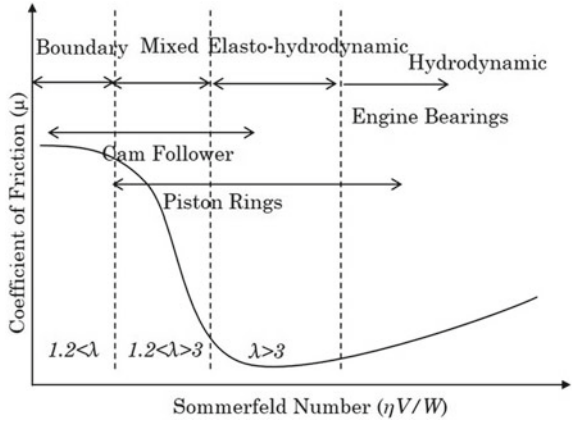
### 2.2.2 Engine Lubrication Regimes and Wear Calculations

Different IC engine components work in different lubrication regimes to achieve better performance. Some components operate in more than one regimes of lubrication. Mostly thrust and journal bearings operate in hydrodynamic regimes of lubrication. Regimes of lubrication also depend on the engine speeds. Generally piston ring assembly, valvetrains and transmission lines operate under boundary and mixed lubrication regimes. Lubrication regimes are also affected by surface roughness of mating interfaces, lubricant degradation and wear of mating surfaces.

Lubrication of engine components can be understood by the modified Stribeck curve, shown in Fig. 2.1 (Dowson 1998; Tayler 1998). It is a plot of coefficient of friction versus Sommerfeld number ( $\eta V/W$ ). The dimensionless parameter  $\lambda$  is defined as the ratio of film thickness to the surface roughness.

$$\text{Lamda } (\lambda) = \text{fluid film thickness } (h) / \text{surface roughness } (R_a)$$

**Fig. 2.1** Lubrication regimes curve for various IC engine components



Engine components design and wear was investigated by numerous researchers. They have given many mechanisms to understand the wear of engine components (Lancaster 1973; Priest et al. 1999). The wear can be simply calculated by using Archard equation, which is as follows:

$$V = kWL \tag{1}$$

where,

- V wear volume (m<sup>3</sup>),
- K wear coefficient (m<sup>3</sup>/mN),
- W load (N),
- L sliding distance (m).

### 2.2.3 Piston Ring Assembly

Piston-ring assembly is the heart of the engine, and it forms a very critical linkage to transform the energy generated by the combustion of fuel into useful kinetic energy. It consists of a ring pack, piston, cylinder liner (wall) and connecting rod. The ring pack acts as dynamic gas seal between the crankcase and combustion chamber, and restricts the oil deportation into the combustion chamber. It also transfers heat from piston to the cylinder wall and eventually into the lubricant. Top two rings are ‘compression rings’ and firing pressure is exerted on to the faces of rings to push them against the cylinder wall, and they experience maximum temperature and loads. Top compression ring is coated with wear resistant materials such as molybdenum and have barrel-faced profile. The second compression ring has tapered face with descending scraping profile. The bottom ring is the oil control ring with two running faces.

For the improvement in performance and durability of piston rings, Priest and Taylor proposed the following solution (Priest and Taylor 2000):

- Improvement of surface roughness, profile and better understanding of mixed lubrication regime.
- Understanding the linkage between chemical and lubrication mechanisms and additive's reaction with the film.

The piston rings are very complicated in tribological aspects since there is a very large variation in speed, load, temperature and availability of lubricant. The lubrication regimes at piston rings and cylinder wall interface is boundary, mixed, elastohydrodynamic and hydrodynamic, all in one engine cycle (Ruddy et al. 2017). As the piston assembly moves from bottom to the top, lubrication regime also changes. It is full film lubrication at the bottom dead center, mixed in the middle of the stroke, and boundary lubrication at the top dead center (Hamilton and Moore 1974; Brown and Hamilton 1977; Wakuri et al. 1978; Dowson et al. 1979). The most common piston ring materials used are gray cast iron, carbide malleable iron and malleable nodular iron. However steels have become more popular off late because of their high strength. Grey cast iron and aluminum alloys are used as cylinder bore materials. Engine piston is mostly made of silicon aluminum alloy. Piston rings, piston and cylinder liner is coated to reduce friction and wear. Friction and wear control is necessary for enhanced engine performance. Hence lubrication study is necessary for clearly understanding the complicated interactions between wear and lubrication. Wear is an after-effect of mechanical interactions, and corrosion takes place in the upper region of the cylinder and dictates the failure of the engine. Wear is also dependent on the surface finish of piston rings and cylinder liner. Surface finish of cylinder liner, piston rings and piston skirt affects retention of oil within surface and reduces scuffing during engine operation.

#### **2.2.4 Engine Bearing**

Crankshaft, camshaft and connecting rod are supported by engine's journal bearing, which rotates during engine operation. Hydrodynamic load bearing capacity is generated by the lubricant film pressure, which balances the load applied. The lubrication of bearings is by jet trespass or by fleeting the lubricant through the shaft holes. The initial wear of bearings is very slow under lubricated conditions of engine operation. If the crankshaft is misaligned or there are contaminants present in lubricant, then excessive wear takes place. Journal bearing tribology is a complex issue of thermal effects, lubricant supply, dynamic loading and elasticity of the surroundings (Booker and Booker 1965). Many assumptions have been considered for the lubricant mobility. The lubrication of engine bearings is assumed entirely to be in hydrodynamic regime. Some researchers have hypothesised that engine bearings operate in mixed lubrication regime and designed the bearings accordingly to improve the engine performance (Priest and Taylor 1998).

### 2.2.5 Valve-Train

The valvetrain consists of valves, valve keys valve springs retainers, valve springs, piston rods, lifter/tappets, rocker arms and a camshaft. The main function of valvetrain is to convert rotary camshaft motion to linear valve motion, in order to control the flow of fluid into the combustion chamber. It also drives water pumps, fuel pumps and power steering pumps. Three main valvetrain systems are sleeve, poppet and rotary valve. The poppet valvetrain system is most popular for exhaust and inlet valves of engine amongst all major engine manufacturers. The opening and closing of valves is controlled by crankshaft driven camshaft and synchronizes the valve movement with the piston movement and hence with the combustion cycle. Each contact undergoes either sliding or rolling friction.

Friction is a very important parameter for the selection of valvetrain. Roller follower, which reduces friction significantly, is the best configuration for valvetrain since roller contact contributes lower coefficient of friction compared to sliding contact. Friction contribution of the valve systems is a small fraction (10%) of mechanical losses compared to piston assembly (50%). The coefficient of friction is reduced by introduction of friction modifier additives such as molybdenum dithiocarbamate (MoDTC) into the lubricating oil (Korcek et al. 1999). Wear of valve seat and its recesses is also a big problem in valvetrains, which affects the engine timing. Hence materials having wear and corrosion resistance, high strength and high temperature stability are selected for the valve seat. Inlet valve materials are hardened low alloy steel with higher strength and wear resistance. Exhaust valve materials is hot hardened stainless steel, which is corrosion resistant and survives the high temperature.

### 2.2.6 Cam Follower

The lubrication of cam follower interface is very difficult in the valvetrain system. The cam follower operates under boundary lubrication regime hence material selection and surface treatment is taken care off. In addition, wear resistant lubricant additives such as zinc di-alkyl di-thio-phosphate (ZDDP) are added into the lubricating oil. Some researchers investigated tribological performance of cam follower under mixed and elastohydrodynamic lubrication regimes (Taylor 1994). Cam follower materials are generally steels or iron with modified surfaces (surface treatments) in order to avoid early failure. Recently, ceramic cam followers are mostly used to minimize the frictional losses (Gangopadhyay et al. 1999). Cam follower failure is due to polishing, pitting and scuffing, which are affected by design, materials, lubrication and operating conditions. Hence durability of cam followers is dependent on materials selection, surface treatment, additives and lubricants.



## 2.3 Transmission and Drive Line Tribology

### 2.3.1 *Transmission Line*

Tribological study of transmission band and clutch are very important because band and clutch performance and durability is controlled by tribology. The transmission clutches include two plates which are friction lined clutch plate and reaction steel plate respectively. The transmission band and clutch is acted as lubricated brake. The clutch plate consists of core plate, adhesive coating and friction facing. The friction facing is confined with the adhesive to steel core on one or both sides. Frictional materials must survive high temperature, compressive forces and shear, and must offer adequate friction. These materials are made of particle fillers, fibers and friction modifiers. These materials have adequate porosity to transmit the transmission fluid to the friction interface as lubricant basin. All transmission fluids consist of base-stock and additives including friction modifiers. Desired friction for smooth engagement of clutch is low static friction and higher stable dynamic friction, which is provided by friction modifiers (Tung and Wang 1989; Stebar et al. 1990).

### 2.3.2 *Traction Drive Components*

Advancements in continuously variable transmission (CVT) enhance the drivability benefits and fuel economy by applying traction drive components. The traction CVT is replacement of bands, clutch and gears with a 'variator', which allows continuous and smooth ratio variation over entire range of operations. The main advantage of traction drive CVT are that engine can be operated over full range of loads and speeds (Heilich 1983). The power transmission by traction drive is through rolling contact via varying forces, which depend on the radius at which traction force is applied. Thin film is formed between two rolling contacts, which experience high load and shear force and forms lubricating oil film in elastohydrodynamic regime. Instantaneous viscosity of fluid is enhanced by many order of magnitude due to these stresses. Then torque is transmitted through this semi-solid lubricant through the drive. Mechanical efficiency is enhanced by traction drive due to efficient rolling motion and their working in elastohydrodynamic lubrication regime (Dowson and Higginson 2014). The traction drive requires high traction coefficient for power transmission along with better lubrication. Traction drive efficiency is greatly dependent on the lubricant used. The traction fluid must survive high temperature and should not deteriorate under repeating shear conditions. Several synthetic fluids and naphthenic base compounds have superior traction properties than paraffinic or aromatic compounds (Hata and Tsubouchi 1998; Machida and Kurachi 1990). Significant new research can be undertaken in future to formulate new traction fluids and optimize its performance for automotive applications.

### **2.3.3 Wheel Bearing**

Most commonly, rolling bearings are applied in the hubs of the wheel. These parts are made of high carbon steel, which is hardened and has excellent surface finish. These bearings are filled with grease and assembled with seals made of elastomeric materials. Bearings fail due to surface damage caused by improper fitting or impacts during operation. Surface damage causes the initiation of fatigue failure and its propagation.

### **2.3.4 Drive Chain**

Chain drives are used for driving and timing of ancillary components. Chains offer their own advantage such as increased durability and relatively simple and cheap, and have high capacity. Chains can be lubricated by splash and jets lubrication methods. In splash lubrication method, chain is dipped into the sump during its move, however in jet lubrication method, a lubricant jet impinges on to the chain at the entrance. Within the roller chain, rollers revolve around the sprocket tooth, while pin slides inside the bush amid enunciation. Hence there is excessive wear of the bush and pin contact, causing elongation of chain after some time.

## **2.4 Trends in Automotive Engine Tribology**

Thinner oil film formations for the lubrication of engine components provide more efficient lubrication and higher power output. Hence lower viscosity engine oils (SAE 0W-20 and 5W-20) are used to improve the fuel economy and reduce the frictional losses (Priest and Taylor 1998).

### **2.4.1 New Material Development**

Currently, heavy cast iron engine blocks are being replaced with non-ferrous lighter materials (Al and Mg). However the lubricants are formulated according to blocks of cast iron, and not for these newer block materials (Tung and Hartfield-Wünsch 1995a; b; Tung et al. 1996). Sleeves of cast iron are used inside the aluminum cylinder bores for better lubrication. Piston skirts and cylinder liners are coated with scuffing and wear resistant materials. These coatings are of amorphous carbon, which offers very low friction and reduces the wear, thus improving engine component durability (Erdemir 2000). These coating materials acts as self-lubricant.

### **2.4.2 Development of Nano-tribology**

The engine component lubrication contact scale moves from micro- to nano-, and the surface adhesion forces start dominating. Nano-lubrication mechanism is different from the conventional lubrication mechanisms (Krauss et al. 2001). Various nano-scale material surfaces are designed for nano-lubrication. These materials are stronger, harder and self-repairing. Such types of materials include structural carbon, ceramic materials, polymer materials, multi-functional materials, nano-particle-reinforced materials, nano-coated materials and nano-particle alloys.

## **2.5 Trends in Automotive Lubricants**

The lubricant used in engines must protect the engine components, which are lubricated. The protection of engine components is provided by the fluid film, which forms a chemical film on the surfaces (boundary lubrication). Lubricant protects the engine components from corrosion by neutralizing the acids generated at hot spots. Lubricants move the protective film to the desired place and displace the unwanted materials from the point of generation. These differing qualities of work unequivocally impacts the selection of physical properties and chemical composition of lubricants. Different engine components require diverse types of protection. Engine oil performances should not degrade with the fuel and combustion product entering the lubricant. Transmission liquids must survive high loads and temperatures. Engine oil must not degrade or evaporate during high temperature engine operating conditions. Different bearings need different liquid film thickness, which separates a spinning shaft around its axes from its bearing surface.

### **2.5.1 Engine Lubricants**

Engine oils operate under harsh conditions, hence there is a big challenge in development of lubricants which can survive the engine environment for longer periods. Fuel, combustion gases, water and solid contaminant (sand, dirt and airborne materials) quicken the oil degradation and also reduce oil life hence require filtration. Properties of engine oil also influences the fuel economy and emissions from the engine. Engine oil designation is done on the basis of their performance. American Petroleum Institute (API), American Society for Testing and Materials (ASTM) and Society for Automotive Engineers (SAE, or currently SAE International) offer the performance framework of the engine lubricants (Hsu 1995). In this framework, performance and service of the engine oil is divided in two series: S and C; which stand for 4-stroke spark ignition engines application, and compression ignition 2-stroke or 4-stroke diesel engines, respectively.

Oil film may not be adequate to offer total wear protection under high pressure and temperature conditions experienced at the cylinder-piston ring interface at the top dead center due to the influence of combustion of fuel. Under these conditions, lubricant should have additives, which form antiwear film at the mating surfaces. One of these additives is zinc di-alkyl di-thio-phosphate (ZDDP). The engine lubricant should also have corrosion resistant additives.

### **2.5.2 Gear Lubricants**

Gears are designed to withstand high load and temperature, which is generated at the point of contact due to friction. Thus lubricant must provide protection from extreme pressure and avoid material failure. Gear material functionality should be for longer duration. Gear lubricant properties must include anti-wear, corrosion protection, low temperature viscosity, resistant to foam formation, oxidative stability, and low friction characteristics (Chapman et al. 1962).

### **2.5.3 Axle Lubricants**

Desired properties of axle lubricant should include viscosity, thermal stability and durability. The viscosity of lubricant should be in the range of 14–15 centistokes at 100 °C. The Kinematic viscosity of lubricant can be measured as standard test method (ASTM D 445). ASTM D 2983 standard test method can be used for the low temperature (–5 to –20 °C) viscosity measurement of the lubricant (Schwartz et al. 2002; Tung et al. 2001). The performance of lubricant should be consistent throughout the service life of the axle. The lubricant should not harm the metal components and also metal components should not degrade the lubricant. The lubricant should also not damage the seals.

### **2.5.4 Solid Lubricants**

Some components of the engine have no space for liquid lubrication. These engine parts are therefore lubricated by using solid lubricants. Generally it is coated on the contacting surfaces by using binder or additives. Some solid lubricants are molybdenum disulphide ( $\text{MoS}_2$ ), graphite and poly-tetra-fluoro-ethylene (PTFE). Polymeric solid lubricants are effective at low temperature range however metallic solid lubricants degradation temperature is higher (up to 650 °C) and hence they can be used at relatively higher temperatures (Booser 1997).

## 2.6 Summary

This chapter provides a comprehensive review of tribological aspects of automotive engine component lubrication. This chapter covers various tribological aspects of engine, which are as follows:

- There is great contribution of automotive lubricants in enhancing the engine efficiency and output from an engine powertrain. For superior power output and efficiency, lubricants should form thinner lubricant film on the mating engine components. The issues of durability and wear are also addressed for the thin film lubrication.
- Tribological requirement of newer non-ferrous automotive materials (Al, Mg) are also discussed.
- Current developments in lubricants are discussed along with future requirements. ASTM standards for automotive engines are also discussed.
- New lubrication methods (nano-lubrication) and their mechanisms is discussed briefly.

**Acknowledgements** The review study is supported by Council of Scientific & Industrial Research—Human Resource Development Group (CSIR—HRDG) and Engine Research Laboratory Department of Mechanical Engineering, Indian Institute of Technology Kanpur, which allowed Dr. Vikram Kumar to stay as CSIR Senior research Associate.

## References

- Andersson BS (1991) Company's perspective in vehicle tribology. In: Leeds-Lyon symposium on tribology, pp 503–506
- Booker JF, Booker JF (1965) Dynamically loaded journal bearings: mobility method of solution. *J Basic Eng* 87(3):537–546
- Booser ER (1997) Solid lubricants. *Tribology data handbook: an excellent friction, lubrication, and wear resource*. CRC Pres, p 156 (Chapter 26)
- Brown SR, Hamilton GM (1977) The partially lubricated piston ring. *J Mech Eng Sci* 19(2):81–89
- Chapman PR, Schimmel JO, Moyer RG (1962) Pure Oil Co, assignee. Method and apparatus for testing lubricants. United States Patent US 3045, 471
- Dowson D (1998) *History of tribology*. Longman, London and New York
- Dowson D, Higginson E (2014) *Elasto-hydrodynamic lubrication: international series on materials science and technology*. Elsevier (2014)
- Dowson D, Economou PN, Ruddy BL, Strachan PJ, Baker AJS (1979) Piston ring lubrication—Part II. Theoretical analysis of a single ring and a complete ring pack. *Energy conservation through fluid film lubrication technology: frontiers in research and design*. ASME 23–52 (1979)
- Dowson D, Taylor CM, Godet CM (1983) Tribology of reciprocating engines. In: 9th Leeds-Lyon symposium on tribology, Butterworth, Oxford, 348 (1983)
- Erdemir A (2000) A crystal-chemical approach to lubrication by solid oxides. *Tribol Lett* 8(2–3):97
- Euler L (1778) *Derepraesentatione superficiae sphaericae super plano*. *Acta Academiae Scientiarum Imperialis Petropolitanae*, pp 107–132

- Gangopadhyay A, McWatt D, Willermet P, Crosbie GM, Allor RL (1999) Effects of composition and surface finish of silicon nitride tappet inserts on valvetrain friction. In: *Lubrication at the Frontier, Leeds-Lyon symposium on tribology*, Lyon, France. Tribology series, vol 36. Elsevier, pp 891
- Hamilton GM, Moore SL (1974) First paper: measurement of the oil-film thickness between the piston rings and liner of a small diesel engine. *Proc Inst Mech Eng* 88(1):253–261
- Hata H, Tsubouchi T (1998) Molecular structure of traction fluids in relation to traction properties. *Tribol Lett* 5:69–74
- Heilich F (1983) *Traction drives: selection and application*. Marcel Dekker Inc 18–51
- Hsu S (1995) National Institute of Science and Technology (NIST) Engine materials and tribology workshop, Gaithersberg, Maryland, pp 3–5
- Jamtveit B, Meakin P (1999) Growth, dissolution and pattern formation in geosystems. In: *Growth, dissolution and pattern formation in geosystems*. Springer, Dordrecht, pp 1–19
- Just HP (1966) *Lubrication: tribology; education and research; Report on the present position and industry's needs* (submitted to the Department of Education and Science by the Lubrication Engineering and Research) Working Group. HM Stationery Office
- Korcek S, Jensen RK, Johnson MD, Sorab J (1999) Fuel efficient engine oils, additive interactions, boundary friction, and wear. Tribology series, vol 36. Elsevier, pp 13–24
- Krauss AR, Auciello O, Gruen DM, Jayatissa A, Sumant A, Tucek J, Mancini DC, Moldovan N, Erdemir A, Ersoy D, Gardos MN (2001) Ultra nano crystalline diamond thin films for MEMS and moving mechanical assembly devices. *Diam Relat Mater* 10(11):1952–1961
- Lancaster JK (1973) Dry bearings: a survey of materials and factors affecting their performance. *Tribology* 6:219–251
- Machida H, Kurachi N (1990) Prototype design and testing of a half toroidal CVT. SAE Technical Paper 900552. <https://doi.org/10.4271/900552>
- Nakasa M (1995) Engine friction overview. In: *Proceedings of international tribology conference*, Japan, Yokohama
- Priest M, Taylor CM (1998) Automobile engine tribology—approaching the surface. In: *AUSTRIB '98: Tribology at work*. The Institution of Engineers, Australia, pp 353–363
- Priest M, Taylor CM (2000) Automobile engine tribology—approaching the surface. *Wear* 241:193–203
- Priest M, Dowson D, Taylor CM (1999) Predictive wear modeling of lubricated piston rings in a diesel engine. *Wear* 231:89–101
- Ruddy BL, Dowson D, Economou PN (2017) A review of studies of piston ring lubrication. In: *Proceedings of 9th Leeds-Lyon symposium on tribology*, pp 109–121 (2017)
- Schwartz SE, Tung SC, McMillan ML (2002) Automotive lubricants. In: *ASTM Handbook of fuels and lubricants* (Chapter 14)
- Stebar RF, Davison ED, Linden JL (1990) Determining frictional performance of automatic transmission fluids in a band clutch. *SAE Trans* 99:914–27
- Taylor CM (1994) Fluid film lubrication in automobile valve trains. *J Eng Tribol Proc Inst Mech Engrs, Part J* 208(J4):221–234
- Taylor CM (1998) Automobile engine tribology—design considerations for efficiency and durability. *Wear* 221:1–8
- Tung SC, Hartfield-Wünsch S (1995a) Advanced engine materials: current development and future trends. In: *NIST (National Institute of Science and Technology), engine materials and tribology workshop*, Gaithersberg, Maryland
- Tung SC, Hartfield-Wünsch S (1995b) The effect of microstructure on the wear behaviour of thermal spray coatings. *ASM Trans* 107
- Tung SC, Wang S (1989) Using electrochemical and spectroscopic techniques as probes for investigating metal-lubricant interactions. *STLE Tribol Trans* 33(4):563–572
- Tung SC, Hill S, Hartfield-Wünsch S (1996) Bench wear testing of common gasoline engine cylinder bore surface/piston ring combinations. *STLE Tribol Trans* 39(4):929–935

Tung SC, Schwartz SE, Kapoor A, Priest M (2001) Automotive tribology. CRC handbook of modern tribology, Chapter 32 (2001)

Wakuri Y, Soejima M, Taniguchi T (1978) On the oil film behaviour of piston rings correction of effective pressure region of oil film. Bull JSME 21(152):295–302

# Chapter 3

## The Potential of Natural Fibers for Automotive Sector



**Shashi Kant Verma, Ashutosh Gupta, Vinay Kumar Patel, Brijesh Gangil  
and Lalit Ranikoti**

**Abstract** Poor quality leads to poor efficiency. As the research progresses, the development in the sustainable material are also progresses. This change leads to enhancement in the efficiency of the product. Novel sustainable material is the need of the hour for the future development. Natural composite fits the best alternative to deal with environment problem. In the past decade natural fibers applications has been increasing as never before. These applications are aerospace, infrastructure, thermal etc. Metal like steel, aluminum, cast iron are some of the materials which have been dominating the industries before the introduction polymer composite. These metals have been dominating the market but for a long time but lacking in the environmental issues. Natural fibers have successfully filling that gap. Being biodegradable, it is nature friendly and easy to dispose off. Decreased weight, nature friendly and easy availability are the attractive characteristics that influences various industries towards natural fiber composite. The current segment deals with the various natural fiber composites and their applications in the industries.

**Keywords** Natural fibre · Mechanical testing · Dynamic mechanical analysis

---

S. K. Verma

Mechanical Engineering Department, IET, Bundelkhand University, Jhansi, Uttar Pradesh, India

A. Gupta · V. K. Patel

Mechanical Engineering Department, G. B. Pant Institute of Engineering and Technology,  
Pauri, Garhwal, Uttarakhand 246194, India

B. Gangil (✉) · L. Ranikoti

Mechanical Engineering Department, H.N.B. Garhwal University, Srinagar Garhwal 246174,  
Uttarakhand, India

e-mail: [brijeshgangil@gmail.com](mailto:brijeshgangil@gmail.com)

© Springer Nature Singapore Pte Ltd. 2019

J. K. Katiyar et al. (eds.), *Automotive Tribology*, Energy, Environment, and Sustainability,  
[https://doi.org/10.1007/978-981-15-0434-1\\_3](https://doi.org/10.1007/978-981-15-0434-1_3)



### 3.1 Introduction

Research, development, and progress of natural or lignocelluloses fibres are supporting eco-system, which leads to positive changes that can be seen in socio-economic development for cultivation and farming. Natural and lingo-cellulosic fibre has been potentially explored in the polymer composite for long since. Plants, crops, and pods from agricultural sources are some viable natural sources for polymer composite industries. To increment the utilizations of renewable and biodegradable materials for ecological safety towards a greener society, the application of natural fibres in the industries as bio-filler/reinforcement materials in composites are the economic issues and are highly preferable factors in the design of automotive parts. For the past decade, various industries are endeavoring to replace synthetic fibre with natural fibre as reinforcements in polymer composite for the development of sustainable composite. Fibres which obtained from the plant or extracted from animals are known as natural fibres. Natural fibres have comprehensive mechanical and physical properties such as tensile, impact strength, stiffness and low density and good damping (Saba et al. 2014; Peças et al. 2018). Natural fibres are lightweight, low density, economical and eco-friendly in nature and have the potential to replace synthetic fibre in many engineering applications like automobiles, furniture, packaging, and construction. The automobile industry is the most benefited among all the industries because of the development in the natural fibre composite fabricated with different polymers like epoxy, Polypropylene (PP), polyethene (PE), and polyvinyl chloride (PVC). The trend of utilization of natural fibre started in the 1990s in Europe and America are shown in the Fig. 3.1.

Demand for natural fibre based composite evolved from the automotive industry because of the need for low cost and superior quality material in the competitive

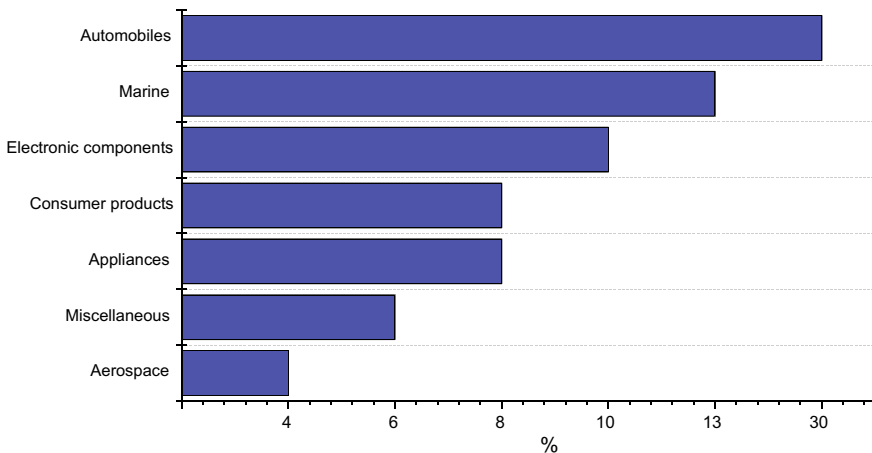
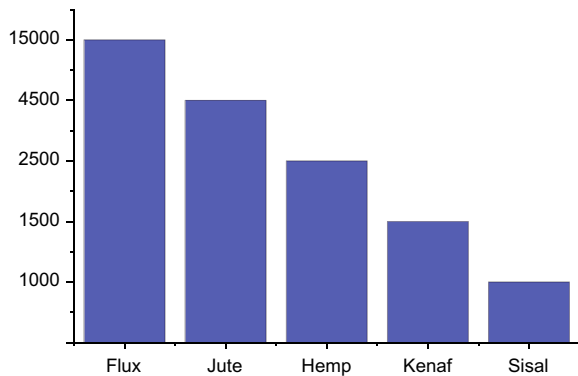


**Fig. 3.1** Contribution of natural fibre in automotive and other sectors (Sherman 1999; Muessig 2002)

world. In this way, the researcher has been trying to increase the renewable resources of raw materials which can be recycled or biodegradable and highly emphasis to reduce petroleum-based synthetics and increase agro-based natural fibres in automotive applications (Ellison et al. 2002). The agro based fibre can reduce the cost of appliances by 20% and weight by 30% (Lan Mair 2000). A market survey found that around 20% of natural fibre is consumed in the automobile sector in North America. German and Austrian automotive industry targeting around 19% increase in the use of natural fibre in the automotive application in 2000, in which major emphasis on the use of jute, hemp and sisal fibre. Around 85% of vehicles are recyclable and reused was targeted by European country at the end of 2015. Toward the development and use of natural fibre, many researchers are working on a combination of matrix material and natural fibre.

Natural fibre composites made up of jute-PP are already in use in German automobile like Vogue to produce different components (Karus and Kaup 2002; Silva et al. 2006). Schuh (Schuh 1999) reported that composites made of natural fibre can be successfully applied in the automotive parts like door panels, rear parcel shelf, seat covering and several damping and insulation parts. Al-Qureshi (Al-Qureshi 1999) fabricated the composites of banana fibre, and analysis shows that they can be a promising material for auto applications. Davoodi et al. (Davoodi et al. 2010) investigated the hybrid composite of kenaf and glass fibre are suggested to be employed in the structural applications of an automobile such as the bumper. Alves et al. (Alves et al. 2010) reported that jute fibre based composite can effectively replace glass fibre for the application of front bonnet of the car. It is found in the survey mostly used natural fibre in tones in the 20th century as shown in the Fig. 3.2.

**Fig. 3.2** Use of natural fibre in the German automotive industry in Tonnes



### 3.2 Applications of Natural Fibre-Reinforced Polymer Composites (NFRC)

As environment friendly, economical and simple to process, NFRPCs have an enormous application region. The automotive industry is the most prominent region of natural fibers apps. Apart from automotive applications there are other areas also where natural fibre can effectively be utilized primarily in health care, fabric packaging, pulp and paper furniture restrictions, electrical equipment, pipes, helmets and transportation. The following different natural fibers and the areas where they can be utilized are:

- Flax use in green wall panels for construction.
- Coir use in making boxes, trays, container for packaging.
- Hemp for bicycles and cases musical instruments panel.
- Balsa, wood for sports.
- Hemp, Jute, Kenaf for automotive and shipping industry.
- Kenaf for Mobile phone casing.
- Wood for modular houses.

### 3.3 Advantages of Natural Fibre-Reinforced Polymer Composites

The natural fibres ousted synthetic fibres in numerous ways such as easily available, low density, low cost, admissible modulus-weight ratio, high acoustic damping, low energy requirement, very less carbon footprint and biodegradable. In comparison to conventional reinforcing fibres such as kevlar and carbon the natural fibres are much cheaper and require low energy for the production. However, natural fibres have a higher variance of mechanical and physical properties, lower durability, lower strength, higher moisture absorption, and lower processing temperature. A comparison of natural and synthetic fibre with respect to cost has been listed in Table 3.1.

Some more attractive properties of natural fibres are their sustainability which makes it environment-friendly. On the other hand, with a business point of view, natural fibres are cheap and keep the economy of the business intact. In addition, some important advantages have been noticed. These are

**Table 3.1** Cost of fibre used in automotive (Huda et al. 2008; Zin et al. 2018)

Fibres	Cost US\$/Ton	Energy GJ/ton
Natural fibres	200–1000	4
Glass fiber	1200–1800	30
Carbon fiber	1250	130

- A low density of natural fibre makes the component around 30% lighter.
- Easily recycled and processed due to the abrasive nature of the natural fibre.
- The satisfactory mechanical property of NFPRCs makes it useful material in non-constructional applications.
- Eliminates the problem of disposal after being used.
- Comparative good mechanical properties like tensile, flexural and impact strength. Good surface finish helps in the construction of better-moulded part.
- High resistance to corrosion.

### 3.4 Disadvantages of Natural Fibre-Reinforced Polymer Composites

Apart from incredible advantages they are certain drawbacks also linked with the usage of natural fibres. Despite being cheap and low weight natural fibres are found to have unstable bonding with various polymers. This instability can be made stable by various surface treatment processes. Somehow prices of composite increases but enhancement of fibre matrix increases which leads to improved physical and mechanical properties. Thus it is worth saying that chemical treatment of fibre is beneficial in the improvement of the fabricated composites. Some most common chemical treatments are Acetylation, Alkalinization, Benzoylation, Silane treatment, Maleated coupling, Peroxide treatment, Permanganate treatment, Isocyanate treatment, Titanate treatment, Plasma treatment, Sodium chlorite treatment etc. (Zin et al. 2018; Kabir et al. 2011; Sanjay et al. 2015).

Regarding the durability, natural fibres are less durable than synthetic fibres with respect to the application of construction. This is due to the chemical absorption and high content of moisture present in the natural fibre. Possibilities of cracks which lead to the swelling and expansion in volume in case of concrete based natural fibre composite. Cementitious material forms the alkaline environment resulted in low interfacial strength between fibre and matrix. The above problem can be avoided by the alkaline treatment of fibre and some other water repelling agents.

### 3.5 Classification of Natural Fibres

Being obtained naturally, natural fibres are categorized in mineral, animal and plant fibres. One of the most important plant fibres is vegetable fibre composed of cellulose, hemicelluloses, and lignin. The main source of vegetable fibres is grass/reed, leaf, seed, fruit, wood, stalk and bast. Plant fibres are highly accepted fibre all over the industries and highly prefer for research point of view. It is due to the fact that plant fibres have a shorter period of growth, availability and renewability (Sanjay et al. 2015) (Fig. 3.3).

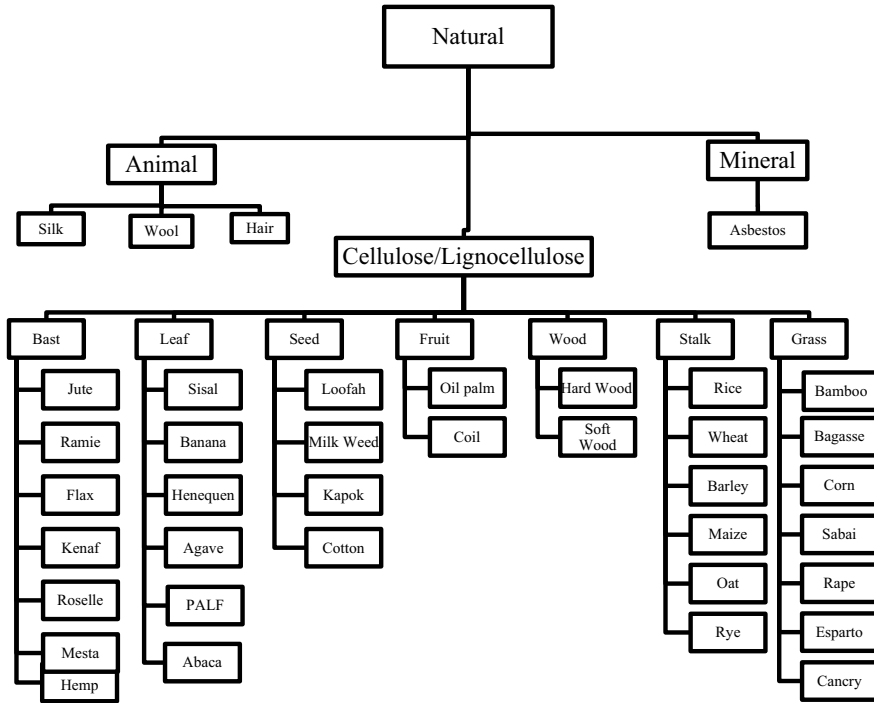


Fig. 3.3 Classification of natural fibre (Sanjay et al. 2015)

### 3.6 Mechanical Testing of Natural-Fibre Composites

The mechanical properties of different natural fiber as shown in Table 3.2.

#### 3.6.1 Tensile Strength of Composite

The main constituents of natural fiber are cellulose, hemicelluloses, pectin, lignin, and waxes. The cellulose molecule in the form of the continuous chain and provide high strength and stiffness to the natural fiber (Mohanty et al. 2005). Generally, the tensile strength and Young’s modulus of natural fibers depends upon cellulose content in natural fiber. The increase in cellulose content of the natural fibers increases the tensile strength and Young’s modulus of natural fiber but the increasing of hemicelluloses content decreases the tensile strength and Young’s modulus of natural fibers (Komuraiah et al. 2014). When the cellulose fibrils are parallel oriented to the fiber axis the natural fiber has high tensile strength, inflexible and high rigidity, if the cellulose fibrils are spiral oriented natural fiber are more ductility. In Table 3.2 is showing the tensile strengths of natural fibers like kenaf, hemp, flax, jute, and sisal,

**Table 3.2** Mechanical properties of natural plant fiber (Mohanty et al. 2005; Mwaikambo 2006)

Fiber type	Fiber	Density (kg/m <sup>3</sup> )	Tensile strength (MPa)	Elongation at break (%)	Young's modulus (GPa)
Bast	Flax	1230	187–773	1.5–3.1	13–26.5
	Hemp	1350	580–1110	1.6–4.5	70
	Kenaf	1200	295–930	2.7–6.9	53
	Ramie	1440	400–938	2–4	61.4–128
Leaf	Sisal	1200	507–885	1.9–3	9.4–22
	Pineapple	1500	170–1627	1–3	34.5–82.5
	Banana	1350	529–914	3–10	8–32
Seed	Cotton	1500–1600	287–587	7–8	7–8
	Coir	1200	175	32	4–7
	Oil palm	700–1500	248	14	3.2
Stalk/grass/wood	Bamboo	800–1400	391–1000	2	11–30
	Bagasse	1200	20–290	1–3	
	Softwood kraft pulp	1500	1000	N.D	40
	Hardwood kraft pulp	1200	950	N.D	37.9
	Wheat straw	1600	273	2.7	4.79–6.58
	Rice straw	1650	449	2.2	1.21–125

are comparatively low than the synthetic fibers like glass and carbon and only bast fibers having better mechanical properties like tensile strength and Young's modulus (Mohanty et al. 2000a). The demand of biodegradable composite increases day by day and biodegradable composite has better mechanical properties than thermo particle polymer (Polypropylene (PP)) composites. The addition of natural fiber in polymer composite affects the tensile strength and Young's modulus of polymer composite. Such as the tensile strength and Young's modulus of Biodegradable polymers (polylactides (PLA)) composites are 62 MPa and 2.7 GPa (Rana et al. 1999) when the addition of 30 wt% flax in PLA decreases the tensile strength from 62.9 to 53 MPa and increases the Young's modulus from 2.7 to 8.3 GPa (Oksman et al. 2003) and the addition of 30 wt% sisal fiber in PLA decreases the tensile strength from 62.9 to 14 MPa and the Young's modulus decreases from 2.7 to 0.7 GPa (Lee and Jang 1999). Therefore, the most of the natural fiber composite used in the automotive, aerospace industry and other industry have a blending ratio of 50:50 wt% for natural fibers because these ratios generate the optimal tensile strengths and Young's modulus. The physical-mechanical properties of natural fibers also depends upon the production method and climatic conditions.

### 3.6.2 Elongation at Break (%)

The natural fibers have ability to resist against the crack formation better than the synthetic fibers. So, elongation at break is considered as an important factor in case of polymer engineering composites. The natural fibers which show weaker strength and Young's modulus have high elongation value. The elongation at break decreases but an increase in Young's modulus when the inclusion of natural fibers and thermoplastics (Mohanty et al. 2005). For improvement in the elongation of fiber, NaOH Surface chemical treatments are required, but it has not beneficial for tensile strength enhancement (Du et al. 2015; Yu et al. 2010). In similar way if we use bagasse contents that improved the percentage elongation and impact strength in the composite and addition of bagasse contents decreases the bending strength and hardness of the material. The elongation of natural fiber is also influence by lignin content when use more lignin content improve the elongation such as leafiran fibers (with 26% lignin) had a greater elongation than kenaf (17% lignin), jute (9% lignin), and pineapple (8.3% lignin) fibers (Agu et al. 2012; Mobasher 2011).

### 3.6.3 Impact Strength

Natural fiber resistance to impact load is described as impact strength. Tests are used in studying the toughness of the material (Ndiyae et al. 2015). Like other mechanical properties, the impact strength of natural fiber increasing with increases in fiber content (Mueller and Krobjilowski 2004). The impact strength of flax fibers is much higher than the other natural fibers (hemp, kenaf) and E glass. Those natural fibers which have high elongation at break it also has ability to absorbed sudden impact. Increasing of the Impact strength of natural fiber is depends on the number layers of fiber and with increment of fiber length but decreases with fiber spacing. The impact strength is also improvement by adequate chemical and physical treatments of natural fibers (Cho et al. 2014). A recent study the toughness of pure polymer composite (such as PLA-based composite and PP based composite) is monotonically decreases by the addition of natural fiber while the addition of natural fiber the presence of cellulose fiber increases of stress concentrations regions that require less energy to elongate the crack propagation potential composite failure (Rana et al. 1998). The impact strength of pure PLA and pure PP are 25 and 29.7 J/m respectively (Fejeskozma and Kargerkocsis 1994) while the addition of bamboo fiber the impact strength are decreases to 19.5 J/m of PLA/bamboo fiber composite and increases to 32.4 J/m of PP/bamboo fiber composite. In study see that when the chemical treated natural fiber is uses the impact strength are improved by 33% (Mueller and Krobjilowski 2003).

**Table 3.3** Stiffness and ultimate stress of different natural fibers (Mohanty et al. 2000; Lilholt and Lawther 2000)

Natural fiber	Fiber type	Stiffness (GPa)	Ultimate stress (MPa)
Hemp	Bast	30–60	300–800
Flax		50–70	500–900
Jute		20–55	200–500
Sisal	Leaf	9–22	100–800
Softwood	Stem	10–50	100–170

### 3.6.4 Flexural Strength

The flexural strength and modulus is also show similar trend as impact strength. The flexural strength and modulus is also depends on fiber length, loading and content. Bast and leaf fibers have the highest flexural strength among all natural fibers, similarly kenaf bast fibers have also higher flexural strength than kenaf core fiber composites (Ishak et al. 2010). The composites whose surfaces are smoother and more homogeneous show the greatest flexural modulus therefore the bleached fiber composites exhibit high flexural properties compared to the untreated bleached fiber composites (Dash et al. 2000). The flexural strength of coir fibers has better than synthetic fibers. The coconut fiber is an excellent reinforcement for polymer concrete, it increasing the fracture and flexural strength. In polymer concrete an increment of 25.1% of coconut fiber and 3.5% bagasse and a decrease of 21% of banana pseudo stem reinforcement have batter flexural strength compared to unreinforced polymer concrete (Reis 2006). The flexural strength and modulus of neat PLA has 98 MPa and 2.6 GPa respectively while the addition of bamboo fiber at 30 wt% the flexural strength decreases to 57 MPa and modulus of elasticity increases to 4 GPa (Mohanty et al. 2002). After addition of wood fibers, there is a growing trend in flexural strength for all the composites. With addition of 30 wt% surface treated fibers, the flexural modulus improves considerably (Mohanty et al. 2000b; Lilholt and Lawther 2000). Stiffness and Ultimate Stress of different natural fibers is shown in Table 3.3.

### 3.6.5 Stiffness

The research in natural fiber proves that lignocellulosic fibers are outstanding in nature of stiffness and strength. Similar to the tensile strength and stiffness of natural fibers is also depending on the cellulose content and spiral angle. Natural Fibers those have high cellulose quantity have been found outstanding mechanical properties. Lignin contents also affects the stiffness properties of natural fibers and how it is implanted in cell structure. Due to excellent stiffness properties of natural are used as filler it's improved the stiffness of the composites (Faruk and Sain 2015). Due to low density of natural plant fibers, the specific properties, strength, and stiffness



of natural fibers are comparable to the values for glass fibers. The Microfibrillar angle is a important factor for stiffness of the natural fibers. The stiffness is directly proportional to Microfibrillar angle. At small Microfibrillar angle ( $<5^\circ$ ), stiffness is 50–80 GPa, and at large Microfibrillar angle ( $40^\circ$ – $50^\circ$ ), stiffness is reduced up to 20 GPa (Page et al. 1977). Strong interactions between the coupling agent and the natural fiber hydroxyl groups are needed to overcome the problem incompatibility problem to increase impact, tensile, and flexural strengths of natural-fiber reinforced composites.

### 3.6.6 Dynamic Mechanical Analysis

Study of response of material to sinusoidal stress is called as Dynamic mechanical analysis (DMA). DMA characteristics of polymer composites are fairly comparable to metals like steel, aluminum and other composite materials (Gupta and Bharti 2017). Thermo Gravimetric Analysis (TGA), Differential Scanning Calorimetry (DSC) and Thermal Mechanical Analysis (TMA) are some of the analysis that can be carried out using DMA. Storage modulus, damping and  $\tan \delta$  are some of the characteristics that can be calculated using DMA. Incorporation of 30% natural fiber to polymer matrix lead to increase in the storage modulus and damping characteristics of the polypropylene composite (Rana et al. 1999; Tajvidi et al. 2006). Modulus decreases only in the case of softening of composite at higher temperature.

The dynamic mechanical properties of neat Polypropylene and the composites with different natural fibers (Wood, Kenaf, Rice Hulls and Newsprint) of 25% shown in Table 3.4 and compared with the pure plastic. As seen in the table all different composites had higher storage and loss modulus values compared with pure Polypropylene, whereas their damping was lower. Therefore, Polypropylenes/natural fiber composite behave more elastically than their pure Polypropylene. Polypropylenes/Kenaf fiber composite show highest storage modulus values and lowest mechanical loss factor and Polypropylenes/Rice Hull composite show lowest storage modulus values and highest mechanical loss factor which indicating better reinforcement efficiency all over the all temperature range ( $-60^\circ\text{C}$ ,  $-20^\circ\text{C}$ ,  $0^\circ\text{C}$ ,  $+20^\circ\text{C}$ ,  $+60^\circ\text{C}$ ). As like all mechanical properties DMA is also improved by increasing fiber content (Tajvidi et al. 2006).

**Table 3.4** Dynamic mechanical analysis of natural fiber (Rana et al. 1999; Tajvidi et al. 2006)

S. No.	Composite	Storage modulus	Loss modulus	$\tan \lambda$
1.	Neat PP	2.9	0.163	0.055
2.	PP/wood flour	3.126	0.189	0.060
3.	PP/kenaf fiber	3.002	0.173	0.058
4.	PP/rice hulls	2.595	0.166	0.064
5.	PP/newsprint	3.046	0.180	0.060

### 3.7 Applications in the Automobile Sector

#### 3.7.1 Interior Components

Interior and an exterior component can be easily manufactured by natural fibre composite (Dash et al. 2000). These are door cladding, seatback lining and in making the space at the back of the rear seat in the sedan i.e. package shelves. Coconut fibre is employed in making of the bottom of seats, cushions and cushion for head support. In automobiles approximately 10–15 kg of natural fibre is used. Figure 3.4 shows the integration of the natural fibre for the automobile application.

Press moulded panels are used to reduce the weight and the cost by using some natural fibres such as hemp, sisal and flax. These are used for an interior application like trimming the door, hear lining, trunk lining etc. Mainly all over the world, manufacturers are using natural fibre in the application of automobiles. Henry Ford first started the manufacturing of hemp fibre composite for the automobile parts in 1940. On the perspective of the automobile industry, the hemp fibres have significant advantages such as lower fuel consumption, lightweight, reduction in waste disposal,

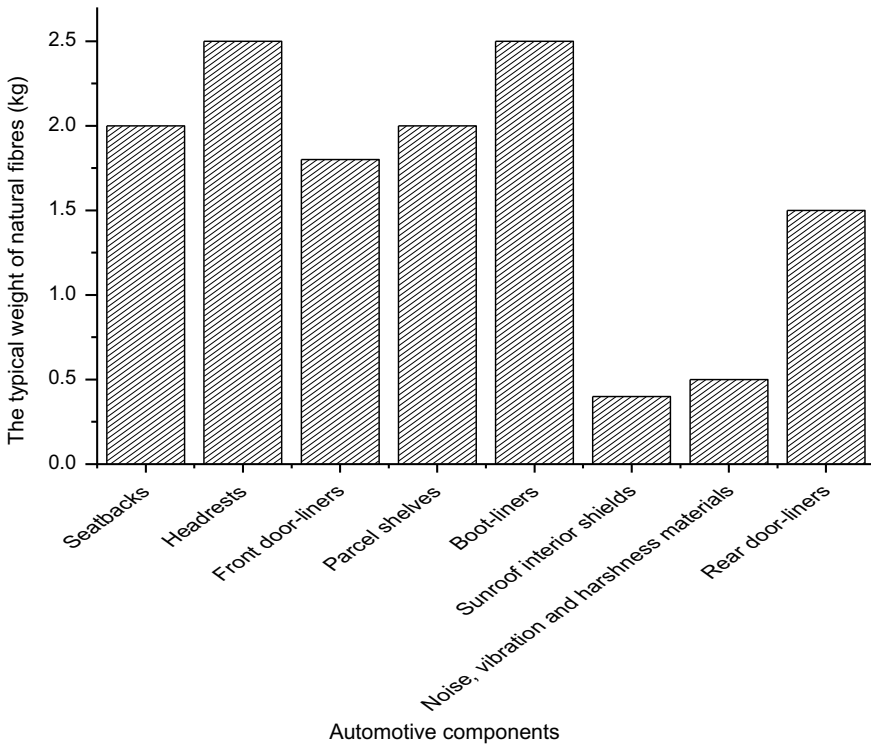
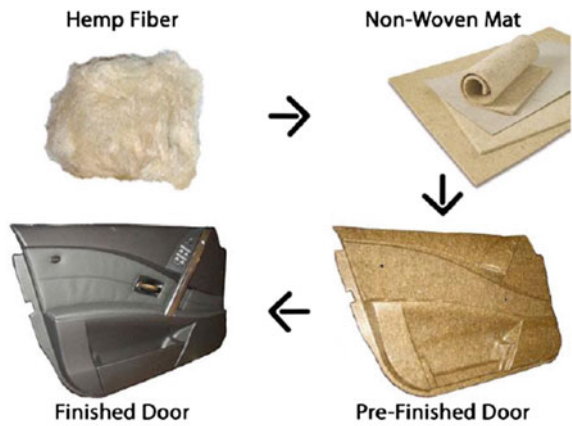


Fig. 3.4 Inclusion of the weight of natural fibre in automotive components

good recycling possibilities and greenhouse emissions. The use of hemp fibre reduces the cost of the automotive part by 20% and a weight reduction of 30% is achieved. Hemp fibre composites are mostly being used for interior parts such as door panels, dashboards, parcel shelves, backrest, seat cushions and cabin linings. Hemp fibre also helps to produce biofuel as an alternative to petroleum-based fuel for the automobile. The stalk and leaves of the hemp plant can be used to produce a cheap and renewable biofuel (Reis 2006) (Fig. 3.5).

Automotive manufacturers have adopted in their new models Natural Fiber Reinforced Polymer Composites NFRPC for interior and exterior vehicle parts such door panels, package trays, trunk liners, seat backs, boot lining, hat rack, spare tyre lining, headliner panel, boot lining, noise insulation panels, molded foot well linings, door trim, Interior door paneling, windshield, dashboard, back cushions, parcel shelf, insulation, rear storage shed, door trim panels (PP matrix with NF), engine or transmission cover side and back, spare wheel compartment cover (Suddell and Evans 2005) (Figs. 3.6 and 3.7).

**Fig. 3.5** Interior door finishing by Hemp fibre (Reis 2006; Dash et al. 2000)



**Fig. 3.6** Coconut coir reinforced PP use for stirring wheel (Witayakran et al. 2017)



**Fig. 3.7** NFRPC use as Seat cover (Witayakran et al. 2017)



NFRPC are a composite material fabricated by a polymer matrix embedded with high-strength natural fibres, like jute, oil palm, sisal, kenaf and flax. NFRPC occupy several industrial areas that prove the perspective of natural fibres as replacements for their synthetic part (Fogorasi and Barbu 2017). Daimler Benz in Germany has also been using natural fibres based composite since 1994. 50 components of Mercedes-Benz E-class are now been made by using various natural fibres such as sisal, flax, hemp, wool and many more. Daimler Benz is also replacing glass fibre with the wide range of natural fibres as European hemp, sisal, flax by using them as reinforcing fibre in polypropylene components. By using the natural fibres like abaca and hemp, Daimler Chrysler increased the use of renewable materials in many vehicles. 27 components have been made by natural fibre composites which are now been used in newest Mercedes S-class vehicle weighing 43 kg.

BMW uses a large number of renewal resources along with 1000 tonnes of the natural fibre. Each BMW 7-series car consists of 24 kg of renewable material with various natural fibres such as hemp, sisal, flax and wool. The mixture of flax and kenaf is used in door panels inserts and package trays for Saturn L300s.

Biodegradable plastic is furnished by Toyota mainly consist of starch obtained from sweet potatoes and other plants. These plastics along with the natural fibre used for garnishing the ES3 concept car's pillars. Lexus package shelves are being made by Kenaf fibre. It is also induced into the body structure of Toyota including I unit concept vehicles. Kenaf fibre imported from Bangladesh obtained from Kenaf reinforced PP composite is used in door panels of the Mondeo model by Ford Motors (Bledzki et al. 2006).

Flex form of fibre which provides better mechanical properties and obtained from natural fibre such as jute, hemp, flax and thermoplastic matrix materials such as PP & PE is used over wool fibres reinforced thermoplastic as they cause 25% strength improvement. Companies named MN, Winona and composite product Inc (CPI) produce composites of flax & PP, as used for Pickups and SUV's field testing was done for instrument panels, door panels and package shelves. For the door panels,

Findlay Industries got 4-star dynamic rating as door panels are made up from LoPref in PP/PET/natural fibre composite. First natural fibre to meet stringent specification was the panels appeared in 9S and 99 Saab. VolcaLite is manufactured by reinforced natural fibre. GMT lite products are made with PP reinforced long chopped basalt fibre (Figs. 3.8 and 3.9).

It provides better chemical resistance, high modulus and more service temperature than glass fibres. It is widely encouraged to replace carbon fibre and glass fibre in composites. VolcaLite causes a 50% reduction compared to GMT product and lowers down ultra thin profile to 3 mm. currently, it is being utilized by Tier-1 Automotive suppliers. Cambridge industries are producing flax/PP composite for Freightliner century COE C-2 heavy trucks.

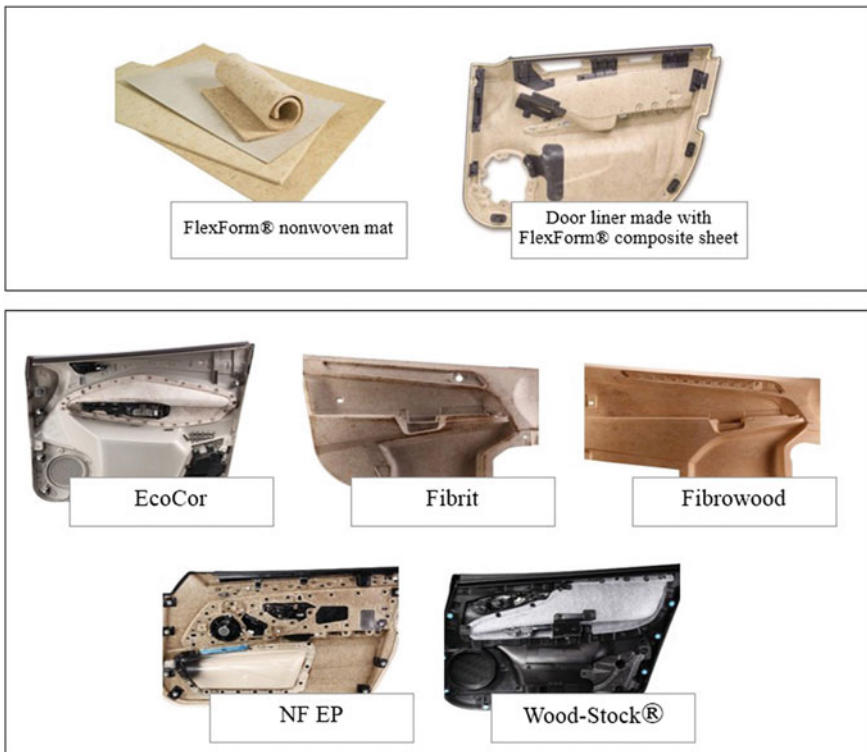


**Fig. 3.8** Interior applications of natural fiber composites products by FlexForm Technologies (above) and Johnson controls (below) (Witayakran et al. 2017)

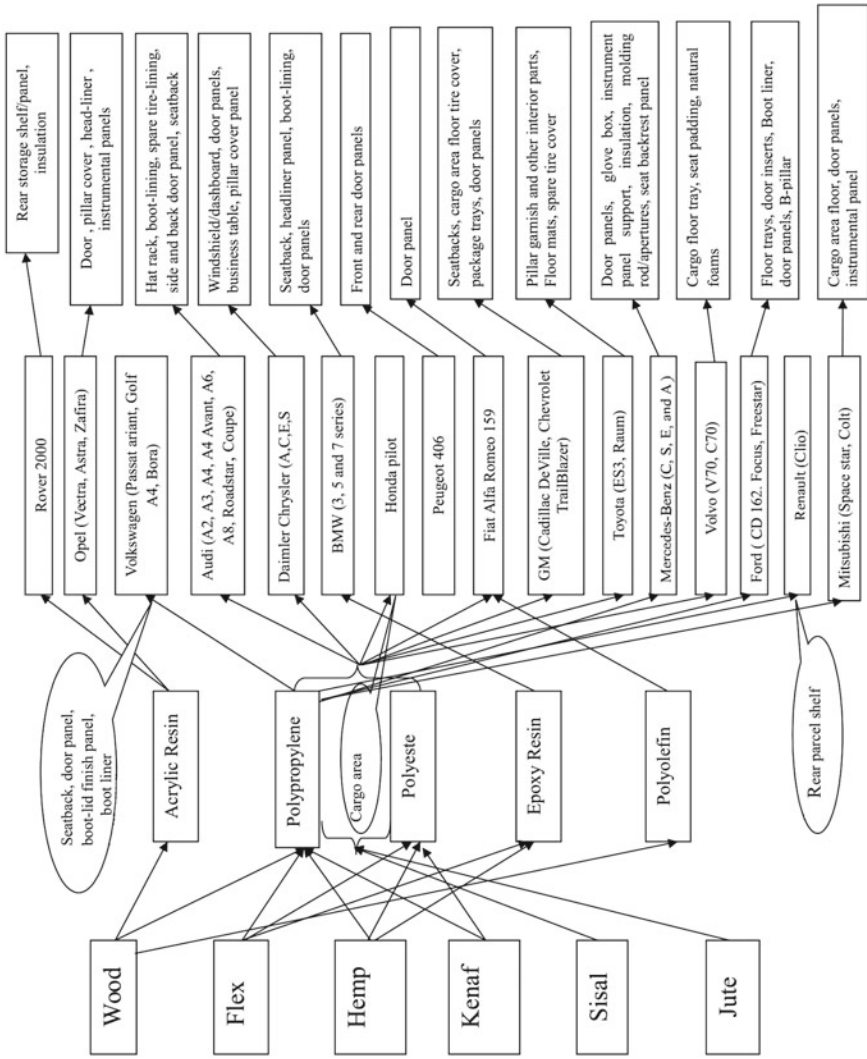


Fig. 3.9 Natural fiber and their use in automobile sector (Witayakran et al. 2017)

### 3.7.2 Exterior Components

To meet the standard of performance of automotive such as door and trim components, bumpers etc., high-performances in along with natural fibre with suitable additives are used. But due to moisture absorbing capacity, their use as the exterior component is restricted. For the application of seat cushions only, the property of water absorption should be taken into account. Due to this reason, the use of these fibres are restricted to inner parts only (Promper 2010; Thomas 2008; Hintermann 2005). However research is under process to use natural fibres as exterior components.

In Mercedes A class an application of Abaca fibres developed by Daimler Chrysler is used for under floor paneling. These fibres are extremely elastic with better tensile strength. Similarly, Mercedes Benz is using flax fibres for the manufacturing the component of Travego (Suddell 2003).

## 3.8 Limitations

Change in the property of natural fibre has been the major drawback of natural fibre reinforced polymer composites. Due to the production of these fibres throughout the world, they have different geographical, different historical and different routes for production and processing, moisture absorbing capacity to a large extent. This limits their applications as exterior components in automobiles (Puglia et al. 2004). Deterioration and dimension stability due to the ingress of moisture is a major drawback of natural fibres. The lower temperature required for processing of natural fibre is one of the major limitations of natural fibre composites because of volatile emission and fibre degradation that may affect composite properties. So the working temperature of natural fibre is limit to 200 °C. Another drawback of natural fibre includes low microbial resistance and high moisture absorption. However, the fair amount of adhesion lowers the amount and rate of water absorption in the interface region of the composite. By encapsulation and good fibre-matrix bonding, the moisture absorption could be reduced. By the acetylating process of hydroxyl group present in fibre, its moisture absorption can also be reduced [57]. Another demerit is the variable range of prices as compared to synthetic fibres such as glass fibres. The cost of flax is increasing consistently but the price of glass fibre is stable for last many years. So cost analysis must be made to avoid this problem.

## 3.9 Conclusions

Most of the bulk material used in the automotive sector has its harmful impacts on the environment and human beings. The new technology and composite are seen as a viable solution to reduce the environmental effects as well as increase the efficiency

of the automobile. The green composites used in the automotive industry largely focus on reducing the fuel consumption, production of lighter equipments and use of low-polluting vehicles. The advancements in the areas of these nanotechnologies have been diverse and manifold. They show diversity from pollution-sensing, and reduction, energy conservation, interior cooling, power train, lightweight construction, surveillance control up to recycle potential, wear reduction and driving dynamics, etc. They also add novel and eco-efficient functionalities to the traditional construction materials.

Natural fibres polymeric composites emerge as a fruitful way to enhance the quality of components of automobile with respect to the economic and technical feasibility safety and environment. Owing to their qualities that include being eco-friendly, light weight, low-cost, resistance to corrosion and being biodegradable among others. Natural fibres polymeric composites is being extensively used in automobile parts such as door panels, seat back panels, door bolsters, side and back walls, headliners, seat backs, car seat covers and mattresses, wrapping paper, rugs, doormats, and many more areas. Also, it not only reduces the automobile cost by around 20–30% but also increases the fuel efficiency by around 20%.

## References

- Agu CV, Njoku OU, Chilaka FC, Okorie SA, Agbiogwn D (2012) Physico-chemical characterization of lignocellulosic fibre from *Ampelocissus cavicaulis*. *Int J Basic Appl Sci* 12(3):68–77
- Al-Qureshi HA (1999) The use of banana fibre reinforced composites for the development of a truck body. In: Second international wood and natural fibre composites symposium, Kassel/Germany, pp 1–8
- Alves C, Silva AJ, Reis LG, Freitas M, Rodrigues LB, Alves DE (2010) Ecodesign of automotive components making use of natural jute fiber composites. *J Clean Prod* 18(4):313–327. <https://doi.org/10.1016/j.jclepro.2009.10.022>
- Bledzki AK, Faruk O, Sperber VE (2006) Cars from bio-fibres. *Macromol Mater Eng* 291(5):449–457
- Cho D, Kim HJ, Drzal TL (2014) Surface treatment and characterization of natural fibers: effects on the properties of biocomposites. In: Sabu T, Kuruvilla J, Malhotra SK, Goda K, Sreekala MS (eds) *Polymer composites, biocomposites*, vol 3. Wiley-VCH, pp 133–178
- Dash BN, Rana AK, Mishra HK, Nayak SK, Tripathy SS (2000) Novel, Low-cost jute-polyester composites II: SEM observation of the fractured surfaces. *Polym-Plast Technol Eng* 39:333–350
- Davoodi MM, Sapuan SM, Ahmad D, Ali A, Khalina A, Jonoobi M (2010) Mechanical properties of hybrid kenaf/glass reinforced epoxy composite for passenger car bumper beam. *Mater Des* 31(10):4927–4932. <https://doi.org/10.1016/j.matdes.2010.05.021>
- Du Y, Yan N, Kortschot MT (2015) The use of ramie fibers as reinforcements in composites. In: Faruk O, Sain M (eds) *Biofiber Reinforcement in Composite Materials*, Woodhead Publishing Series in Composites Science and Engineering, vol 5, pp. 104–137
- Ellison GC, McNaught R, Eddleston EP (2002) The use of natural fibers in nonwoven structures for applications as automotive component substrates. Research Report, Ministry of Agriculture Fisheries and Food, UK
- Faruk O, Sain M (2015) *Biofiber reinforcement in composite materials*. Woodhead Publishing, Cambridge



- Fejeskozma Z, Kargerkocsis J (1994) Fracture-mechanical characterization of a glass- fiber mat-reinforced polypropylene by instrumented impact bending. *J Reinf Plast Comp* 13(9):822–834
- Fogorasi MS, Barbu I (2017) The potential of natural fibers for the automotive sector—review. In: IOP conference on series: materials science and engineering 252:012044. <https://doi.org/10.1088/1757-899x/252/1/012044>
- Gupta MK, Bharti A (2017) Natural fibre reinforced polymer composites: a review on dynamic mechanical properties. *Current Trends in Fashion Technology & Textile Engineering* 1(3):555563. <https://doi.org/10.19080/CTFTTE.2017.01.555563>
- Hintermann M (2005) Automotive exterior parts from natural fibers, RIKO-2005. Hannover, Germany
- Huda MS, Drzal LT, Ray D, Mohanty AK, Mishra M (2008) Natural-fiber composites in the automotive sector. In: Properties and performance of natural-fibre composites. Woodhead Publishing, Oxford. ISBN 9781845692674.1
- Ishak MR, Leman Z, Sapuan SM, Edeerozey AMM, Othman IS (2010) Mechanical properties of kenaf bast and core fibre reinforced unsaturated polyester composites. *Mater Sci Eng* 11(1):1–6. <https://doi.org/10.1088/1757-899X/11/1/012006>
- Kabir MM, Wang H, Aravinthan T, Cardona F, Lau K-T (2011) Effects of natural fibre surface on composite properties: a review. *Energy Environ Sustain* 2011:94–99
- Karus M, Kaup M (2002) Natural fibres in the European Automotive Industry. *J Ind Hemp* 7(1):119–131. [https://doi.org/10.1300/J237v07n01\\_10](https://doi.org/10.1300/J237v07n01_10)
- Komuraiah A, Shyam Kumar N, Durga Prasad B (2014) Chemical composition of natural fibers and its influence of their mechanical properties. *Mech Compos Mater* 50(3):359–376
- Lan Mair R (2000) Tomorrow's plastic cars, ATSE Focus no. 113
- Lee NJ, Jang J (1999) The effect of fiber content on the mechanical properties of glass fiber mat/polypropylene composites. *Compos A* 30:815–822
- Lilholt H, Lawther JM (2000) Natural organic fibres. Chapter 10. In: Kelly A, Zweben C (eds) *Comprehensive composite materials*. Elsevier Science, pp 303–325
- Mobasher B (2011) *Mechanics of fiber and textile reinforced cement composites*. CRC Press, New York, p 562
- Mohanty AK, Misra M, Hinrichsen G (2000a) Biofibers, biodegradable polymers and biocomposites: an overview. *Macromol Mater Eng* 276(277):1–2
- Mohanty AK, Misra M, Hinrichsen G (2000) Biodegradable polymers and biocomposites: an overview. *Macromol Mater Eng* 276/277:1–25
- Mohanty AK, Misra M, Drzal LT (2002) Sustainable bio-composites from renewable resources: opportunities and challenges in the green materials world. *J Polym Environ* 10(1–2):19–26
- Mohanty AK, Misra M, Drzal T (2005) *Natural fibers, biopolymers, biocomposites*. CRC Press, New York
- Mueller DH, Krobjilowski A (2003) Improving the impact strength of natural fiber reinforced composites by specifically designed material and process parameters. *Int Nonwovens J* 12(2):31–38
- Mueller DH, Krobjilowski A (2004) Improving the impact strength of natural fiber reinforced composites by specifically designed material and process parameters. *Int Nonwovens J* 13(4)
- Muessig J (2002) Influence of fiber fineness on the properties of natural fiber composites. In: Proceedings 4th international wood and natural fiber composites symposium, Kassel/Germany, 10–11 Apr 2002
- Mwaikambo LY (2006) Review of the history, properties and application of plant fibres. *Afr J Sci Technol (AJST) Sci Eng Ser* 7:120–133
- Ndiyae D, Gueye M, Thiandoume C, Badji AM, Tidjani A (2015) Reinforcing fillers and coupling agents' effects for performing wood polymer composites. Chapter 12. In: Thakur VJ, Kessler M (eds) *Green biorenewable biocomposites: from knowledge to industrial applications*. CRC Press, Boca Raton
- Oksman K, Skrifvars M, Selin JF (2003) Natural fibers as reinforcement in polylactic acid (PLA) composites. *Compos Sci Technol* 63:1317–1324

- Page DH, El-Hosseiny F, Winkler K, Lancaster APS (1977) Elastic modulus of single wood pulp fibers. *Tappi* 60:114–117
- Peças P, Carvalho H, Salman H, Leite M (2018) Natural fibre composites and their applications: a review. *J Compos Sci* 2:66. <https://doi.org/10.3390/jcs2040066>
- Promper E (2010) Natural fibre reinforced polymers in automotive interior applications. In: Mussig J (ed) *Industrial applications of natural fibres: structure, properties and technical applications*. Wiley, Chichester, pp 423–436
- Puglia D, Biagiotti J, Kenny JM (2004) A review on natural fiber-based composites Part II: application of natural reinforcements in composite materials for automotive industry. *J Nat Fibres* 1(3):23–65
- Rana AK, Mandal A, Mitra BC, Jacobson R, Rowell R, Banerjee AN (1998) Short jute fiber-reinforced polypropylene composites: effect of compatibilizer. *J Appl Polym Sci* 69:329–338
- Rana AK, Mitra BC, Banerjee AN (1999) Short jute fiber-reinforced polypropylene composites: dynamic mechanical study. *J Appl Polym Sci* 71:531–539
- Reis JML (2006) Fracture and flexural characterization of natural fiber-reinforced polymer concrete. *Constr Build Mater* 20(9):673–678
- Saba N, Tahir PMd, Jawaid M (2014) A review on potentiality of nano filler/natural fiber filled polymer hybrid composites. *Polymers* 6:2247–2273. <https://doi.org/10.3390/polym6082247>
- Sanjay MR, Arpitha GR, Yogesha B (2015) Study on mechanical properties of natural glass fibre reinforced polymer hybrid composites: a review. *Mater Today Proc* 2:2959–2967
- Schuh TG (1999) Renewable materials for automotive applications. Daimler-Chrysler AG, Stuttgart
- Sherman LM (1999) Natural fibers: the new fashion in automotive plastics. *Plast Technol Online* 10
- Silva RV, Spinelli D, Bose Filho WW, Claro Neto S, Chierice GO, Tarpani JR (2006) Fracture toughness of natural fibers/castor oil polyurethane composites. *Compos Sci Technol* 66(10):1328–1335. <https://doi.org/10.1016/j.compscitech.2005.10.012>
- Suddell B (2003) The current situation and future outlook for natural fibers within the automotive industry, Joint Meeting of the Intergovernmental Group on Hard Fibers and on Jute; Kenaf and Allied Fibers. Salvador, Brazil
- Suddell BC, Evans WJ (2005) Natural fiber composites in automotive applications. In: Mohanty AK, Misra M, Drzal LT (eds) *Natural fibers, biopolymers and biocomposites*. CRC Press, New York, p 113
- Tajvidi M, Falk RH, Hermanson JC (2006) Effect of natural fibers on thermal and mechanical properties of natural fiber polypropylene composites studied by dynamic mechanical analysis. *J Appl Polym Sci* 101:4341–4349
- Thomas GS (2008) Renewable materials for automotive applications. Daimler Chrysler AG, Stuttgart
- Witayakran S, Smitthipong W, Wangpradid R, Chollakup R (2017) Natural fiber composites: review of recent automotive trends. <https://doi.org/10.1016/b978-0-12-803581-8.04180-1>
- Yu T, Ren J, Li S, Yuan H, Li Y (2010) Effect of fiber surface-treatments on the properties of poly(lactic acid)/ramie composites. *Compos A Appl Sci Manuf* 41(4):499–505
- Zin MH, Abdan K, Mazlan N, Zainudin ES, Liew KE (2018) The effects of alkali treatment on the mechanical and chemical properties of pineapple leaf fibers (PALF) and adhesion to epoxy resin. *IOP Conf Ser Mater Sci Eng* 368:012035

# Chapter 4

## Future of Metal Foam Materials in Automotive Industry



Ankur Bisht, Vinay Kumar Patel and Brijesh Gangil

**Abstract** With the growing industrial development and reliance on fossil fuels, green house gas emission has become a major problem. Transportation plays a massive role in producing CO<sub>2</sub> gas emission with personal vehicles producing the largest share. Light weighting is a possible solution of reducing the CO<sub>2</sub> gas emissions. On an average, 100 kg of mass reduction achieved on a passenger car saves about 9 g of CO<sub>2</sub> per km at the car exhaust. Some lightweight materials are already being used in automobile sector such as aluminum, magnesium, their alloys, composite materials, etc. A novel category is metal foams, which are one of the metal matrix composites, having uniformly distributed gaseous pores as reinforcement embedded in the metal matrix. A high porosity in metal foams makes them potential candidates to absorb the large amount of mechanical energy, damping vibrations and ability of sound absorption which can be well exploited in automotive industry. As per requirement in different sectors, metal foam of different metals has been developed like Al, Mg, Fe, etc. Based on the porosity of metal foams, they have found their applications in the functional and structural field. This book chapter emphasizes on the recent development in the field of metal foams, mechanical properties, which can be exploited in the automotive industry, processing method and also gives the overview of existing and as well as the potential field where these novel material can be utilized.

**Keywords** Metal foam · Structural application · Energy absorption characteristic

---

A. Bisht · B. Gangil (✉)

Department of Mechanical Engineering, S.O.E.T., H.N.B,  
Garhwal University Srinagar, Garhwal 246174, Uttarakhand, India  
e-mail: [brijeshgangil@gmail.com](mailto:brijeshgangil@gmail.com)

V. K. Patel

Mechanical Engineering Department, Govind Ballabh Pant Institute of Engineering and  
Technology, Pauri, Garhwal 246194, India

© Springer Nature Singapore Pte Ltd. 2019

J. K. Katiyar et al. (eds.), *Automotive Tribology*, Energy, Environment, and Sustainability,  
[https://doi.org/10.1007/978-981-15-0434-1\\_4](https://doi.org/10.1007/978-981-15-0434-1_4)

## 4.1 Introduction

Metal foams are the cellular solids in which the gaseous pores are integrated uniformly in their structures. Metal foam is one of the hottest developing topics among the researchers due to their interesting combinations of physical and mechanical properties, such as high stiffness to weight ratio or high gas permeability combined along with high thermal conductivity. Though, the development of metal foam as engineering application started in near the beginning of 20th century when filters, batteries and self lubricated bearings were manufactured by sintered powder and meshes but the first patent on metal foam was registered by a French in 1925 (Nils-son 2007; Meller 1925). The commercialization started three decades later in USA, where some quality research was obtained for about 10 years as a recent development on metal foams. But the great surge of research and development started from 1996 when USA launched Multidisciplinary Research Initiative on Ultralight Metals (MURI) which helped in funding the projects focused on cellular metals (Banhart and Weaire 2002).

Nature has also developed cellular material like wood, bones etc. Man made cellular materials which is frequently used are polymeric foams having great variety of applications. Metals and alloys are also being converted in foam are less known (compare to polymer foams), which can produce interesting structural and functional applications in the near future. The need behind the development of metal foam is their unique set of physical and mechanical properties such as high strength to weight ratio, low thermal conductivity, good electric insulating properties, non inflammability, high gas permeability, high impact energy absorption, sound absorbing capacity etc. The produced metal foam can find suitable application as light weight construction material in automotive, naval and aerospace field. Moreover, it can be suitable in producing heat exchanger, silencers, fire arresters, filters, bullet proof jackets, heat radiators, structured templates and supports, electrode muffling devices etc. (Banhart 2001, 2003, 2005; Davis and Zhen 1983; Stöbener et al. 2005; Chen et al. 2011; Sanz et al. 2008; Wang et al. 2011; Xu et al. 2008; Hong and Herling 2006; Gomez Alvarez-Arenas and Gonzalez Gomez 2007).

On the basis of structure, metal foam can be divided in three categories closed cell, open cell, combination of both and lotus type. As the name suggests close cell metal foam are such type of structures in which the pores are completely enclosed by thin layer of metallic wall, while open cell structures have unified pores. The third type is a novel development in which there are long cylindrical pores aligned in one direction (Hyun et al. 2001; Hyun and Nakajima 2003; Simone and Gibson 1997). The close cell metal foam finds suitable application in structural load-bearing applications, while open porosity is used in functional field where load bearing is not a primary goal. In last three decades different metals and alloys foams have been developed like Al, Al-Zn (Bisht and Gangil 2018; Bisht et al. 2019), Al-Mn (Xia et al. 2013), Zn (Banhart et al. 2001), Cu (Zhao et al. 2005; Irretier and Banhart 2005; Park and Nutt 2001), Pb (Park and Nutt 2000), Fe, Steels (Park and Nutt 2001; Ikeda et al. 2005), Mg, Ti (Wuebben et al. 2000), Ti-5W alloy foams (Hyelim et al. 2017),

Al–Si, Ni<sub>3</sub>Al (Bart-Smith et al. 1998), Al–Cu, MMCs, open-cell Al–Mg/Al<sub>2</sub>O<sub>3</sub> and Al–Mg/SiC–Al<sub>2</sub>O<sub>3</sub> composite prefoams (Sharifi et al. 2017), foamed-copper reinforced composites (Ji et al. 2014) etc. Among these wide varieties of metal foam Al has gained tremendous interest and is being developed by different industries through different trade name like Alporas, Alulight, Cymat, Duocel etc.

Being a multifunctional property material, the research in all directions covering, material processing, mechanism of foam development, enhancing the desired properties, searching suitability in different applications and the development of predictive models for foaming process are being conducted by researchers. This article is devoted towards the development in the field of processing techniques, characterization and applications of close cell Aluminum metal foam.

### 4.2 Production Methods of Close Cell Metal Foams

There are several techniques to manufacture the metal foam. The fundamental idea for foam production is to produce uniform pores throughout the metal matrix. In this article classification is based on gas source used for foams production. Different processing methods are summarized in Fig. 4.1.

In this article the focus will be given on the techniques which are used worldwide commercially.



Fig. 4.1 Processing method of metal foam based on gas source used

### 4.2.1 *Blowing Agent Techniques*

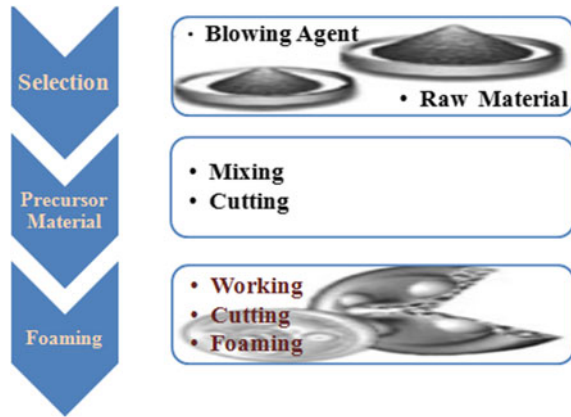
A blowing agent is a substance which is capable of producing a cellular structure via a foaming process for variety of material that undergo hardening or phase transition. They are typically applied when the blown material is in a liquid stage. Generally the foaming agents must undergo thermal decomposition and generate gas pressure in the matrix sufficient to overcome atmospheric pressure and cause foaming (Li et al. 2012). Blowing agents preferably decomposes with liberation of gases, these generated gases should be virtually insoluble in the matrix and the corrosive gases should be avoided from the decomposition products. Blowing agents have different decomposition temperature. The temperature required for the foaming has to be slightly above the liquids temperature of the used alloy. Generally hydrides and carbonates are used as blowing agents.  $\text{TiH}_2$ ,  $\text{ZrH}_2$ ,  $\text{MgH}_2$  etc. are hydrides, generally used in low melting point metals. On the other hand  $\text{CaCO}_3$ ,  $\text{SrCO}_3$ ,  $\text{MgCO}_3$  etc. are used in high melting point base metals. The melting behavior and decomposition characteristic of the blowing agent must be coordinated to obtain good quality foam. If the general conditions are met and heating and cooling are properly controlled, the foam with acceptable porosity can be produced. The processes based on blowing agent are melt route and powder metallurgy method.

### 4.2.2 *Powder Metallurgy Technique (Trade Name—Alulight)*

The fundamental idea is to use the metal in powder form so called as powder metallurgy technique but the final expansion occurs in liquid state. In the process metal powders or alloy powders with blowing agent are uniformly mixed which are then compacted to get a yield semi-finished product. Compaction is completed generally by iso-static compression, rod extrusion or powder rolling method (Baumeister 1990; Baumeister and Schrader 1991; Weber et al. 1997; Yu et al. 1998). The care has to be taken to produce semi finished precursor in which blowing agent is uniformly embedded without any residual porosity. Now in which form the final shape is needed, semi finished precursors are converted through rolling process. Heat treatment process near the melting point of matrix material is the last step, where the blowing agent which is distributed uniformly in matrix decomposes and releases gas which applies the force on the compressed precursor to form highly porous structure (Fig. 4.2).

Aluminium alloys foams. For steels, carbonates are well suited due to their high decomposing temperature (Irretier and Banhart 2005; Park and Nutt 2000, 2001).  $\text{SrCO}_3$  is most frequently used as blowing agent in production of such foams. (Park and Nutt 2001, 2002). A content of less than 1% is sufficient for using metal hydrides as blowing agent. The method is generally used for producing foam of tin, zinc, brass, lead, gold and some other metals and alloys by selecting correct blowing agents with appropriate process parameters (Banhart 2001). Fraunhofer-Institute in Bremen (Germany) developed this technique for producing PM precursor with blowing agent

**Fig. 4.2** Powder metallurgy process



or sintering of hollow spheres. So 'Foaminal' is other trade name for such products. Foaminal are integral metal foams with a closed cell structure and a closed surface. (Baumeister 1992, 1996; Baumeister et al. 1996, 1997; Fraunhofer-Institute Bremen 1999).

### 4.2.3 Melt Route Method (Trade Name—Alporas)

This method is also known as casting method, in which metal or metal alloy is melted in crucible where viscosity enhancer is added at 680 °C between 2 and 3%. The viscosity enhancer generally used are liquid metal matrix composites (MMCs) containing 10–20 vol% particles (typically 10 μm silicon carbide or alumina particles), 5% of 70 nm SiC, 4 wt% of TiC particles (200–1000 nm), Ca metal between 2 and 3%. Viscosity enhancer is used to enhance the viscosity which adhere on metal interface and prevent pore coalescence. In most of the cases Ca granules are added as viscosity enhancer at 680 °C and stirred up to several minutes which helps in enhancing the viscosity by a factor up to 5 due to the formation of calcium oxide (CaO), calcium–aluminium oxide (CaAl<sub>2</sub>O<sub>4</sub>) or perhaps even Al<sub>4</sub>Ca intermetallics which thicken the liquid metal (Simone and Gibson 1998; Miyoshi et al. 2000). Stirring time shows increasing effect on the viscosity as well as also increases with increase in percentage of viscosity enhancer (Banhart 2001). After this process blowing agents are introduced in viscous melt at 680–730 °C which is again stirred for few minutes. At constant pressure due to reaction, molten metal starts to expand slowly and gradually and fills the foaming vessel. After cooling solid metal foam is released and cut into desired shape for further processing (Fig. 4.3).

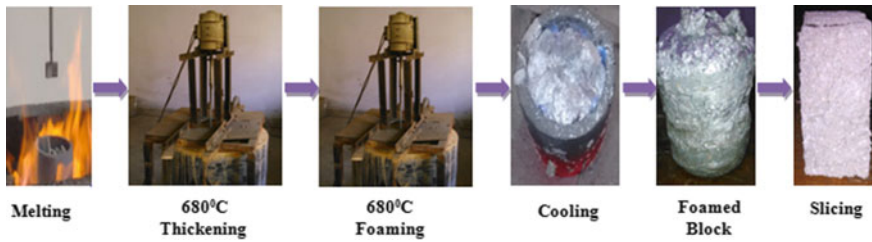


**Fig. 4.3** Melt route process for metal foam

#### 4.2.4 *Foaming by Gas Injection (Trade Name—Alcan or Cymat)*

In this process shown in Fig. 4.4 viscosity enhancer like silicon carbide, aluminium oxide or magnesium oxide particles are added in the melt. The viscosity enhancer or reinforcing agent is added from 10 to 20% having moderate particle size from 5 to 20  $\mu\text{m}$  (Banhart 2001). These particles help in stabilizing the foam by accumulating on the cell walls which depends on the wetting angle. So the proper selection of reinforcement particle is needed whose wetting angle with respect to melt must provide optimum stabilizing effect. In the next step gas (air, nitrogen, argon) is injected in viscous melt, where it is stirred by rotating impeller or vibrating nozzle to produce uniformly distributed fine gas bubbles. The foam in semi liquid state is pulled out by the help of conveyor belt and then allowed to cool down in normal air. Canadian company Cymat is the large producer of Al metal foam through this method. Same process is patented originally by Hydro Aluminium in Norway named as Alcan International. (Jin et al. 1990, 1992; Ruch and Kirkevåg 1991; Thomas et al. 1994; Sang

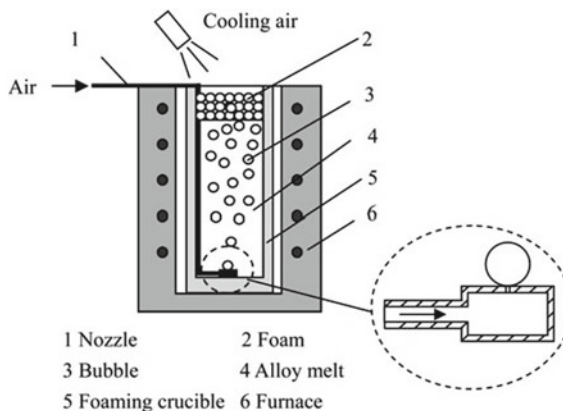


**Fig. 4.4** Schematic diagram of gas injection foaming process (Liu et al. 2015). Copyright: © materials research society 2015



et al. 1992; Sholt et al. 1997). The problem associated in such foam is brittleness caused due to the reinforcement particles. The main feature of reinforcement particles is to enhance viscosity of melt. To avoid brittleness caused from reinforcement particles an alternate way is used, in which pure metal is foamed at lower temperature near the melting point of parent metal without using reinforcement particles (Wood 1998).

### 4.3 Properties of Some of the Commercially Available Al Foams

Figure 4.5 shows the compressive stress strain curve of different commercially produced metal foam. The curve shows three regions namely elastic, plastic and densification region.

First region shows the stiffness of particular foam which depends on the density, chemical composition, distribution, shape and curvature of cell walls. The next region is plateau region which is caused by homogeneous plastic deformation of uniformly distributed pores. ERG and Alporas foams have a flat plateau region which is helpful in increasing the energy absorption capacity of metal foam. In Alcan foam serrations is observed caused by fracture of cell walls. The last region is densification region

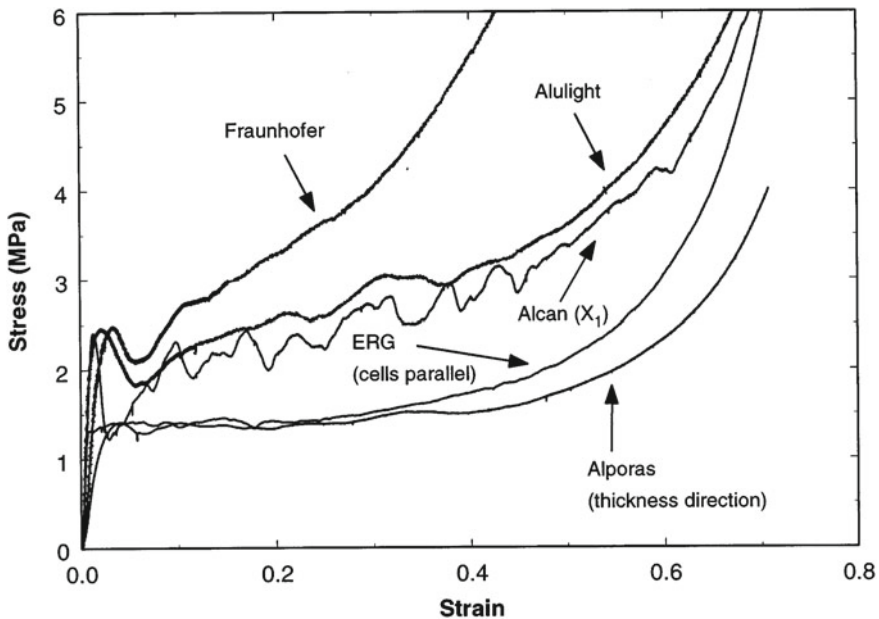


**Fig. 4.5** Stress–strain curve of different metal foam (Andrews et al. 1999). Copyright © 1999 Elsevier science S.A

**Table 4.1** Commercially available foams mechanical properties (Guner et al. 2015; Ashby et al. 2000; FOAMINAL)

Materials	Al–SiC	Al–Mg–Si	AlSi12	Al–5Ca–Ti	Al 6061 T6
Trade Name	Cymat, Alcan	Mepura, Alulight	Foaminal	Shinko Wire, Alporas	ERG, Duocel
Relative density	0.02–0.2	0.1–0.35	0.5–0.8	0.08–0.1	0.05–0.1
Structure	Closed cell	Closed cell	Closed cell	Closed cell	Open cell
Young’s Modulus (MPa)	0.02–2.0	1.7–12	3.5–8.4	0.4–1.0	0.06–0.3
Poisson’s ratio, $\nu$	0.31–0.34	0.31–0.35		0.31–0.36	0.31–0.37
Compression strength (MPa)	0.04–7.0	1.9–14.0	7.9–22.8	1.3–1.7	0.9–3.0
Tensile strength (MPa)	0.05–8.5	2.2–30	2.76–5.99	1.6–1.9	1.9–3.5
Fracture toughness (MPa m <sup>1/2</sup> )	0.03–0.5	0.3–1.6	0.03–1.19	0.1–0.9	0.1–0.2
Thermal conductivity (W/m K)	0.3–10	3.0–3.5	16.7	3.5–4.5	6.0–11

where cell wall collapses and a steep rise is seen in stress corresponding to strain (Andrews et al. 1999) (Table 4.1).

#### 4.4 Applications and Commercialization of Close-Cell Metal Foam

Due to multifunctional properties of metal foam it is attracting different industrial sectors like automobile, naval, aerospace etc. towards itself. Reliance on fossil fuels and adverse green house effect is inspiring different sectors to use metal foam. A survey shows that in future major application about 32% by using metal foam will be in automotive and aerospace sector. Among them 26% will be used in automobile industry. Moving further it is necessary to know essential properties helpful in automotive sector (Srivastava and Sahoo 2006; Banhart 2009).

Figure 4.6. shows the important properties of Aluminum metal foam which can be utilized in transportation field. Low density and high strength to weight ratio can help it in using as light weight construction material. The long and flat plateau region in compressive stress–strain curve helps in providing high energy absorption

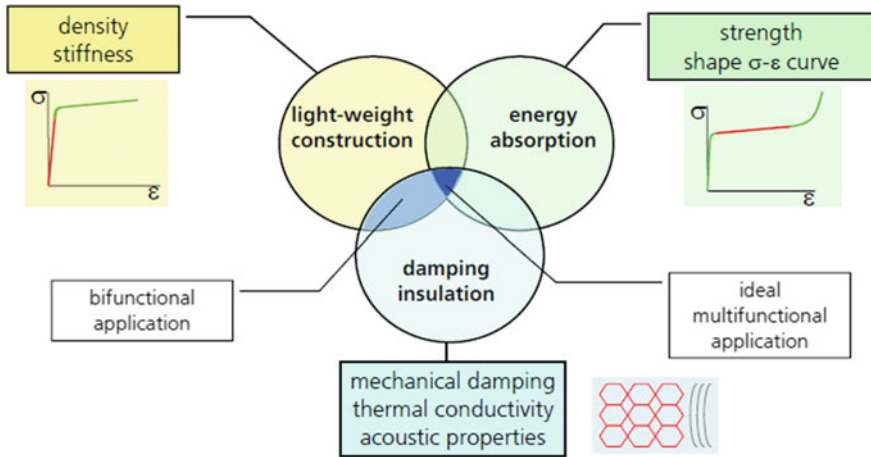


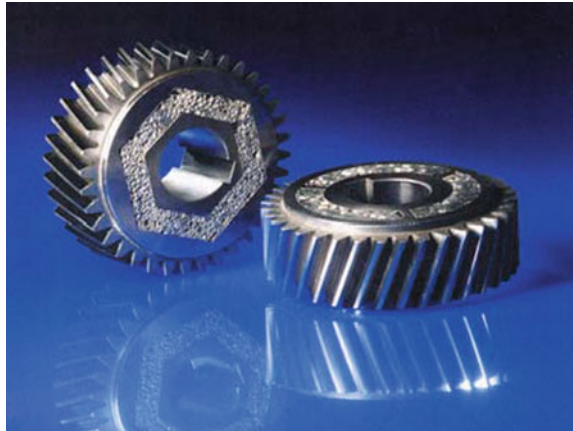
Fig. 4.6 Possible application field for metal foam (Li et al. 2012)

capacity so can be used as energy absorption material. Due to uniform distribution of pores throughout the matrix, metal foams are useful as damper insulator and noise absorber. Exploitation of two or more properties can make them an effective material to be used in automobile field. Many products had been successfully prepared and some are under prototype stages.

#### 4.4.1 Light Weight Construction and Energy Absorption Applications

Lightweight construction applications depend on two properties of metallic foams: reversible quasi-elastic deformation and high stiffness to mass ratio. By using aluminum sandwich structures on the vehicle body frame where weight and stiffness are a primary concern, the number of components needed in the car can be significantly reduced, decreasing fabrication cost (Duarte and Oliveira 2009; Šimančík 2015). Foamed panels could also be very helpful in reducing the energy consumption of elevators; light weight construction is an important issue because of the high frequency. Another possible application can be the car wheel. The cast wheel having metal foam inserted as core can reduce the weight of the wheel by 2 kg.

**Fig. 4.7** Gear-wheel with an anti-vibration layer of aluminium foam



#### ***4.4.2 Light Weight Construction with Damping Insulation***

Gear wheel with anti vibrating layer of Aluminum foam can be used in future. This product can help in reducing the weight as well as provide sound proof mating of wheel and reducing the value of thrust force (Fig. 4.7).

#### ***4.4.3 Multi-functional Application***

These applications can play a vital role in automobile industry. In Fig. 4.8a engine brackets are shown which are currently being used by BMW. These engine brackets helps in reducing the weight, noise and prevents engine from shock. Figure 4.8b represents the prototype of engine carrier having bulk aluminum shell with aluminum foam core.

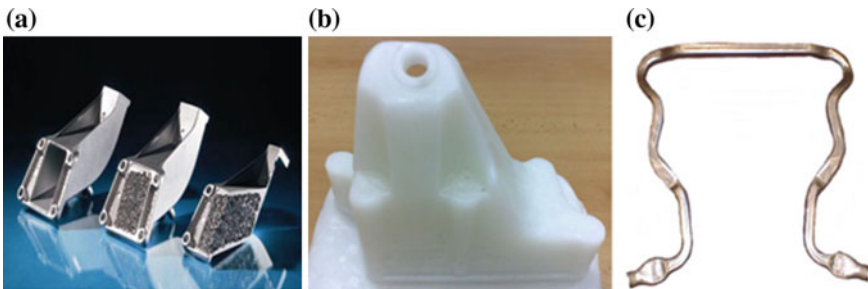


**Fig. 4.8** a Engine bracket, b engine carrier, c car front safety bar

Latest study is being carrying out on engine carrier, the requirement for good engine carrier must be high strength, better performance, no change in outer shape and low cost. These engine carriers can provide safety from the crashing as well as will increase the performance of vehicle by reducing the noise. Figure 4.8c shows the car front safety bar prototype which are used for absorbing energy while crash. They can be stiff, able to absorb deformation energy and increase damping properties.

## 4.5 Conclusion

Recently many works had been carried out on processing techniques of close cell metal foam. It is clear that close cell foam will be new futuristic structural material in automotive sector. Some improvement is further needed to develop techniques for super alloys. The main issue is to produce similar density of foam maintaining the uniformity in pores. This is due to the lack of understanding of physics foaming. It seeks improvement in material development technique, characterization and understanding the foaming physics afterward searching the applications in various engineering fields. Their multi functional properties can be well utilized by developing versatile models for processing and properties. The future of metal foam in innovative engineering applications look bright and it is anticipated that the growth on various scenario of metal foam keep on going on faster rates.

## References

- Andrews E, Sanders W, Gibson LJ (1999) Compressive and tensile behaviour of aluminum foams. *Mater Sci Eng A* 270:113–124
- Ashby MF, Evans AG, Fleck NA, Gibson LJ, Hutchinson JW, Wadley HNG (2000) Making metal foams. *Metal foams: a design guide*. Butterworth-Heinemann, Woburn, MA, USA, pp 6–23
- Banhart J (2001) *Prog Mater Sci* 46:559
- Banhart J (2003) *MRS Bull.* 290
- Banhart J (2005) *Indian Foundry J* 51:36
- Banhart J (2009) *Metallic foams II—properties & applications*
- Banhart J, Weaire D (2002) *Phys Today* 55:37
- Banhart J, Bellmann D, Clemens H (2001) *Acta Mater* 49
- Bart-Smith H, Bastawros AF, Mumm DR, Evans AG, Sypeck DJ, Wadley HNG (1998) Compressive deformation and yielding mechanisms in cellular Al alloys determined using X-Ray tomography and surface strain mapping. *Acta Mater* 46(10):3583–3592
- Baumeister J (1990) German Patent 4,018,360
- Baumeister J (1992) US Patent 5,151,246
- Baumeister J (1996) European Patent 0,460,392
- Baumeister J, Schrader H, (1991) German Patent DE 4,101,630
- Baumeister J, Banhart J, Weber M (1996) German Patent DE 4(424):157
- Baumeister J, Banhart J, Weber M (1997) German Patent DE 4,426,627
- Bisht A, Gangil B (2018) Structural and physico-mechanical characterization of closed-cell aluminum foams with different zinc additions. *Sci Eng Compos Mater* 25789–25795

- Bisht A, Gangil B, Patel VK (2019) Physico-compression, sliding wear and energy absorption properties of Zn/Mg infiltrated closed cell aluminum foam. *Mater Res Express* 6:106583
- Chen Z, Ren W, Gao L, Liu B, Pei S, Cheng H-M (2011) Three-dimensional flexible and conductive interconnected graphene networks grown by chemical vapour deposition. *Nat Mater* 10:424–428
- Davis GJ, Zhen S (1983) *J Mater Sci* 18:1899
- Duarte I, Oliveira M (2009) Aluminium alloy foams: production and properties
- Fraunhofer-Institute Bremen (1999) Product information sheet of “Foaminal” and (<http://www.ifam.fhg.de>)
- Gomez Alvarez-Arenas T, Gonzalez Gomez I (2007) Spatial normalization of the high frequency ultrasound energy loss in open-cell foams. *Appl Phys Lett* 90:201903
- Guner A, Arkan MM, Mehmet N (2015) *Metals* 5:1553–1565. <https://doi.org/10.3390/met5031553>
- H Choi, S Shilko, J Gubicza, H Choea (2017) Study of the compression and wear-resistance properties of freeze-cast Ti and Ti-5W alloy foams for biomedical applications. *J Mech Behav Biomed Mater* 72:66–73
- Hong ST, Herling DR (2006) Open-cell aluminum foams filled with phase change materials as compact heat sinks. *Sci Mater* 55:887–890
- Hyun SK, Nakajima H (2003) *Mat Lett* 57:3149
- Hyun SK, Murakami K, Nakajima H (2001) *Mater Sci Eng A* 299:241
- Ikeda T, Aoki T, Nakajima H (2005) *Met Mat Trans* 36A
- Irretier and Banhart J (2005) *Acta Mater* 53:4903
- Ji K, Xu Y, Zhang J, Chen J, Dai Z (2014) Foamed-metal-reinforced composites: tribological behavior of foamed copper filled with epoxy–matrix polymer. *Mater Des* 61:109–116
- Jin I, Kenny LD, Sang H (1990) US Patent 4,973,358 (Int. Patent Application WO 91/03578)
- Jin I, Kenny LD, Sang H (1992) US Patent 5,112,697
- Li A-B, Xu H-Y, Geng L, Li B-L, Tan Z-B, Ren W (2012) Preparation and characterization of SiCp/2024Al composite foams by powder metallurgy
- Liu X, Li Y, Chen X (2015) Bubble size control during the gas injection foaming process in aluminum alloy melt. *J Mater Res* 30(7):1002–1010
- Meller MA (1925) *Produit Métall.* pour l’obtention d’objets Laminés, Moulés ou Autres, et Proc. Pour sa Fabrication, French Patent 615.147
- Miyoshi T, Itoh M, Akiyama S, Kitahara A (2000) *Adv Eng Mater* 2:179
- Nilsson O (2007) Substitution of rechargeable NiCd batteries: a background document to evaluate the possibilities of finding alternatives to NiCd batteries. <http://www.rechargebatteries.org/07.NilssonSubstitution.pdf>
- Park C, Nutt SR (2000) *Mater Sci Eng A* 288:111
- Park C, Nutt SR (2001a) *Mater Sci Eng A* 299:68
- Park C, Nutt SR (2001b) *Mater Sci Eng A* 297:62
- Park C, Nutt SR (2002) Strain rate sensitivity and defects in steel foam. *Mater Sci Eng A* 323, 358–366
- Ruch W, Kirkevåg B (1991) Int. Patent Application WO 91/01387 (European Patent Application EP 0,483,184, B1)
- Sang H, Thomas M, Kenny LD (1992) Int. Patent Application WO 92/03582
- Sanz O, Javier Echave F, Sánchez M, Monzón A, Montes M (2008) Aluminium foams as structured supports for volatile organic compounds (VOCs) oxidation. *Appl Catal A* 340:125
- Sharifi H, Ostovan K, Tayebi M, Rajaei A (2017) Dry sliding wear behavior of open cell Al-Mg/Al<sub>2</sub>O<sub>3</sub> and Al-Mg/SiC-Al<sub>2</sub>O<sub>3</sub> composite prefoams produced by a pressureless infiltration technique. *Tribol Int.* <https://doi.org/10.1016/j.triboint.07.023>
- Sholt A, Metallschaume P, Banhart J (eds) (1997) Proc. Symp. Metallschaume, Bremen, Germany, 6–7 March. MIT Press, Verlag, Bremen, p 27 [partially in German]
- Simančík F (2015) Lightweight materials for future cars. In: 2nd symposium on Innovation, cooperation in technology and international transfer of technology 2015
- Simone E, Gibson LJ (1997) *Mater Sci* 32:451
- Simone AE, Gibson LJ (1998) *Acta Mater* 46:3109

- Srivastava C, Sahoo KL (2006) Metallic foams: current status and future prospects
- Stöbener K, Baumeister J, Rausch G, Busse M (2005) Metal powder report, January 12
- Thomas M, Kenny LD, Sang H (1994) Int. Patent Application WO 94/17218
- Wang JS, Liu P, Sherman E, Verbrugge M, Tataria H (2011) Formulation and characterization of ultra-thick electrodes for high energy lithium-ion batteries employing tailored metal foams. *J Power Sour* 196:8714–8718
- Weber M, Knuwer M, Metallschaume, Banhart J (eds) (1997) Proc. Symp. Metallschaume, Bremen, Germany, 6–7 March. MIT Press, Verlag, Bremen, p 73 [in German]
- Wood J. (1998) In: Banhart J, Eifert H (eds) Proc. Fraunhofer USA Symposium on Metal Foams, Stanton, USA, 7–8 October. MIT Press, Verlag, Bremen. p 31
- Wuebben T, Odenbach S, Banhart J (2000) Proc Eurofoam
- Xia X, Feng H, Zhang X, Zhao W (2013) The compressive properties of closed-cell aluminum foams with different Mn additions. *Mater Des* 51:797–802
- Xu J, Ji X, Zhang W, Liu G (2008) Pool boiling heat transfer of ultra-light copper foam with open cells. *Int J Multiph Flow* 34:1008–1022
- FOAMINAL (2004) Properties overview and design guideline. Fraunhofer IFAM Institute Manufacturing and Advanced Materials
- Yu CJ, Eifert H, Knuwer M, Weber M, Baumeister J (1998) Porous and cellular materials for structural applications. In: Schwartz DS, Shih DS, Evans AG, Wadley HNG (eds) *MRS Symp. Proc.* vol 521, p 145
- Zhao YY, Fung T, Zhang LP, Zhang FL (2005) *Scripta Mater* 52:295

# Chapter 5

## Study of Tribo-Performance and Application of Polymer Composite



Hemalata Jena

**Abstract** Research on composite materials has got much attention for the development of social and economic growth. The Polymer composite is a material which is highly advantageous in the area of construction, packaging and automotive application due to its high strength to the weight ratio, self-lubrication properties, improved fatigue resistance, higher resistance to thermal expansion, wear, and corrosion resistance. Tribo-performance of polymer composite indicates the behaviour of friction and wear of polymer composite which is basically decided by amount and types of polymer matrix and reinforcement. In the past decade, a large number of studies have been carried out the feasibility of the application of polymer composite in tribological applications. However, a very few study has been conducted on the tribological performance of composite material in an automotive application. Here attempts have been to provide a review on tribological performance of polymer and its composites which deals with the application of polymer composite in automotive application and recent developments of polymer composite in tribo-performance. It also deals with the effects of different process and material parameters on tribological properties of the polymer composite.

**Keywords** Polymer · Composites · Tribology · Reinforcement · Matrix

### 5.1 Introduction

Polymers and their composites are being increasingly used in the automobile and aircraft industries. It is mainly due to their good strengths, low densities, ease of manufacturing and ability to be tailored to achieve any combination of strength and stiffness (ASM Handbook 1992). The composite material is defined as a material is composed of at least two constituent materials. The combination of materials are superior properties to those of the individual constituents. Composites are of two phases in which one of the phases is in the form of fibre, particles or sheets which

---

H. Jena (✉)

School of Mechanical Engineering, KIIT Deemed to be University Bhubaneswar, Bhubaneswar, Odisha 7541024, India

e-mail: [hemalata.jenafme@kiit.acin](mailto:hemalata.jenafme@kiit.acin)

© Springer Nature Singapore Pte Ltd. 2019

J. K. Katiyar et al. (eds.), *Automotive Tribology*, Energy, Environment, and Sustainability, [https://doi.org/10.1007/978-981-15-0434-1\\_5](https://doi.org/10.1007/978-981-15-0434-1_5)



is known as reinforcing phase and the other phase is called the matrix phase. The matrix phase binds the fibre into the proper place and protects from external damage, whereas the fibres help to improve the stiffness and strength of the matrix and resist cracks and fractures. The common synthetic fibres such as carbon, glass are widely used in engineering and other applications while the matrix materials are used in the form of plastic, ceramic, or metals. The density and mechanical property of composites over conventional metals are better than the metals (Jang 1994). The properties of the composites depend upon the following factors:

- (1) The bonding strength between fibre and matrix
- (2) The basic structure of the reinforcing material (shape and size)
- (3) The concentration and congregational diffusion (volume fraction of the reinforcement)
- (4) The geometric configuration of the reinforcing phase (random or preferred).

The property of the constituent materials greatly influences the property of the composites. The distribution of the materials and the interaction among them also influence the property of a composite (Aggarwal et al. 2006; Jones 1999). The most commonly used fibres in polymer matrix composites in tribo-applications in automotive are glass, carbon, graphite, aramid fibres and natural fibres etc (Bijwe 2002; Suh 1986). The basalt fibres are also an important fibre which is obtained from melting basalt rock.

## 5.2 Tribology

Tribology deals with friction, wear and lubrication where surfaces are interacting under relative motion. The word “Tribology” is originated from the Greek word *tribos* means “rubbing”. It is mandatory to know the wear property of any engineering materials, where materials used in the wear related application in particular industry and automotive application. Many studies reported on the wear resistance of polymer and its composite (Ray and Gnanamoorthy 2007; Cirino et al. 1988). The study of tribology helps to improve service life, reliability, safety of the spacecraft to household components and also increase the economic growth. Friction and wear are two important terms used in tribology. Friction is an opposing force when a body slide against a surface and it is known as surface resistance of an object. Friction causes various types of wear. As per Gahr, wear is defined as the “progressive loss of substance from the operating surface of a body occurring as a result of relative motion at the surface” (Zum Gahr 1987).

Wear is classified into six types. These are mainly (Burwell 1957; Sharma et al. 2011):

- (1) Abrasive: Abrasive wear can be defined as a cutting or loss of mass when a hard surface slides or roll under pressure on another surface. In abrasion wear test, the sample can be slide against a rough counter face or abrasion by hard particles. Abrasion may be two bodies or three bodies depending upon the number of the interacting surfaces. Figure 5.1 shows the schematic representations of the abrasion wear.

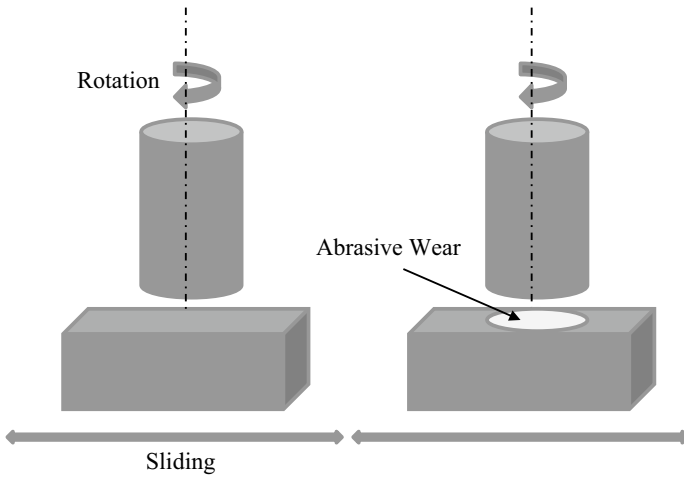


**Fig. 5.1** Schematic representations of the abrasive wear

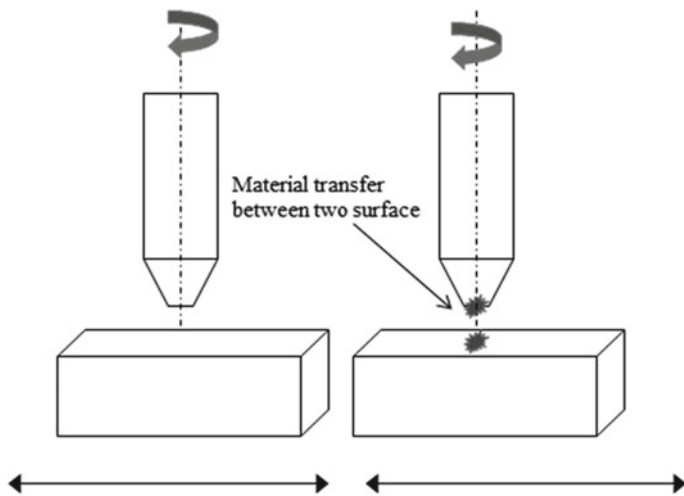


**Fig. 5.2** Schematic representations of the adhesive wear

- (2) Adhesive: Adhesive wear can be defined as mutual affinity between the materials which causes material exchange between the two mating surfaces or the loss from either surface. Figure 5.2 shows the schematic representations of the adhesive wear.
- (3) Erosive: Erosive wear is a material removal process when a solid particles impact on a surface. This material removal process may be occurred by gas or liquid which flow with and without carrying solid particles. Figure 5.3 shows the schematic representations of the erosive wear.

**Fig. 5.3** Schematic representations of the erosive wear

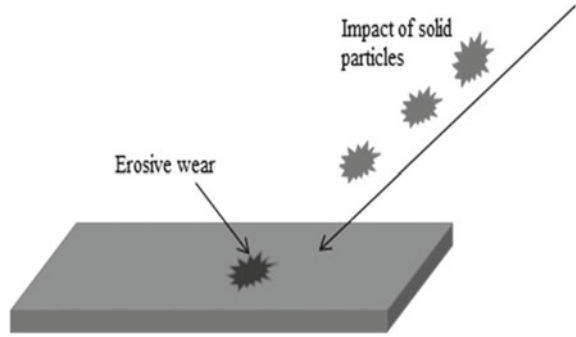
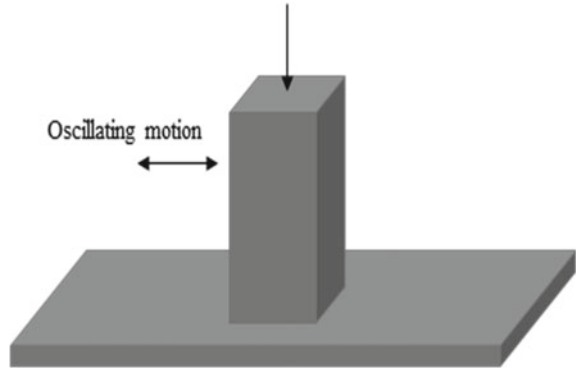


**Fig. 5.4** Schematic representations of the fretting wear



- (4) Surface fatigue: Fatigue wear of a solid surface is a process by which the surface of the material gets fractured by cyclic loading. Due to the loading and unloading which involves tension and compression, propagates pre-existing microcrack. After reaching the critical limit, the materials get removed out from the parent metal.
- (5) Corrosive: Corrosive wear is defined as a material removal process due to a chemical reaction between the material and a medium which can be a chemical reagent (acid, gas, alkalis etc.), reactive lubricant or atmosphere. The combination of mechanical and chemical give rise to corrosion wear.
- (6) Fretting: Fretting wear occurs when a mechanical assembly parts undergo a small oscillation. The materials get removed from the one or both surfaces in contact when the sliding between two mating parts is at the micron level. It is inevitable in joints, bearing, flanges, gears, seals etc. Figure 5.4 shows the contact between two bodies which undergoes in a short amplitude reciprocating sliding for a large number of cycles. In fretting wear for most of the machinery equipment, the centre of the contact may remain stationary and the edges reciprocate. Due to this wear debris form and this retain in between the mating surface which further causes the wear damage.

These wears have different wear mechanism and carried out by different tribo testing machine. Following section describe the different type of tribo-testing machines and its relevance.

### **5.2.1 Tribo-Testing Machines**

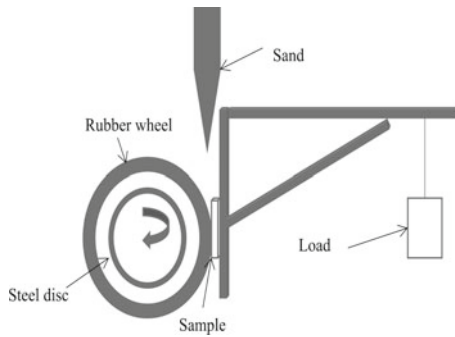
Tribo-testing is required to evaluate the tribological property of the products. Various tribo-elements decide the design and manufacturing of tribo-testing machine and based on these elements tribo-testing machines are classified. These elements are: materials, contact geometry (point, line, area), between test sample and counterface, loading, motion (rotating, sliding), environment (Dry, or wet with water or contaminants). The main differences between various tribo-test is based on the contact geometry of the tested material with the counterface (Yousif 2013).

## **5.3 Tribological Properties of Polymer**

Polymer tribology is an important parameter to decide the friction and wear property of polymers and polymer-based composites. Polymers are blended with various fillers and fibres and the ability to change the tribological property of the polymer composite. So it is important to know the tribological property of polymers before deciding the property of polymer based composites. Polymers and polymer composites are extensively used in the field of self lubricating material. From a tribological point of view, addition of graphite in polymer is most suitable for storage of hydrogen at room temperature and liquid hydrogen (Theiler and Gradt 2007). This is the reason why composite materials replaced may conventional metallic materials for the tribological application. The overview of various polymers used in tribology and their properties are given in Table 5.1 (Myshkin et al. 2015).

Polymers are classified as thermoplastic, thermosetting, and elastomers. Thermosetting polymers as matrices materials are widely used for brakes, clutches, and other frictional units. Antifriction composites are made of thermosetting polymer with incorporation of graphite or molybdenum disulfide as filler material which is used in linings of machine guides (Kong et al. 1998). Addition of filler like graphene and liquid lubricants (such as base oil SN150) in epoxy matrix can improve its performance with low coefficient of friction and high wear resistance. A tribological coating made epoxy and SU-8 (an epoxy-based polymer) is used to protect the machine components (Samad and Sinha 2010). Various studies have been carried out on addition of micro/nano-filler in epoxy and also other thermosetting polymers for tribological performance enhancement (Prabakaran et al. 2013; Lau et al. 2009; Khun et al. 2012). It is observed that epoxy-based composite shows higher wear resistance than polyester-based composite (Chand et al. 1993) (Table 5.2).

**Table 5.1** Tribo-testing equipment and its relevance



Rubber wheel abrasion test

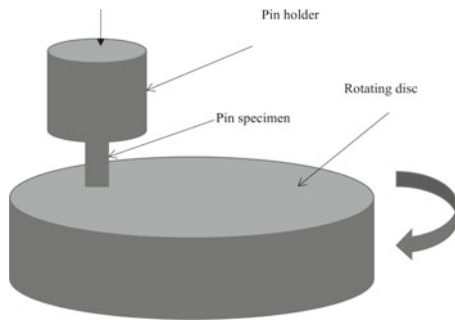
(i) **Rubber wheel test** (Stevenson and Hutchings 1996; Namdeo et al. 2015)

(i) Dry Sand Rubber Wheel (DSRW) follows ASTM-G65

(ii) Wet Sand Rubber Wheel (WSRW) follows ASTM-G105

(iii) Sand/Steel wheel (SSW) test in wet/dry conditions follows ASTM-B 611

- Abrasive wear behaviour of materials under three-body conditions
- Dimension of the specimen is 70 mm × 20 mm × 7 mm
- The rubber wheel get in touch with the specimen under a load
- Silica sand particles (i.e. fine, grain or coarse) are then introduced between the specimen and a rotating rubber wheel
- Used also for adhesive testing
- Operating parameters: applied load, rubber hardness, sliding speed
- Applications: tyres, bushes, bearings and rollers



Pin-on-disk abrasion test

(ii) **Pin-on-disk test** (Ahmed et al. 2012; Olofsson et al. 2018)

• Abrasion test follows ASTM G99-05

• Dimension of the specimen is 10 mm × 10 mm × 20 mm

• The test specimen is set perpendicular under loading against rotating counterface

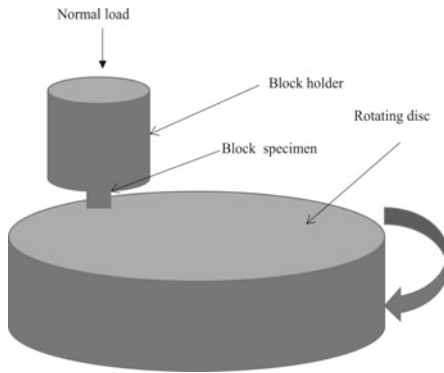
• Contact area is not varying with respect to sliding time

• Operating parameters: sliding velocity, sliding distance, normal load, wet or dry sliding, abrasive or adhesive contact condition

• Application: sliding wear of various materials where constant contact area of interest

(continued)

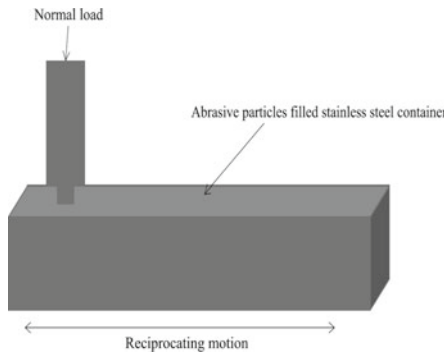
**Table 5.1** (continued)



Block on disc test

(iii) **Block on disc test** (Yousif et al. 2010)

- Block on disc test follows ASTM G99
- Dimension of the specimen is 10 mm × 10 mm × 20 mm
- The test specimen is placed vertically to the counterface which is rotating
- An infrared thermometer can be used for the measuring interfaces temperatures during the interaction of sample and counterface
- Contact area is not varying with respect to sliding time
- Test can be adhesive and abrasive
- Operating parameters: sliding velocity, sliding distance, normal load, wet or dry sliding, abrasive or adhesive contact condition
- Applications: sliding wear of various materials where constant contact area of interest



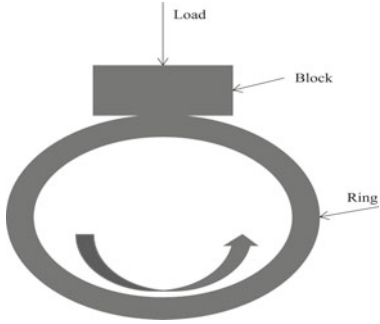
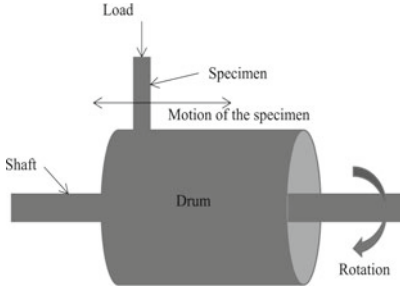
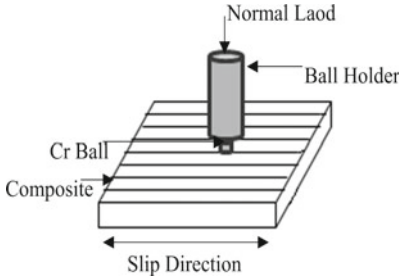
Linear reciprocating abrasion testing

(iv) **Linear reciprocating test** (Yousif et al. 2010; Tyagi 2015)

- Linear reciprocating abrasion test follows ASTM G133-05e1
- Abrasive wear behaviour of materials under three-body conditions
- It has space for a variety of sample geometries to form point, line and area contacts
- Stainless steel container filled with abrasive moves linearly with the help of the power screw which is directly coupled to the motor and the specimen slides in the abrasive particles filled container
- Test is abrasive in the presence of abrasive particles in the stainless steel container, otherwise the test is purely adhesive
- Operating parameters: sliding velocity, wet or dry sliding, abrasive types, applied load
- Application: linear sliding of window panels, door handles, lock mechanisms

(continued)

**Table 5.1** (continued)

 <p>The diagram shows a rectangular block positioned on top of a thick, circular ring. A downward arrow labeled 'Load' is applied to the top of the block. A curved arrow on the inner surface of the ring indicates its rotation. Labels 'Block' and 'Ring' point to their respective parts.</p> <p>Block on ring test</p>	<p>(v) <b>Block on ring test</b> (Nirmal et al. 2011)</p> <ul style="list-style-type: none"> <li>• Block on ring test follows ASTM G77, G137-95 standards</li> <li>• Dimension of the specimen is 10 mm × 20 mm × 50 mm</li> <li>• Test sample place parallel to the side of the counterface and contact surface varies with the sliding time</li> <li>• Operating parameter: sliding velocity, sliding distance, applied load, temperature, wet or dry sliding</li> <li>• Applications: crankshafts, camshafts, piston pins, connecting rods, suspensions, lubricants</li> </ul>
 <p>The diagram shows a cylindrical drum with a shaft passing through its center. A curved arrow on the right end of the shaft indicates 'Rotation'. A specimen is mounted on top of the drum, with a downward arrow labeled 'Load' and a horizontal arrow labeled 'Motion of the specimen' pointing to the left. Labels 'Shaft' and 'Drum' are also present.</p> <p>Pin on drum test</p>	<p>(vi) <b>Pin on drum test</b> (Nirmal et al. 2011, 2015)</p> <ul style="list-style-type: none"> <li>• Pin on drum test follows ASTM A514</li> <li>• Specimen travels linearly which is placed horizontally against a rotating drum</li> <li>• The drum is covered with abrasive paper. Without abrasive paper, test is simply adhesive</li> <li>• Operating parameters: sliding distance, sliding velocity, applied load, wet or dry sliding, abrasive or adhesive contact condition</li> <li>• Applications: conveyor belts, rotating rollers etc.</li> </ul>
 <p>The diagram shows a rectangular composite specimen with a grid of lines on its top surface. A double-headed arrow below it is labeled 'Slip Direction'. A cylindrical ball holder is mounted on top of the specimen, with a downward arrow labeled 'Normal Load' and a label 'Cr Ball' pointing to the ball inside the holder. A label 'Composite' points to the specimen.</p> <p>Low-amplitude oscillating test</p>	<p>(vii) <b>Low-amplitude oscillating test</b> (Sharma and Bijwe 2011)</p> <ul style="list-style-type: none"> <li>• Known as fretting wear 10 mm × 10 mm × 3–4 mm</li> <li>• A polished chromium steel ball of having surface roughness values in the range 0.01–0.015 μm oscillates against the specimen. The diameter of the ball is 10 mm</li> <li>• Operating parameter: load, sliding velocity, number of cycles, slip amplitude, slip, frequency, contact geometry, material properties, environment</li> <li>• Application: bearings, gears, bushes, flanges, multilayer leaf springs, palliatives</li> </ul>

(continued)

**Table 5.1** (continued)

	<p>(viii) <b>Erosion test</b> (Jena et al. 2016)</p> <ul style="list-style-type: none"> <li>● Erosion test follows ASTM: G76–07</li> <li>● Dimension of the specimen 20 mm × 20 mm</li> <li>● The dry and compressed air with the solid sand particles hit on the test sample at various speeds and angle at constant feed rate through converging nozzle</li> <li>● Stand of distance is 10 mm</li> <li>● Operating parameters: impingement angle, impact velocity, erodent type</li> <li>● Application: rotor blade, convener belt</li> </ul>
--	---

Erosion test

**Table 5.2** Tribological properties of polymers (Myshkin et al. 2015)

Material	Friction coefficient	Operating parameter	Advantage	Disadvantage
Aliphatic polyamides	0.2–0.5	–40 to +85	Low wear and high fatigue resistance	Water sorption, high coefficient of friction
Aromatic polyamides	0.1–0.3	–100 to +200	Low wear, high fatigue resistance and heat stability	High cost, water sorption
Fluoroplastics	0.01–0.05	–269 to +260	Low friction, resistance to aggressive media	Creep and low mechanical strength
Polycarbonate	0.2–0.5	–60 to +125	Rigidity and resistance to aggressive media	Low fatigue strength
Polyacetals	0.1–0.3	–50 to +120	High wear and fatigue resistance	Abrasive effect due to high rigidity
Polyolefins	0.1–0.3	–100 to +100	High resistance to aggressive media	Low mechanical strength
Polyalkylene terephthalate	0.1–0.3	–20 to +115	Resistance to aggressive media and heat resistance	Sensitivity to hot water
Thermoplastic elastomers	0.3–0.6	–60 to +120	High elasticity and resistance to ambience	High friction and low mechanical strength
Polyetherether ketone	0.2–0.4	–30 to +250	High heat and ambient resistance, and $\gamma$ -radiation	High cost
Polyphenylene sulfide	0.2–0.5	–30 to +220	High wear and fatigue resistance	High cost



Polyetheretherketone (PEEK) is an important polymer in engineering materials. PEEK is a high performance composite which has good mechanical strength, high melting temperature, low wear rate at high temperature, chemical inertness, bio-resistance and easy to process (Patel et al. 2011). A large number of investigations have been carried out on tribological behaviour of PEEK and its composite. And found that incorporation of fibre into PEEK has improved the wear property of the PEEK polymer (Karandikar et al. 2014; Ovaert and Cheng 1991).

Polytetrafluoroethylene (PTFE) is a thermoplastic polymer which has a self-lubricating property, high resistance to temperature, low friction, quasi-absence of sticking effect, corrosion resistance and chemical inertness, outstanding anti-ageing performance (Myshkin et al. 2015). PTFE gives a pollution free lubrication and used as a solid lubricant both as a filler and matrix (Chaudhari and Shekhawat 2013). It is one of the most promising polymers used in shaft seals, sliding bearing, piston rings etc. The drawback (poor mechanical property and unsuitability as lubricants at UV condition) of PTFE can be overcome by adding some filler and solid lubricants (Song et al. 2016). It is observed that neat PTFE has lower wear property compared to filler (Glass fibre, MoS<sub>2</sub>, polyether ether ketone (PEEK) particles, carbon) filled PTFE composite (Desale and Pawar 2018). Similarly, in another study the wear resistance of PTFE with fillers such as bronze, carbon, graphite, glass fibre, carbon fibre, and polymer is enhanced (Ye and Xingrong 2014). Tribological property of the PTFE with filler addition is largely influenced by filler content, type, shape and size. Both organic and inorganic filler are also used to enhance the tribological property of the composite.

Polybutylene terephthalate (PBT) is another thermoplastic polymer which is semicrystalline in nature. It is widely used in automotive sector, electrical industry and building sectors. It has good mechanical strength, water absorption resistance, chemical inertness, good dimensional stability (Carrión-Vilches et al. 2015). The main problem associated with PBT is low surface resistance under sliding wear and abrasion conditions. In order to improve the tribological property of the PBT, different fillers, fibres are added and also surface coating is applied (Georgescu et al. 2014; Lugscheider et al. 2004).

Polyamides are thermoplastic polymers which have low wear and high fatigue resistance. It can be natural (wool, silk) or produce by artificially (nylons, aramids). It is reinforced with glass fibre is used in the manufacture of parts under engine hood of the automobile to improve their friction and wear performances (Strumberger et al. 2005; Li et al. 2013). Filler filled Polyamides are also used to make sliding bearings, gears and thin polymer coatings. Thermoplastic polymer like polyformaldehyde, polycarbonate, and polyarylate are also used in gears, bushings, and sliding bearings.

Polyetherimide (PEI) is another important high temperature thermoplastic polymer which is amorphous in nature. It is also known for ductile polymer and hard (Bijwe et al. 2001). It has potential in fluoropolymer coatings applications, good mechanical, electrical and thermal properties and most important thing is that it has resistance to chemical solvents, radiation, etc. (Serfaty 1984). Hanchi and Eiss (1994) have conducted tribological test on blends of PEI and PEEK. This blend gives better wear resistance to its neat polymer. PEI has similar characteristics to PEEK in the

aspect of amorphous, transparent, and thermoplastic. But it is different with PEEK with respect to lower heat resistant, cost, and in impact strength (McKeen 2006)

Rubbers and polyurethanes are examples of elastomers which are widely used in automotive tires. Another important application of elastomers is in reciprocating and rotary seals materials for the automotive. They have low modulus of elasticity and high elongation-to-brake; high Poisson's ratio (close to 0.5) and low shear modulus (Zhang 2004). Anti-abrasion lining of metal surfaces is also an example of application of elastomers.

## 5.4 Tribological Properties of Fibre Reinforced Polymer Composite Materials

Fibre as reinforcement in polymer matrix plays an important role to decide its mechanical, tribological, electrical and thermal property of the composite. Fibre may be continuous or discontinuous. Continuous fibre is divided into:

- (i) Unidirectional long fibre
- (ii) Woven (cross-ply or multidirectional).

Discontinuous fibre is divided into:

- (i) Unidirectional short fibre
- (ii) Randomly oriented fibre.

Again fibre is classified into two groups depending upon its occurrence. One is synthetic fibre (man-made) and another one is natural fibre (non-man made). Synthetic fibres like glass and carbon fibres are most important fibre in the polymer composite. They are well known for its research and application. But due to its non-recyclability, non-degradability, high cost and CO<sub>2</sub> emission during its synthesis, researchers are bound to search an eco-friendly material. And found the possibility to replace the synthetic fibre with natural fibre. Natural fibres are not man-made fibres which are suitable as reinforcement in polymer matrix. Table 5.3 shows the different type of natural fibres. In present study focuses on plant fibre which is basically divided into two; one is non-wood fibre and another is wood fibre. These plant fibres are composed of cellulose, hemicelluloses, lignin, wax, oil and other impurities. The presence of lignin, wax and other impurities make the natural fibre incompatibility with polymer which in turn give improper adhesion between fibre and matrix. Fibre and matrix adhesion is a very important aspect for mechanical, tribological property of the composites. Different surface treatments are available for improving the surface roughness and mechanical inter-locking between fibre and matrix. These chemical treatments are: Alkaline, Acetylation, Acrylation, Bleaching, Permanganate, Isocyanate, Peroxide, Maleated Coupling agent, Benzoylation (Li et al. 2007). The chemical treatments are improved the wear property, mechanical property of the composite. On the other hand, certain behaviour of natural fibre reinforced

**Table 5.3** Classification of natural fibre (Faruk et al. 2012; Mohanty et al. 2005)

Non wood fibre					Wood fibre	Animal fibre	Mineral fibre
Bast fibre	Leaf fibre	Seed fibre	Fruit fibre	Stalk fibre			
Jute	Sisal		Coir	Barley	Soft wood	Wool	Asbestos
Bamboo	Banana		Betel nut	Wheat	Hard wood	Hair	
Hemp	Palm			Rice	Sawdust	Silk	
Rattan	Abaca	Alfalfa		Grass		Feather	
Flax	Pineapple	Kapok		Corn			
Sugarcane	Date Palm	Oil palm seed					
Kenaf	Manila	Cotton					
Banana							

composite still make it difficult to use in structural application like hydrophilic in nature, dimensional instability, variation of properties depending upon growth in soil, viscoelastic, viscoplastic or time-dependent behaviour due to creep and fatigue loading (Gassan 2002).

It is observed that short fibre reinforced composites are better tribological properties as compared to long or non-woven fibres (Almajid et al. 2011). It may be due to improved cross-linking of thermosetting polymers. The further advantage of using short fibre is low cost of making short fibre as compared to make fibre mat and no problem of directionality (El-Tayeb 2008).

For structural application, polymer composites are encountered with friction and wear. Hence calculating the coefficient of friction, mechanical load carrying capacity and wear resistance are important factor to decide its application. Different modes of wear including abrasive, adhesive and erosive are available in the literature. Cirino et al. (1988) have studied the abrasive wear in unidirectional composite where surface is worn in three principal directions like normal, parallel and anti-parallel with respect to the fibre orientation. Parallel and antiparallel wear direction are considered as in-plane and normal wear direction is considered as out-of-plane. In the case of woven fabric, the weave types respond differently in different wear mode and wear mechanism. Bijwe and Rattan (2007) have studied on different type of weave (plain, twill and satin 4-H) of fibre to analyse its tribological properties at different wear modes. It is found that the role of wear modes varied with different weaves.

Compared to unidirectional, bidirectional is more advantageous due to its ease of handling and imparting strength in two directions. Friction and wear rate of the composites depends on reinforcement (types, size, orientation, volume fraction etc), matrix and manufacturing process of the composites. The performance of the composite also depends on fibre-matrix adhesion which can be improved by treating the fibre with some functional groups. Beside the fibre-matrix adhesion, tribo-properties

of the composites also depend on different operating conditions. Parikh and Gohil (2015) have done a literature review on effect of filler, fibre type, fibre orientation and the operating parameters such as load, sliding distance for different synthetic and natural fibre composites.

### 5.4.1 Glass Fibre Composite

Glass fibre reinforced polymer (GFRP) composite is extensively used as tribo-materials. It has excellent corrosion resistance, low weight, and high strength. It is widely used in aircraft, automobile, sports utility and many others. The wear mechanism of GRFP is a complex nature due to the anisotropic behaviour of composite. Any wear application, it is essentially required to avoid the damage propagation during wear. Various studies have been carried out to reduce the wear rate in the glass fibre composite. Incorporation of fillers, tested on various kinds of polymer matrix in glass fibre, fibre content, its orientation and selecting the appropriate testing parameters are different techniques to avoid the wear damage at minimal in glass fibre composite. Glass fibre is available in the form of unidirectional fibre, chopped and woven fibre mat. It is found that the wear rate of chopped glass fibre reinforced polymer composite is better than bidirectional glass fibre reinforced polymer composite (Siddhartha and Gupta 2012)

Glass fibre-reinforced in polymer resin is a desirable material for tribological property. Various studies have reported that the wear rate has been reduced when the polymers are reinforced with glass fibre. Carrion-Vilches et al. (2015) have conducted scratch test according to ASTM D7027-05 on 20 and 30 wt% of glass fibre in PBT polymer and found that friction coefficients increase with the increasing fibre content and 20 wt% of fibre loading gives higher scratch resistance than that of neat polymer.

Further improvement of wear resistance of glass fibre reinforced polymer composite, various metallic, nonmetallic, conventional and nonconventional fillers have been added. Shivamurthy et al. (2009) have observed that 6 wt% of  $\text{SiO}_2$  filler addition gives better wear resistance and further increase of filler content is not beneficial to the composite. Addition of SiC and graphite filler addition to the glass fibre composite improve the wear property of the composite (Shivamurthy et al. 2009). Addition of 20 wt% of chopped carbon, 5 wt% glass fibre and 5 wt% of  $\text{MoS}_2$  in PTFE polymer have improved the wear property of the composite (Song et al. 2016). Suresha et al. (2007) have investigated that incorporation of graphite filler into glass fibre epoxy reduces the wear rate as compared to neat epoxy. Similarly, incorporation aluminium nitride in E-glass fibre reinforced improves the wear resistance (Panda et al. 2014).

Bijwe et al. (2001) have examined the different wear test like adhesive, abrasive (abrading in single pass and multi-pass against silicon carbide abrasive paper and three-body abrasion), erosive and fretting wear test on three materials viz. neat polyetherimide (PEI), PEI with 20% short glass fibre and PEI with 25% short glass fibre, 15% PTFE and 15%  $\text{MoS}_2$  and graphite. Wear performance of different material is different in different wear mode. Operating parameters such as load, speed,

temperature etc. affect the wear mode of the materials. Pihtili and Tosun (2002) have concluded that sliding load is more predominant over the sliding speed of the glass fibre and aramid fibre composite and also found that wear resistance of glass fibre is less as compared to the aramid fibre. Table 5.4 shows the tribological analysis of glass fibre composite with operating parameters. From the table, it is found that the wear resistance of the polymers have been improved when it is reinforced with glass fibre. The performance of the glass fibre reinforced polymer composite is influenced by experimental parameters such as speed of sliding, load and environment etc.

### 5.4.2 Carbon Fibre Composite

Among all synthetic fibre, Carbon fibre has maximum strength, modulus, self lubricating, chemical inertness and offers good thermal conductivity which is very essential for tribological application. Furthermore, due to the layer lattice structure of graphite, it gives self-lubricity in the structure (Lancaster 1972). It is also a good candidate for the brake friction material with good performance. Hence it is very important to optimise the content of carbon fibre in friction materials due to its high cost. The composite at 15 wt% of fibre content gives highest friction and wear property (He et al. 2019).

Various studies have been carried out on the incorporation of carbon fibre in polymer matrix where the wear property of the composite has been improved. Table 5.5 shows the effect of carbon fibre on the tribological property of the polymer matrix composite. Researchers have found that addition of carbon fibre in polymer results into low wear rate and no damage to the worn pair and the friction coefficient is less affected by outside conditions (Bijwe and Rattan 2007). Polymer matrix degradation can be avoided by incorporation of carbon fibre which is quickly dissipated the frictional heat. Gopal et al. (1995) have studied the effect on wear rate and friction coefficient by addition of carbon fibre in phenolic resin and various operating conditions like different loadings and sliding speeds. It is found that at 34.5 vol% of fibre, the friction coefficient and wear rate are reduced with an increase in normal load sliding speed is increasing. Guan et al. (2004) have found that with an increase in wt% of carbon fibre (12, 15 and 18 wt%) is increased both friction coefficient and wear resistance. Under the dry and wet working condition, carbon-epoxy composite performs well in wet condition where maximum percentage reduction in wear rate is 30% and for dry working conditions is 18.5% when compared with the neat epoxy (Algbory 2011). Zhao et al. (2018) have added polyethersulfone (PES) in short carbon fibre and found that it reduces the friction coefficient and wear rate at 20 vol% of carbon fibre. Maximum reduction of specific wear rate is 95.7% achieved with the addition of 20 vol% fibre.

The carbon fibre is required to be treated before use in the composite Untreated carbon fibres are inherently inert toward the matrix, and hence treated carbon fibre is essential to improve the fibre matrix adhesion including tribological in adhesive and abrasive wears (Tiwari et al. 2011a, b). The treatment of carbon fibre increases

**Table 5.4** Tribological analysis of glass fibre reinforced polymer composite

Matrix	Fibre type/fibre length/content	Tribo-test	Process parameter	Wear type	Dry sliding coefficient of friction	Wear resistance	Refs.
PEI	Bidirectional plain woven/20, 25 wt%	<ul style="list-style-type: none"> <li>Pin-on-disc— for Adhesive and abrasive</li> <li>Rubber wheel abrasion</li> <li>tester- third body abrasive</li> <li>Erosive wear test rig</li> <li>SRV optinol tester-for Fretting wear</li> </ul>	<p><b>Filler:</b> Solid lubricants: Graphite, MoS<sub>2</sub>, PTFE (15 wt%)</p> <p><b>Adhesion:</b> Load: L, 43 N Speed, 2.1 m/s</p> <p><b>Abrasion:</b> Load: 2, 4, 6, 8, 10, 12 N</p> <p><b>Third body abrasion:</b> Load: 4.45, 8.90, 13.35, 17.85</p> <p><b>Erosion:</b> Impact angle: 15, 30, 45, 60, 90° Amount of erodent: 3, 6, 9, 12, 15 kg</p> <p><b>Fretting wear</b> Load: 70, 80, 90, 100 N</p>	<ul style="list-style-type: none"> <li>Adhesive wear mode</li> <li>Erosive wear mode</li> <li>Abrasive wear mode</li> <li>Fretting wear mode</li> </ul>	–	Improved	(Li et al. 2013)
Unsaturated polyester	<ul style="list-style-type: none"> <li>Chopped fibres/1, 5, and 10 mm/3–4 wt%</li> <li>Unidirectional, fibre mates/80 mm × 80 mm, 7–8 gm/mat/30–40 wt%</li> </ul>	Pin-on-disc test	<p><b>Filler:</b> ND</p> <p>Load: 20, 40, 60, 80 N</p> <p>Fibre length-1, 5, 10 mm</p> <p>Fibre orientation: parallel, anti-parallel with respect to the sliding direction</p>	Adhesive	Decrease	Improved	(Li et al. 2007)

(continued)

Table 5.4 (continued)

Matrix	Fibre type/fibre length/content	Tribo-test	Process parameter	Wear type	Dry sliding coefficient of friction	Wear resistance	Refs.
Epoxy	<ul style="list-style-type: none"> <li>• Bidirectional glass fibre/15 20 25 30 35 wt%</li> <li>• Chopped/15 20 25 30 35 wt%</li> </ul>	Rubber wheel abrasion test	<b>Filler:</b> ND Sliding speed: 0.48, 0.72, 0.96, 1.20, 1.44 m/s Normal load: 2.5, 5, 7.5, 10, 12.5 kgf Sliding distance: 50, 60, 70, 80, 90 m Abrasive size: 125, 210, 355, 420, 600 $\mu\text{m}$	Abrasive	–	Chopped glass fibre reinforced composites > bi-directional glass fibre	(Siddhartha 2012)
Epoxy	bidirectional plain woven/200 $\text{g}/\text{m}^2$ /50 wt%	Pin-on-disc	<b>Filler:</b> $\text{SiO}_2$ (0, 3, 6, 9 wt%) Load: 30, 60, 90 N	Adhesive	Decrease	Improved	(Shivamurthy et al. 2009)
Epoxy	Bidirectional plain woven Woven fibre/8 mil/40, 50, 60 vol%	Pin-on-disc test	<b>Filler:</b> Graphite (10 wt%), SiC (10 wt%), Load: (20, 40, 60 N), Sliding Velocity: 3, 4, 5 m/s Sliding Distance: 1000, 2000, 3000 m	–	–	Improved	(Basavarajappa et al. 2009)
Polyester	Woven fibre/300, 500 $\text{g}/\text{m}^2$ /30 vol%	Block-on-shaft	<b>Filler:</b> ND Sliding distance: 235.5, 471.0, 706.5, 942.0, 1177.5, 1413.0, 1648.5, 1884.0 Sliding speed: 500, 710 rpm Load: 500, 1000 g	Detachment of matrix, Fibre breakage,	–	Aramid fibre has better wear resistance than glass fibre composite	(Pihiti and Tosun 2002)

(continued)

Table 5.4 (continued)

Matrix	Fibre type/fibre length/content	Tribo-test	Process parameter	Wear type	Dry sliding coefficient of friction	Wear resistance	Refs.
Epoxy	Bidirectional plain woven/360 g/m <sup>2</sup> /50 wt%	Erosion wear test rig	<b>Filler:</b> Tungsten Carbide (4 wt%) Impingement angle: 30°, 60°, 90° Impact velocity: 40, 80 m/s	Erosion	Decrease	Improved	(Mohan et al. 2013)
Epoxy	Bidirectional plain woven/600 GSM/-	A pin-on-disc machine	<b>Filler:</b> ND Load: 40, 80, 120 N Sliding speed: 2.51, 3.14 m/s Sliding distance: 1.507, 2.827 km Lubrication: dry, oil and argon gas	Adhesive wear	Argon > Dry > Oil	Improved	(Agrawal et al. 2016)
Nylon6	Bidirectional glass fibre/-/0, 10, 20, 30 wt%	Pin on disc	<b>Filler:</b> ND Load: 5, 10, 15, 20 N	Abrasive	-	Improved	(Kumar and Panneerselva 2016)
PEEK	Short fibres/-/30 wt%	Ball-on-disc	<b>Filler:</b> ND Sliding time: 10, 20, 30, 40, 50, 60, 70, 80, 90, 100, 110, 120 min Load: 100, 200, 300, 400 N	Adhesion	Increase	Improved	(Li et al. 2013)
Unsaturated Polyester	Short Fibre/30 mm/-/40, 45 wt%	Rubber wheel abrasion test	<b>Filler:</b> CaCO (5 wt%) Load: 3, 4.5, 6 and 7.5 N Sliding speed: 0.83, 1.66, 2.5, 3.34, 4.16 m/s Sliding distance: 100, 200, 300, 400, 500, 600, 700, 800 m	Abrasive	-	Improved	(Chand et al. 2000)

ND—Not Done



**Table 5.5** Tribological analysis of carbon fibre reinforced polymer composite

Matrix	Fibre type/fibre length/content	Tribo-test	Variables	Wear type	Dry sliding coefficient of friction	Wear Resistance	Refs.
Polyethersulfone (PES)	Bidirectional twill weave	Low-amplitude oscillating Test	<b>Filler:</b> ND Load: 200, 400, 600 N	Fretting wear	Decrease	Improved	(Sharma and Bijwe 2011)
Polyetherimide	Bidirectional woven carbon fibre (plain weave CP, twill Weave CT and satin 4-H CS)/1960, 1980, 1930 kg/m <sup>2</sup> /65 wt%	Pin-on-disc; Erosion wear test	<b>Filler:</b> ND <b>• Adhesive:</b> Sliding speed: 1.0466 m/s; Load: 200, 300, 400, 500 N Sliding time: 2 h Sliding distance: 7.536 km. <b>• Fretting:</b> Load: 100, 150, 200, 250, 300 N <b>• Abrasive:</b> Speed: 2 m/min; Load: 10, 20, 30, 40 N Sliding distance: 1.5 m. <b>• Erosive</b> Mass of erodent: 80 g; Flux rate: 8 g/min; Impinging velocity: 18.66 m/s; Duration of erosion: 10 min	Adhesive, low amplitude oscillating wear Abrasive, Erosive	-	<ul style="list-style-type: none"> <li>• <b>Adhesive:</b> CT &gt; CP &gt; CS</li> <li>• <b>Low amplitude oscillating wear:</b> CP &gt; CT &gt; CS</li> <li>• <b>Abrasive:</b> CS &gt; CT &gt; CP</li> <li>• <b>Erosive</b> CP &gt; CS &gt; CT</li> </ul>	(Bijwe and Rattan 2007)

(continued)

Table 5.5 (continued)

Matrix	Fibre type/fibre length/content	Tribo-test	Variables	Wear type	Dry sliding coefficient of friction	Wear Resistance	Refs.
Epoxy	Short fibre/3 mm/3, 6, 9 vol%	Pin-on-disc	<b>Filler:</b> ND Load: 4, 8, 12, 16 N Sliding speed: 0.4, 0.8, 1.2, 1.6 m/sec. Sliding time: 5, 10, 15, 20 min Environment: dry and wet	Abrasive	–	Improved	(Algbory 2011)
Polyethersulfone (PES)	Short fibre/-5, 10, 20, 30 vol%	Pin-on-disk	<b>Filler:</b> ND Normal load: 800 g Sliding speed: 364 rpm	<ul style="list-style-type: none"> <li>• Adhesive at low fibre content.</li> <li>• Fatigue worn and peeling at high fibre content</li> </ul>	Decrease	Improved	(Zhao et al. 2018)
Phenolic	Short fibre: 0, 1, 2 and 4 vol%	In-house ring type	<b>Filler:</b> Barite 19, 21, 22, 23 vol% Sliding speed: 700 rpm Load: 440 N	–	Decrease	Improved	(Ahmadijokani et al. 2019)
Epoxy	Bidirectional plain-woven carbon fibre/200 g/m <sup>2</sup> /60 wt%	Erosion wear test rig	<b>Filler:</b> Graphite (2, 4, 6, 8 wt%)	Semi-ductile erosive wear	–	Decreased	(Rao et al. 2015)

the surface roughness and adhesion toward the polymer through treatments of some functional groups. Lin et al. (2015) have found that the wear rate and the coefficient of friction are decreased in the case of recycled cryogenic treated carbon fibre composite as compared to the recycled carbon fibres composite. Similarly, carbon fibre treated with cold remote nitrogen improves wear resistance of the composite as compared to untreated carbon fibre composite (Sharma and Bijwe 2011). Another technique to improve the service performance and wear-resistance of carbon fibre with SiC is through prepared by hot press sintering. Again carbon fibre is treated with air oxidation and liquid oxidation methods to increase wear resistance (Yang et al. 2019).

### 5.4.3 *Natural Fibre Composite*

Tribological property is an important property when natural fibre composites are going to use in structural application. Wear property of the polymer have been improved by adding the natural fibre into the polymer matrix as shown in the Table 5.6. Again fibre loading in the polymer matrix composite increases the wear resistance of the composite (Dwivedi and Chand 2008).

In abrasive wear, the nature of wear mechanism is different for different fibre directions i.e parallel orientation, anti-parallel orientation and normal orientation. Various authors have studied the effect of natural fibre orientation with respect to sliding distance on abrasive wear. El-Sayed et al. (1995) have found that at 15 wt% of fibre gives the lowest wear rate in normal direction than transverse and the longitudinal orientation of fibres in linen composite and jute composite. Where Mishra and Acharya (2010) have concluded that wear rate of Bagassae composite in normal direction is lowest followed by antiparallel and parallel direction.

Operating parameters and material parameters have a significant role in the tribo-property in the natural fibre composite (Sumithra and Sidda Reddy 2018). Akpan et al. (2018) have studied the tribological properties using a block-on-ring test on hard wood and soft wood of various length in water soluble acrylic resin and make a fully bio degradable composite material. The increasing in fibre length is increased the wear rate of the composite which attributes that longer fibre length have an affinity of poorer impregnation quality. Table 5.6 indicates the various natural fibre polymer composite in tribological test and its various process parameter and material parameters. It may help to gather the knowledge of how the natural fibre content improves the wear resistance of the composites.

## 5.5 **Tribological Application of Composite Materials**

The research on development of fibre reinforced composite for improving vehicle efficiency through weight reduction is an emerging trend in automotive application. Rathnakar and Pandian (2015) have reported that the highest consumption of the

**Table 5.6** Tribological analysis of natural fibre reinforced polymer composite

Fibre-matrix	Fibre type/fibre length/content/treatment	Tribo-test	Process variables	Wear type	Dry sliding coefficient of friction	Wear resistance	Reference
Sugarcane-unsaturated polyester	Short fibre/1, 5, 10 mm/3–4 wt% Unidirectional fibre/7–8 gm/mat/3–4 wt%/ND	Pin on disc machine	Filler: ND Load: 20, 40, 60, 80 N Fibre length: 1, 5, 10 mm	Adhesive	Decrease	Improved	(El-Tayeb 2008)
Linen fibre-polyester	Woven fibre/ND/5, 12, 21, 33 wt%/ND	Pin-on-disc machine	Speed: 200–500 rev/min Fibre volume fraction Fibre orientation	Abrasive	Decrease	Improved	(El-Sayed et al. 1995)
Bagasse-epoxy	Unidirectional fibre/ND	Pin-on-disc	Loads: 1, 3, 5 and 7 N Grit sizes (150, 180, 320 and 400) Fibre orientation	Abrasive	–	Improved	(Mishra and Acharya 2010)
Borassus fruit fibre-epoxy	Short fibre/50 to 110 mm/35 wt%/Alkali treatment	Pin on disc machine	Load: 15, 20, 25, 30 N Sliding velocities: 1.413, 1.884, 2.355 m/s	Abrasive	Decrease	Improved	(Boopathi et al. 2012)
Rice husk-epoxy	Particulate fibre/ND/5, 10, 15, 20 wt%/Benzoylation	Pin-on disc	Load: 5, 7.5, 10, 15 N Sliding distance: 1000, 2000, 3000 mm Fibre volume fraction	Abrasive	–	Improved	(Majhi et al. 2012)
Coir-epoxy	Short fibre/ND/10, 20, 30/benzoylation	Pin-on-disc	Load: 10, 20 and 30 N Sliding speed: 200, 300, 400 rpm	Abrasive	–	Improved	(Chandra Rao et al. 2012)

(continued)

Table 5.6 (continued)

Fibre-matrix	Fibre type/fibre length/content/treatment	Tribo-test	Process variables	Wear type	Dry sliding coefficient of friction	Wear resistance	Reference
Kenaf-polyurethane	Unidirectional fibre/100 mm/25% wt sodium hydroxide	Block-on-disc	Load: 50, 60, 70, 80 N sliding distances: 0, 2.7 km Fibre orientation	Wet Adhesive	-	Improved	(Singh et al. 2011)
Coir-epoxy	Coir dust/10, 20, 40, 60 wt%	Pin-on-disc	5, 10, 15, 20, and 25 N sliding distances i.e. 20, 40, 60, 80, and 100 m	Abrasive	-		(Aireddy and Mishra 2011)
Coir-epoxy	Coir dust/10, 20, 40, 60 wt%	Erosion wear	Impingement angle 30°, 45°, 60°, 75°, 90° Impact velocity 34, 48, 60, 78, 92 m/sec Erodent particle size 200, 300, 400, 500, 600 µm	Erosive	-	Improved	(Aireddy and Mishra 2011)
Cotton-polyester	Single wound/7 count/18 wt%	Pin-on-disc	Filler: Graphite(0, 3, 5 wt%) Load: 2, 3, 4 kg Sliding speed: 1.66, 2.49, 3.33 m/s Sliding distance: 1, 1.5, 2 km	Abrasive	-	Improved	(Parikh and Gohil 2017)
Kenaf-epoxy	Short fibre/300 mm/48 vol%	Block-On-Disk	Load: 30, 50, 70, 100 N Sliding velocity: (1.1-3.9) m/s Sliding distance: (0-5 km) Fibre direction	Abrasive	-	Improved	(Chin and Yousif 2009)

polymer composite is in automotive industry. It is mainly due to the high strength to weight ratio, higher stiffness to weight ratio, wear resistance, higher resistance to thermal expansion, improved fatigue resistance, corrosion resistance, etc. Around 20% utilization of polymer composite is made by aerospace application.

Some of the important applications of FRP in tribological area from literature are listed below (Rathnakar and Pandian 2015; Mittmann and Czichos 1975; Fiore et al. 2015; Kurokawa et al. 2003; Ahmadijokani et al. 2019):

- Aramid fibre reinforced rubber composite for convener belt
- Continuous carbon fibre composites for multi layered leaf springs
- Short or continuous fibre reinforced polymer composites for bearings in aerospace application
- Short fibre reinforced and self lubricated thermoplastic blends are used for mechanical assemblies like gears or racks etc.
- Basalt fibre reinforced polymer composite is used to make roofs, clutch facing, car headliners, brake disc pads etc.
- Plastic gear made of Polymer carbon fibre reinforced polyamide
- Phenolic resin-based friction composites are used for disc brake pads and brake linings in automobiles, airplanes, racing cars, trucks and other vehicles
- Fibre-reinforced polymer (FRP) in automotive and aerospace applications like gears, seals, bushes and cams.

The reinforcement and polymer affect the tribological performance of the machine elements like gears, friction brake and spring are studied and the details are discussed below.

### 5.5.1 Gears

Gears are basically used to transmit power and motion from one shaft to others. It gives better transmission as compared to other drive such as belt, rope and chain drives. It may be due to less slipping between the teeth of two mating gears. Gears are made of polymer and its composite are now used to replace the metallic gears which can be used in low load condition. It provides the low cost, light weight, self-lubricity, high damping resistance and low noise. The main reasons for failure in polymer composite gears are fatigue and wear (Mao 2007). Life test is used to measure fatigue where continuous monitored is required to record the wear of the gear. Extensive researches have been carried out on power transmission of polymer gears which can be used in motorcycle and electric vehicle lightweight gearbox applications. Senthilvelan and Gnanamoorthy (2006) have studied the performance of spur gear made of short carbon fibre reinforced Nylon 66. The property of polymer gear largely depends upon the time, temperature and stress levels. Table 5.7 shows the spur gears are made of polymers and polymer composites. In the given table, all spur gears are manufactured by injection moulding method.

**Table 5.7** Spur gears parameters

Refs.	Polymer	Reinforcement	Operating parameter	Minimum wear rate at
Singh and Vashishtha (2018)	Polyamide 66	0, 15, 30 wt% of glass fibres	Rotational speed:(500–1700 rpm) Torque: (0.8–3.2 N·m).	30 wt% glass fibre composite
Singh et al. (2018)	Acrylonitrile Butadiene Styrene, High Density Polyethylene, Polyoxymethylene	ND	Rotational speeds: 600, 800, 1000 and 1200 rpm Torque: 0.8, 1.2, 1.6 and 2.0 Nm	POM
Mao et al. (2019)	Polyoxymethylene	28 wt% glass fibre	Rotation speed: 2000 rpm Torque: 3 to 8.5 Nm	Glass fibre Polyoxymethylene composite
Kurokawa (2003)	Polyamide 6, Polyamide 12, Polyamide 46, Polyamide 66	Carbon fibre	Rotation speed: 200 rpm Torque = $\pm 3-5$ MPa	Carbon fibre polyamide 12 composite

### 5.5.2 Brake Pads

Asbestos is used to manufacture the brake pads, brake linings, brake couplings etc. But its use causes the harmful effects and hence studies are carried to use alternative eco-materials for brake pads. Carbon, glass, aramid fibres are used an alternative material for asbestos brake pads (Xin et al. 2005; Kato 1994).

Wears are major problem occurred in brake pads. These are: outer pad wear, inner pad wear, tapered pad wear, cracking, glazing, or lifted edges on the pads, overlapping friction material (Arman et al. 2018). To improve the wear and friction property different techniques are adopted. Phenolic resin and its composite are widely used as friction composites for brake pads and brake linings in automobiles and other sectors. The ingredients of the friction composite to improve the wear and other properties are classified into four different types viz., polymer matrix(thermoset), fibrous ingredients, fillers (functional filler and space filler) and friction modifiers. Functional fillers are basically abrasive or lubricants where space filler are barites. Short fibres are basically used for brake friction material which is available in the form of chopped and milled (Cox 2011). Table 5.8 shows the ingredients used for the friction composite for automobiles and aeroplanes etc.

Fibre as reinforcement in polymer matrix is a suitable composite material in brake friction materials. A single fibre may not full fill the desired performance alone, hence the incorporation of different fibre or so called hybridisation of composite by the number of fibres are emerging technique in friction material. Abadi et al. (2010) have mixed the carbon fibre with steel and improve the friction property of the composite. Similarly, Farhad et al. (Ahmadijokani et al. 2019) have introduced aramid and glass fibre in carbon fibre in phenolic resin with other additives.

**Table 5.8** Response of fibre in tribological properties of brake friction materials

Matrix	Fibre	Other ingredients	Observation	Ref.
Phenolic resin	Carbon fibre	<ul style="list-style-type: none"> <li>Fibrous ingredients: Aramid and glass</li> <li>Filler: Barite, Copper powder, Alumina, Calcium Carbonate, Friction dust, Vermiculate</li> <li>Lubricant: Graphite</li> </ul>	<b>Improvement:</b> Storage modulus, stiffness, wear resistance <b>Reduction:</b> Thermal stability, friction coefficient	(Ahmadijokani et al. 2019)
Phenolic resin	<ul style="list-style-type: none"> <li>Sisal fibre</li> </ul>	<ul style="list-style-type: none"> <li>Filler: Copper, Barite, Felspar, ZnO, Friction power, Sb2S3, Clay</li> </ul>	<b>Improvement:</b> Friction coefficient, Wear resistance at different friction temperatures	(Xin et al. 2007)
<ul style="list-style-type: none"> <li>Phenolic resin</li> <li>Modified Phenolic resin</li> </ul>	ND	<ul style="list-style-type: none"> <li>Fibrous ingredients: Aramid, PAN, Lapinus Rb 220, glass, steel, brass</li> <li>Friction modifiers: Alumina, Cashew</li> <li>Space filler</li> </ul>	<b>Improvement:</b> Modified Phenolic resin have better Friction Coefficient, Wear resistance, shelf life, no emission of noxious volatiles, near zero shrinkage and void then conventional phenolic resin	(Gurunath and Bijwe 2007)
Epoxy resin	Palm kernel fibre	Filler: Aluminium oxide, Graphite, Calcium carbonate	<b>Improvement:</b> Wear, friction, mechanical, moisture effects, surface oil and water absorptions property	(Ikpambese et al. 2016)

(continued)



**Table 5.8** (continued)

Matrix	Fibre	Other ingredients	Observation	Ref.
Phenolic resin	Aramid fibre	Filler: Flyash	<b>Improvement:</b> Friction coefficient, Recovery factor, Fade resistance	(Dadkar et al. 2009)
Phenolic resin	Glass fibre	<ul style="list-style-type: none"> <li>• Fibrous ingredients: Aramid fibre</li> <li>• Filler: ZrSiO<sub>4</sub>, Barite</li> <li>• Lubricant: Graphite</li> </ul>	<b>Improvement:</b> Friction coefficient, Wear resistance	(Gweon et al. 2016)
Phenolic resin	Palm kernel fibre	<ul style="list-style-type: none"> <li>• Fibrous ingredients: Wheat fibre and Nile rose fibre</li> <li>• Filler: Al<sub>2</sub>O<sub>3</sub>, Graphite</li> </ul>	Improvement: Friction coefficient, Wear resistance, oil absorptions property	(Pujari and Srikiran 2019)

These synthetic fibres performed comparatively good mechanical and friction properties. The high cost and friction-induced noise are the main problems with these fibres. To overcome this, the natural fibre composite is the best solution. Xin et al. (2007) have found that the sisal fibre reinforced phenolic composite is a substitute of asbestos in brake composite. 20 wt% sisal fibre with copper and other fillers gives the highest wear property for the friction composites. Different friction modifiers (copper chips, alumina, graphite, SiO<sub>2</sub> power, cashew dust) are added in the friction composite (Xin et al. 2007; Gurunath and Bijwe 2007). Similarly, other natural fibres like banana fibre (Idris et al. 2015), coir fibres (Maleque and Atiqah 2013), palm kernel fibres (Ikpambese et al. 2016), bamboo fibres (Purboputro et al. 2017), Kenaf (Koya and Fono 2009) bagasse (Aigbodion et al. 2010) etc. are used for brake pad. It is well proven that natural fibres can replace asbestos in brake friction composites.

### 5.5.3 Springs

Springs plays an important role in vehicle suspension system which is made of steel. Replacing steel with fibre reinforced polymer composite offers higher strength to weight ratio, higher stiffness, elastic strain energy storage capacity, corrosion resistance and high impact energy absorption (Subramanian and Senthilvelan 2010). Different fibre reinforced polymer composites are widely used for preparing the

spring for vehicle system. The helical springs are mostly used in the suspension system in automobiles. The objective is to improve the shock absorption and comfort of the passengers. It is found from Table 5.9 that carbon fibre composite has better stiffens characteristic as compared to glass fibre composite.

Kumar et al. (2013) have compared a single-leaf spring made of glass fibre epoxy composite and jute-glass epoxy composite. It is concluded that stresses are the same for both steel and composite leaf spring. Nearly 75% weight of multi-leaf steel spring is reduced by composite material in suspension leaf spring. It is not only reducing the fuel consumption but also improve the riding qualities.

Foard et al. (2019) have studied the Belleville springs and their application. It is manufactured by a polymer composite of woven prepreg material. It is well proven that it can perform in a vibration isolation system like vehicle suspension.

Choi and Choi (2015) have prepared a coil spring of carbon fibre reinforced epoxy composite by resin transfer moulding (RTM) process. It is found that coil spring made of CFRP is provide weight reduction about 55% than that of steel and the magnitude of the shear modulus of the composite is about 16.8% of that of steel.

Manjunatha and Budan (2012) have prepared a helical spring made of glass fibre, carbon fibre, and glass-carbon fibre in  $+45^\circ$  orientation by filament winding technique (FWT). Helical spring made of carbon fibre is 24% more than glass fibre and 10% more that glass-carbon hybrid composite in mechanical property. Kara (2017) have reviewed more on leaf spring of polymer composite and concluded that the advantage, acceptability of polymer composite in leaf spring more than metal leaf spring.

## 5.6 Conclusions

The present work discusses the variety of wears encounter in the composite material along with different types of tribo-testing machines and their applications to find the wear behaviour of materials in real time conditions. It is observed that neat polymer and fibre/filler associated with polymer has great role on tribological property of the composite which could be a potential candidate to replace a metal in wear related application. Operating parameters like normal load, sliding velocity, sliding distance, temperature and material parameters like volume/weight fraction, fibre orientation, fibre length, surface treatment have a influence the tribological property. Tribological study on filler filled natural fibre reinforced polymer composite is an emerging technique in tribological world. Addition of filler in polymer matrix composites play a vital role in improving the wear property of the composite. Application of these composite materials in gear, brake pad etc. have evolved in automobile and low load condition for their tribological property. In addition to this, fuel efficiency and weight reduction by polymer composites in automobile application have a reason to replace the conventional metal.

Table 5.9 Mechanical property of leaf spring

Fibre + Matrix	Fabrication technique	Weight of spring (g)	Spring constant (N/mm)	Shear stress (N/mm <sup>2</sup> )	Deflection (mm)	Maximum compression load (N)	Failure load (N)	Refs.
<b>Steel (55Si2Mn90)</b>		13,400	31.98	-	-	-	-	(Kumar et al. 2013)
<b>Glass epoxy</b>	Hand lay up technique	3590	-	-	74.00	-	400	(Kumar et al. 2013)
<b>Jute glass epoxy</b>		2590	-	-	125.00	-	520	(Kumar et al. 2013)
Glass + Epoxy	Filament winding method		4.83	83.00	83.00	388.80	1000	(Manjunatha and Budan 2012)
Carbon + Epoxy			6.36	79.67	80.00	511.75	1500	(Manjunatha and Budan 2012)
<b>Unidirectional laminates</b>	Filament winding method	90	14.03	-	21.37	-	275	(Chiu et al. 2007)
Carbon + Epoxy								
<b>Rubber core unidirectional laminates</b>			14.31	-	24.47	-	300	(Chiu et al. 2007)
Carbon + Epoxy)								

(continued)

Table 5.9 (continued)

Fibre + Matrix	Fabrication technique	Weight of spring (g)	Spring constant (N/mm)	Shear stress (N/mm <sup>2</sup> )	Deflection (mm)	Maximum compression load (N)	Failure load (N)	Refs.
<b>Unidirectional laminates with a braided outer layer</b> Carbon + Epoxy)			16.23	–	21.03	–	320	(Chiu et al. 2007)
<b>Rubber core unidirectional laminates with a braided outer layer</b> Carbon + Epoxy			16.27	–	22.10	–	340	(Chiu et al. 2007)

## 5.7 Future Works

The current finding is a broad, but not in-depth study. Hence the present work can be expand in future:

- There are still many other varieties of natural fibres and synthetic fibre should have been explored elaborately.
- Other than spur gear should be studied in the wear related application.
- The influence of manufacturing process of composite on wear behavior of break pad, gear and spring should be explored.
- Its application is not limited only automotive but more finding is required in other industries also.

## References

- Abadi SBK, Khavandi A, Kharazi Y (2010) Effects of mixing the steel and carbon fibres on the friction and wear properties of a PMC friction material. *Appl Compos Mater* 17(2):151–158
- Aggarwal BD, Lawrence J, Broutman K et al (2006) *Analysis and performance of fibre composites*, 3rd edn. ISBN: 978-0-471-26891-8. 2
- Agrawal S, Singh KK, Sarkar PK (2016) A comparative study of wear and friction characteristics of glass fibre reinforced epoxy resin, sliding under dry, oil-lubricated and inert gas environments. *Tribo Int* 96:217–224
- Ahmadijokani F, Shojaei A, Arjmand M et al (2019a) Effect of short carbon fibre on thermal, mechanical and tribological behaviour of phenolic-based brake friction materials. *Compos* 68:98–105
- Ahmadijokani F, Alaei Y, Shojaei A et al (2019b) Frictional behaviour of resin-based brake composites: effect of carbon fibre reinforcement. *Wear* 420–421:108–115
- Ahmed KS, Khalid SS, Mallinatha V, Amith Kumar SJ (2012) Dry sliding wear behavior of SiC/Al<sub>2</sub>O<sub>3</sub> filled jute/epoxy composites. *Mater Des* 36:306–315
- Aigbodion VS, Akadike U, Hassan SB et al (2010) Development of asbestos- free brake pad using bagasse. *Tribol Ind* 32:12–18
- Aireddy H, Mishra SC (2011) Tribological behaviour and mechanical properties of bio-waste reinforced polymer matrix composites. *J Metall Mater Sci* 53(2):139–152
- Akpan EI, Wetzel B, Friedrich K (2018) A fully biobased tribology material based on acrylic resin and short wood fibres. *Tribo Int* 120:381–390
- Algbory AMRM (2011) Wear rate behaviour of carbon/epoxy composite materials at different working condition. *Iraqi J Mech Mater Eng* 11(3):475–485
- Almajid A, Friedrich K, Floeck J, Burkhart T (2011) Surface damage characteristics and specific wear rates of a new continuous carbon fibre (CF)/polyetheretherketone (PEEK) composite under sliding and rolling contact conditions. *Appl Compos Mater* 18(3):211–230
- Arman M, Singhal S, Chopra P et al (2018) A review on material and wear analysis of automotive Brake Pad. *Mater Today Proc* 5:28305–28312
- ASM Handbook (1992) vol 8. ASM International, Materials Park. Qhio, USA
- Basavarajappa S, Arun KV, Paulo Davim J (2009) Effect of filler material on dry sliding wear behaviour of polymer matrix composites-A Taguchi approach. *J Miner Mater Character Eng* 8:379–391

- Bijwe J (2002) Wear failure of polymer composites. In: Hawk J, Wilson R (eds) Failure analysis and prevention. In: Becker WT, Shipley RJ (eds) ASM handbook, vol 11. ASM Intl., OH, USA, p 1028–1043
- Bijwe J, Rattan R (2007) Influence of weave of carbon fabric in polyetherimide composites in various wear situations. *Wear* 263:984–991
- Bijwe J, Indumathi J, John Rajesh J et al (2001) Friction and wear behaviour of polyetherimide composites in various wear modes. *Wear* 249:715–726
- Boopathi L, Sampath PS, Mysamy K (2012) Influence of fibre length in the wear behaviour of borassus fruit fibre reinforced epoxy composites. *Int J Eng Sci Tech* 4(9):4119–4129
- Burwell JT (1957) Survey of possible wear mechanisms. *Wear* 58:119–141
- Carrion-Vilches FJ, Gonzalez-Vivas A, Martinez-Mateo IJ et al (2015) Study of the abrasion resistance under scratching of polybutylenetereftalate–glass fibre composites. *Tribo Int* 92:365–378
- Carrion-Vilches FJ, Gonzalez-Vivas A, Martinez-Mateo IJ et al (2015) Study of the abrasion resistance under scratching of polybutylenetereftalate–glass fibre composites. *Trib Int* 92:365–378
- Chandra Rao CH, Madhusudan S, Raghavendra G et al (2012) Investigation in to wear behaviour of coir fibre reinforced epoxy composites with the Taguchi method. *Int J Eng Res Appl* 2(5):371–374
- Chand N, Fahim M, Hussain SG (1993) Effect of 60Co gamma-irradiation on interface and abrasive wear of glass-reinforced polyester composite. *J Mater Sci Lett* 12:1603–1605
- Chand N, Naik A, Neogi S (2000) Three-body abrasive wear of short glass fibre polyester composite. *Wear* 242:38–46
- Chaudhari SB, Shekhawat SP (2013) Wear analysis of Polytetrafluoroethylene (PTFE) and its composites under wet condition. *IOSR J Mech Civil Eng* 8(2):7–18
- Chin CW, Yousif BF (2009) Potential of kenaf fibres as reinforcement for tribological applications. *Wear* 267:1550–1557
- Chiu CH, Hwan CL, Tsai HS et al (2007) An experimental investigation into the mechanical behaviours of helical composite springs. *Compos Struct* 77:331–340
- Choi BL, Choi BH (2015) Numerical method for optimizing design variables of carbon-fibre-reinforced epoxy composite coil springs. *Compos Part B: Eng* 82:42–49
- Cirino M, Friedrich K, Pipes RB (1988) The effect of fibre orientation on the abrasive wear behaviour of polymer composite materials. *Wear* 121:127–141
- Cox RL (2011) Engineered tribological composites: the art of friction material development. SAE International
- Dadkar N, Tomar BS, Satapathy BK (2009) Evaluation of flyash-filled and aramid fibre reinforced hybrid polymer matrix composites (PMC) for friction braking applications. *Mater Des* 30:4369–4376
- Desale DD, Pawar HB (2018) Performance analysis of Polytetrafluoroethylene as journal bearing material. *Proc Manuf* 20:414–419
- Dwivedi UK, Chand N (2008) Influence of wood flour loading on tribological behaviour of epoxy composites. *polym. Compos* 29:1189–1192
- El-Sayed AA, El-Sherbiny MG, Abo-El-Ezz AS et al (1995) Friction and wear properties of polymeric composite materials for bearing applications. *Wear* 184:45–53
- El-Tayeb NSM (2008) A study on the potential of sugarcane fibres/polyester composite for tribological applications. *Wear* 265(1–2):223–235
- Faruk O, Bledzki AK, Fink H, Sain M (2012) Biocomposites reinforced with natural fibres: 2000–2010. *Prog Polym Sci* 37(11):1552–1596
- Fiore V, Scalici T, Bella GD et al (2015) A review on basalt fibre and its composites. *Compos Part B Eng* 74:74–94
- Foard JHD, Rollason D, Thite AN, Bell C (2019) Polymer composite Belleville springs for an automotive application. *Compos Struct*. <https://doi.org/10.1016/j.compstruct.2019.04.063>
- Ganguly A, George R (2008) Asbestos free friction composition for brake linings. *Bull Mater Sci* 31(1):19–22
- Gassan J (2002) A study of fibre and interface parameters affecting the fatigue behaviour of natural fibre composites. *Compos Part A* 33:369–374

- Georgescu C, Deleanu L, Botan M (2014) Dry sliding of composites with PBT matrix and micro glass beads on steel. *Ind Lubr Tribol* 66:424–433
- Gopal P, Dharani LR, Blum FD (1995) Load, speed and temperature sensitivities of a carbon-fibre-reinforced phenolic friction material. *Wear* 181:913–921
- Guan QF, Li GY, Wang HY, An J (2004) Friction-wear characteristics of carbon fibre reinforced friction material. *J Mater Sci* 39(2):641–643
- Gurunath PV, Bijwe J (2007) Friction and wear studies on brake-pad materials based on newly developed resin. *Wear* 263:1212–1219
- Gweon JH, Joo BS, Jang H (2016) The effect of short glass fibre dispersion on the friction and vibration of brake friction materials. *Wear* 362–363:61–67
- Hanchi J, Eiss NS (1994) The tribological behavior of blends of PEEK, PEI at elevated temperatures. *Tribol Trans* 37:494–504
- He Q, Zhou Y, Qu W et al (2019) Wear property improvement by short carbon fibre as enhancer for rubber compound. *Polym Test*. <https://doi.org/10.1016/j.polymertesting.2019.04.026>
- Idris UD, Aigbodion VS, Abubakar IJ et al (2015) Ecofriendly asbestos free brake-pad: using banana peels. *J King Saud Univ Eng Sci* 27:185–192
- Ikpambese KK, Gundu DT, Tuleun LT (2016) Evaluation of palm kernel fibres (PKFs) for production of asbestos-free automotive brake pads. *J King Saud Univ Eng Sci* 28(1):110–118
- Jang BZ (1994) *Advanced polymer composites: principles and applications*. ASM International, Materials Park, OH, USA Chapter 2
- Jena H, Pradhan AK, Pandit MK (2016) Study of solid particle erosion wear behavior of bamboo fibre reinforced polymer composite with cenosphere filler. *Adv Polym Technol*. <https://doi.org/10.1002/adv.21718>
- Jones RM (1999) *Mechanics of composite materials*, 2nd edn. ISBN Number 13: 978-1-56032-712-7
- Kara Y (2017) A review: fibre reinforced polymer composite helical springs. *J Mater Sci Nanotechnol* 5(1):101–106
- Karandikar PM, Kharde RR, Bhojar SB et al (2014) Study the tribological properties of PEEK/PTFE reinforced with glass fibres and solid lubricants at room temperature. *Int J Cur Eng Tech* 4(4):2401–2404
- Kato T, Magario A (1994) The wear of aramid fibre reinforced brake pads: the role of aramid fibres. *Tribol Trans* 37(3):559–565
- Khun NW, Zhang H, Yang JL et al (2012) Tribological performance of silicone composite coatings filled with wax-containing microcapsules. *Wear* 296:575–582
- Kong H, Han HG, Yoon ES et al (1998) Evaluation of the wear life of MoS<sub>2</sub>-bonded-films in tribo-testers with different contact configuration. *Wear* 215(1–2):25–33
- Koya OA, Fono TR (2009) Palm kernel shell in the manufacture of automotive brake pad. International Seminar on Harnessing Natural Resources for National Development, Raw Materials Research & Development Council, 10–13 Feb 2009
- Kumar S, Panneerselva K (2016) Two-body abrasive wear behavior of Nylon 6 and glass fibre reinforced (GFR) Nylon 6 composite. *Procedia Tech* 25:1129–1136
- Kurokawa M, Uchiyama Y, Iwai T, Nagai S (2003) Performance of plastic gear made of carbon fibre reinforced polyamide 12. *Wear* 254:468–473
- Lancaster JK (1972) In: Jenkins AD (ed) *Polymer science: a material science handbook*. North Holland, Amsterdam
- Lau KT, Zheng BF, Rong MZ et al (2009) Imparting ultra-low friction and wear rate to epoxy by the incorporation of microcapsulated lubricant. *Macromol Mater Eng* 294:20–24
- Lin LM, Ahsan Q et al (2015) Wear behaviour of cryogenic treated recycled carbon fibres filled epoxy composite. *Appl Mech Mater* 761:489–493
- Li X, Tabil LG, Panigrah S (2007) Chemical treatments of natural fibre for use in natural fibre-reinforced composites: a review. *J Polym Environ* 15:25–33
- Li DX, You YL, Deng X et al (2013a) Tribological properties of solid lubricants filled glass fibre reinforced polyamide 6 composites. *Mater Des* 46:809–815

- Li EZ, Guo WL, Wang HD et al (2013b) Research on tribological behavior of PEEK and glass fibre reinforced PEEK composite. *Physics Procedia* 50:453–460
- Lugscheider E, Bobzin K, Maes M et al (2004) On the coating of polymers—basic investigations. *Thin Solid Films* 459:313–317
- Majhi S, Samantarai SP, Acharya SK (2012) Tribological behavior of modified rice husk filled epoxy composite. *Int J Scient Eng Res* 3(6):1–5
- Maleque MA, Atiqah A (2013) Development and characterization of coir fibre reinforced composite brake friction materials. *Arab J Sci Eng* 38(11):3191–3199
- Manjunatha TS, Budan DA (2012) Manufacturing and experimentation of composite helical springs for automotive suspension. *Int J Mech Eng Robot Res* 1:229–241
- Mao K (2007) A new approach for polymer composite gear design. *Wear* 262:432–441
- Mao K, Greenwood D, Ramakrishnan R, Goodship V, Shrouti C, Chetwynd D, Paul L (2019) The wear resistance improvement of fibre reinforced polymer composite gears. *Wear* 426–427:1033–1039
- McKeen L (2006) Fluorinated coatings and finishes handbook
- Mishra P, Acharya SK (2010) Anisotropy abrasive wear behaviour of bagasse fibre reinforced polymer composite. *Int J Eng Sci Tech* 2(11):104–112
- Mittmann HU, Czichos H (1975) Reibungsmessungen und Oberflächenuntersuchungen an Kunststoff-Metall-Gleitpaarungen. *Materialprüfung* 17:366–372
- Mohanty AK, Misra M, Drzal TL (2005) Natural fibres, biopolymers, and bio composites. CRC Press, Technology & Engineering, Boca Raton
- Mohan N, Mahesha CR, Rajaprakash BM (2013) Erosive wear behaviour of WC filled glass epoxy composites. *Procedia Eng* 68:694–702
- Myshkin NK, Pesetskii SS, Grigoriev AYA (2015) Polymer tribology: current state and applications. *Trib Ind* 37(3):284–290
- Namdeo R, Tiwari S, Manepatil S (2015) Development of rubber wheel abrasion testing machine for estimation of three body abrasive wear of automobile components. *Int J Des Manuf Technol* 9(1)
- Nirmal U, Hashim J, Lau STW (2011) Testing methods in tribology of polymeric composites. *Int J Mech Mater Eng* 6(3):367–373
- Nirmal N, Hashim J, Megat Ahmad MMH (2015) A review on tribological performance of natural fibre polymeric composites. *Tribol Int* 83:77–104
- Olofsson U, Minghui Tu, Nosko O, Lyu Y, Dizdar S (2018) A pin-on-disc study of airborne wear particle emissions from studded tyre on concrete road contacts. *Wear* 410–411:165–172
- Ovaert TC, Cheng HS (1991) Counterface topographical effects on the wear of polyetheretherketone and a polyetheretherketone-carbon fibre composite. *Wear* 150:150–157
- Panda P, Mantry S, Mohapatra S et al (2014) A study on erosive wear analysis of glass fibre-epoxy-AlN hybrid composites. *J Compos Mater* 48(1):107–118
- Parikh HH, Gohil PP (2017) Experimental investigation and prediction of wear behaviour of cotton fibre polyester composites. *Friction* 5(2):83–193
- Parikh HH, Gohil PP (2015) Tribology of fibre reinforced polymer matrix composites—a review. *J Reinf Plast Compos* 34(16):1340–1346
- Patel P, Richard Hull T, Lyon Richard E et al (2011) Investigation of the thermal decomposition and flammability of PEEK and its carbon and glass-fibre composites. *Polym Degrad Stab* 96:12–22
- Pihtili H, Tosun N (2002) Effect of load and speed on the wear behaviour of woven glass fabrics and aramid fibre-reinforced composites. *Wear* 252:979–984
- Prabakaran S, Satyanarayana N, Sinha SK (2013) Self-lubricating SU-8 nano-composites for micro electro mechanical systems applications. *Tribol Lett* 49:169–178
- Pujari S, Srikanth S (2019) Experimental investigations on wear properties of Palm kernel reinforced composites for brake pad applications. *Defence Technol.* <https://doi.org/10.1016/j.dt.2018.11.006>



- Purboputro PI, Hendrawan MA, Hariyanto A (2017) Use of bamboo fibre as a brake pad lining material and the influence of its portion on hardness and durability. In: 1st International conference on engineering and applied technology (ICEAT), IOP conference series: materials science and engineering. <https://doi.org/10.1088/1757-899x/403/1/012100>
- Rao KS, Varadarajan YS, Rajendra N (2015) Erosive wear behaviour of carbon fibre-reinforced epoxy composite. *Mater Today Proc* 2:2975–2983
- Rathnakar G, Pandian PP (2015) A review on the use and application of polymer composites in automotive industries. *Int J Res Appl Sci Eng Technol* 3(4):898–903
- Ravi Kumar V, Lalitha Narayana V, Srinivas Ch (2013) Analysis of natural fibre composite leaf spring. *Int J Latest Trends Eng Technol* 3(1):182–191
- Ray D, Gnanamoorthy R (2007) Friction and wear behavior of vinyl ester resin matrix composites filled with fly ash particles. *J Reinf Plast Compos* 26:57–63
- Samad MA, Sinha SK (2010) Nanocomposite UHMWPE–CNT polymer coatings for boundary lubrication on aluminium substrates. *Tribol Lett* 38:301–311
- Senthilvelan S, Gnanamoorthy R (2006) Carbon fibre reinforced nylon 66 spur gears: development and performance. *Appl Compos Mater* 13(1):43–56
- Serfaty IW (1984) Polyetherimide: a versatile, processable thermoplastic. In: Mittal KL (ed) *Polyimides*. Springer, Boston, MA
- Sharma M, Bijwe Singh K (2011) Studies for wear property correlation for carbon fabric-reinforced PES composites. *Tribol Lett* 43:267–273
- Shivamurthy B, Siddaramaiah, Prabhuswamy MS (2009) Influence of SiO<sub>2</sub> fillers on sliding wear resistance and mechanical properties of compression moulded glass epoxy composites. *J Min Mater Charact Eng* 8:513–530
- Siddhartha V, Gupta K (2012) Mechanical and abrasive wear characterization of bidirectional and chopped E-glass fibre reinforced composite materials. *Mater Des* 35:467–479
- Singh PK, Siddhartha, Singh AK (2018) An investigation on the thermal and wear behavior of polymer based spur gears. *Tribol Int* 118:264–272
- Singh N, Yousif BF, Rilling D (2011) Tribological characteristics of sustainable fibre Reinforced thermoplastic composites under wet adhesive wear. *Tribol Trans* 54:736–748
- Singh AK, Vashishtha S (2018) Thermal and wear behavior of glass fibre-filled functionally graded material-based polyamide 66 spur gears manufactured by a novel technique. *J Tribol* 140(2):021601
- Song F, Wang Q, Wang T (2016) Effects of glass fibre and molybdenum disulfide on tribological behaviours and PV limit of chopped carbon fibre reinforced Polytetrafluoroethylene composites. *Trib Int* 104:392–401
- Stevenson ANJ, Hutchings IM (1996) Development of the dry sand/rubber wheel abrasion test. *Wear* 195:232–240
- Strumberger N, Gosopic A, Bratulic C (2005) Polymeric materials in automobiles. *Promet Traffic Traffico* 17(3):149–160
- Subramanian C, Senthilvelan S (2010) Effect of reinforced fibre length on the joint performance of thermoplastic leaf spring. *Mater Des* 31:3733–3741
- Suh NP (1986) *Tribophysics*. Prentice-Hall, Englewood Cliffs, New Jersey
- Sumithra H, Sidda Reddy B (2018) A review on tribological behaviour of natural reinforced composites. *J Reinf Plast Compos* 37(5):349–353
- Suresha B, Chandramohan G, Renukappa MN et al (2007) Mechanical and tribological properties of glass-epoxy composites with and without graphite particulate filler. *J Appl Polym Sci* 103:2472–2480
- Theiler G, Gradt TH (2007) Polymer composites for tribological applications in hydrogen environment. In: International conference in hydrogen safety, Sept 2017
- Tiwari S, Bijwe J, Panier S (2011a) Influence of plasma treatment on carbon fabric for enhancing abrasive wear properties of polyetherimide composites. *Tribol Lett* 41:153–162
- Tiwari S, Sharma M, Panier S et al (2011b) Influence of cold remote nitrogen oxygen plasma treatment on carbon fabric and its composites with specialty polymers. *J Mater Sci* 46:964–974

- Tyagi R (2015) Processing techniques and tribological behavior of composite materials. IGI Global
- Xin X, Guangxu C, Feiqing L (2005) Research progress of friction properties for fibre reinforced resin matrix composite materials. *J Mater Sci Eng* 23(3):457–461
- Xin X, Xu CG, Qing LF (2007) Friction properties of sisal fibre reinforced resin brake composites. *Wear* 262:736–741
- Yang L, Hui T, Peng W (2019) Tribological properties of carbon fibre toughened SiC prepared by hot pressing sintering. *Ceram Int* 45:832–838
- Ye Sujuan, Xingrong Z (2014) Tribological properties of PTFE and PTFE composites at different temperatures. *Trib Trans* 57:382–386
- Yousif BF (2013) Design of newly fabricated tribological machine for wear and frictional experiments under dry/wet condition. *Mater Des* 48:2–13
- Yousif BF, Lau Saijod TW, Mc William S (2010a) Polyester composite based on betelnut fibre for tribological applications. *Tribol Int* 43:503–511
- Yousif BF, Nirmal U, Wong KJ (2010b) Three-body abrasion on wear and frictional performance of treated betelnut fibre reinforced epoxy (T-BFRE) composite. *Mater Des* 31(9):4514–4521
- Zhang SW (2004) *Tribology of elastomers*. Elsevier, Amsterdam
- Zhao ZK, Du SS, Li F et al (2018) Mechanical and tribological properties of short glass fibre and short carbon fibre reinforced polyethersulfone composites: A comparative study. *Compos Commun* 8:1–6
- Zum Gahr KH (1987) *Microstructure and wear of materials*. Tribology series, vol 10. Elsevier, Amsterdam

# Chapter 6

## Mechanical and Erosion Characteristics of Natural Fiber Reinforced Polymer Composite: Effect of Filler Size



Ankush Sharma, Vishal Bhojak, Vikas Kukshal, S. K. Biswas, Amar Patnaik and Tapan Kumar Patnaik

**Abstract** The thermosetting and thermoplastic materials reinforced with natural fiber are widely used in the automotive sector. Variety of natural fibers like jute, kenaf, hemp, banana, sisal, etc. are used in FRP composite due to lightweight, eco-friendly, easy availability and low cost. In addition, FRP composite also meets the structural and robustness demands of interior and exterior components of the vehicles. However, the erosion behavior of the FRP composites is a critical parameter in the dusty environment. In this work, needle punched nonwoven fiber composite is prepared using vacuum assisted resin transfer molding (VARTM) process with variation in filler size (10, 25 and 50  $\mu\text{m}$ ). The composites are prepared using 4 layers of needle punched jute fiber of  $250 \times 250$  mm and mill scale is added 10 wt% of epoxy. Tensile and flexural properties are evaluated. The erosion tests are carried out using irregular silica sand at different impingement angles, impact velocities and environment temperatures. It is observed that the composite C1 with 10  $\mu\text{m}$  filler size shows the maximum tensile and flexural strength  $45.564 \pm 0.72$  MPa and  $73.16 \pm 1.34$  MPa respectively. It is also observed that the composite C1 (10  $\mu\text{m}$ ) exhibited lower erosion rate of 216.67 mg/kg at  $30^\circ$  impingement angle compared to C2 (25  $\mu\text{m}$ ) and C3 (50  $\mu\text{m}$ ).

**Keywords** Jute fiber · VARTM · Mechanical properties · Erosion rate

---

A. Sharma · V. Bhojak · A. Patnaik (✉)

Mechanical Engineering Department, Malaviya National Institute of Technology Jaipur, Jaipur 302017, India

e-mail: [patnaik.amar@gmail.com](mailto:patnaik.amar@gmail.com)

V. Kukshal

Mechanical Engineering Department, National Institute of Technology Uttarakhand, Srinagar 246174, India

S. K. Biswas

Department of Metallurgical and Materials Engineering, Malaviya National Institute of Technology Jaipur, Jaipur 302017, India

T. K. Patnaik

Department of Physics, GIET University, Gunupur 765022, India

© Springer Nature Singapore Pte Ltd. 2019

J. K. Katiyar et al. (eds.), *Automotive Tribology*, Energy, Environment, and Sustainability, [https://doi.org/10.1007/978-981-15-0434-1\\_6](https://doi.org/10.1007/978-981-15-0434-1_6)

## 6.1 Introduction

Composite material is a combination of two or more divergent element on a macro scale. A composite is fabricated by embedding one or more discontinuous phases into the continuous phase (Agarwal et al. 2015). The discontinuous phase inculcates hard and strong particles termed as *reinforcement*, whereas, matrix usually acts as the continuous phase. Natural fiber reinforced hybrid composites can be a viable substitute to the man-made fiber reinforced polymer composites for various lightweight structural applications (Sathishkumar et al. 2013; Yusriah et al. 2014). These days, utilization of natural fibers has tremendously increased replacing synthetic fibers in automotive industries owing to its superior properties, environmental impact and social benefits (Verma and Senal 2019). Therefore, engineers and professionals across the world are showing their keen interest in utilization of natural fiber composites for the various applications especially automotive sectors. These natural fibers retains enormous characteristics such as enhanced mechanical properties, better thermal and acoustic insulating characteristics and higher resistance to fracture which are highly desirable for various lightweight structural applications (Deng et al. 2016). Other industrial applications that have been explored previously are namely, automotive panels and filling, door and window structures, gardening components, packaging, shelves etc., other purposes where higher mechanical resistance is not of much importance but do require reducing overall purchasing and maintenance costs are in aerospace, sports, leisure and construction based industries (Al-Oqla and Sapuan 2014; La Mantia and Morreale 2011). Ragupathi et al. (2018) compared the impact strength, cost and weight of the fabricated jute composite car bumper with the existing steel car bumper. The weight and cost of composite car bumper compared to steel was observed to be reduced by 58% and 56.1% respectively with 7.14 J/mm<sup>2</sup> impact strength. The mechanical and tribological properties of the natural fiber composites could be modified by adding conventional and nonconventional fillers. Sharma and Patnaik (2018) studied the effect of marble dust particulate filled jute fiber composite. The flexural and interlaminar shear strength was identified to be increased with the increase in filler amount from 0 to 30 wt%. Choudhary et al. (2019a, b) examined the effect of varying marble powder in glass fiber reinforced epoxy composites. 30 wt% inclusion of marble powder in the composite presented better erosion resistance at 45° impingement angle.

Considering other reinforcing fillers available as industrial waste/by-product, mill scale is one of them. Mill scale is a by-product pit out from the surface of steel substrates during the process like rolling, forming, forging etc. (Sista et al. 2019). In India, there are large number of rolling mill industries that produces a huge amount of mill scale on daily basis. Mill scale is contaminated with lubricants and grease from the equipment associated with the rolling mills simultaneously, it is considered as a rich source of iron with minimum impurities (Sen et al. 2015). It is generally dumped nearby the industrial areas becoming one of the reasons for infertility of

the soil, whereas some proportion finds its application for road construction purpose. Researchers are consistently discovering new methods to utilize this waste/by-product mill scale in some useful applications. Mill scale is rich source of iron oxide and displays a potential to be used as filler due to its distinctive mechanical properties. Soni and Patnaik (2019) investigated the effect of mill scale on mechanical properties of carbon fiber reinforced composites. The results shown that the tensile strength increases with increasing the mill scale in the composite by 4.73% whereas the maximum flexural strength was observed at 5 wt% of mill scale. Durowaye et al. (2018) examined the effect of silicon carbide, mill scale and magnesia particulates as reinforced in unsaturated polyester resin. The results shown that 15 wt% reinforcement exhibited the maximum tensile strength, flexural strength, impact energy and hardness.

In the present era, the automotive industries are adopting new materials based on the market situations, economic situations and environmental regulations. As per international protocols, manufactures are responsible for the reduction in fuel consumption, pollution emissions and recyclability of the parts after their use. This is a chance to develop new material for the automotive components. The composites are the combination of two or more constituents with distinct properties combined at macroscopic level to get the desired features which are not possible from the original individual material. The composites are light material with tailorable properties. Many automobile companies are using natural fiber composites for interior and exterior parts. The European car manufacturers have been used natural fiber composites for headliners, seat backs, dashboards, door panels, etc. (Holbery and Houston 2006). Hence, this work is aimed to show the effect of filler size on mechanical and erosion properties and the feasibility of mill scale filled jute fiber reinforced hybrid composites for the automotive components.

## 6.2 Types of Natural Fibers

The natural fibers are classified based on their genesis, as shown in Fig. 6.1. The plant fibers such as Jute, Flax, hemp, Kenaf, coir and many more are commercially used in the automotive applications (Bharath and Basavarajappa 2016). For various interior and exterior applications in the cars, major car manufacturing industries in Germany such as Audi, Mercedes, Ford is using natural fiber reinforced polymer composites due to its moderate strength, low cost, available in bulk quantity and environment-friendly nature.

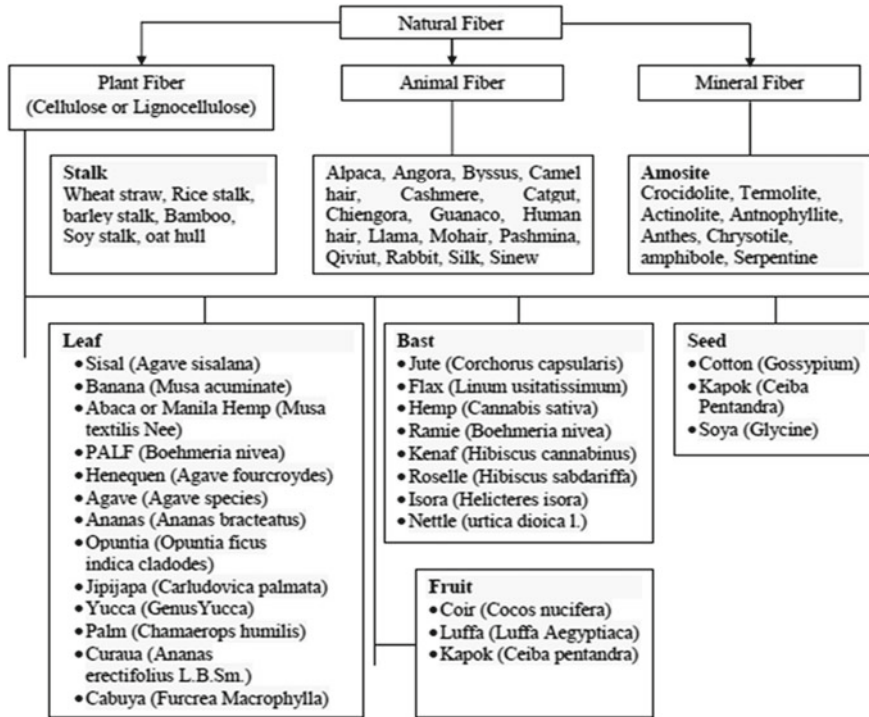


**Fig. 6.1** Classification of natural fiber (Kicinska-Jakubowska et al. 2012; Thakur 2013; Thakur and Thakur 2014; Bharath and Basavarajappa 2016; Mochane et al. 2019)

### 6.2.1 Composite Fabrication Techniques

The properties of natural fiber composites are dependent upon the fabrication methods. There are many factors on which selection of fabrication technique is dependent such as production time, volume of production, complexity, etc. (Lau et al. 2018). The various composite fabrication methods are shown in Fig. 6.2.

In present work, vacuum infusion resin transfer molding process adopted for the fabrication of different size of mill scale filled jute fiber reinforced epoxy composites (Sharma and Patnaik 2018; Choudhary et al. 2019a, b). The materials used in the present work are tabulated in Table 6.1 and the complete set of VARTM is shown in Fig. 6.3. Firstly, 10 wt% Mill scale of different size (10, 25 and 50  $\mu\text{m}$ ) dispersed in epoxy using magnetic stirrer at 800 rpm for 2 h at room temperature. Initially, a layer of wax and PVA is placed over a glass mold for easy removal of composite panel. Then, four layers of jute fiber are stacked on glass mold followed by peel ply with infusion mesh. The matrix material is uniformly distributed in radial and longitudinal direction by infusion mesh. The spiral tube is laid down at the two ends of the infusion mesh. The first spiral tube is connected with the one end of the inlet pipe and the spiral tube of the other corner is connected with catch port followed by

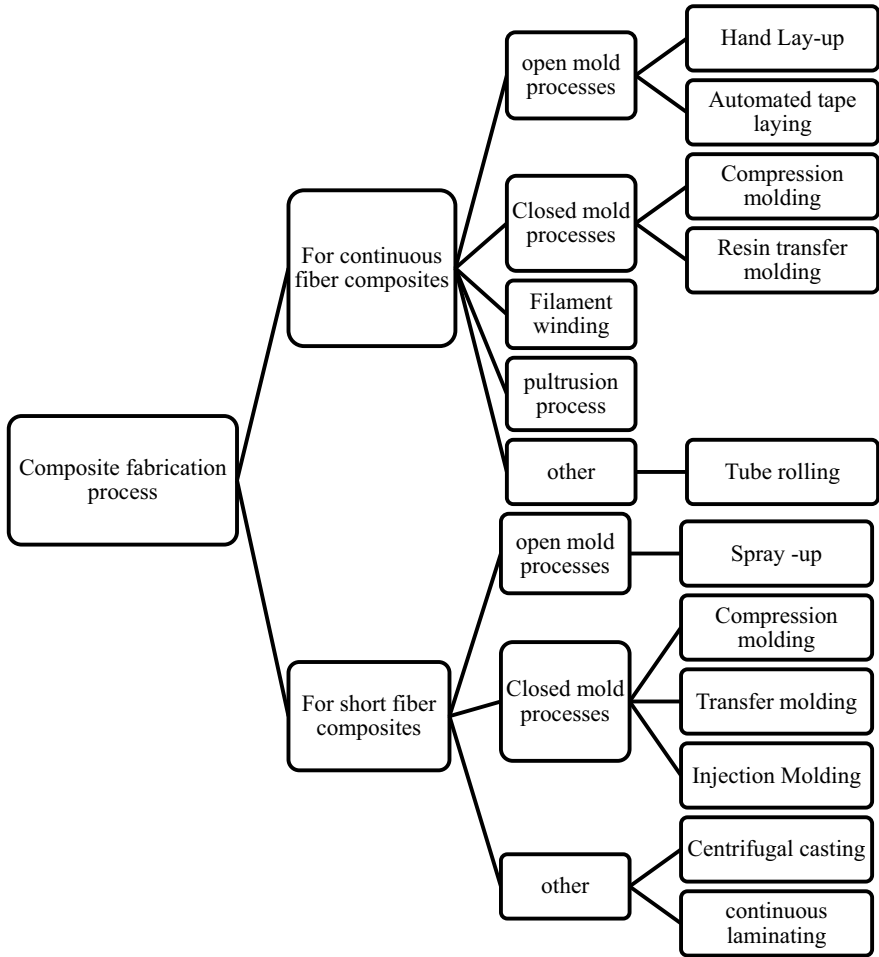
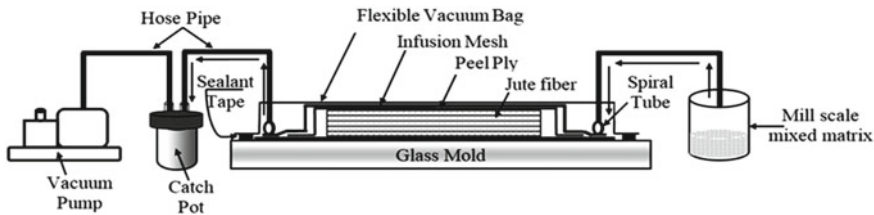


Fig. 6.2 Composite fabrication techniques

Table 6.1 Materials for composite fabrication

Material	Supplier	Size
Reinforced material: needle punched nonwoven jute fiber	Eskay International, Kolkata, India	400 GSM
Matrix material: epoxy (CY-230) and corresponding hardener	Excellence Resin, Meerut, India	–
Filler: mill scale	From local rolling industry: Sarda Industrial Enterprises, Jaipur, India	10, 25 and 50 $\mu\text{m}$



**Fig. 6.3** Schematic of VARTM process

a vacuum pump. Now the mold area is covered with the flexible transparent vacuum bag and locked down using sealant tube and vacuum is created inside the covered area. Thereafter the mill scale filled resin mixture flows inside the covered area. Once all layers impregnate with filler mixed matrix material, resin flow is stopped and the mold is kept for 24 h to cure at room temperature. The composite with 10, 25 and 50  $\mu\text{m}$  size mill scale filled hybrid composites are designated as C1, C2 and C3 respectively.

### 6.2.2 Particle Size Distribution of Mill Scale

The particle size of mill scale is measured using particle size analyzer (Model: Mastersizer 3000, Make: Malvern Panalytical, UK). The particle size distribution of 10, 25 and 50  $\mu\text{m}$  is shown in Fig. 6.4. It can be seen from the graphs that the more than 90% particles are less than 10.2, 25.4 and 50.3  $\mu\text{m}$ .

### 6.2.3 Mechanical Characterization

The tensile and flexural test is performed under displacement control mode using Heico fatigue testing machine (Fig. 6.5) equipped with 25 kN load cell according to ASTM D3039 and ASTM D7264. Three samples for each fabricated composites are tested for both the tests. The tensile test is performed with rate of loading of 2 mm/min and flexural test is conducted under three point bending mode with 1 mm/min rate of loading and flexural modulus is calculated as per the ASTM D7264.

Figure 6.6 shows the effect of particle size of mill scale on tensile strength and tensile modulus of jute fiber reinforced epoxy hybrid composites. The tensile strength and tensile modulus decreases with increasing the mill scale size from 10 to 50  $\mu\text{m}$  (Fig. 6.6). The maximum tensile strength ( $45.564 \pm 0.72$ ) is observed for C1 composite compared to C2 and C3. With the increase in filler size the contact surface between particle and epoxy tends to decrease which results in poor bonding amongst epoxy and filler that yields in poor tensile strength (Yilmaz et al. 2008). The tensile modulus is evaluated from slope of initial portion of the stress-strain curve. The



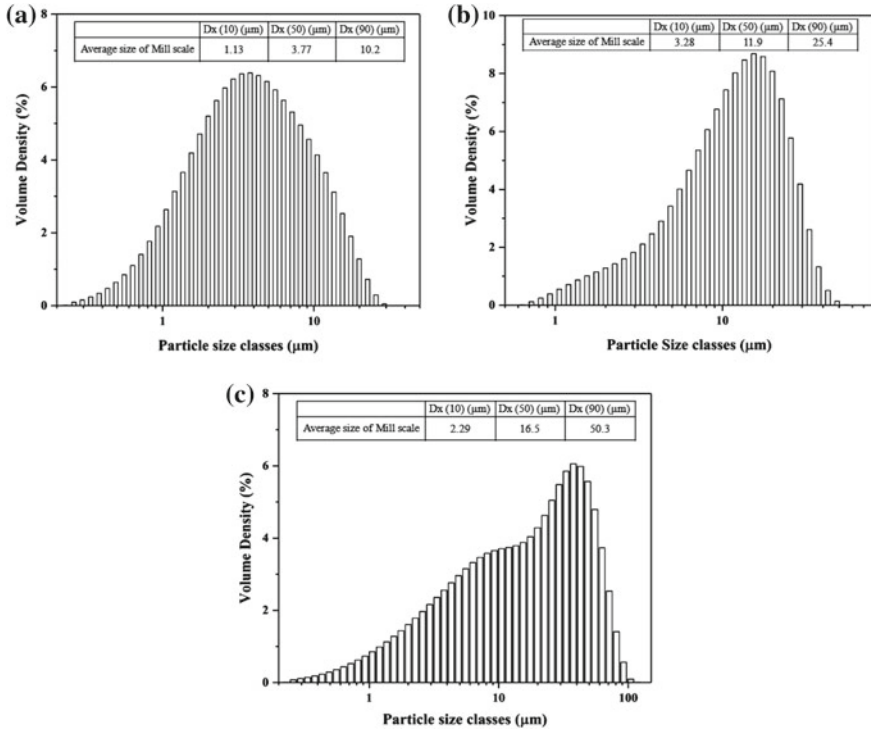


**Fig. 6.4** Particle size analysis of mill scale particles

tensile modulus shows the similar trend as tensile strength with respect to mill scale size. It has been seen from the past studies that the modulus is dependent upon the interfacial adhesion and at minimal load the large particles easily debond, hence the modulus of C1, C2 and C3 composites is in decreasing trend (Dányádi et al. 2006, 2007; Renner et al. 2009; Fiore et al. 2014).

The flexural strength is decreasing with the increase in mill scale size from 10 to 50 μm and trend is similar as observed for the tensile strength of the composites. The maximum flexural strength for C1, C2 and C3 composite is found as  $73.16 \pm 1.34$  MPa,  $69.212 \pm 1.53$  MPa and  $58.63 \pm 1.14$  MPa respectively. The flexural strength of C1 is 24.79% higher than C3 and 5.70% higher than C2. In C1 composite, the smaller particle size provides higher interface area and stiffness which produces good rigidity and hence enhanced flexural and modulus strength is attained in comparison to C2 and C3 composites. Also, the smaller size of filler possesses larger surface area hence act as a crack growth barrier. Similarly, the flexural modulus of C1 composite is 32.99% higher than C3 and 10.29% higher than C2 (Fig. 6.7).



Fig. 6.5 Photograph of fatigue testing machine

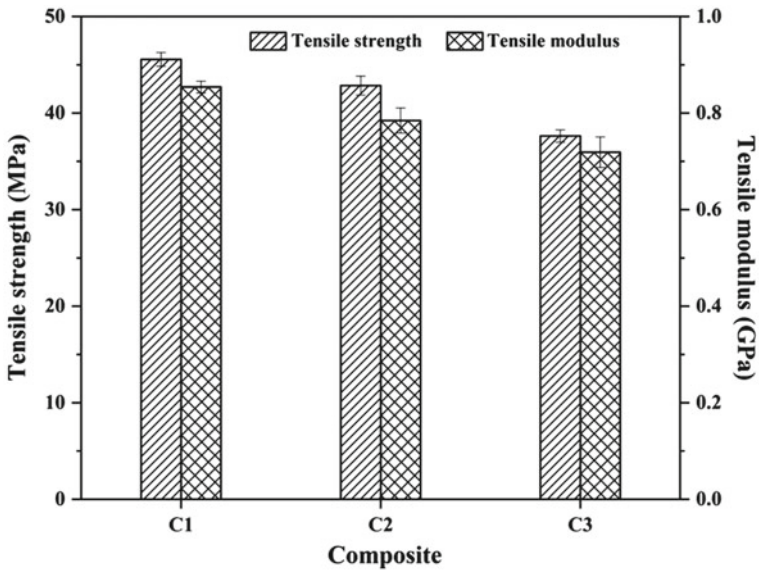


Fig. 6.6 Effect of mill scale particle size on tensile strength and tensile modulus of hybrid composite

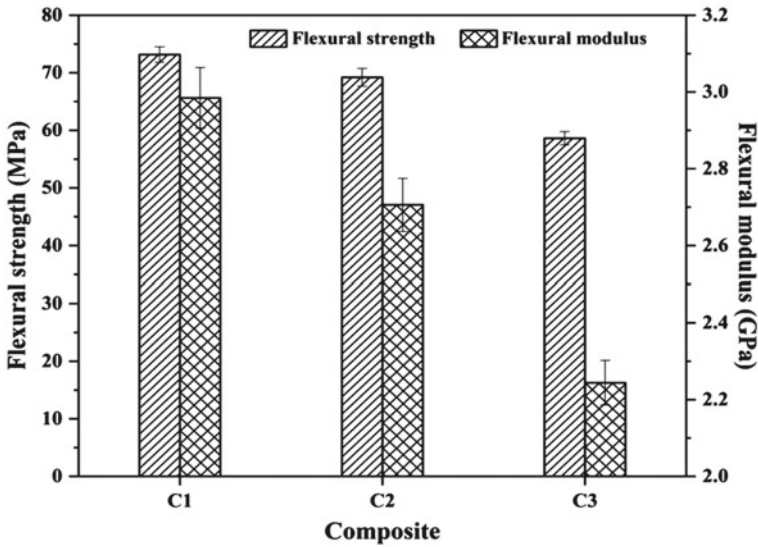
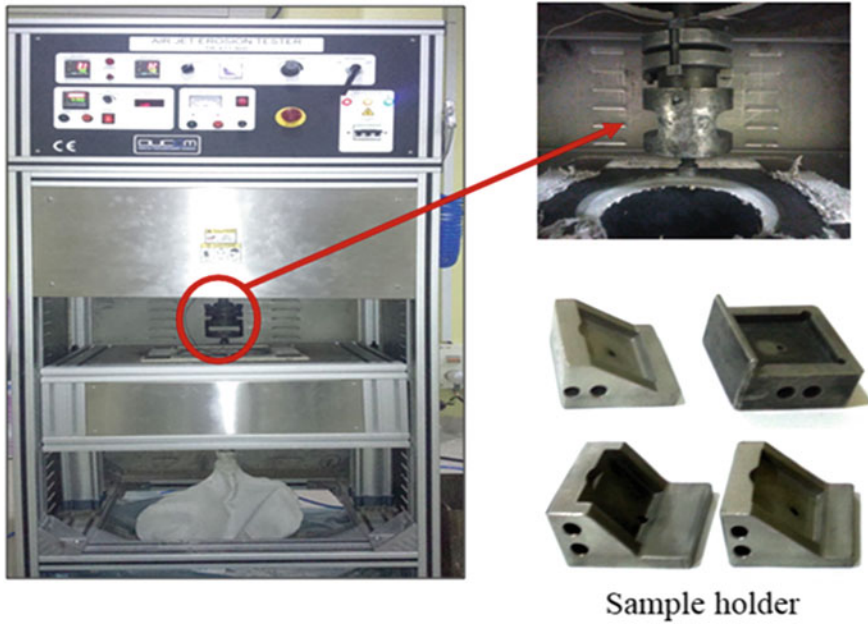


Fig. 6.7 Effect of mill scale particle size on flexural strength and flexural modulus of hybrid composite

### 6.3 Erosion Behavior of NFRP Composites

#### 6.3.1 Air Jet Erosion Test Rig

The solid particle erosion tests are conducted using air jet erosion test rig (Model: TR 471, Make: Bangalore, India) containing the facility to mix particles with compressed air and passed through nozzle confirming to ASTM D76. The Pictorial view of equipment is shown in Fig. 6.8. The solid particles are feed from the hopper and the velocity of the conveyor belt controls the mass flow rate. The conveyor belt drops the particle in the stream of air and carried with the stream through a nozzle of 1.5 mm diameter to hit the target material. The velocity of erodent ejected from the exit of the nozzle is varying from 30 to 60 m/s, and stand-off distance is 10 mm. The erosion test is performed with varying the impingement angle from 15 to 90°, increment in the step of 15°. River silica sand (Size: ~150  $\mu\text{m}$ ) is used as erodent material in the present study and maintained the discharge rate of 2 g/min. The square samples of 25 mm  $\times$  25 mm are cut from the composite slab for slurry erosion wear test. The fixed parameters and control factors for slurry jet erosion test are depicted in Table 6.2.



**Fig. 6.8** Air jet erosion tribometer

**Table 6.2** Parameters for solid particle erosion test

Control factor		Fixed parameter	
Impact velocity	30, 40, 50 and 60 m/s	Erodent	Silica sand
Impingement angle	15, 30, 45, 60, 75 and 90°	Erodent size	~150 μm
Temperature	40, 50 and 60 °C	Erodent feed rate (g/min)	2 g/min
Filler size	10, 25 and 50 μm	Carrier fluid	Air
		Nozzle diameter (mm)	1.5 mm

### 6.3.2 *Effect of Impingement Angle on Erosion Rate with Varying Mill Scale Size in Composites*

The effect of impingement angle on the erosion rate is identified starting from 15 to 90°, increment in the step of 15° by keeping other parameters constant as impact velocity 30 m/s, erodent flow rate of 2 g/min and erodent size ~150 μm. In general

thermoplastic matrix composites usually show ductile erosion whereas the thermosetting ones erode in a brittle manner (Patnaik et al. 2009a). From the Fig. 6.9, it can be easily visualized that the erosion rate increases initially up to 30° and then the curve shows a downhill thereby reducing the erosion loss, which shows the ductile behaviour of the fabricated composites (Hutchings 1992; Finnie 1995; Barkoula and Karger-Kocsis 2002; Patnaik et al. 2010; Sharma et al. 2018). At lower impingement angle, the erosion phenomenon may take place via micro-cutting or micro-ploughing due to penetration of the solid particles on the surface of the composite (Kaundal 2017). It is reported in the literature (Patnaik et al. 2009a, b, c; Choudhary et al. 2019a, b) that at lower impingement angle the impact force due to erodent particles is split into two components: (i) tangential component ( $P_T$ ) and (ii) vertical or normal component ( $P_N$ ).  $P_T$  results in shear component of force and controls the abrasive flow whereas  $P_N$  represents the impact phenomenon. The influence of  $P_N$  is insignificant as the impact angle shifts towards 90° (Patnaik et al. 2009b). From Fig. 6.9, it can be seen that all three composites shows same trend of erosion behaviour with respect to the impingement angle. Composite C1 exhibits the lowest erosion rate (216.67 mg/kg) at 30° angle as compared to C2 and C3, which is attributed to smaller the filler size, more the active sites for bonding with the matrix material thus stronger the bonding and higher the wear resistance (Raja et al. 2013). Other reason may be that increase in the size of mill scale results in the formation of air bubbles and void in composites thereby increasing the non-homogeneity in microstructure which results in decrease in erosive resistance (Patnaik et al. 2009a, b, c).

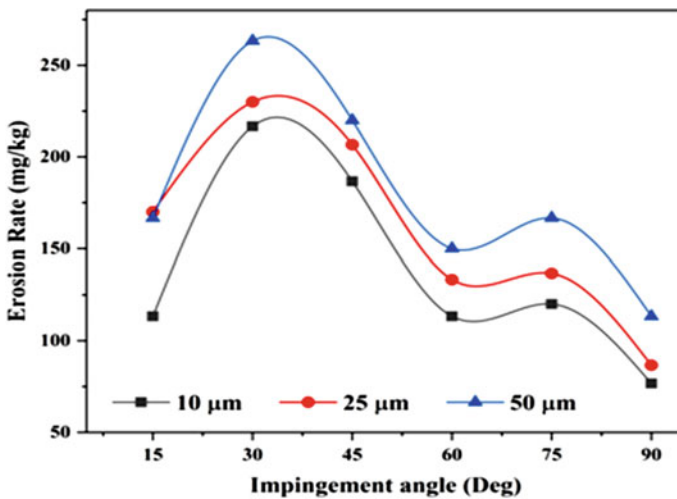


Fig. 6.9 Effect of impingement angle on erosion rate with varying mill scale size in composites

### 6.3.3 Effect of Impact Velocity on Erosion Rate with Varying Mill Scale Size in Composites

The erosion wear as a function of impact velocity is studied at different velocities of 30, 40, 50 and 60 m/s keeping other parameters (impingement angle 30°, erodent rate 2 g/min) constant. The general trend obtained from the Fig. 6.10 is that erosion wear increases with impact velocity which is supported by the fact that for medium to high velocities, a power law used to describe the relationship between wear rate and impact velocity is given as (Stachowiak and Batchelor 1993):

$$\frac{-dm}{dt} = kv^n \quad (6.1)$$

where,  $m$  represents the mass of eroded sample,  $t$  denotes the test duration,  $k$  and  $n$  are the empirical constant and velocity exponent respectively. 'n' is a function of erodent and target material characteristics and varies from 2 to 3 for polymeric materials possesses ductile behavior.

The erosion of fiber is mainly caused by damage mechanisms as micro-cracking or plastic deformation due to the impact of silica sand, such damage increases with the increase of kinetic energy (Stachowiak and Batchelor 1993). The impact velocity shows proportional relationship with the erosion rate for all the three composites as can be illustrated from Fig. 6.10. Thus with the increase in filler size, the erosion wear tends to increase and this effect may be explained due to the fact that there is better adhesion between matrix and the smaller size filler which results in hindering the stress propagation (Raja et al. 2013).

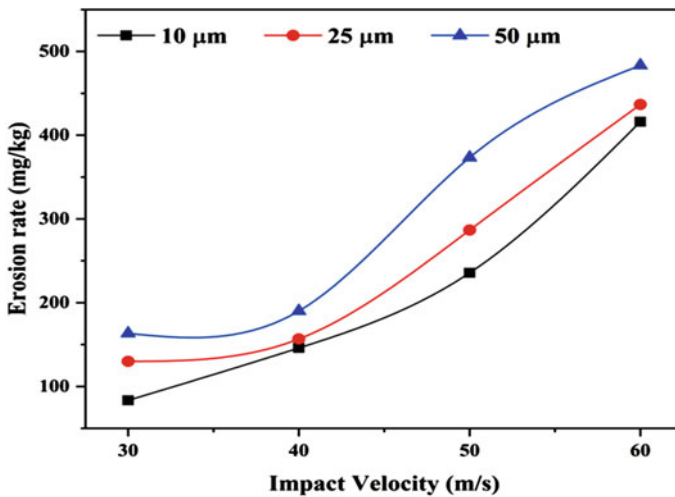


Fig. 6.10 Effect of impact velocity on erosion rate with varying mill scale size in composites

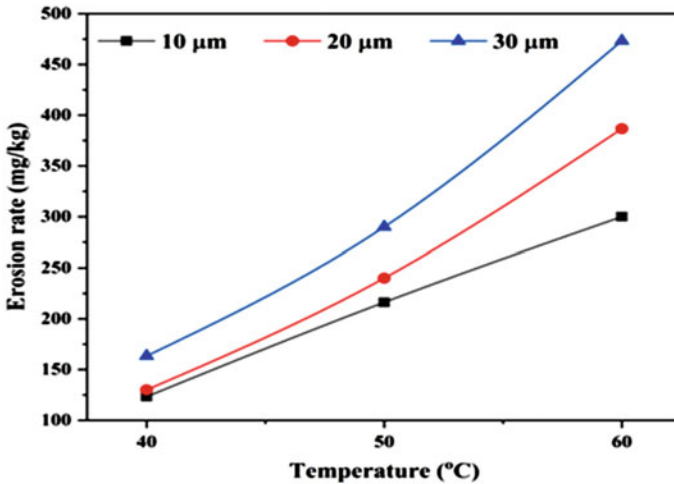


Fig. 6.11 Effect of environment temperature on erosion rate with varying mill scale size in composites

### 6.3.4 Effect of Environment Temperature on Erosion Rate with Varying Mill Scale Size in Composites

Figure 6.11 illustrates the influence of environment temperature on erosion rate with varying mill scale size in composites. It can be identified that the erosion rate of fabricated composite increases with increase in temperature while keeping all other parameters constant (30 m/s impact velocity, 30° impingement angle and 150 μm erodent size).

Composite C1 shows least erosion rate as compared to C2 and C3 (Fig. 6.11). With the elevated temperatures, the stress required for plastic flow of material decreases due to thermal softening thus leading to enhanced wear (Patnaik et al. 2011). Impingement of particles also results in heat generation in the surface of composite thereby leading to softening of the matrix and resulting in easy material removal (Patnaik et al. 2009c).

## 6.4 Conclusion

The effect of filler size shows the significant impact on the mechanical and tribological characteristics of jute fiber reinforced epoxy composite and following conclusions are derived:

- The tensile strength and tensile modulus of mill scale filled hybrid composite decreases with increasing the mill scale size from 10 to 50 μm. The maximum

tensile strength ( $45.564 \pm 0.72$ ) is observed for C1 composite compared to C2 and C3.

- The flexural strength and flexural modulus of the fabricated composites are decreasing with increase in mill scale size. The maximum flexural strength and flexural modulus is found for C1 composite as  $73.16 \pm 1.34$  MPa and  $2.985 \pm 0.073$  GPa respectively. The flexural strength of C1 is 24.79% higher than the C3 and 5.70% higher than the C2.
- Composite C1 has shown better erosion resistance with respect to impingement angle, impact velocity and environment temperature followed by C2 and C3. The smaller size of the filler results in higher the erosion resistance which is attributed to the good interfacial bonding between the constituents.
- The overall results shows the potential use of mill scale ( $10 \mu\text{m}$  particle size) filled jute fiber reinforced composite for automotive application.

**Acknowledgements** The authors are grateful to the TEQIP-III, MNIT Jaipur for providing the financial support, Advanced research lab for Tribology, MNIT Jaipur and Materials research center, MNIT Jaipur for providing fabrication and testing facilities.

## References

- Agarwal BD, Broutman LJ, Chandrashekhara K (2015) Analysis and performance of fiber composites, 23rd edn. Wiley India Pvt. Ltd., New Delhi, pp 2–16
- Al-Oqla FM, Sapuan SM (2014) Natural fiber reinforced polymer composites in industrial applications: feasibility of date palm fibers for sustainable automotive industry. *J Clean Prod* 66:347–354
- Barkoula NM, Karger-Kocsis J (2002) Effects of fibre content and relative fibre-orientation on the solid particle erosion of GF/PP composites. *Wear* 252(1–2):80–87
- Bharath KN, Basavarajappa S (2016) Applications of biocomposite materials based on natural fibers from renewable resources: a review. *Sci Eng Compos Mater* 23(2):123–133
- Choudhary M, Sharma A, Dwivedi M, Patnaik A (2019a) A comparative study of the physical, mechanical and thermo-mechanical behavior of GFRP composite based on fabrication techniques. *Fibers Polym* 20(4):823–831
- Choudhary M, Singh T, Dwivedi M, Patnaik A (2019b) Waste marble dust-filled glass fiber-reinforced polymer composite part I: physical, thermomechanical, and erosive wear properties. *Polym Compos*
- Dányádi L, Renner K, Szabó Z, Nagy G, Móczó J, Pukánszky B (2006) Wood flour filled PP composites: adhesion, deformation, failure. *Polym Adv Technol* 17(11–12):967–974
- Dányádi L, Renner K, Móczó J, Pukánszky B (2007) Wood flour filled polypropylene composites: interfacial adhesion and micromechanical deformations. *Polym Eng Sci* 47(8):1246–1255
- Deng Y, Paraskevas D, Tian Y, Van Acker K, Dewulf W, Duflou JR (2016) Life cycle assessment of flax-fibre reinforced epoxidized linseed oil composite with a flame retardant for electronic applications. *J Clean Prod* 133:427–438
- Durowaye S, Sekunowo O, Shittu S, Duru P (2018) Effects of silicon carbide, mill scale, and magnesia particulates on the mechanical properties of hybrid unsaturated polyester resin matrix composites. *Usak Univ J Eng Sci* 1(1):28–37
- Finnie I (1995) Some reflections on the past and future of erosion. *Wear* 186:1–10
- Fiore V, Scalici T, Vitale G, Valenza A (2014) Static and dynamic mechanical properties of Arundo Donax fillers-epoxy composites. *Mater Des* 57:456–464



- Holbery J, Houston D (2006) Natural-fiber-reinforced polymer composites in automotive applications. *JOM* 58(11):80–86
- Hutchings IM (1992) Ductile-brittle transitions and wear maps for the erosion and abrasion of brittle materials. *J Phys D Appl Phys* 25(1A):A212
- Kaundal R (2017) Role of process variables on solid particle erosion of polymer composites: a critical review. *Silicon* 9(2):223–238
- Kicińska-Jakubowska A, Bogacz E, Zimniewska M (2012) Review of natural fibers. Part I—vegetable fibers. *J Nat Fibers* 9(3):150–167
- La Mantia FP, Morreale M (2011) Green composites: a brief review. *Compos A Appl Sci Manuf* 42(6):579–588
- Lau KT, Hung PY, Zhu MH, Hui D (2018) Properties of natural fibre composites for structural engineering applications. *Compos B Eng* 136:222–233
- Mochane MJ, Mokhena TC, Mokhothu TH, Mtibe A, Sadiku ER, Ray SS, Ibrahim ID, Daramola OO (2019) Recent progress on natural fiber hybrid composites for advanced applications: a review
- Patnaik A, Satapathy A, Mahapatra SS, Dash RR (2009a) Tribo-performance of polyester hybrid composites: damage assessment and parameter optimization using Taguchi design. *Mater Des* 30(1):57–67
- Patnaik A, Satapathy A, Mahapatra SS, Dash RR (2009b) Modeling and prediction of erosion response of glass reinforced polyester-flyash composites. *J Reinf Plast Compos* 28(5):513–536
- Patnaik A, Satapathy A, Mahapatra SS (2009c) Study on erosion response of hybrid composites using Taguchi experimental design. *J Eng Mater Technol* 131(3):031011
- Patnaik A, Satapathy A, Chand N, Barkoula NM, Biswas S (2010) Solid particle erosion wear characteristics of fiber and particulate filled polymer composites: a review. *Wear* 268(1–2):249–263
- Patnaik A., Biswas S, Satapathy A, Kaundal R (2011) Processing, characterisation and erosion wear analysis of SiC filled glass-epoxy-composites: *Int J Comput Mater Sci Surf Eng* 4(2):168–184
- Ragupathi P, Sivaram NM, Vignesh G, Selvam MD (2018) Enhancement of impact strength of a car bumper using natural fiber composite made of jute. *i-Manager's J Mech Eng* 8(3):39–45
- Raja RS, Manisekar K, Manikandan V (2013) Effect of fly ash filler size on mechanical properties of polymer matrix composites. *Int J Min Metall Mech Eng* 1:2320–4060
- Renner K, Móczó J, Pukánszky B (2009) Deformation and failure of PP composites reinforced with lignocellulosic fibers: effect of inherent strength of the particles. *Compos Sci Technol* 69(10):1653–1659
- Sathishkumar TP, Navaneethakrishnan P, Shankar S, Rajasekar R, Rajini N (2013) Characterization of natural fiber and composites: a review. *J Reinf Plast Compos* 32(19):1457–1476
- Sena R, Dehiya S, Pandel U, Banerjee MK (2015) Utilization of low grade coal for direct reduction of mill scale to obtain sponge iron: effect of reduction time and particle size. *Procedia Earth Planet Sci* 11:8–14
- Sharma A, Patnaik A (2018) Experimental investigation on mechanical and thermal properties of marble dust particulate-filled needle-punched nonwoven jute fiber/epoxy composite. *JOM* 70(7):1284–1288
- Sharma A, Purohit A, Nagar R, Patnaik A (2018) Effect of marble dust as filler on erosion behaviour of needle-punched-nonwoven jute/epoxy composite. In: *Epoxy composite*, 13 Dec 2018
- Sista KS, Dwarapudi S, Nerune VP (2019). Direct reduction recycling of mill scale through iron powder synthesis. *ISIJ Int ISIJINT-2018*
- Soni A, Patnaik A (2019) Study the effect of mill scale filler on mechanical properties of bidirectional carbon fibre-reinforced polymer composite. *Innovative design, analysis and development practices in aerospace and automotive engineering (I-DAD 2018)*. Springer, Singapore, pp 121–130
- Stachowiak GW, Batchelor AW (1993). *Engineering tribology*. In: *Tribology series*, vol 24, p 586
- Thakur VK (2013) Green composites from natural resources. CRC Press, Boca Raton
- Thakur VK, Thakur MK (2014) Processing and characterization of natural cellulose fibers/thermoset polymer composites. *Carbohydr Polym* 109:102–117

- Verma D, Senal I (2019) Natural fiber-reinforced polymer composites: feasibility study for sustainable automotive industries. In: Biomass, biopolymer-based materials, and bioenergy. Woodhead Publishing, UK, pp 103–122
- Yilmaz MG, Unal H, Mimaroglu A (2008) Study of the strength and erosive behaviour of CaCO<sub>3</sub>/glass fibre reinforced polyester composite. *Express Polym Lett* 2:890–895
- Yusriah L, Sapuan SM, Zainudin ES, Mariatti M (2014) Characterization of physical, mechanical, thermal and morphological properties of agro-waste betel nut (*Areca catechu*) husk fibre. *J Clean Prod* 72:174–180

# Chapter 7

## Erosive Wear Behaviour of Carbon Fiber/Silicon Nitride Polymer Composite for Automotive Application



Vikas Kukshal, Ankush Sharma, Vinayaka R. Kiragi, Amar Patnaik and Tapan Kumar Patnaik

**Abstract** The automotive industry is experiencing a radical change where the metallic components are replaced with the light weight fiber reinforced composite materials. Fiber reinforced polymer (FRP) components are an effective alternate offering improved properties such as reduced weight, good mechanical strength, corrosion resistance etc. Carbon fiber reinforced polymer (CFRP) is lighter than aluminum and stronger than iron and exhibits higher elasticity than titanium. In the present study, the carbon fiber and Silicon Nitride ( $\text{Si}_3\text{Ni}_4$ ) filler is used to fabricate FRP composite. Carbon fiber has high strength to volume ratio, high chemical resistance, low weight, high stiffness and high tensile strength whereas  $\text{Si}_3\text{Ni}_4$  is an abrasion resistant and thermally conductive material. Carbon fiber reinforced epoxy matrix composite is fabricated using vacuum assisted resin transfer molding (VARTM) technique with different weight percent of silicon nitride (0, 10, 20 and 30 wt%). 10 layers of carbon fiber are stacked in the glass mould for the fabrication of the composite. The erosion test is performed with varying impingement angle from  $45\text{--}90^\circ$ , impact velocity from 30 to 60 m/s and filler content from 0 to 30 wt%. It is found from the Taguchi design of experiment that the impact velocity is most significant factor and the filler content is the least significant factor. However, increase in the filler content increase the wear resistance of the fabricated composite.

**Keywords** Automotive industry · CFRP · Erosion wear · Taguchi design of experiment

---

V. Kukshal  
Mechanical Engineering Department, National Institute of Technology Uttarakhand, Srinagar,  
Uttarakhand 246174, India

A. Sharma · V. R. Kiragi · A. Patnaik (✉)  
Mechanical Engineering Department, Malaviya National Institute of Technology Jaipur, Jaipur  
302017, India  
e-mail: [patnaik.amar@gmail.com](mailto:patnaik.amar@gmail.com)

T. K. Patnaik  
Department of Physics, GIET University, Gunupur 765022, India

## 7.1 Introduction

The automotive industry is experiencing a radical change where the metallic components are replaced with the light weight fiber reinforced composite materials. The attention was focused more on the use of metals and alloys for the development of automotive components in the past. However, fiber reinforced polymer (FRP) composites are replacing metallic components in structures, housing, bushing, windshield wiper motors, shock absorbers, steering shaft joints and door hinges (Forintos and Czigany 2018). One of the most critical parameter for design of any product is the reduction in weight while increasing the load carrying capacity (Chung 2017). High-performance fiber reinforced composite is one of the key solution in designing new materials for such applications (Adam 1997). The application of composite in automotive sector has increased manifold in the recent years and is expected to increase tremendously in the future. The use of carbon fibre reinforced plastic (CFRP) in automotive industry is expected to increase to \$6.3 billion by 2021 with an average increase of 17.5% (Mazumdar 2016).

Fiber reinforced polymer (FRP) composite generally possesses high specific strength and enhanced stiffness as compared to the other materials such as metal, alloys, metal matrix composite. Both the natural fiber and the synthetic fiber are widely used as the reinforcement in the composite material and provide improved mechanical and wear resistance property for application in various industries (Gangil et al. 2019; Ghalia and Abdelrasoul 2019; Harsha and Jha 2008; Patnaik et al. 2010). However, synthetic fiber reinforced composites are more advantageous as compared to the natural fiber composites in terms of the mechanical properties. The synthetic fiber reinforced composites are widely used for the development of large number of automotive components. The common synthetic fibers used for the development of the composites are Carbon, Glass, Aramid and Kevlar. The property of epoxy such as high mechanical strength, low viscosity, low volatility and low shrinkage further enhances the performance of the composite. The weight of the carbon-fiber composites is about one-fifth of the steel and also comparable in terms of the stiffness and strength. This leads to the improved efficiency of the automobiles.

A number of automotive components are subjected to the impact of the particles resulting in the removal of materials from the surface. Most of the automobiles used in the desert area are subjected to the impact of the sand particles resulting in the loss of materials. Polymer composite are finding increased application under the arid conditions (Friedrich 2018). The use of filler along with the fiber as reinforcement has attracted many researchers to enhance the performance of the composites in the automotive industry. In the present study, Silicon Nitride ( $\text{Si}_3\text{Ni}_4$ ) is used as a filler and the carbon fiber as reinforcement in the polymer matrix composite. Carbon fiber reinforced polymer matrix composite is fabricated using vacuum assisted resin transfer molding (VARTM) technique with different weight percentage of silicon nitride. The present work investigates the erosive wear behavior of particulate filled carbon fiber reinforced epoxy composites. Design of experiments is used to study

the effect of impact velocity, impingement angle and filler content on the erosive wear behavior of composites.

## 7.2 Materials and Methods

Different types of materials are used as matrix in composites such as polymers, metals and ceramics. In modern composites, polymers are widely used as a matrix material because of its light weight, ease of fabrication and its compatibility with variety of reinforcements. Polymer matrices such as Epoxy, vinylester, phenolics and polyester are the most commonly used thermosets. Biphenol A epoxy (CY230) is used as a matrix material along with the Amide hardener Aradur (HY951) for the fabrication of composite.

Carbon fiber is used as reinforcement in the present study due to high strength to volume ratio, high chemical resistance, low weight, high stiffness and high tensile strength. These properties are very much advantageous in the automotive application. Filler or particulate are used along with the fiber to develop hybrid composite to further enhance the mechanical properties. Silicon Nitride ( $\text{Si}_3\text{Ni}_4$ ) particle of size 5 microns procured from Jayshree spheres and measures, Pune, India with 99.5% purity is used as a particulate for the fabrication of the composite material. The properties of the raw materials used in the current study are presented in Table 7.1. Various fibers and fillers used in the fabrication of the composite available in the literature are listed in Table 7.2.

### 7.2.1 Composite Fabrication

Carbon fiber reinforced epoxy matrix composite is fabricated using vacuum assisted resin transfer molding (VARTM) technique with different weight percentage of silicon nitride as given in Table 7.3. 10 number of carbon fiber layers are stacked in the glass mould for the fabrication of the composite samples. The VARTM technique is

**Table 7.1** Properties of raw materials used for fabrication of composite (Callister and Rethwisch 2007)

Material	Density, $\text{gm/cm}^3$	Ultimate tensile strength, MPa	Elastic modulus, GPa
Epoxy	1.176	35.79	2.4
Silicon Nitride	3.44	–	247
Carbon fiber	1.8	580	228

**Table 7.2** Effect of fiber/filler used in the fabrication of the composites

Author	Fibre/filler	Matrix	Effect of filler/fiber
Hyuga et al. (2004)	Carbon fibre	Silicon nitride	Carbon fibre helps in maintaining the low friction coefficient. Fracture strength decrease with increase in carbon fibre content
Guo et al. (1982)	Carbon fibre	Silicon nitride	Issue of incompatibility of carbon fibre and silicon nitride at high temperature
Suzuki et al. (1992)	Carbon fibre	Silicon nitride	Pullout fibre length is determined and considered in the pullout mechanism and processes
Xie et al. (2016)	Silicon nitride/carbon fibre	Bismaleimide (BMI) resin	Flexural strength and interlaminar shear strength and thermal resistance properties of the composites are improved
Friedrich et al. (2005)	Silicon nitride	Polyetheretherketone (PEEK) matrix nano composite	Reduction in frictional coefficient
Ramdani et al. (2015)	Silicon nitride (10–70 wt%)	Polybenzoxazine matrix	Improve thermal conductivity, thermal stability
Shimamura et al. (2015)	Both alpha and beta phase Silicon nitride	Epoxy resin	Increased thermal conductivity and influence on fracture pattern of composite is addressed
Ramdani et al. (2014)	Silicon nitride nanoparticles	Polybenzoxazine	Increase tensile strength and micro hardness. Increase in thermal and mechanical properties
Bodis et al. (2017)	Graphine	Silicon carbide	Fracture toughness (FT) increases 20% for 1 wt% MLG. FT is calculated at different sintering temperatures

(continued)

**Table 7.2** (continued)

Author	Fibre/filler	Matrix	Effect of filler/fiber
Ahmed and Ibrahim (2014)	Zirconium oxide nanofiller	Polymethyl-methacrylate (PMMA)	Best mechanical properties achieved at 7% ZrO <sub>2</sub> concentration. Increment in fracture toughness is seen
Sedlek et al. (2017)	Graphene Platelet (GPLs) (4–10wt%)	Boron carbide	Fracture toughness w. r. t GPLs addition is calculated and it increase with increase in wt% of GPLs
Li et al. (2017)	Multi layered graphene	Al <sub>2</sub> O <sub>3</sub> /TiC	Composite with 0.2 wt% MLG has highest fracture toughness
Rahman and Radford (2017)	Alumina nano-fiber, silicon carbide whisker, carbon nanofiber	Geopolymer matrix	2 vol% silicon carbide whisker shows largest improvement in K <sub>IC</sub> of geopolymer
Emiroglu et al. (2017)	Alumina Nanoparticles (0.5, 1.0, 2.0, and 3.0 wt%) of epoxy resin	Polymer concrete	Incorporation of ANPs into PC mixes steadily improved its fracture toughness
Belmonte et al. (2016)	Graphenenanoplatelets and reduced graphene oxide (rGO)	Silicon carbide	Outstanding mechanical performance and increment in fracture toughness of composites containing just 5 vol% of rGOs is observed
Basu et al. (2011)	HAp (Hydroxyapatite) and Al <sub>2</sub> O <sub>3</sub>	High density Polyethylene (HDPE)	Fracture toughness increase with increase in filler volume

**Table 7.3** Composition of carbon fiber reinforced composite

Designation	Composition
EC	Epoxy + carbon fiber
EC10	Epoxy + carbon fiber + 10 wt% silicon nitride
EC20	Epoxy + carbon fiber + 20 wt% silicon nitride
EC30	Epoxy + carbon fiber + 30 wt% silicon nitride

successfully used by many researchers to fabricate the composites (Sharma and Patnaik 2018; Choudhary et al. 2019a). The mould consists of a single die and preform over it. The  $\text{Si}_3\text{Ni}_4$  particles are sprayed over the carbon fiber and are placed over the mould before the entire vacuum bag is sealed. The vacuum is maintained in the complete set up and the mixture of resin and hardener is injected in the mould. The samples are allowed to cure for 24 h before removal from the mould. The tooling cost and the time required to fill the mould is very less as compared to the other fabrication process. The complete fabrication process is performed at room temperature. Concentration of the fibers and the adhesion between the layers is improved by the application of the pressure. The flowchart of the different processes involved in the fabrication process of composites using VARTM process is shown in Fig. 7.1.

### 7.2.2 Solid Particle Erosion

The solid particle erosion tests were performed using Ducom TR 471 according to ASTM D76 (Sharma et al. 2018). The pictorial diagram of solid particle erosion test rig is shown in Fig. 7.2. The solid particles are fed from hopper and the mass flow rate is controlled by the conveyor belt. The mix is carried by the conveyor belt and through the nozzle of diameter 1.5 mm made to strike the composite sample with desired velocity. The velocity of the erodent is selected in the range of 30–60 m/s. The stand-off distance between the sample and the nozzle is kept 10 mm. The impingement angle is selected as 45, 60, 75 and 90°. Silica is used as a erodent and the discharge is maintained at constant rate i.e. 2 g/min. The test coupon of size 25 mm × 25 mm were used to perform the erosion test. Taguchi design of experiment is selected for performing solid particle erosion test (Choudhary et al. 2019b; Kiragi et al. 2019). Taguchi method is one of the robust design which helps to improve the quality of response by reducing the variation in the experimentation as a result of efficient and systematic utilization of fixed table of array. It is a tool for designing a set of experiment providing much-reduced variance with optimum control parameters. The method uses an integrated approach for finding the influence of process parameters on performance on the developed composite with minimum number of experiments. The selected control factors for solid particle erosion along with their levels are shown in Table 7.4.

## 7.3 Result and Discussion

The performance of control factor (signal-to-noise ratio) is measured using Taguchi design of experiment technique. The signal-to-noise (S/N) ratio considers both the mean and the unpredictability into account. Considering smaller is better characteristic, S/N ratio for minimum erosion rate can be calculated as logarithmic value of the loss function as given in Eq. (7.1). Lower is the better characteristic:



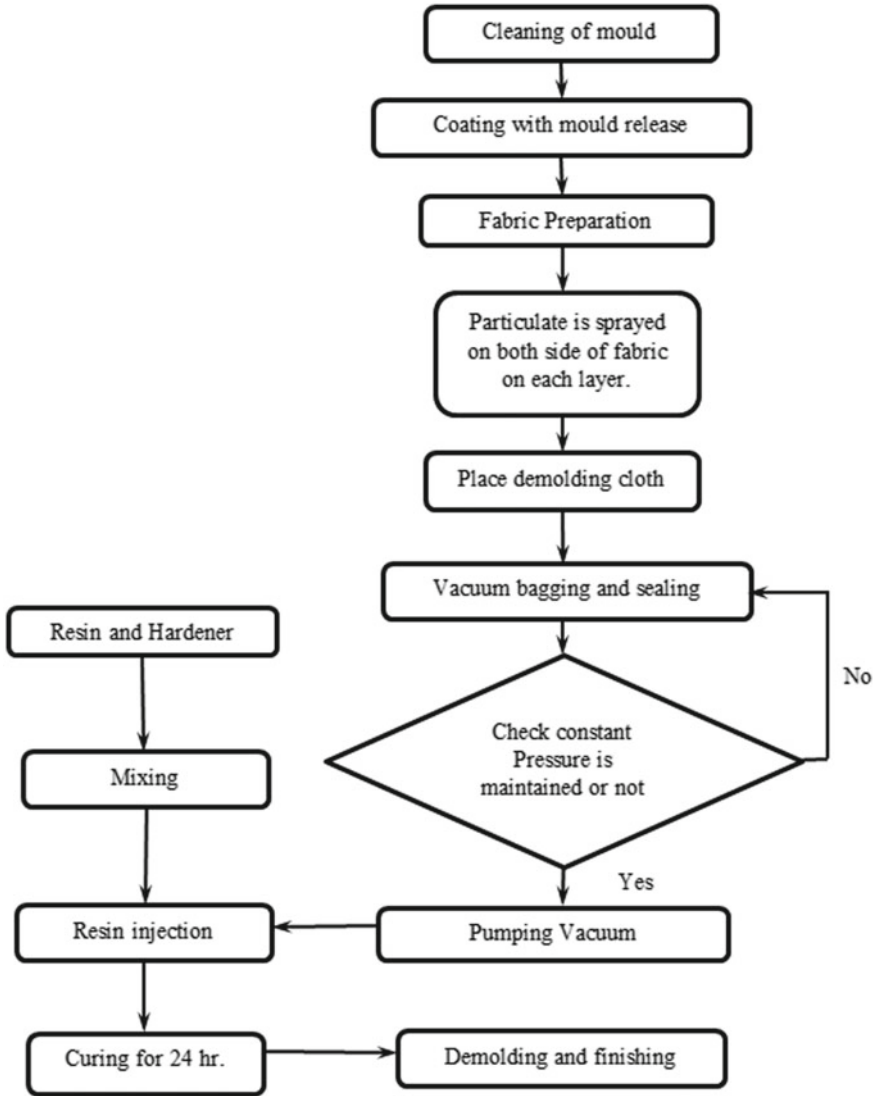
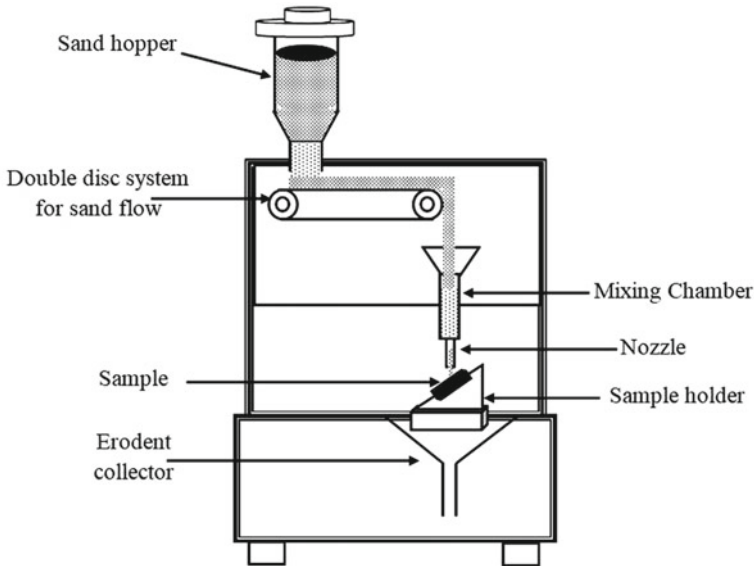


Fig. 7.1 Flowchart of the fabrication process of composite material using VARTM technique



**Fig. 7.2** Pictorial diagram of solid particle erosion test rig

**Table 7.4** Levels of various control factors

Control factor	Level				Unit
	I	II	III	IV	
A: Impact velocity	30	40	50	60	m/s
B: Impingement angle	45	60	75	90	Degree
C: Filler content ( $\text{Si}_3\text{Ni}_4$ )	0	10	20	30	wt%

$$\frac{S}{N} = -10 \log \frac{1}{n} \left( \sum_{i=1}^n (y_i^2) \right) \quad (7.1)$$

where,  $n$  is the number of observations, and  $y_i$  the observed data (Taguchi 1990).

The present work involves the systematic study of erosive wear performance of  $\text{Si}_3\text{Ni}_4$  based CFRP with the help of Taguchi analysis. The most important factors i.e. impact velocity, impingement angle and filler content are considered for the erosion tests with  $L_{16}$  orthogonal array. Analysis of variance (ANOVA) technique in-turn resembles the dominant factor that has significant contribution in erosive wear of CFRP. In Taguchi method, after assigning the individual factor to its appropriate levels, the obtained result is transformed to the output called Signal to Noise (S/N) ratio, which helps in predicting the quality characteristic of the obtained result. As the current study is based on wear analysis, it is desired to have small is the better characteristic condition in the three factors drawn at three levels with its corresponding S/N ratio as presented in Table 7.5.

**Table 7.5** L<sub>16</sub> orthogonal design for the set of experiment

S. No	Impact velocity	Impingement angle	Filler content	W1	W2	Mass loss (mg)	Erodent discharge (kg)	ER (mg/kg)	SNRAI	RESI1
1.	30	45	0	1.7229	1.717	0.0059	0.02	0.295	10.6036	1.14652
2.	30	60	10	1.9199	1.9132	0.0067	0.02	0.335	9.4991	-0.51704
3.	30	75	20	2.0566	2.0494	0.0072	0.02	0.36	8.8739	0.62289
4.	30	90	30	2.1634	2.1562	0.0072	0.02	0.36	8.8739	-1.25236
5.	40	45	10	1.9385	1.9278	0.0107	0.02	0.535	5.4329	-1.41037
6.	40	60	0	1.8212	1.8103	0.0109	0.02	0.545	5.2721	0.78089
7.	40	75	30	2.0433	2.0336	0.0097	0.02	0.485	6.2852	1.73891
8.	40	90	20	2.0707	2.0589	0.0118	0.02	0.59	4.5830	-1.10944
9.	50	45	20	2.0888	2.0756	0.0132	0.02	0.66	3.6091	1.66640
10.	50	60	30	2.0917	2.0764	0.0153	0.02	0.765	2.3268	0.91601
11.	50	75	0	1.8795	1.838	0.0415	0.02	2.075	-6.3404	-3.43581
12.	50	90	10	1.993	1.975	0.018	0.02	0.9	0.9151	0.85340
13.	60	45	30	2.0171	1.9982	0.0189	0.02	0.945	0.4914	-1.40256
14.	60	60	20	1.9398	1.9185	0.0213	0.02	1.065	-0.5470	-1.17986
15.	60	75	10	1.9729	1.951	0.0219	0.02	1.095	-0.7883	1.07401
16.	60	90	0	1.8045	1.7838	0.0207	0.02	1.035	-0.2988	1.50840

Where W1 = Initial weight, W2 = Final weight, ER = Erosion rate, SNRAI = Signal to noise ratio, RESI = Residua

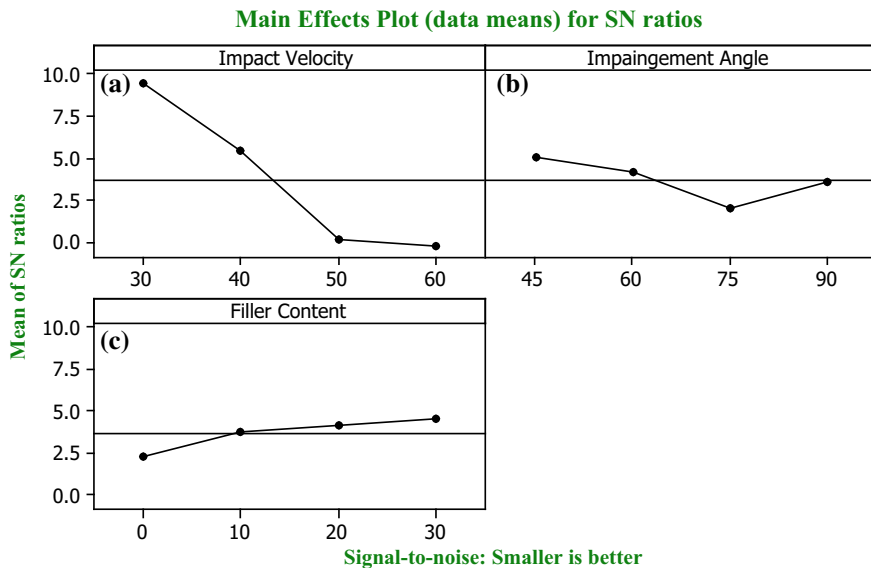


**Fig. 7.3** Main effect plot of S/N Ratio

Figure 7.3 shows the main effect plot of S/N ratio. The increase in impact velocity from 30 m/s implies decrease in mean of S/N ratio in turn implies the increased erosive wear rate. This may attributes to the reduced time of travel to reach the target material with the increased velocity and also the increased kinetic energy of the impacting erodent. Also, Fig. 7.3 implies that the decrease in S/N ratio results in increased wear rate of the  $\text{Si}_3\text{Ni}_4$  induced CFRP. Wear rate of the CFRP composite is found to increase up to  $75^\circ$  impingement angle irrespective of impact velocity. This behavior may be due to the brittle nature of the fabricated composites as well the dominant normal component of the impacting erodent. However,  $90^\circ$  impingement angle shows reduction in the wear rate due to the impact of the erodent normal to the samples thereby reducing the removal of material. In case of the filler content, it is observed that with the increase in the wt% of  $\text{Si}_3\text{Ni}_4$ , there is a continuous increase in the S/N ratio. This implies that the addition of the filler content in the composite results in the decrease in the wear rate. This may be attributed to the presence of the hard  $\text{Si}_3\text{Ni}_4$  particles in the CFR composite resulting in the decrease in the wear rate.

In Taguchi, ANOVA is a subsequent step followed to find out statistical significance of factors adopted like impact velocity, impingement angle and filler content on erosion wear rate on experimental data. A confidence of 95% was considered in the analysis. The ANOVA results for the erosion rate of  $\text{Si}_3\text{Ni}_4$  filled carbon fiber reinforced composite are shown in Table 7.6. The last column of Table 7.6 indicates significance of individual control factor on erosion rate. Smaller the p-value, better is the significance of the control factor on the erosion rate. From Table 7.6, it is

**Table 7.6** ANOVA table for Si<sub>3</sub>Ni<sub>4</sub> filled CFRP composite

Source	DF	Seq SS	Adj SS	Adj MS	F	P
A: Impact velocity	3	258.879	258.879	86.293	15.53	0.003
B: Impingement angle	3	19.466	19.466	6.489	1.17	0.397
C: Filler content	3	11.007	11.007	3.669	0.66	0.606
Error	6	33.329	33.329	5.555		
Total	15	322.681				

Where DF = Degree of freedom, Seq SS = Sequential sum of square, Adj SS = Adjusted sums of square, Adj MS = Adjusted mean squares

observed that the p-value of impact velocity is smallest and hence it the most significant factor that controls the erosion rate of the composite. Similarly, the second most influential factor is the impingement angle with p-value equivalent to 0.397 and the filler content is the third significant factor with p-value of 0.606.

## 7.4 Conclusion

The carbon fiber/silicon nitride polymer composite were successfully fabricated using VARTM technique with different weight percent of silicon nitride (0, 10, 20 and 30 wt%). Influence of various factors such as impact velocity, impingement angle and filler content on the erosion wear behavior of the composite is determined. It is found that the impact velocity is most significant factor and the filler content is the least significant factor. However, increase in the filler content increase the wear resistance of the fabricated composite. The fabricated composites have shown the better wear resistance and hence can be used in the development of automotive components subjected to the impact of solid particles.

## References

- Adam H (1997) Carbon fibre in automotive applications. *Mater Des* 18(4–6):349–355
- Ahmed MA, Ebrahim MI (2014) Effect of zirconium oxide nano-fillers addition on the flexural strength, fracture toughness, and hardness of heat-polymerized acrylic resin. *World J Nano Sci Eng* 4(02):50
- Basu B, Jain D, Kumar N, Choudhury P, Bose A, Bose S, Bose P (2011) Processing, tensile, and fracture properties of injection molded Hdpe-Al<sub>2</sub>O<sub>3</sub>-HAp hybrid composites. *J Appl Polym Sci* 121(5):2500–2511
- Belmonte M, Nistal A, Boutbien P, Román-Manso B, Osendi MI, Miranzo P (2016) Toughened and strengthened silicon carbide ceramics by adding graphene-based fillers. *Scripta Mater* 113:127–130

- Bodis E, Cora I, Balazsi C, Nemeth P, Karoly Z, Klebert S, Fazekas P, Keszler AM, Szepvolgyi J (2017) Spark plasma sintering of graphene reinforced silicon carbide ceramics. *Ceram Int* 43(12):9005–9011
- Callister WD, Rethwisch DG (2007) *Materials science and engineering: an introduction*, Vol 7. Wiley, New York, pp 665–715
- Choudhary M, Sharma A, Dwivedi M, Patnaik A (2019a) A comparative study of the physical, mechanical and thermo-mechanical behavior of GFRP composite based on fabrication techniques. *Fibers Polym* 20(4):823–831
- Choudhary M, Sharma A, Shekhawat D, Kiragi VR, Nigam R, Patnaik A, (2019b) Parametric optimization of erosion behavior of marble dust filled aramid/epoxy hybrid composite. *Epoxy hybrid composite* 31 Mar 2019
- Chung DDL (2017) Processing-structure-property relationships of continuous carbon fiber polymer-matrix composites. *Mater Sci Eng R Rep* 113:1–29
- Emiroglu M, Douba AE, Tarefder RA, Kandil UF, Taha MR (2017) New polymer concrete with superior ductility and fracture toughness using alumina nanoparticles. *J Mater Civ Eng* 29(8):04017069
- Forintos N, Czigany T (2018). Multifunctional application of carbon fiber reinforced polymer composites: electrical properties of the reinforcing carbon fibers—a short review. *Compos Part B Eng*
- Friedrich K, Zhang Z, Schlarb AK (2005) Effects of various fillers on the sliding wear of polymer composites. *Compos Sci Technol* 65(15–16):2329–2343
- Friedrich K (2018) Polymer composites for tribological applications. *Adv Ind Eng Polym Res*
- Gangil B, Kukshal V, Sharma A, Patnaik A, Kumar S (2019) Development of hybrid fiber reinforced functionally graded polymer composites for mechanical and wear analysis. *AIP Conf Proc* 2057(1):020059
- Ghalia MA and Abdelrasoul A (2019) Compressive and fracture toughness of natural and synthetic fiber-reinforced polymer. In: *Mechanical and physical testing of biocomposites, fibre-reinforced composites and hybrid composites*. Woodhead Publishing, pp 123–140
- Guo JK, Mao ZQ, Bao CD, Wang RH, Yan DS (1982) Carbon fibre-reinforced silicon nitride composite. *J Mater Sci* 17(12):3611–3616
- Harsha AP, Jha SK (2008) Erosive wear studies of epoxy-based composites at normal incidence. *Wear* 265(7–8):1129–1135
- Hyuga H, Jones MI, Hirao K, Yamauchi Y (2004) Influence of carbon fibre content on the processing and tribological properties of silicon nitride/carbon fibre composites. *J Eur Ceram Soc* 24(5):877–885
- Kiragi VR, Patnaik A, Singh T, Fekete G (2019) Parametric optimization of erosive wear response of TiAlN-coated aluminium alloy using Taguchi method. *J Mater Eng Perform* 28(2):838–851
- Li ZL, Zhao J, Sun JL, Gong F, Ni XY (2017) Reinforcing effect of graphene on the mechanical properties of Al<sub>2</sub>O<sub>3</sub>/TiC ceramics. *Int J Miner Metall Mater* 24(12):1403–1411
- Mazumdar S (2016) The road to success in carbon composites for the automotive market. *JEC composites magazine*, pp 21–23
- Patnaik A, Satapathy A, Chand N, Barkoula NM, Biswas S (2010) Solid particle erosion wear characteristics of fiber and particulate filled polymer composites: a review. *Wear* 268(1–2):249–263
- Rahman AS, Radford DW (2017) Evaluation of the geopolymer/nanofiber interfacial bond strength and their effects on Mode-I fracture toughness of geopolymer matrix at high temperature. *Compos Interfaces* 24(8):817–831
- Ramdani N, Derradji M, Feng TT, Tong Z, Wang J, Mokhnache EO, Liu WB (2015) Preparation and characterization of thermally-conductive silane-treated silicon nitride filled polybenzoxazine nanocomposites. *Mater Lett* 155:34–37
- Ramdani N, Wang J, Wang H, Feng TT, Derradji M, Liu WB (2014) Mechanical and thermal properties of silicon nitride reinforced polybenzoxazine nanocomposites. *Compos Sci Technol* 105:73–79

- Sedlak R, Kovalcikova A, Mudra E, Rutkowski P, Dubiel A, Girman V, Bystricky R, Dusza J (2017) Boron carbide/graphene platelet ceramics with improved fracture toughness and electrical conductivity. *J Eur Ceram Soc* 37(12):3773–3780
- Sharma A, Patnaik A (2018) Experimental investigation on mechanical and thermal properties of marble dust particulate-filled needle-punched nonwoven jute fiber/epoxy composite. *JOM* 70(7):1284–1288
- Sharma A, Purohit A, Nagar R, Patnaik A (2018) Effect of marble dust as filler on erosion behaviour of needle-punched-nonwoven jute/epoxy composite. *Epoxy composite*
- Shimamura A, Hotta Y, Hyuga H, Kondo N, Hirao K (2015) Effect of amounts and types of silicon nitride on thermal conductivity of  $\text{Si}_3\text{N}_4$ /epoxy resin composite. *J Ceram Soc Jpn* 123(1441):908–912
- Suzuki T, Sato M, Sakai M (1992) Fiber pullout processes and mechanisms of a carbon fiber reinforced silicon nitride ceramic composite. *J Mater Res* 7(10):2869–2875
- Taguchi G (1990) Introduction to quality engineering. Asian Productivity Organization, Tokyo
- Xie C, Han Y, Zhao R (2016) Highly thermal conductivity silicon nitride/carbon fibres/bismaleimide composites. *Polym Compos* 37(2):468–471

# Chapter 8

## Effects of Reinforcement on Tribological Behaviour of Aluminium Matrix Composites



Manoj Kumar Gupta, Lalit Ranakoti and Pawan Kumar Rakesh

**Abstract** This segment encompasses the tribological changes usher by the addition of various reinforcements to the aluminium metal matrix composite. Aluminium matrix composites (AMCs) are being successfully tailored to achieve certain mechanical properties for specific applications. AMCs can be called as advance engineering materials with excellent properties. High hardness, high thermal conductivity, good yielding strength, strength to weight ratio, low coefficient of thermal expansion and excellent wear resistance are some of the attractive properties which AMCs possess. Applications like automobile, aerospace and several other industrial applications are being attracted towards AMCs due to its qualities. Various reinforcements are available in the market which can be added to aluminium metal to further enhance its properties. Particularly, in the field of tribology, these reinforcements have proved their worth in AMCs. To examine the effects of various reinforcements, a comprehensive study has been reported in the field of tribology for AMCs.

**Keywords** Metal Matrix Composite · Tribology · Mechanical Properties · Aluminum · Automobile

### 8.1 Introduction

Two different material with different characteristics is brought together to obtain the desired properties and termed as composite materials. This composite usually possess special features which are generally better than the features of the individual section. Composite materials have the fundamental advantage of being lightweight, low density, good quality and reduced weight of the completed part (Guo and Leu 2013). Phenomenal attention leading to innovation in the application has been received by

---

M. K. Gupta  
Mechanical Engineering Department, H.N.B. Garhwal University, Srinagar Garhwal,  
Uttarakhand, India

L. Ranakoti · P. K. Rakesh (✉)  
Mechanical Engineering Department, National Institute of Technology Uttarakhand, Srinagar  
Garhwal, Uttarakhand, India  
e-mail: [pawanrakesh@nituk.ac.in](mailto:pawanrakesh@nituk.ac.in)



composite materials in recent years. Metals are characterized by their physical, chemical and mechanical properties (Helu et al. 2011; Nair et al. 1985). These properties are influenced by the addition of reinforcements to it. Method of reinforcement, size of reinforcement particle and the level of dispersion are some of the variables which control the property of the output composite. In addition, the surface between the base metal and the reinforced particle has a critical role to play (Lalit et al. 2018). Moreover, environmental condition like dry or lubricated sliding condition provides the basis for the choice of metal matrix and reinforcing materials. The metal matrix composites (MMC) derived from the combination of the reinforcing element to the base metal. This reinforcing element can be of metal, ceramic or organic nature. MMCs are produced by the dispersion of reinforcement to the base metal. When the base is selected as aluminium, then the metal matrix is called Aluminum matrix composites (AMCs). Fly ash, silicon carbide (SiC), graphite, red mud, rice husk, cow dung and some common agro-based filler are reinforcing fillers which are added to the aluminium metal for the enhancement of its mechanical and tribological properties (Prasad and Asthana 2004). The demand for AMCs in the industries have been increasing due to its attractive properties such as high strength, high thermal conductivity, high specific modulus, good abrasion and wear resistance, and low density etc. Particularly, in the field of tribology, extensive research has been carried out for aluminum metal. An experimental result has been reported by various researchers which explained the potential of aluminium metal to be used as a competent tribological material (Kumar et al. 2011). In this regards, several techniques have been evolved to fabricate the AMCs using various reinforcing material (Surappa 2003). Being the case, the tribological behaviour of AMCs with the addition of various reinforcing materials and their criticalities has been discussed in the coming section.

## 8.2 Reinforcement Particle in AMC

The reinforcement materials in AMCs may be oxides, carbides, borides and nitrides of ceramics materials. The important conventional reinforcement materials used in the aluminium matrix composites are carbon/graphite, silicon carbide, alumina, zirconia, zircon, titanium oxides, titanium carbide, molybdenum disulphate, boron carbide, tungsten carbide, cerium oxide, titanium nitride, ferric oxide, titanium diboride, chromium oxide and carbon nanotubes. These reinforcement materials may be in the form of particulate, whisker or fibers. The physical, mechanical, tribological and other desired properties of composite depend upon factors like fabrication techniques and processing temperature, and reinforcement shape, size, chemical affinity and wettability with the matrix material. The selection of the reinforcement mostly depends on the targeted application and compatibility with matrix materials. Boron carbide ( $B_4C$ ) offers outstanding neutron absorptivity along with thermal and wears resistance. The  $B_4C$  reinforced composites contain the excellent neutron absorbing capability and used as main neutron shield material in reactors (Dinaharan et al. 2016). The mechanical property of Mg–CNT composites is outstanding whereas

Mg–Al<sub>2</sub>O<sub>3</sub> composite possesses greater wear resistance (Lu et al. 2013). The reinforcement particle dimension is an important factor and required to be considered in composite fabrication. Normally, two scales viz. micrometer and nanometer of particles are incorporated in the composites. The coarse particles have larger grains during recrystallization whereas fine particle reduces grain size. The dimensions and volume fraction of the reinforcements extensively affect the properties and microstructure of surface composites.

The availability and high-cost ceramic reinforcing materials have a major constraint for the development of metal matrix composites particularly in developing countries (Bhandakkar et al. 2014). Other challenges of metal matrix composites are poor ductility and fracture toughness. The various researchers addressed and resolved these problems by selecting the proper reinforcing materials. The reinforcing materials have a major role in determining the whole performance of the composite materials. Mainly three strategies are used to improve the performance of composites materials as well as to curtail the cost (Kok 2005). The first strategy involves finding alternative and cheaper reinforcements. The aim is to provide a solution to the problems of high-cost conventional reinforcements. The agro and industrial wastes ashes such as rice husk, coconut shell and sugar cane bagasse, bamboo leaf, pine needle ash and fly ash are some of the alternatives reinforcing materials that have been used to resolve issues of high cost and limited availability of conventional reinforcements (Loh et al. 2013; Ubolluk et al. 2010; Lancaster et al. 2013). The use of these alternative reinforcements showed noteworthy enhancement in the properties of the composites as compared to the matrix material. The second strategy is to optimize the properties of composites by using nanoscale particle size of reinforcement materials instead of micron-scale particles (Madakson et al. 2012; Anilkumar et al. 2011). The third strategy involves using two or more reinforcing materials are called as hybrid composites. The aim of this approach is to reduce the cost of composite coupled with property optimization (Gupta and Rakesh 2019; Gupta et al. 2016; Gupta 2018). Some of the commonly used reinforcement materials in the aluminum matrix are listed in Table 8.1.

### 8.3 Techniques of Manufacturing AMCs

Many ways have been evolved to fabricate the AMCs. Powder metallurgy and casting method are some of the frequently used techniques. Powder metallurgy produces quality AMCs with higher cost as compared to AMCs produced by the casting method. Thus only specially assigned components are produced by powder metallurgy with specific characteristics. Widely applied techniques in the production of AMMCs are squeeze casting, compo casting and stir casting.

**Table 8.1** Reinforcement and their effects in aluminium matrix

Reinforcement	Matrix	Effects
TiO <sub>2</sub>	Al and Al–Mg	<ol style="list-style-type: none"> <li>1. Formation of reactive layers MgO/Ti leads to covering of particles</li> <li>2. Significant reduction in the formation of Al<sub>4</sub>C<sub>3</sub></li> </ol>
Al <sub>2</sub> O <sub>3</sub>	Al and Al–Mg	<ol style="list-style-type: none"> <li>1. Good protection in whiskers but no protection in Particulates</li> </ol>
SiO <sub>2</sub>	Al and Al–Mg	<ol style="list-style-type: none"> <li>1. The reaction between Al reacts SiC precede only after Al reacts with SiO<sub>2</sub></li> <li>2. The interfacial reaction depends on the alloy composition and thickness of the SiO<sub>2</sub> layer</li> </ol>
Al <sub>2</sub> O <sub>3</sub>	Al	<ol style="list-style-type: none"> <li>1. Good reaction barrier but poor wettability</li> </ol>
SiO <sub>2</sub>	Al	<ol style="list-style-type: none"> <li>1. Modulus of elasticity increases</li> <li>2. Degradation of fiber resulted in lower strength</li> </ol>
SiC	Al	<ol style="list-style-type: none"> <li>1. Fibers are protected during processing and improved mechanical properties</li> </ol>
Titanium	Al	<ol style="list-style-type: none"> <li>1. Promote wetting</li> <li>2. Improvement in interfacial reaction between Al and C</li> <li>3. Reaction troubles the coating</li> </ol>
Nickel	Al	<ol style="list-style-type: none"> <li>1. Formation of NiAl<sub>3</sub> around the fibers including wetting</li> </ol>
Copper	Al	<ol style="list-style-type: none"> <li>1. Wetting and uniformity of fibers get improved</li> </ol>

### 8.3.1 Squeeze Casting

It is one of the oldest and most frequently applied techniques in the industry. It is primarily used for the production of automotive parts (Aghajanian et al. 1991). The schematic diagram of squeeze casting has been shown in Fig. 8.1. This technique is based on the melting of metal, matrix and alloys. Metals in melting state and at a pressure above 100 MPa are allowed to take the space of pores and volume of preform (Vencl et al. 2004). The preform must have a property of porosity enough to confirm the appropriate filling and it is made up of particles of reinforcement materials. A strong bond between the matrix and reinforcement can be assured due to the following characteristics of the preform. This method deals with the sudden change of phase of metal from liquid to solid state which results in a composite structure of finer grains (Ruehle and Evans 1989). In addition, a product with a smoother surface is obtained. Rapid pressing is applied in this technique which leads to increased productivity and greater significance towards practical approach (Rohatgi and Asthana 2001). Disadvantages of this method are expensive tools and their maintenance as higher pressure and temperature has to be sustained by the tool. Damaging of the tool can lead to error in the dimension of the final product.

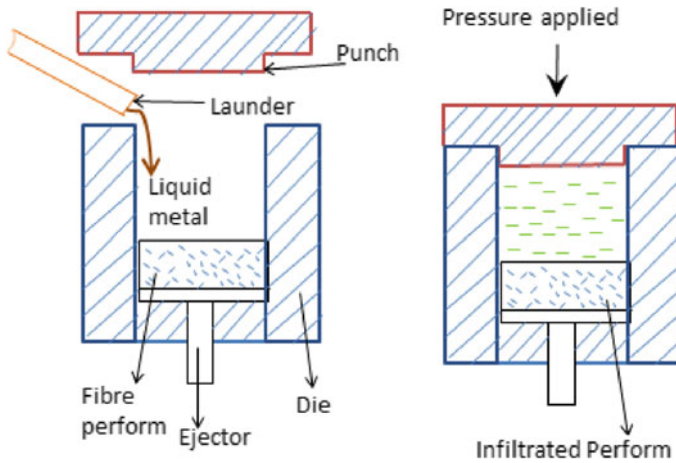


Fig. 8.1 Schematic diagram of squeeze casting

### 8.3.2 Compoasting

Hypo and hyper-eutectic alloys which are in the semi-solid state can be reformed by the semi-solid forming which comprises various methods and composting is one of them. Semi-solids are those materials which act as pseudo-plastic fluid when undergoes shear forces (Rohatgi 1991). Thus the viscosity of the fluid does not remain constant but depends upon the intensity of the force. This change in viscosity allows easy penetration and entanglement of particulates into the matrix material. Generation of fumes at the boundary of reinforcement and matrix is another advantage of solving the problem of wettability. Compo casting can be carried out at lower temperature and pressure. This makes it the best suited method with respect to energy consumption and tool life. Shear rate and mixing rate ratio are varied which makes it suitable for the distribution of reinforcement into the matrix (Mehrabian et al. 1974). The main drawback is the non-processability of eutectic alloys by this method but still, alloys with semi-solid states are considered to be processed by compo casting for the most appropriate output.

### 8.3.3 Stir Casting

Schematic diagram of stir casting has been shown in Fig. 8.2. The reinforcement melted above the liquidus temperature and along with stirring is performed to attain appropriate distribution. It is the simplest among all the three and productive also. Pure metals with matrices at eutectic state can be easily cast by this technique (Hosking et al. 1982; Ghosh and Ray 1988). Low-cost casting can be easily executed with

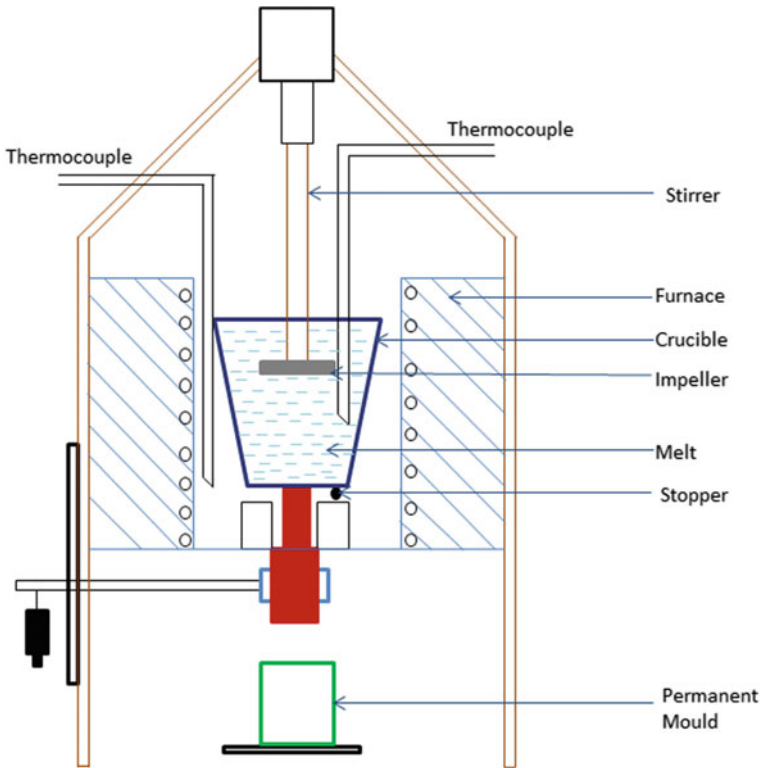


**Fig. 8.2** Schematic diagram of stir casting setup

complex geometry such as thin walls products. The major drawback is the wettability of the reinforced particle in the melt of matrix.

## 8.4 Tribology of AMCs

Study of friction and wear is termed as tribology study. Wear is a phenomenon in which the material removes gradually from the surface of a body. It occurs due to the continuous rubbing of materials in the contact surface of two bodies. For the wear to take place, plastic deformation at a localized place and microcracks are two major reasons. Physical, chemical and mechanical are other phenomena that lead to wear. The mechanism of wear depends upon adhesion, corrosion, oxidation, fatigue, fretting and abrasion. These mechanisms are partially or fully in relation to one another. Wear cannot be completely suppressed but can be reduced to some extent by the application of lubrication. Lubrication forms a smooth layer between the mating bodies and helps in smooth operation with a reduction in wear. Basically,

wear in AMCs occur due to two main reasons (Wilson and Alpas 1997). First one is the wear due to oxidation and the second one is wear of metallic surface. Wear due to oxidation is considered as mild wear while the severity of metallic wear appears to be higher. The severe wear initiates the seizure which is called seizure point. Several studies have been reported in relevance to the analysis of effects of load, sliding velocity and composition on the seizure point. These variables affect the seizure point until its initiation but as the execution of seizure point starts, the effects of the variables also start diminishing. Seizure point has harmful effects on the body as the surface deteriorates with the occurrence of seizure. Many particulates are being added to aluminium as being discussed earlier. Silicon is most commonly used particulate in the aluminium base metal. Wear properties of aluminium generally increase with the addition of Silicon. Literature available in tribology of AMCs is in support of the reinforcement of metal particulates to the aluminium. An alloy of Al–Cu has been investigated for the wear loss. It was found that addition of 30%  $\text{Al}_2\text{O}_3$  to Al–Cu alloy leads to reduction in wear rate from  $2 \times 10^{-3}$  to  $0.5 \times 10^{-3}$   $\text{mm}^3/\text{min}$  under the dry test condition, withstanding 10 N loads at 3.6 m/s of sliding speed (Deuis et al. 1997). Similarly, the wear rate reduces significantly while using SiC as reinforcement. It was reported that wear rate down to  $4 \times 10^{-12}$  to  $12 \times 10^{-3}$   $\text{mm}^3/\text{min}$  on the addition of 10% SiC to the Al–Cu alloy in the similar dry condition at 1 m/s sliding speed with a sliding distance of 500 m (Casati and Vedani 2014). This reduction in wear rate varied according to the material properties. In case of Al356 aluminium alloy, the addition of 5% SiC brings the wear rate down to  $12 \times 10^{-3}$   $\text{mm}^3/\text{min}$  from  $18 \times 10^{-3}$   $\text{mm}^3/\text{min}$  under the 5 N load at 0.4 m/s of sliding speed and 1000 m of sliding distance (Yalcin and Akbulut 2006). As the percentage of particle reinforcement increase the wear strength of the metal matrix composite increases. The total wear loss carried on pin-on-disc has been found for the AlMgSi metal to be 35 mg which was reduced to 25 mg and 20 mg at 3% and 5% of SiC respectively at sliding speed of 2.64 m/s and sliding distance of 3200 m a distinct grade of aluminium known as Al6061 has been investigated for the wear loss. Load conditions were set at 150 N with the sliding speed of 2000 rpm (Gürler 1999). It was found that total wear loss reduced from 3 mg to 1.2 mg with the incorporation of 30% SiC to the Al6061 (Reihani 2006). It has been shown that wear loss increases as the load increases. The properties of reinforcement also affect the tribological properties of the fabricated composite. Figure 8.3 revealed wear rate of hybrid composite is superior to the  $\text{B}_4\text{C}$  and TiC mono reinforced composites. Furthermore,  $\text{B}_4\text{C}$  reinforced composite exhibited less wear. Figure 8.4 showed that coefficient of friction of  $\text{B}_4\text{C}$  reinforced composite is least as compared to other composite and matrix material as a result this composite exhibited less wear rate.

Composite of Al–Cu with 13% addition of SiC has been investigated at 1 m/s of sliding speed with the sliding distance of 1000 m. The wear loss was found to be 3 mg, 4 mg and 5 mg under the load of 30 N, 50 N and 70 N respectively (Lim et al. 1999). It was also reported that oxidation wear is independent of load, percentage of reinforcement and particle size. The tribological properties of composites depend upon the surface roughness of testing disc. The effect of surface roughness of GCr15

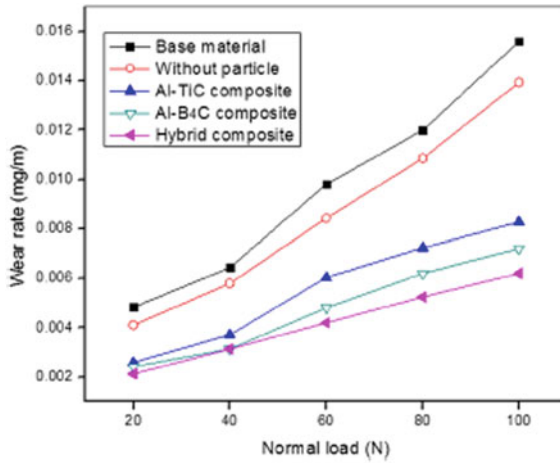


Fig. 8.3 Wear properties of composites (Yuvaraj et al. 2017)

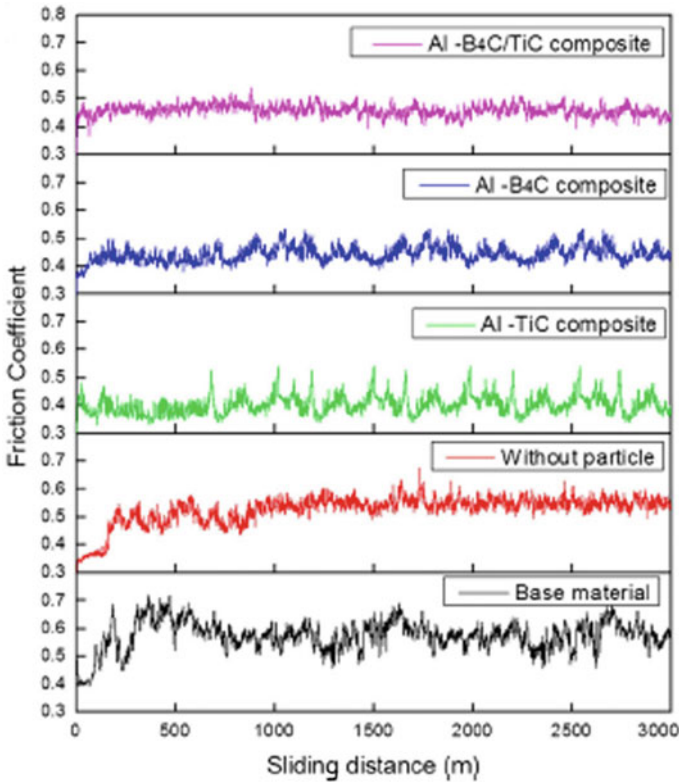
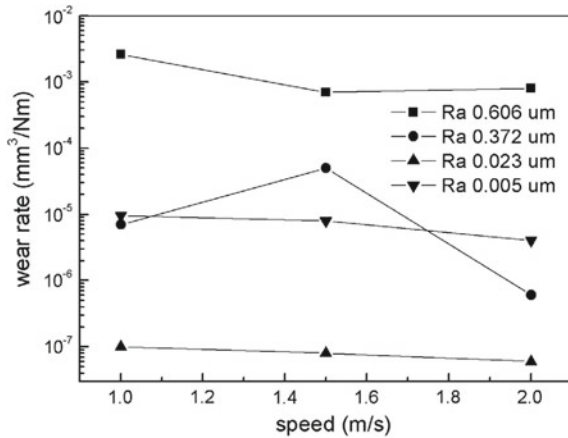


Fig. 8.4 Coefficient of friction of composites (Yuvaraj et al. 2017)

**Fig. 8.5** Wear rate of  $TiB_2/Al$  composite against GCr15 bearing steel as a function of sliding speed and surface roughness under dry sliding condition (Tian et al. 2014)



steel disc (Ra 0.606, 0.372, 0.023, 0.005  $\mu m$ ) on  $TiB_2/2024Al$  composites investigated shows that Ra 0.023  $\mu m$  disc exhibited lowest friction coefficient and wear rate as shown in Fig. 8.5.

A comparative study for the AMC, grey cast iron and semi-metallic material of brake shoe lining has also been reported (Natarajan et al. 2006). It was reported that MMCs are more wear resistant as compared to grey cast iron and metallic brake shoe lining under similar working condition.

## 8.5 Mechanical Properties of AMCs

Various studies are also available related to the mechanical properties of the aluminium based metal matrix. One of the work was carried out to compare the mechanical properties of the Al6061 and Al7075 with the reinforcement of SiC and  $Al_2O_3$  respectively (Kumar et al. 2010). The composite was prepared with the help of stir casting. It was observed that hardness increased from 97 VHN and 109 VHN for Al6061 and Al7075 respectively. Improvement in the tensile strength was also reported in their studies which were observed to be 68% and 24% for Al6061 and Al7075 respectively. Concluding remarks show that reinforcement of SiC brings better mechanical and tribological properties than  $Al_2O_3$ . Mechanism of wettability is also the main concern during the processing of aluminium metal matrix. Factors like free silicon kinetics of SiC and wetting angle have an enormous effect on the wettability (Jones and Atkinson 1993). However, it should be noted that incorporation time is the most important factor for the wetting reaction to take place. Particulate to be wetted fully need more time but the incorporation of magnesium and titanium reduces the wetting time of particulate (Kobashi and Choh 1993). Discussion on the interface bonding of the particulate and the aluminium matrix would be valuable. Silicon takes time to melt with the aluminium thus processing time is generally kept



large. This leads to an increase in the concentration of silicon at the interface thus prevent the formation of  $Al_4C_3$  at the interface which further makes the composite uniform (Sozhamannan and Prabu 2009).  $TiB_2$  is commonly known reinforcement used in the aluminum metal matrix. Incorporation of 12%  $TiB_2$  in Al6061 leads to an increase in tensile, hardness and young modulus but decreases the ductility (Christy et al. 2010). If we look at the stress-strain behaviour of aluminium metal matrix composite, silicon carbide with 40% volume in Al6061 shows higher modulus of elasticity but lower ductility. The type of reinforcement i.e. whisker, nodule particulate or discontinuous, and the matrix used also has a greater role in the properties of the composite (McDanel 1985).

On the other hand, using the atmosphere of argon during the processing of aluminium metal matrix affects the fluidity due to the presence of silicon. Argon prevents the formation of oxides film at the surface and wetting has no role to play in the presence of argon. Moreover, the presence of magnesium acts as a catalyst which enhances the phenomena of wetting (Moraes et al. 2006). Percentage of particulate has a major role in the aluminium metal matrix composite. Increase in the percentage of  $TiB_2$  in Al6061 leads to an increase in yield and ultimate stress. Generally, the percentage of  $TiB_2$  is kept below 15%. The increase in yield and ultimate stress is found to be about 53% and 44% respectively (Sreenivasan et al. 2011; Lü et al. 2001; RC and Ramakrishnan 1996). In case of formation of  $\alpha-Al_2O_3$  at the surface of the metal matrix, particulates like  $TiO_2$  and  $B_2O_3$  gets segregated at the grain boundaries which lead to uniformity of the particulate at in the metal matrix (Zhu et al. 2007). Several studies have also been reported regarding the machinability of the aluminum metal matrix. Various parameters like speed, feed, depth of cut, angle of cut etc. have been optimized in the work carried out earlier. Effect of tool material, the lubricant used and the reinforcement material on the aluminium metal matrix are also been discussed. Machining of Al–SiC requires low feed and high speed for good surface finish (Manna and Bhattacharayya 2005). The similar parameter is required for the machining of A356–SiC composite to obtain better surface finish (Muthukrishnan et al. 2008) but the case of Al2024 reinforced with  $Al_2O_3$  is different as the surface gets rough as the speed is increased. Particle size and their percentage have a significant role to play. Smaller particle size increases the surface roughness and vice versa (Kök 2011).

## 8.6 Applications of AMCs

Engineering industries require lightweight, strong and durable material. High corrosion resistance and thermal resistance would be the icing on the cake. Aluminium is lighter in weight as compared to conventional material like cast iron and steel. Applications of AMMCs in industries would lead to a reduction in mass, higher efficiency which further resulted in low fuel requirement and low vehicle emission. AMCs are better tribological material which extends their applications in a field where higher wear takes place. Primarily, AMCs are treated as an avionics material but later made

its place in the field of automotive also. A product like engine blocks, pistons, brakes, and the cylinder is now being developed by AMCs. Numerous reports have been presented for the further possible applications of AMCs. A diesel engine was developed by Toyota motor in 1985 by squeeze casting method with the incorporation of  $\text{Al}_2\text{O}_3$  into the Al metal matrix. Later on, Honda motor has employed a similar technique in its manufacturing system since 1990 (Surappa 2003). Applications of AMCs can also be seen in power plant components like heat exchanger, cooling transmission etc. (Vencl et al. 2004). Reinforcing the Al with solid lubricants shows anti-galling and anti-seizing properties which have extensive application in high-temperature tribosystems.

## 8.7 Conclusion

The sets of microscopic interaction are the basic causes of friction and wear. The tribological field requires those materials which require high wear resistant along with optimum strength. Aluminium is a lightweight, strong, durable material but lack in tribological properties. Various reinforcements can be added to aluminium to enhance its wear and resistance. Percentage, type, and size of aluminium are the crucial variables that can enrich the tribological behaviour of aluminium metal. Applied load, sliding velocity and environment condition are the deciding factor for the tribological behaviour of aluminium metal.

## References

- Aghajanian MK, Rocazella MA, Burke JT, Keck SD (1991) The fabrication of metal matrix composites by a pressureless infiltration technique. *J Mater Sci* 26(2):447–454
- Anilkumar HC, Hebbar HS, Ravishankar KS (2011) Mechanical properties of fly ash reinforced aluminium alloy (Al6061) composites. *Int J Mech Mater Eng* 6(1):41–45
- Bhandakkar A, Prasad RC, Sastry SM (2014) Fracture toughness of AA2024 aluminum fly ash metal matrix composites. *Int J Compos Mater* 4(2):108–124
- Casati R, Vedani M (2014) Metal matrix composites reinforced by nano-particles—a review. *Metals* 4(1):65–83
- Christy TV, Murugan N, Kumar S (2010) A comparative study on the microstructures and mechanical properties of Al6061 alloy and the MMC Al6061/TiB<sub>2</sub>/12p. *J Miner Mater Charact Eng* 9(01):57
- Deuis RL, Subramanian C, Yellup JM (1997) Dry sliding wear of aluminium composites—a review. *Compos Sci Technol* 57(4):415–435
- Dinakaran I, Murugan N, Thangarasu A (2016) Development of empirical relationships for prediction of mechanical and wear properties of AA6082 aluminum matrix composites produced using friction stir processing. *Eng Sci Technol Int J* 19(3):1132–1144
- Ghosh PK, Ray S (1988) Influence of process parameters on the porosity content in Al (Mg)– $\text{Al}_2\text{O}_3$  cast particulate composite produced by vortex method. *Trans Am Foundrymen's Soc* 96:775–782
- Guo N, Leu MC (2013) Additive manufacturing: technology, applications and research needs. *Front Mech Eng* 8(3):215–243

- Gupta MK (2018) Controlling factors in aluminum Matrix composites fabrication. *Anusandhan* 8(14):141–151
- Gupta MK, Rakesh PK (2019) Characterization of pine needle ash particulates reinforced surface composite fabricated by friction stir process. *Mater Res Express* 6(4). <https://doi.org/10.1088/2053-1591/aafaea>
- Gupta MK, Rakesh PK, Singh I (2016) Application of industrial waste in metal matrix composite. *J Polym Compos* 4(3):2321–8525
- Gürler R (1999) Sliding wear behavior of a silicon carbide particle-reinforced aluminum–magnesium alloy. *J Mater Sci Lett* 18(7):553–554
- Helu M, Vijayaraghavan A, Dornfeld D (2011) Evaluating the relationship between use phase environmental impacts and manufacturing process precision. *CIRP Ann* 60(1):49–52
- Hosking FM, Portillo FF, Wunderlin R, Mehrabian R (1982) Composites of aluminium alloys: fabrication and wear behaviour. *J Mater Sci* 17(2):477–498
- Jones H, Atkinson HV (1993) The wettability of silicon carbide by liquid aluminium: the effect of free silicon in the carbide and of magnesium, silicon and copper alloy additions to the aluminium. *J Mater Sci* 28(10):2654–2658
- Kobashi M, Choh T (1993) The wettability and the reaction for the SiC particle/Al alloy system. *J Mater Sci* 28(3):684–690
- Kok M (2005) Production and mechanical properties of Al<sub>2</sub>O<sub>3</sub> particle-reinforced 2024 aluminium alloy composites. *J Mater Process Technol* 161(3):381–387
- Kök M (2011) Modelling the effect of surface roughness factors in the machining of 2024Al/Al<sub>2</sub>O<sub>3</sub> particle composites based on orthogonal arrays. *Int J Adv Manuf Technol* 55(9–12):911–920
- Kumar GV, Rao CSP, Selvaraj N, Bhagyashekar MS (2010) Studies on Al6061-SiC and Al7075-Al<sub>2</sub>O<sub>3</sub> metal matrix composites. *J Miner Mater Charact Eng* 9(01):43
- Kumar GV, Rao CSP, Selvaraj N (2011) Mechanical and tribological behaviour of particulate reinforced aluminium metal matrix composites—a review. *J Miner Mater Charact Eng* 10(01):59
- Lalit R, Mayank P, Ankur K (2018) Natural fibers and biopolymers characterization: a future potential composite material. *Strojnícky casopis—J Mech Eng* 68(1):33–50
- Lancaster L, Lung MH, Sujun D (2013) Utilization of agro-industrial waste in metal matrix composites: towards sustainability. *World Acad Sci Eng Technol* 73:1136–1149
- Lim SC, Gupta M, Ren L, Kwok JKM (1999) The tribological properties of Al–Cu/SiCp metal–matrix composites fabricated using the rheocasting technique. *J Mater Process Technol* 89:591–596
- Loh YR, Sujun D, Rahman ME, Das CA (2013) Sugarcane bagasse—the future composite material: a literature review. *Resour Conserv Recycl* 75:14–22
- Lu D, Jiang Y, Zhou R (2013) Wear performance of nano-Al<sub>2</sub>O<sub>3</sub> particles and CNTs reinforced magnesium matrix composites by friction stir processing. *Wear* 305(1):286–290
- Lü L, Lai MO, Su Y, Teo HL, Feng CF (2001) In situ TiB<sub>2</sub> reinforced Al alloy composites. *Scripta Mater* 45(9):1017–1023
- Madakson PB, Yawas DS, Apasi A (2012) Characterization of coconut shell ash for potential utilization in metal matrix composites for automotive applications. *Int J Eng Sci Technol* 3(4):1190–1198
- Manna A, Bhattacharayya B (2005) Influence of machining parameters on the machinability of particulate reinforced Al/SiC–MMC. *Int J Adv Manuf Technol* 25(9–10):850–856
- McDanel DL (1985) Analysis of stress-strain, fracture, and ductility behaviour of aluminium matrix composites containing discontinuous silicon carbide reinforcement. *Metall Trans A* 16(6):1105–1115
- Mehrabian RGR, Riek RG, Flemings M (1974) Preparation and casting of metal-particulate non-metal composites. *Metall Trans* 5(8):1899–1905
- Moraes EES, Graça MLA, Cairo CAA (2006) Study of aluminium alloys wettability on SiC preform. In: *Congresso Brasileiro de Engenharia e Ciência dos Materiais*, vol 15, no 19, pp 4217–4224
- Muthukrishnan N, Murugan M, Rao KP (2008) Machinability issues in turning of Al-SiC (10p) metal matrix composites. *Int J Adv Manuf Technol* 39(3–4):211–218
- Nair SV, Tien JK, Bates RC (1985) SiC-reinforced aluminium metal matrix composites. *Int Metals Rev* 30(1):275–290

- Natarajan N, Vijayarangan S, Rajendran I (2006) Wear behaviour of A356/25SiCp aluminium matrix composites sliding against automobile friction material. *Wear* 261(7–8):812–822
- Prasad SV, Asthana R (2004) Aluminium metal-matrix composites for automotive applications: tribological considerations. *Tribol Lett* 17(3):445–453
- RC P, Ramakrishnan P (1996) Deformation and fracture behaviour of the cast and extruded 7075Al-SiCp composites at room and elevated temperatures. *Mater Trans, JIM* 37(3):223–229
- Reihani SS (2006) Processing of squeeze cast Al6061–30vol% SiC composites and their characterization. *Mater Des* 27(3):216–222
- Rohatgi P (1991) Cast aluminum-matrix composites for automotive applications. *JOM* 43(4):10–15
- Rohatgi P, Asthana R (2001) Solidification science in cast MMCs: the influence of Merton Flemings. *JOM* 53(9):9–13
- Ruehle M, Evans AG (1989) Structure and chemistry of metal/ceramic interfaces. *Mater Sci Eng, A* 107:187–197
- Sozhamannan GG, Prabu SB (2009) Evaluation of interface bonding strength of aluminium/silicon carbide. *Int J Adv Manuf Technol* 44(3–4):385–388
- Sreenivasan A, Paul Vizhian S, Shivakumar ND, Muniraju M, Raguraman M (2011) A study of microstructure and wear behaviour of TiB<sub>2</sub>/Al metal matrix composites. *Latin Am J Solids Struct* 8(1):1–8
- Surappa MK (2003) Aluminium matrix composites: challenges and opportunities. *Sadhana* 28(1–2):319–334
- Tian SF, Jiang LT, Guo Q, Wu GH (2014) Effect of surface roughness on tribological properties of TiB<sub>2</sub>/Al composites. *Mater Des* 53:129–136
- Ubolluk R, Prinya C, Prasert S (2010) Development of high volume rice husk ash alumino silicate composites. *Int J Miner Metall Mater* 17(5):654–668
- Venci A, Rac A, Bobic I (2004a) Tribological behaviour of Al-based MMCs and their application in the automotive industry. *Tribol Ind* 26(3–4):31–38
- Venci A, Rac A, Bobic I (2004b) Tribological behaviour of Al-based MMCs and their application in the automotive industry. *Tribol Ind* 26(3–4):31–38
- Wilson S, Alpas AT (1997) Wear mechanism maps for metal matrix composites. *Wear* 212(1):41–49
- Yalcin Y, Akbulut H (2006) Dry wear properties of A356-SiC particle reinforced MMCs produced by two melting routes. *Mater Des* 27(10):872–881
- Yuvaraj N, Aravindan S, Vipin (2017) Wear characteristics of Al5083 surface hybrid nano-composites by friction stir processing. *Trans Indian Inst Met* 70(4):1111–1129
- Zhu HG, Wang HZ, Ge LQ, Shi CHEN, Wu SQ (2007) Formation of composites fabricated by exothermic dispersion reaction in Al-TiO<sub>2</sub>-B<sub>2</sub>O<sub>3</sub> system. *Trans Nonferrous Met Soc China* 17(3):590–594

**Part III**  
**New Lubricants for Automotive**  
**Applications**

# Chapter 9

## Current and Future Trends in Grease Lubrication



Sooraj Singh Rawat and A. P. Harsha

**Abstract** The traditional greases are composed of mineral or synthetic oil, thickening agent, additives and fillers. Thickeners having fibrous matrix are generally made of fatty acid soaps (calcium, lithium, aluminum, sodium) and non-soaps (clay, PTFE, polyurea, silica). The tribological performance of the grease is depends upon the viscosity of the base oil, type and its concentration of thickening agent. A variety of additives and fillers were added to the grease to obtain the desired properties of the grease. Lubricating greases are widely used in numerous automotive applications such as gears, cams, ball and roller bearings. A significant amount of power is lost due to the friction (i.e. friction in brakes, engine, tires, and transmission) in the automotive components. By reducing the frictional losses, the significant amount of power can be saved and this will improve the efficiency of the parts. The lubrication by the grease help in separation of the contacting surfaces to achieve low friction, wear, and long life. In the last decades, the researchers have contributed for enhancing the tribological performance of the grease with different fillers. In recent time the nano-additives is gaining importance for improving the tribological performance of the mating surface. Further, due to environmental concern, bio-based greases are explored in the formulation of the lubricating grease. This chapter enumerates the recent developments in the formulation of grease and their important aspect for improving the tribological performance of automotive components.

**Keywords** Grease · Fibrous Matrix · Nano additives · Bio-based Grease

---

S. S. Rawat · A. P. Harsha (✉)  
Department of Mechanical Engineering, Indian Institute of Technology (Banaras Hindu University), Varanasi 221005, India  
e-mail: [apharsha.mec@itbhu.ac.in](mailto:apharsha.mec@itbhu.ac.in)

S. S. Rawat  
e-mail: [soorajsr.rs.mec15@itbhu.ac.in](mailto:soorajsr.rs.mec15@itbhu.ac.in)

© Springer Nature Singapore Pte Ltd. 2019  
J. K. Katiyar et al. (eds.), *Automotive Tribology*, Energy, Environment, and Sustainability,  
[https://doi.org/10.1007/978-981-15-0434-1\\_9](https://doi.org/10.1007/978-981-15-0434-1_9)

## 9.1 Introduction

### 9.1.1 Background

Friction is a resistance which opposes the relative motion of interacting surfaces. Many tribological situations demand less friction and wear such as ball bearing, gears etc. High friction often leads to adverse impact on efficiency, wear rate, reliability and component life. It is great challenge for a human being to minimize friction in moving components. On average 33% energy of the fuel is utilized to overcome friction in the various parts (i.e. gearbox, engine, clutches, tries etc.) of the passenger cars and heavy-duty vehicles (Holmberg et al. 2012, 2014). This is an enormous amount of energy lost due to frictional losses. The global demand for energy consumption is increasing tremendously due to the increase in automobile and industrial activities. The share of energy used by various transportation vehicles is summarized in Table 9.1. The proper lubrication in the interacting surfaces can minimize the frictional losses. Improved efficiency and operation age of machinery is obtained by reducing the frictional losses. A noticeable amount of energy can be saved with best lubrication practices which reduce the frictional losses.

### 9.1.2 Overview of Lubricants

Lubricants are those having inherent lubricious property as well as have the capability to reduce friction between the rubbing pairs and prevent the surfaces against wear. Lubricants are generally a mixture of base stock and additives. Additives are added to enhance the performance of the base stock. The classification of the lubricants is generally based on their physical appearance and, their source of origin, as shown in Fig. 9.1. As per physical appearance, lubricants are classified as solid, semi-solid, and liquid lubricants. Sometimes gas is also used as a lubricant. Based on the source of origin, lubricants are classified as non-biological and biological derivatives. Paraffinic, naphthenic, and aromatic oils are non-biological lubricants. Synthetic oils

**Table 9.1** Global energy consumption in automobile sector by transportation vehicles (Holmberg et al. 2014)

Transportation sector	Consumption of energy (%)
Light duty vehicles	52
Trucks	17
Buses	4
Aviation	10
Marine	10
Rail	3
Others	3

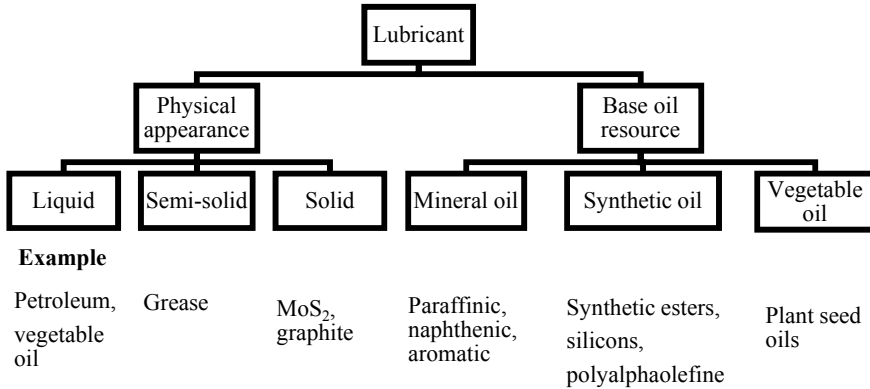


**Fig. 9.1** Classification of lubricants

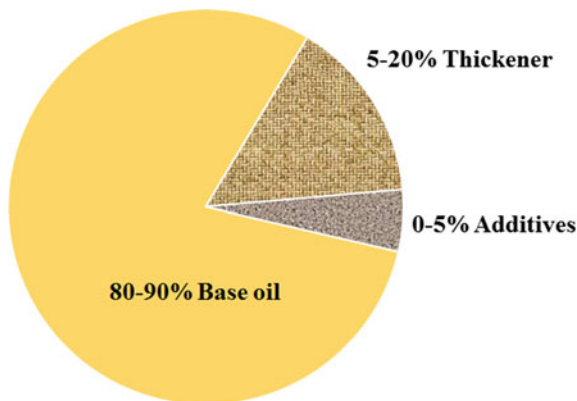
are chemically modified version of mineral oils, which is artificially developed in the laboratory. Synthetic esters, silicones and polyalphaolefins are examples of synthetic oils. Synthetic oils have superior performance at elevated temperature as compared to mineral oils. While oil extracted from plants seeds are coming under the category of biological lubricants.

## 9.2 Grease

The term ‘grease’ is a Latin language originated word ‘crassus’ which means fat. Grease is a semi-solid in physical appearance and the semifluid product obtained by the dispersion of thickening agent in a liquid lubricant. The other ingredients are added to impart unique properties (Melville 1984). A grease has three basic ingredients: base stock, thickening agent and additives. A typical grease consists of 80–90% base oil, 5–20% thickening agent, and 0–5% additives, as shown in Fig. 9.2. The base oil used in the formulation of the grease may be synthetic, mineral or vegetable oil while the thickening agent may be soap or non-soap. The fundamental requirement of the lubricating grease is to achieve the desired level of wear, friction, and life expectancy of the machinery. The consumption of grease at a worldwide scale is estimated about 1296 Kiloton while 691 Kiloton grease used in industrial applications till 2017 (Panchal et al. 2017). Approximately 90% of grease of global demand is manufactured with petroleum oils. Remaining 9 and 1% share of global demand is manufactured with synthetic esters and vegetable oils, respectively.

Grease protects the surfaces against wear and corrosion. The solid additives dispersed in the lubricating oil tends to settle down with time while in the grease solid additives remain fully dispersed. Textiles, pharmaceutical and food industry need to maintain hygiene and purity in the development of the product. Lubricating oil is



**Fig. 9.2** Grease composition

prone to splash or leak, which is not desirable in these industries. This problem is well controlled with the lubricating grease. The viscoelastic behavior of the lubricating grease imparts a consistency which restricts to leak out easily. Bearing lubricated with lubricating oil needs seal to prevent dirt, contamination particles and leakage. Grease acts as an inherent seal against dirt and foreign particles. Grease is more viscous, so it is more water-resistive as compared to lubricating oil. The viscosity of lubricating oil is affected with rise in temperature while grease has apparent viscosity, which is less influenced by temperature. Along with these advantages, lubricating grease has some demerits as compared to lubricating oil. Grease has very poor thermal conductivity and high oxidative characteristics.

## 9.3 Grease Composition

### 9.3.1 Base Oil

The base oil is the key ingredient of lubricants/greases. Further, the base oil is classified into mineral, synthetic and vegetable oils. In addition to this, mineral oil is categorized into paraffinic, naphthenic and aromatic oils.

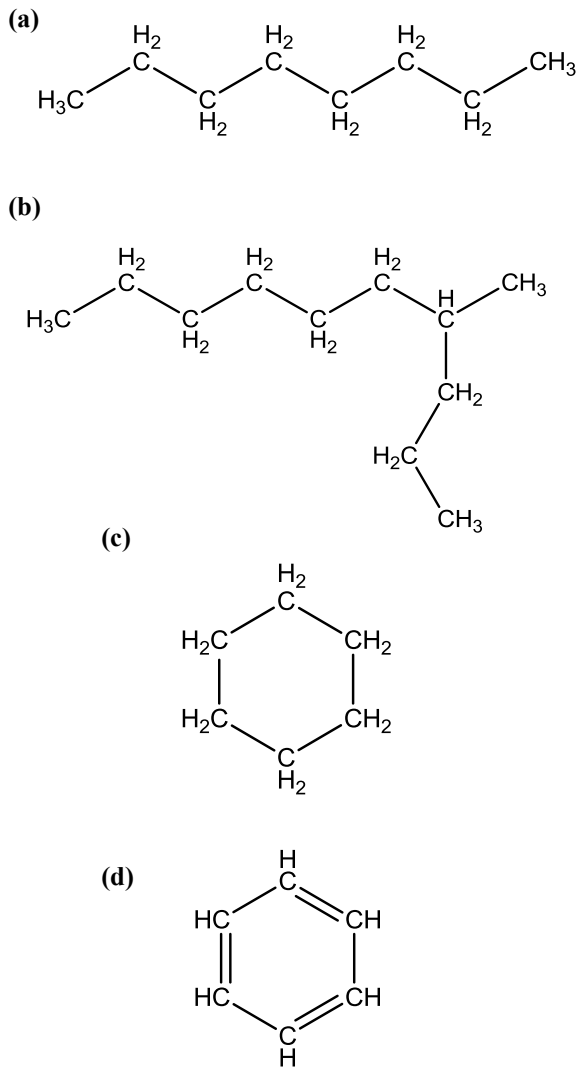
**Mineral oil** Mineral oils are derived through the fractional distillation process of crude oil. Mineral oil is widely used in the formulation of commercially available engine oils, industrial lubricants, greases, transmission oil etc. Low cost, available in a wide assortment of viscosities and ample availability of mineral oil, makes it most preferable base stock. Available mineral oil consists of basic three forms:

**Paraffinic** Paraffin oil comprises a blend of alkenes (hydrocarbon). It has straight or branched hydrocarbon chain structures. Paraffin oil exhibited higher viscosity index, oxidation stability, and pour point as compared with naphthenic oils. As the degree of branching of hydrocarbon increases in the paraffin oil, the decay observed

in the melting point and viscosity index of the oil. Figure 9.3 shows the structure of different mineral oils.

*Naphthenic* Naphthenic oils have a cyclic structure; generally, it contains six carbon rings with no unsaturation. This oil has good solubility property, low viscosity index, low temperature flowability properties. This oil displays poor oxidation stability and viscosity-temperature characteristic at elevated temperature applications. Naphthenic oils have better compatibility with polar additives. The solubility of metallic soap is better in naphthenic oil as compared to paraffinic oil. The mechanical stability of the grease developed with metallic soap and naphthenic oil is higher as

**Fig. 9.3** Structure of different mineral oils  
**a** straight chain paraffin  
**b** branched chain paraffin  
**c** Naphthenic and  
**d** Aromatic



compared with the grease developed with paraffin oil and metallic soap. Therefore, naphthenic oil has gained more preference as a base oil for grease formulation. Furthermore, this oil is more preferable in the production of metal working applications, turbine oils, and hydraulic oils.

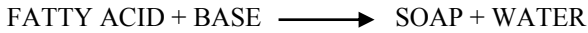
**Aromatic** Aromatic oils have a cyclic structure of six carbon atoms with alternating single and double bonds. It has a high density, oxidation resistance, good thermal stability. Aromatic oils display better thermal stability to a certain degree than either paraffin or naphthenic oil. Absence of wax in the base stock imparts it good low-temperature fluidity and low melting point. Aromatic oil has high polarity causes a strong affinity to water to dissolve it.

**Synthetic oil.** Synthetic oils are artificially developed in the laboratories to enhance the desired properties of the mineral oils. Polyphenyl ethers, polyalphaolefins (POA), perfluoropolyalkylether (PFPE), polyalkylene glycols, synthetic hydrocarbon oils, polysiloxanes, synthetic esters, silicones etc. are the examples of the synthetic oils. Synthetic oil-based greases are formulated where mineral oil-based greases are unable to fulfil the service requirements. Generally, synthetic base oils are not companionable with conventional thickening agents. Clay, polyurea, fumed silica, Teflon, are commonly preferable thickening agents in the formulation of synthetic grease.

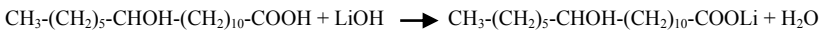
**Vegetable oil** Vegetable oils are extracted from plants seeds, which is renewable and biodegradable. Those vegetable oils are consumed by human beings are categorized into edible vegetable oil. Sunflower, peanut, soybean, olive, rapeseed, coconut, palm are the most common examples of edible oils. On the other hand, which is not consumed by human beings are called non-edible vegetable oils. Mahua, Karanja, cottonseed, sesame, linseed, neem, castor are the most common examples of non-edible oils. In the past decades, edible and non-edible vegetable oils gained popularity as biofuels, which shows significant potential as an alternative for fuels (Sumathi et al. 2008). Non-edible oils are used in agrochemicals, varnishes, soaps, and paints etc. Vegetable oils contain almost all desired properties for lubrication applications, i.e. excellent lubricity, good metal adherence, high flash point, non-toxic, higher load bearing capacity, higher shear stability, higher viscosity index, low volatility, low evaporative losses, and environmentally friendly relative to the conventional mineral oil (Fox and Stachowiak 2007; Reeves et al. 2017). Therefore, vegetable oils are gaining more attention as lubricating base stock for lubrication engineers. In addition to vegetable oils have lower oxidation stability and pour point as compared with conventional mineral oils. These issues of conventional vegetable oils are rectified with chemical modification in the structure of fatty acids (Kashyap and Harsha 2016; Gupta et al. 2018).

### 9.3.2 Thickener

The thickener is also termed as ‘soap’ which is a reaction product of fatty acid and a strong base (alkali). Water is obtained as a by-product in the neutralization process of fatty acid and base (Honary and Erwin 2011).

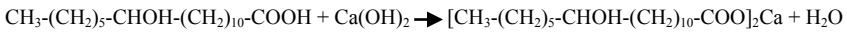


For example-



12-hydroxy stearic acid      Lithium hydroxide      lithium 12-hydroxy stearate      water

Lithium soap



12-hydroxy stearic acid      Calcium hydroxide      Calcium di (12-hydroxy stearate)      water

Calcium soap



Stearic acid      Aluminum hydroxide      Aluminum tristearate      water

Aluminum soap

The product of the neutralization process, ‘soap’ is mixed with a base oil to obtain grease. The length of thickener fibers varies in the range between 1 and 100 microns and length to diameter ratio varies from about 10 to 100 (Lugt 2009). The thickener imparts a unique property to the lubricating oil. The lubricating oil is reinforced by the thickening agent, which formed a three-dimensional network. Thickening capacity of the grease is directly proportional to the chain length of the hydroxystearate soap (Mang and Dresel 2007). The matrix of the soap behaves as a reservoir of the lubricating oil, release the lubricating oil at the contact of friction surfaces. An enormous variety of thickeners are used for grease lubrication. Figure 9.4 shows the classification of thickeners. Thickeners are broadly classified into two groups (a) soap and (b) non-soap. Soaps are generally metallic soap (fibrous structure) which is further classified into four groups (a) alkali metals (b) alkaline-earth metals (c) aluminum metal and (d) heavy metals. Each category of soap is further subdivided into straight and complex soap. Chloride, carbonate, benzoate, metallic acetate is a

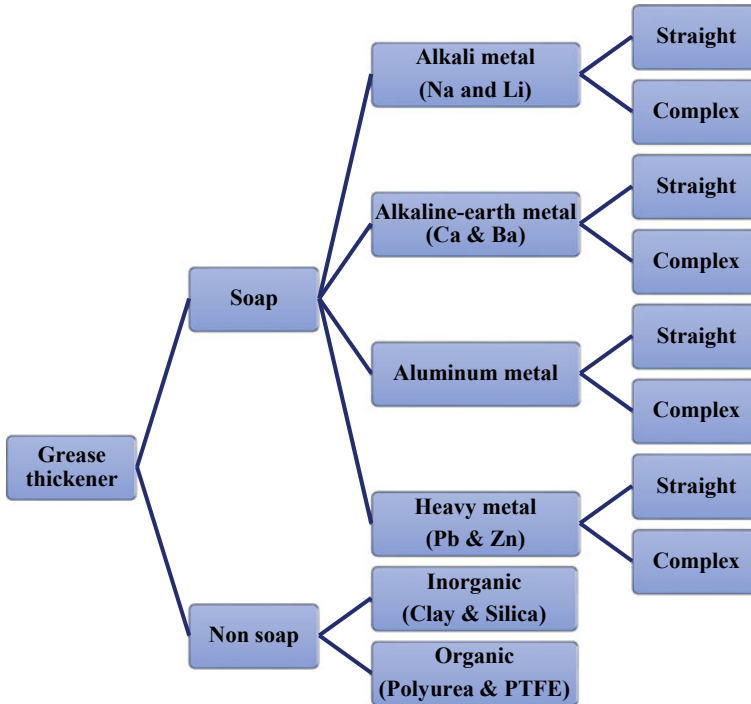


**Fig. 9.4** Classification of thickeners

common type of complex agents. The complex agent is added in grease to improve its heat resistance property or, we can say to improve the dropping point of the grease. Straight soaps are excluded from complexing agents. The carboxylic acid containing 18 carbon atoms exhibited maximum thickening impression (Mang and Dresel 2007).

Non-soaps are broadly classified as inorganic and organic soaps. Lithium grease preferably used globally. The estimated amount of different grease formulate with simple and complex soap worldwide is given in Table 9.2.

### 9.3.3 Additives

Additives are added in the lubricating grease to improve its desired properties and to minimize its undesired features. Generally, antioxidants, antiseizure, antifricition, antiwear, extreme pressure, anticorrosive, and tackiness additives are used in the grease to enhance its performance. Some additives modify the grease structure (Adhvaryu et al. 2005), or some additives ameliorate the base oil characteristics.

**Table 9.2** Share of different grease formulated with straight and simple soap at worldwide scale (Honary and Erwin 2011)

Type of soap	Percentage (%)
Lithium complex grease	40
Conventional lithium grease	29
Calcium soap grease	11
Aluminum soap grease	7
Polyurea grease	5
Organophilic clay thickeners	4
Sodium and other metallic soap grease	2
Other non-soap grease	2

**Table 9.3** Commonly used additives in commercially available greases

Additives	Examples
Antioxidants	Diphenylamine, paraoxydiphenylamine, butyl-4-methyl-phenol, zinc dithiophosphate, phenolic thioesters, diaryldisulfides etc
Antiseizure	Graphite, molybdenum disulfide, zinc dialkyl dithiophosphate
Antifriction and antiwear	zinc dialkyl dithiophosphate, Lead naphthanate
Anticorrosion	zinc dialkyl dithiophosphate, triethanolamine Amines, dextramin, lanolin, amides, sulfonates, disodium sebacate etc
Viscous	Polyisobutylene, vinytol, atapol, latex etc
Thickening	Atapol, Polybutene, low-pressure high-density polyethylene
Tackifiers	Polyisobutylene, methacrylates, ethylene-propylene copolymer, olefin copolymer

The prime function of the antioxidants additives to protect the grease against oxidation and elongate service life at elevated temperature situations. Antiseizure additives prevent the tribo-pairs against the high friction sticking under high load condition. The primary purpose of antifriction and antiwear additives are to reduce friction and protect the surface against wear. Tackifiers additives are added to the grease to enhance its adhesion and cohesion with the mating surface. Commonly used additives in commercially available greases are tabulated in Table 9.3.

## 9.4 General Method for Grease Synthesis

The basic idea in development of the lubricating grease is by the dispersion of readymade soap into the base oil at high temperature with continuous stirring. The remaining base oil is added to the dispersion to control the consistency of the grease. Further, additives are added in the cooling phase of the grease. For the synthesis

of in situ soap-based grease, a measured amount of the fatty acid is added to the pre-heated base oil followed by the addition of a measured amount of alkali with continuous stirring. The saponification reaction takes place which allows dispersion of the soap in the base oil. The addition of remaining base oil and additive is done during the cooling phase of the grease. In the final stage, the grease is milled for the homogenization of the dispersion.

The lithium 12-hydroxy stearate is the most commonly used thickening agent in the synthesis of lubricating grease. Various researchers were adopted lithium soap (Sahoo and Biswas 2014; Rawat et al. 2018, 2019; Wang et al. 2008; Ji et al. 2011), titanium complex (Chen 2010; Shen et al. 2016), calcium soap (Kamel et al. 2016; Dai et al. 2017), bentonite clay (Chen et al. 2014), PTFE (Ge et al. 2015a, b) and different mineral or synthetic oils adopted as a base oil for the synthesis of lubricating grease. A great diversity showed in the synthesis procedure of lubricating grease. The cooking temperature of the grease varies according to the type of thickener used and play an important role in the property of the grease.

Incorporation of additives in the grease is an important issue. Some additives are sensitive to heat and, they lose their effectiveness at a cooking temperature of the grease. Therefore, in normal practice, the addition of additive is done during the cooling phase of the grease, when the temperature is less than 85 °C. Some additives are unaffected with heat so it can be incorporated in the grease at any time. In industry, the greases are manufactured in large grease kettle in batch or continuous grease plants. Rawat et al. (2018) have developed the paraffin grease blended with SiO<sub>2</sub> nanoparticles by in situ dispersion method. SiO<sub>2</sub> nanoparticles were dispersed in the base oil at the very beginning for homogenous dispersion of the nanoparticles. Further 12-hydroxy stearic acid was added in the base oil with continuous stirring and temperature was maintained at 90 °C. The aqueous solution of the lithium hydroxide monohydrate added in the solution in a dropwise manner. Saponification reaction took place and temperature was raised up to 180 °C to dehydrate the colloidal solution for 2 h. Further, leave the grease to cool down at room temperature for the next 24 h.

## 9.5 Test Methods

Grease testing is broadly classified into the following two categories:

- Physical property testing
- Tribological performance testing.

### 9.5.1 Physical Property Testing

National Lubricating Grease Institute (NLGI) of the United States is the pioneer institute in the field of grease. NLGI with the association of American Society of

Testing Materials (ASTM) develops the technical standards for the grease. Numerous ASTM standards are available to evaluate the various common physical property of grease, i.e. dropping point, cone penetration, water washout, grease mobility test, evaporation loss, oxidation stability, leakage tendency etc. and these are tabulated in Table 9.4.

**Dropping point** Dropping point test is used to determine the melting point of the grease as per ASTM D566 (ASTM D566-16 2016). It is a critical property to evaluate the performance of the grease. When the grease is heated, it softens and turns its phase from semi-solid to liquid. This test indicates the temperature at which thickener is able no more to hold the base oil in its matrix. This test method is limited to bath temperature up to 288 °C. Figure 9.5 shows the schematic diagram of drop point apparatus. Furthermore, ASTM D2265 (2017) is used for the high-temperature range. Dropping point is also dependent on the type of thickener used in the synthesis of the grease. Dropping point and working temperature of some types of greases are tabulated in Table 9.5.

**Cone penetration** The cone penetration test is used to determine the consistency of the lubricating grease as per ASTM D217 (ASTM D217-02 2003). Figure 9.6 shows the schematic diagram of the cone penetrometer. The concentration of the thickening agent governs the consistency of grease. The importance of this test is to find the NLGI grade of the grease. NLGI classified grease based on the consistency as measured by worked penetration. This test is performed at room temperature (25 °C). The worked and unworked penetration is measured when specified weight and dimension cone dropped freely in the grease cup filled with grease for 5 s. The unworked penetration test is carried out without disturbing the grease structure. In a worked penetration test, before the measurement of penetration depth of the cone, the grease sample was subjected to 60 double strokes in grease worker and, the remaining procedure is the same as unworked penetration. The digital image of the one-quarter scale grease worker is shown in Fig. 9.7.

The various grades of grease designated by NLGI are tabulated in Table 9.6. The temperature shows an adverse effect on the consistency of the grease. As temperature increases, the penetration depth of the grease also increases. The grease becomes softer when it is heated. At dropping point grease converts its phase from semi-solid to liquid. At this temperature, the structure of the grease has been destroyed. Dropping point is the critical temperature at which grease loses its consistency. A grease does not recover its same consistency when it is heated above its drop point and followed by cooling.

**Water washout** Water wash out test is used to evaluate the resistance capability of lubricating grease against water to wash out under prescribed conditions as per ASTM D1264 (ASTM 1264 2017). The ball bearing (D2PP version, 6204) was packed with grease and encountered with a jet of water under standard conditions. The amount of grease washout through water indicates the resistance of grease against washout. After completion of the test, the shields and bearing were dried at 77 °C for 15 h and then weighed to estimate the loss of grease. If the base oil of the grease is highly volatile, then some weight loss may be possible during drying. Therefore, this test is not preferred for some greases which comprise highly volatile constituents. Any



**Table 9.4** List of physical characterization of lubricating grease

Designation	ASTM Standard	Purpose
D 217	Cone penetration of lubricating grease	To determine the consistency of the lubricating grease
D 566	Dropping point of lubricating grease	To determine the dropping point of lubricating grease
D 942	Oxidation stability of lubricating grease by the oxygen pressure vessel method	To determine resistance capacity of lubricating grease to oxidation when stored statically in an oxygen atmosphere
D 972	Evaporation loss of lubricating greases and oils	To determine the evaporation loss of lubricating grease
D 1092	Measuring apparent viscosity of lubricating greases	To measurement of apparent viscosity of lubricating grease in the temperature range from $-54$ to $38$ °C
D 1263	Leakage tendencies of automotive wheel bearing greases	To evaluate the leakage tendency of wheel bearing greases
D 1264	Determining the water washout characteristics of lubricating greases	To evaluate the resistance capacity of a lubricating grease to washout by water from a bearing
D 1403	Cone penetration of lubricating grease using one-quarter and one-half scale cone equipment	To determine the consistency of the lubricating grease
D 1742	Oil separation from lubricating grease during storage	To determine the tendency of a lubricating grease to separate oil during storage in both normally filled and partially filled containers
D 1743	Determining corrosion preventive properties of lubricating greases	To determine the corrosion preventive properties of lubricating grease under wet conditions
D 1831	Roll stability of lubricating grease	To determine the change in consistency of lubricated grease when worked in a roll stability test apparatus
D 2265	Dropping point of lubricating grease over wide range temperature range	To determine the dropping point of lubricating grease up to temperature $400$ °C
D 2595	Evaporation loss of lubricating greases over wide- temperature range	To determine the evaporation loss of lubricating grease up to temperature $316$ °C
D 4048	Detection of copper corrosion from lubricating grease	To determine the corrosiveness to copper of lubricating grease
D 4289	Elastomer compatibility of lubricating greases and fluids	To determine the compatibility of lubricating greases and fluids with standard elastomer sheets

(continued)

**Table 9.4** (continued)

Designation	ASTM Standard	Purpose
D 4290	Determining the leakage tendencies of automotive wheel bearing grease under accelerated conditions	To evaluate the leakage tendency of wheel bearing greases
D 5969	Corrosion-preventive properties of lubricating greases in presence of dilute synthetic sea water environments	To determine the corrosion-preventive properties of lubricating grease exposed under dilute synthetic sea water environment
D 6138	Determination of corrosion-preventive properties of lubricating greases under dynamic wet conditions (Emcor test)	To determine the corrosion preventive properties of greases under dynamic wet conditions
D 6184	Oil separation from lubricating grease (Conical sieve method)	To determine the tendency of lubricating grease to separate oil at an elevated temperature

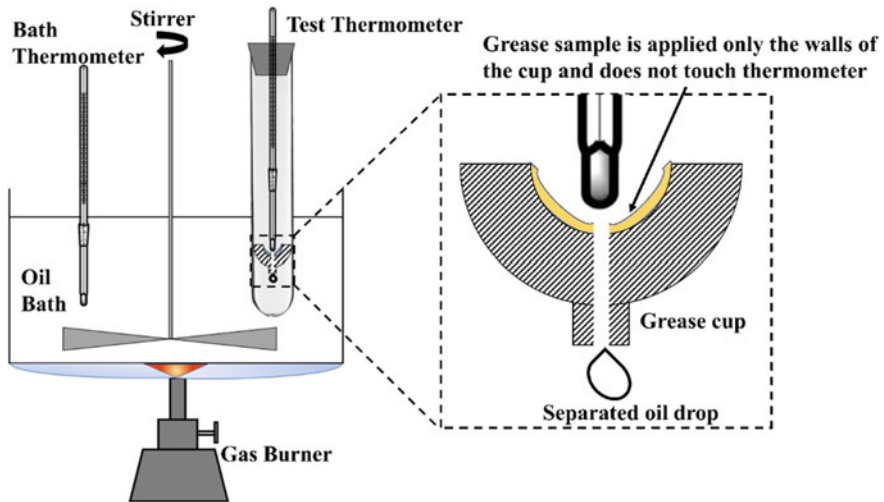


**Fig. 9.5** Schematic diagram for drop point apparatus

loss due to leakage occurred during drying of the grease should not be added in the account of grease loss.

**Leakage tendency** This test is performed to estimate the leakage of base oil, grease or both from the wheel bearing grease when it is tested as per ASTM D1263 (ASTM 1263 2017). Separation of oil from grease or grease from the bulk grease or overflow of grease may be caused by bearing rotation and high temperature. After completion of the test, apparatus permitted to cool down, weigh the hub cap and leakage collector to estimate the leakage loss.

**Evaporation loss** This test is performed to determine the evaporation loss of the base oil and grease when grease is encountered with elevated temperature. As per

**Table 9.5** Effect of thickener on the dropping point of the grease (Melville 1984)

Thickener	Dropping point (°C)	Working limit (°C)
Sodium soap	163–177	121
Lithium soap	177–204	135
Lithium complex soap	250–320	177
Hydrated calcium soap	70–104	60
Anhydrous calcium soap	130–140	100
Aluminium soap	100–120	79
Aluminium complex soap	200–260	150
Barium soap	120–150	100
PTFE	230–300	177

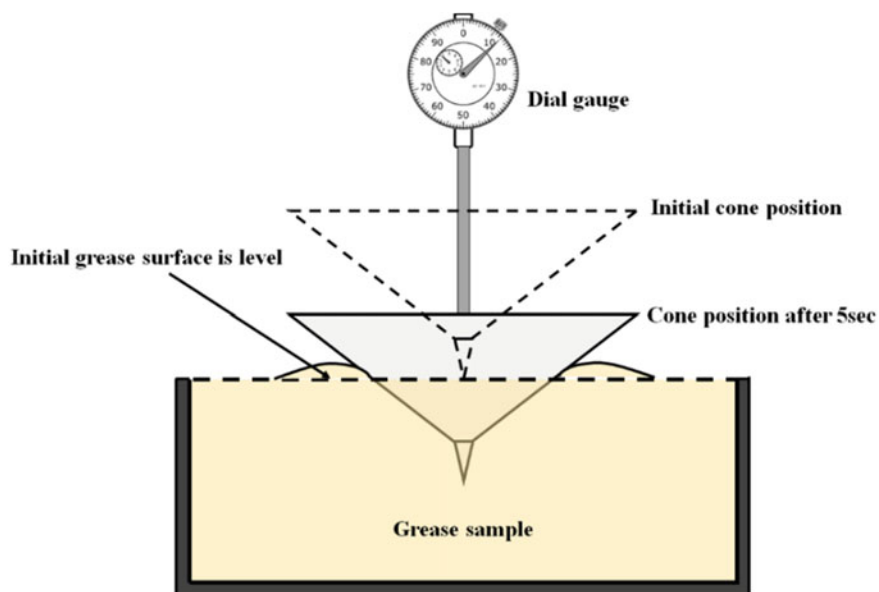


**Fig. 9.6** Schematic diagram for cone penetration apparatus

**Fig. 9.7** The digital image of one-quarter scale grease worker



**Table 9.6** NLGI classification of grease (ASTM D217-02 2003)

NLGI grade	Work penetration depth after 60 strokes at 25 °C (0.1 mm)	Appearance
000	445–475	Fluid
00	400–430	Semi-fluid
0	355–385	Very soft
1	310–340	Soft
2	265–295	Normal
3	220–250	Firm
4	175–205	Very firm
5	130–160	Hard
6	85–115	Very hard

ASTM D972 (ASTM D972-16 2017), this test is carried out in the temperature range between 100 to 150 °C. Further, ASTM D2595 is preferred for the higher temperature range between 93 to 316 °C. The performance of the grease is affected by the loss of volatile components in the base oil and grease.

The test parameters of above-mentioned physical properties in accordance with ASTM standards are summarized in Table 9.7.

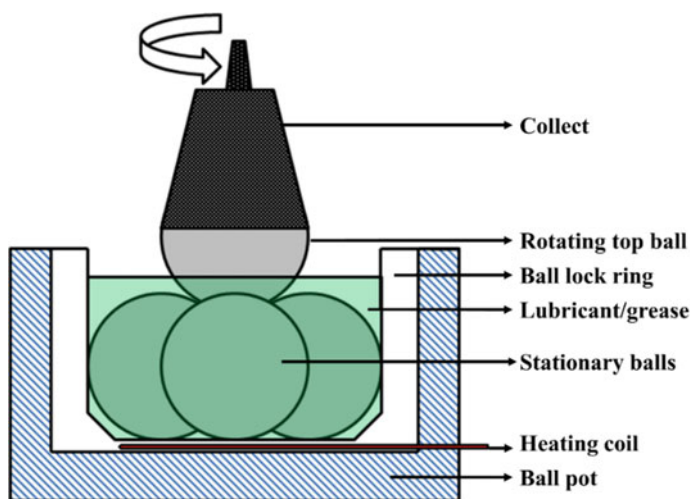
### 9.5.2 Tribological Performance Testing

The friction and wear play an important role in any tribological situation. The lubricating grease is used for reducing the wear and for improving the asperity to asperity separation capability. The tribological testing is performed to evaluate the antiwear, antifricition, and load carrying capacity properties of the grease. Most commonly

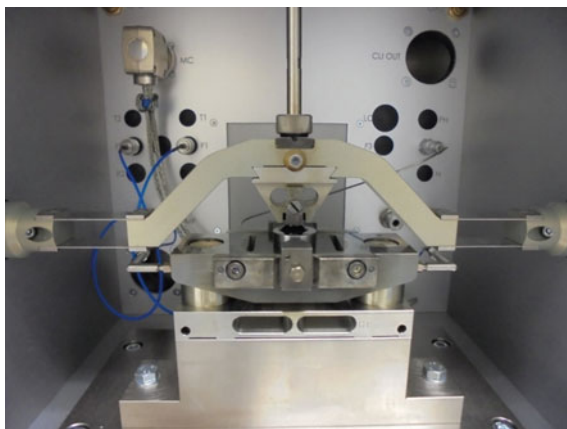
**Table 9.7** Test conditions required for the evaluation of some physical properties of the grease as per ASTM standard

Test specification	Cone penetration	Drop point	Evaporation loss	Leakage tendency	Water washout
Standard test	ASTM D217	ASTM D566	ASTM D972	ASTM D1263	ASTM D1264
Quantity of grease (gm)	400	2	20	90 ± 1	4 ± 0.05
Speed (rpm)	–	–	–	660 ± 30	600 ± 30
Temperature (°C)	25 ± 0.5	–5 to +288	100–150	105 ± 1.2	38 or 79
Duration (min)	0.0833	–	1320 ± 5	360 ± 5	60 ± 1
Flow rate (ml/sec)	–	–	2000 (air)	–	5 ± 0.5 (water)
Heat rate (°C/min)	–	4–7	–	–	–

used tribometers are four-ball tester, SRV tribometer, and Timken tester, etc. The schematic diagram of four-ball and digital image of SRV tribometers are shown in Figs. 9.8 and 9.9 respectively. Timken tester is used to determine the extreme pressure property of lubricating grease as per ASTM D2509 (ASTM 2509 2015). This test consists of a rotating cup and stationary test block tribo-pair. In this test, the minimum load (score value) and the maximum load (OK value) is used for test evaluation. When adhesion between the test cup and stationary test block takes place by

**Fig. 9.8** Schematic diagram four-ball tester

**Fig. 9.9** Typical photograph of SRV V model



rupturing of the lubricant film is called minimum load. If the adhesion takes place between the test cup and test block without rupturing of the lubricant film is called maximum load. Four-ball tester, SRV tribometer is used to measure antiwear and extreme pressure property of the lubricating grease, test specifications are summarized in Table 9.8.

**Table 9.8** The details of test conditions used in various tribometers for the evaluation of antiwear and extreme pressure property of the grease

Test specifications	Wear test		Extreme pressure test	
	Four-ball tester	SRV machine	Four-ball tester	SRV machine
Test standard	ASTM D2266	ASTM D5707	ASTM D2596	ASTM D5706
Load (N)	392 ± 2	50 N for 30 s (pre load) Then 200 N	6, 8, 10, 13, 16, 20, 24, 32, 40, 50, 63, 80, 100, 126, 160, 200, 250, 315, 400, 500, 620, 800	50 N for 30 s (pre load) 100 N for 15 min, then 100 N steps with a duration of 2 min till seizure
Speed (rpm)	1200 ± 60	–	1760 ± 40	–
Stroke (mm)	–	1.0	–	1.5
Duration (min)	60 ± 1	120 ± 0.25	0.167 at each load	53.5
Temperature (°C)	75 ± 2	50 or 80 or 120	27 ± 8	50 or 80

## 9.6 Grease Specification for Automotive Industry

Society of Automotive Engineers (SAE) in association with ASTM incorporated the ideas of NLGI and established ASTM D 4950 standard for automotive service application. As per ASTM D 4950 (ASTM D4950-14 2015) the service greases are categorized into two class: general chassis grease (“L” category) and wheel bearing grease (“G” category). L category grease is used in service lubrication of universal joints, ball joints, steering pivots, suspensions, and other chassis components. While G category grease is used in service lubrication of wheel bearings, both the category of service greases is applied to passenger cars, buses, light-duty trucks and high-duty trucks etc. Further, service grease category is subdivided based on the severity of service (ASTM D4950-14 2015), and summarized in Table 9.9.

Some commercially available grease is termed as ‘multipurpose grease’. This product indicates that it is compatible for lubrication of both chassis and wheel bearings. If grease is suitable to lubricate both chassis and wheel bearing, it should be designated with both “L” and “G” specification (i.e. LB-GC). ASTM D 4950 for service grease consists of other 12 ASTM standards, and these are summarized in Table 9.10, which also includes acceptance limit.

## 9.7 Grease Lubrication Mechanism

The property of grease lies between liquid and solid. Therefore, it shows viscous and elastic properties like liquid and solid, respectively. It can be referred to as ‘viscoelastic’ material. Grease is a non-Newtonian fluid which shows thixotropy behavior (Singh et al. 2017a). Grease has a fibrous structure like that sponge. Thickener is a gelling agent which immobilizes the base oil into the matrix by weak Van der Waals forces and capillary forces (Lugt 2009). The lubricating oil is trapped between the voids available in the matrix. The base oil and thickener both play a role in lubrication mechanism. Antiwear performance of lubricating grease evaluated as per ASTM D2266 with four-ball tester and the Hertzian contact stress was found to be 3.4 GPa (Rawat et al. 2019). The soap molecules of lubricating grease squeeze under high Hertzian contact stress and bleed the lubricating oil on the contacting surfaces and develops a tribo-film. Schematic diagram of grease lubrication is depicted in Fig. 9.10. The lubricating oil comprises the additives which also exposed to tribo-pairs. These additives are nano-sized, which enters easily between the tribo-pairs and provide a better tribo-film for lubrication (Rawat et al. 2018). Spherical morphology of nano-additives transforms the sliding friction into rolling friction, which promotes the reduction in direct contact of asperity to asperity (Kashyap and Harsha 2016; Ge et al. 2015a). High Hertzian contact stress compels the grease molecules and nano-additives to fuse and gets deposited on the contact interfaces. This deposition of nano-additives on the surface forms a protective layer which assists the lubricating film (Rawat et al. 2019). Nano-additives also behaves as a self-healing agent which

**Table 9.9** List of service grease category and performance description

Grease	Category	Application	NLGI Grade	Relubrication interval	Temperature
Chassis grease	LA	To lubricate universal joints and chassis component in vehicles operated under mild duty situation and noncritical applications	2	Frequent relubrication (approx. 3200 km or less for passenger cars)	-
	LB	To lubricate universal joints and chassis component in vehicles operated under mild to severe duty situation and exposure to water or other contaminations	2	Prolonged lubrication intervals (more than 3200 km for passenger cars)	-40 to 120 °C
Wheel bearing grease	GA	To lubricate wheel bearings of the vehicles operated under mild duty situation and noncritical applications		Frequent relubrication	-20 to 70 °C
	GB	To lubricate wheel bearings of the vehicles operated under mild to moderate duty situation such as highway and off-highways service	2	Less frequent relubrication	-40 to 120 °C
	GC	to lubricate wheel bearings of the vehicles operated under mild to severe duty situation, such as severe braking service, frequent stop-and-go service	2	-	-40 to 160 °C



**Table 9.10** Requirements for service grease for chassis and wheel bearing applications

Test	Property	Acceptance limit						
		Chassis grease			Wheel bearing grease			
		LA	LB	GA	GB	GC		
D217	Work penetration, mm/10	220–340	220–340	220–340	220–340			
D566	Dropping point (°C)	80	150	80	175			220
D1264	Water resistance @ 80 °C (%), max	–	–	–	15			15
D1742	Oil separation (%), max	–	10	–	10			6
D1743	Rust, max	–	Pass	–	Pass			Pass
D2266	Four ball, scar diameter (mm), max	0.9	0.6	–	0.9			0.9
D2596	Four ball EP Load wear index (kgf), min Weld point (kgf), min	–	30 200	–	–			30 200
D3527	High temp. life (h), min	–	–	–	40			80
D4170	Fretting protection (mg loss), max	–	10	–	–			–
D4289	Elastomer compatibility 3217/3B CR (%) volume change 3217/3B CR hardness change 3217/2B NBR-L volume change (%) 3217/2B NBR-L hardness change	0–40 –15 to 0 – –	0–40 –15 to 0 – –	– – – –	– – –5 to 30 –15 to 2			– – –5 to 30 –15 to 2

(continued)

**Table 9.10** (continued)

Test	Property	Acceptance limit					
		Chassis grease			Wheel bearing grease		
		LA	LB	GB	GA	GB	GC
D4290	Leakage tendency (g) max	-	-	-	-	24	10
D4693	Low temp. torque @ -40 °C (N-m)	-	15.5	15.5	15.5	15.5	15.5

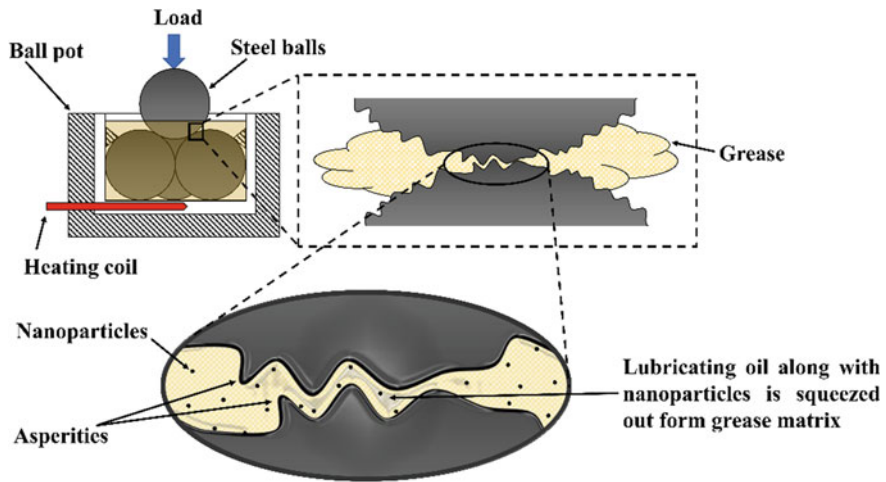


**Fig. 9.10** Schematic diagram for grease lubrication

heals the dimples of the contact interfaces and it is called mending effect (Gupta and Harsha 2018). The sandwiched nano-additives between contact interfaces decreases the real area of contact causes a decrement in the contact pressure (Rawat et al. 2019; Ghaednia and Jackson 2013). The grease becomes soft due to the flash temperature developed by Hertzian contact stress and shear rate, facilitating the exposure of lubricating oil with the degradation of grease matrix. The induced temperature in the grease due to Hertzian contact stress also affects the film thickness between the contact interfaces. As the temperature increases in the grease, the decrement in the film thickness was observed (Gonçalves et al. 2017). Experiments unveiled that at low-speed grease develop a thicker tribo-film as compared to the corresponding base oil. While at high speed formation of tribo-film similar to the base oil properties alone (Kanazawa et al. 2017).

## 9.8 Grease Tribology

The amount and type of thickening agent, dropping point, consistency, extreme pressure additives, antioxidant additives, volatility and ambient conditions are some important factors which influence the properties and performance of the lubricating grease. The tribological performance of the lubricating grease is entirely reliant on the properties of the ingredient involved in their composition. In recent decades, the researchers have demonstrated the excellent tribological performance of nanoparticles in the lubrication system. A variety of nano-sized materials were explored as a lubricant additive to enhance the tribological performance (Gulzar et al. 2016). The presence of additives in the grease enhances the tribological performance as well as

it affects the microstructure of the grease (Adhvaryu et al. 2005). Various morphologies of solid nano-sized materials such as Sn (Chang et al. 2015), Cu (Qiang et al. 2017),  $\text{CaF}_2$  (Wang et al. 2007),  $\text{MoS}_2$  (Sahoo and Biswas 2014; Rawat et al. 2019; Chen et al. 2014; Gänshemer and Holinski 1972; Czarny 2007),  $\text{SiO}_2$  (Rawat et al. 2018; Chen 2010; Ge et al. 2015a),  $\text{CuO}$  (Peña-Parás et al. 2015; Chang et al. 2014),  $\text{TiO}_2$  (Chen 2010; Ge et al. 2015a; Peña-Parás et al. 2015; Chang et al. 2014),  $\text{Al}_2\text{O}_3$  (Singh et al. 2017a, b; Peña-Parás et al. 2015),  $\text{CeF}_3$  (Wang et al. 2008),  $\text{CeO}_2$  (Shen et al. 2016; He et al. 2018), carbon nanotubes (Kamel et al. 2016; Ge et al. 2015b; Peña-Parás et al. 2015; Mohamed et al. 2015; Yang et al. 2011; Hongtao et al. 2014), carbon black (Ge et al. 2015b), carbon nanohorn (Kobayashi et al. 2005),  $\text{CaCO}_3$  (Ji et al. 2011; Chen et al. 2014; Singh et al. 2017a, b), reduced graphene oxide (Singh et al. 2017a, b), graphite (Chen et al. 2014; Czarny 2007; Silver and Stanley 1974), graphene (Fan et al. 2014; Wang et al. 2017; Kamel et al. 2017; Singh et al. 2016; Cheng and Qin 2014), quartz-enriched rice husk ash (Akhtar et al. 2016), calcium borate (Zhao et al. 2013), zirconium phosphate (Dai et al. 2017), polytetrafluoroethylene (Chen 2010; Chen et al. 2014; Czarny 2007), nanocomposites (Wu et al. 2018) were explored as an additive to enhance the tribological performance of the lubricating grease. The effect of nanoparticles on the tribological performance of the grease is summarized in Table 9.11. A variety of additives were added in the grease to improve the antiwear as well as load bearing capacity of the grease. Each nanoparticle added in the grease exhibited their significant potential to minimize the friction and wear. Rawat et al. (2018) have obtained a ~20% reduction in coefficient of friction with a dispersion of 0.03% w/w  $\text{SiO}_2$  nanoparticles in paraffin grease, whereas ~42% reduction in the mean wear volume. Furthermore, ~42% reduction in the coefficient of friction and ~55% in mean wear volume has achieved at a concentration of 0.04% w/w addition of  $\text{MoS}_2$  in paraffin grease (Rawat et al. 2019). This reduction in coefficient of friction directly decreases the demand for energy, which improves the efficiency and working life of the machinery.

Vegetable oils have excellent lubrication property, and environment-friendly nature are gaining more attention of lubrication engineers. Vegetable oils have poor oxidation stability, which makes it incompetent to use straight as base stock for development of the grease. This deficiency of vegetable oil can overcome by different chemical modification techniques. Various chemical modification route has been discovered for bio-lubricants viz transesterification (Panchal et al. 2015), estolide formation (García-Zapateiro et al. 2013), hydrogenation (Fernández and Tonetto 2009), and epoxidation (Kashyap and Harsha 2016; Gupta et al. 2018). An investigation conducted by Panchal et al. (2015) is a shred of transesterification of non-edible vegetable oil (Karanja oil). Chemically modified Karanja oil (Transesterified esters) has chosen as the base oil, and lithium-12-hydroxy stearate opted as a thickening agent in the formulation of grease samples. The tribological results showed that vegetable oil-based grease has good antiwear and load carrying capacity as compared to mineral oil (SN 500) based commercially available lithium grease. Researchers are trying to find an effective alternative of conventional thickening agents (metallic soap, clay, or polyurea etc.) in the formulation of grease, which is also biodegradable and eco-friendly. Alternative thickeners derived from natural resources should

**Table 9.11** Tribological performance of lubricating grease dispersed with numerous nano-additives

References	Base oil	Thickener	Nanoparticles	Optimum concentration	Coefficient of friction ( $\mu$ )	Wear scar diameter (WSD)/Mean wear volume (MWV)	Extreme pressure (EP)
Gänsheimer et al. (1972)	Mineral oil	Lithium soap	MoS <sub>2</sub> (lamellar t = 5–10 $\mu$ m)	3% w/w	–	–	EP $\uparrow$ 100–220 kg
Kobayashi et al. (2005)	Mineral oil	Lithium soap	CNH (horn-shaped tip, d < 80–100 nm) HT-CNH (horn-shaped rounded tip, d = 600 nm) Graphite (Flake)	Less than 1 mass% Less than 1 mass% 3 or more mass%	$\mu$ ↓ $\mu$ ↓ $\mu$ ↓	WSD↓ WSD↓ WSD↓	– – –
Wang et al. (2007)	Commercial lithium grease		CaF <sub>2</sub> (cubic, l = 60–65 nm)	1.0% w/w	$\mu$ ↓ 29%	WSD↓ 19%	EP $\uparrow$ 48%
Wang et al. (2008)	Paraffin oil	Lithium soap	OA-CeF <sub>3</sub> (hexagonal, d = 20 nm)	2.0% w/w	$\mu$ ↓	WSD↓	EP $\uparrow$
Chen (2010)	Mixture of Neopentyl polyol ester, soy bean oil and commercial 650SN (4.5:2.5:1)	Titanium complex soap	PTFE TiO <sub>2</sub> SiO <sub>2</sub>	2.0 wt% 0.5 wt% 1.5 wt%	$\mu$ ↓ 34.58% $\mu$ ↓ 22.97% $\mu$ ↓ 24.47%	WSD↓ 4.95% WSD↓ 4.35% WSD↓ 1.80%	– – –

(continued)

Table 9.11 (continued)

References	Base oil	Thickener	Nanoparticles	Optimum concentration	Coefficient of friction ( $\mu$ )	Wear scar diameter (WSD)/Mean wear volume (MWV)	Extreme pressure (EP)
Yang et al. (2011)	Commercial greases (Daphne Alphasel ET) (Daphne Eponecks SR) Alvania grease S2)		CNTs (tubular, d = 150 nm, l = 10–20 $\mu$ m)	0.3 wt%	$\mu$ ↓	WSD↓	–
Ji et al. (2011)	PAO	Lithium soap	CaCO <sub>3</sub> (cubic, l = 45 nm)	5.0 wt%	$\mu$ ↓	WSD↓	EP↑
Zhao et al. (2013)	Mineral oil	Lithium soap	Calcium borate (spherical, d = 70 nm)	6.0 wt%	$\mu$ ↓	WSW↓	EP↑
Sahoo and Biswas (2014)	Mineral oil	Lithium soap	MoS <sub>2</sub> (lamellar, 1–350 nm)	0.2 wt%	$\mu$ ↓	–	–
Hongtao et al. (2014)	PAO (DURASYN-166)	Calcium-sodium soap	CNTs (tubular, d = 1.4 nm, l = 0.5–40 $\mu$ m)	–	$\mu$ ↓	Wear ratio↓	–
Chen et al. (2014)	PAO-40	Attapulgit/Bentonite clay	PTFE MoS <sub>2</sub> CaCO <sub>3</sub> Graphite	3.0 wt%	$\mu$ ↓ $\mu$ ↓ $\mu$ ↑ $\mu$ ↓	MWV↑ MWV↓ MWV↑ MWV↑	–

(continued)

Table 9.11 (continued)

References	Base oil	Thickener	Nanoparticles	Optimum concentration	Coefficient of friction ( $\mu$ )	Wear scar diameter (WSD)/Mean wear volume (MWV)	Extreme pressure (EP)
Zhao et al. (2013)	Mineral oil	Lithium soap	Calcium Borate (spherical, d = 70 nm)	6.0 wt%	$\mu$ ↓	WSD↓	No change
Fan et al. (2014)	PAO-40	Bentone soap	Graphene (lamellar, t = 1.3 nm)	0.1 wt%	$\mu$ ↓ 10.4%	MWV↓ 25–50%	–
Chang et al. (2014)	Commercial lithium grease	Commercial lithium grease (LB80102)	TiO <sub>2</sub> (spherical, d = 40–60 nm) CuO (spherical, d = 90–110 nm)	1.0 wt% 2.0wt%	$\mu$ ↓ 40% $\mu$ ↓	WSD↓ WSD↓ 60%	– –
Cheng and Qin (2014)	Commercial lithium grease	Commercial lithium grease	Graphene oxide (flake)	0.075%w/w	$\mu$ ↓ 40–60%	WSD↓ 50%	–
Ge et al. (2015a)	Naphthenic oil	PTFE	TiO <sub>2</sub> (spherical, d = 35 nm) SiO <sub>2</sub> (spherical, d = 30 nm)	0.1 wt% 0.1wt%	$\mu$ ↓ $\mu$ ↓	WSD↓ WSD↓	– –

(continued)

Table 9.11 (continued)

References	Base oil	Thickener	Nanoparticles	Optimum concentration	Coefficient of friction ( $\mu$ )	Wear scar diameter (WSD)/Mean wear volume (MWV)	Extreme pressure (EP)
Panchal et al. (2015)	Karanja oil	Lithium soap	-	-	$\mu$ ↓	WSD↓	EP↑
Peña-Parás et al. (2015)	Commercial grease (Moligrase 28 and Uniflor 8623B)		TiO <sub>2</sub> (spherical, d < 21 nm) Al <sub>2</sub> O <sub>3</sub> (spherical, d < 50 nm) CuO (tubular, d = 6–9 nm) MWNTs (tubular, l = 5 $\mu$ m)	0.1 wt% 0.1 wt% 0.1 wt% 0.01 wt%	$\mu$ ↓ 30% $\mu$ ↓ 7.5% $\mu$ ↓ 36% $\mu$ ↓ 16%	WSD↓ 20% WSD↑ 11% WSD↓ 14% WSD↓ 4%	- - - -
Mohamed et al. (2015)	Commercial lithium grease		CNTs (tubular, d = 10 nm, l = 5 $\mu$ m)	1.0 wt%	$\mu$ ↓ 81.5%	WSD↓ 63%	EP↑ 52%
Chang et al. (2015)	Commercial lithium grease		Sn1 (spherical, d = 60 nm) Sn2 (spherical, d = 80 nm) Sn3 (spherical, d = 120 nm)	1.0 wt%	$\mu$ ↓ 63.5%	WSD↓ 58.9%	-

(continued)



Table 9.11 (continued)

References	Base oil	Thickener	Nanoparticles	Optimum concentration	Coefficient of friction ( $\mu$ )	Wear scar diameter (WSD)/Mean wear volume (MWV)	Extreme pressure (EP)
Akhtar et al. (2016)	Commercial lithium grease		Rice husk ash (flake)	0.5 wt%	$\mu$ ↓	WSD↓	EP↑
Shen et al. (2016)	Mixed oil (350SN and 650 SN) (1:1 weight ratio)	Titanium complex soap	CeO <sub>2</sub> (spherical, d = 10 nm)	3.0 wt%	$\mu$ ↓	WSD↓	EP↑
Ge et al. (2015b)	PAG	PTFE	CB (spherical, d = 35 nm) MW/CNTs (tubular, d = 50 nm) CMW/CNTs (tubular, d = 50 nm) SWCNTs (tubular, d = 1–2 nm)	1.0 wt% 1.0 wt% 1.0 wt% 1.0 wt%	$\mu$ ↓ $\mu$ ↓ $\mu$ ↓ $\mu$ ↓	MWV↓ MWV↓ MWV↓ MWV↓	– – – –
Kamel et al. (2016)	Commercial calcium grease (MERKAN 23)		MW/CNTs (tubular, d = 10–12 nm, l = 1–20 $\mu$ m)	3.0 wt%	$\mu$ ↓ 50%	WSD↓ 32%	EP↑ 38%

(continued)

Table 9.11 (continued)

References	Base oil	Thickener	Nanoparticles	Optimum concentration	Coefficient of friction ( $\mu$ )	Wear scar diameter (WSD)/Mean wear volume (MWV)	Extreme pressure (EP)
Singh et al. (2016)	Commercial lithium grease		rGO (lamellar)	0.4 wt%	$\mu$ ↓ 30%	-	-
Dai et al. (2017)	POA-8	Calcium soap	Zirconium phosphate	3.0 wt%	$\mu$ ↓	WSD↓	EP↑
Qiang et al. (2017)	Commercial lithium grease		Cu (spherical, d = 10 nm)	0.25 wt%	$\mu$ ↓	WSD↓	-
Wang et al. (2017)	Commercial oil (MVI500)	Lithium soap	Graphene (lamellar)	0.5 wt%	$\mu$ ↓ 18.9%	WSD↓ 10.4%	-
Kamel et al. (2017)	Commercial calcium grease (MERKAN 23)		Graphene (lamellar, t = 1.3 nm, l = 2 $\mu$ m)	3.0 wt%	$\mu$ ↓ 61%	WSD↓ 45%	EP↑ 60%
Singh et al. (2017a)	Commercial lithium grease		rGO (lamellar, l = 500 nm) CaCO <sub>3</sub> (cubic, l = 50 nm) Al <sub>2</sub> O <sub>3</sub> (random, l = 40 nm)	0.4 wt% 5.0 wt% 0.8 wt%	$\mu$ ↓ 35% $\mu$ ↓ 27% $\mu$ ↓ 10%	- - -	- - -

(continued)

Table 9.11 (continued)

References	Base oil	Thickener	Nanoparticles	Optimum concentration	Coefficient of friction ( $\mu$ )	Wear scar diameter (WSD)/Mean wear volume (MWV)	Extreme pressure (EP)
Singh et al. (2017b)	Commercial lithium grease		rGO (lamellar, l = 500 nm) CaCO <sub>3</sub> (cubic, l = 50 nm) Al <sub>2</sub> O <sub>3</sub> (random, l = 40 nm)	0.4 wt% 5.0 wt% 0.8 wt%	- - -	- - -	EP $\uparrow$ 45% EP $\uparrow$ 25% No Change
Wu et al. (2018)	Commercial grease		Zinc borate & MoS <sub>2</sub> (nanocomposite)	0.06 wt%	$\mu$ $\downarrow$ 28.2%	WSD $\downarrow$ 23.1%	EP $\uparrow$ 23.1%
Rawat et al. (2018)	Paraffin oil	Lithium soap	SiO <sub>2</sub> (spherical, d = 70 nm)	0.03% w/w (COF) 0.05% w/w (MWV)	$\mu$ $\downarrow$ 20%	MWV $\downarrow$ 42%	No change
He et al. (2018)	Commercial lithium grease		CeO <sub>2</sub> (random, l < 500 nm)	0.6 wt%	$\mu$ $\downarrow$ 28%	WSD $\downarrow$ 13%	-
Rawat et al. (2019)	Paraffin oil	Lithium soap	MoS <sub>2</sub> (lamellar, t = 3–7 nm, l = 50–150 nm) MoS <sub>2</sub> -ODT (lamellar, t = 3–7 nm, l = 50–150 nm)	0.04% w/w (COF&MWV) 0.01% w/w (COF) 0.04% w/w (MWV)	$\mu$ $\downarrow$ 42% $\mu$ $\downarrow$ 42%	MWV $\downarrow$ 55% MWV $\downarrow$ 61%	No change

$\downarrow$  decrement;  $\uparrow$  increment; t = thickness; l = length; d = diameter

include gel-like characteristics, non-toxicity, thermal resistance, biodegradability property. Apart from that, it should have a similar potential to minimize wear and friction as achieved by conventional non-renewable thickening agents. García-Zapateiro (García-Zapateiro et al. 2014) and coworkers developed biodegradable grease with vegetable oil (castor oil, High-oleic sunflower acid oil and a ricinoleic acid-derived estolide) with biopolymers (chitosan and Kraft cellulose pulp). These biopolymers are renewable and proposed as an alternative to conventional thickening agents for the formulation of lubricating grease.

## 9.9 Compatibility of Greases

Sometimes some base oils and some thickening agents are not compatible with each other. Therefore, it is not recommended for mixing of two greases with each other. The mixing of two incompatible greases deteriorates the physical and tribological behavior of the grease. The compatibility of lubricating greases with bearing seals is also a significant aspect, which is mainly considered on the basis of base oil. ASTM D6185 (ASTM D6185-11 2018) protocol covers the evaluation of compatibility of one or more mixtures of lubricating greases.

The mixing of two greases is possible only when the similar base oil (chemical structure), similar thickening agent (including concentration), similar additives (concentration also) and similar formulation technique is followed for the preparation of greases.

## 9.10 Application of Grease

The grease has great demand in railroad, agriculture, steel mills, cement, mining, textile, food industry, and automobile sector etc. The operating conditions of grease often encountered with wet and humid conditions, dusty environment, exposure of water, and corrosive environment. Draglines and excavators used in mining industry furnished with kilometers long wire ropes lubricated with grease. The wire ropes met with shock loads, high wear rate, and dusty environment. The wire ropes greases should have a high concentration of AW and EP as well as anticorrosion additives. In aviation application, the applied grease in aircraft flew at high altitude and encountered with temperature in the range between  $-75$  and  $200$  °C. Therefore, synthetic oil preferred as base stock for aviation application. In space, the grease confronts the vacuum environment, so outstandingly low volatility base oil is ideal. Specially designed seals controlled the evaporation loss in the space. If grease applied at water contamination area, then grease should possess high viscosity base oil and water-resistant thickener. Water wash out property can be minimized with the addition of tackiness additives. In the situation of heavy or shock load, high viscosity lubricating oil grease preferred as well as it should contain a higher concentration of antiwear

**Table 9.12** Application of grease in various parts of the passenger cars (Mang and Dresel 2007)

Automobile systems	Automobile parts
Steering system	Rack and pinion steering gear, pivots joints of steering linkages, steering intermediate shafts
Suspension system	Ball joints of cross-bar and antiroll-bar, shock absorbers, half shaft joints
Brake system	Caliper pins, ABS follower
Power transmission system	Universal joints, cardan joint, constant velocity joint, belt-pulley bearing, clutch bearing/spline, fan clutch bearing, turbo/supercharger, differential gear, hypoid rear axle
Wheel bearing	Roller bearings, needle bearings
Body hardware	Door locks, door check hinges, windshield wiper gear, window levers, seat adjustment gears
Electrical system	Electrical contacts, alternator bearing
Others	Water pump bearing, cable actuators

and extreme pressure additives. The grease selection for a specific application is based on the operating temperature, operational life, load, speed, type of component and, the environment. The application of grease in various parts of a passenger car is summarized in Table 9.12.

## 9.11 Summary

The fundamental of lubricants, greases and its composition has been discussed in this chapter. Large varieties of base oils and thickening agents are used in the formulation of lubricating grease. Blending of additives in the grease is a common practice to enhance properties of the grease. Lubricating greases are widely used in locomotive, automotive, mining, steel, food industry, textile, and agriculture applications. Besides this, greases are extensively used in a large variety of severe operating environmental situations viz. higher temperature higher load, speed, and extreme pressure. Various ASTM protocol for physical and tribological characterization of grease is also discussed. From the last decade, the nano-additives are gaining more attention for improvising the tribological performance of the grease. Remarkable reduction in coefficient of friction and wear is reported which indicates the significant potential of nano-additives for improving the tribological performance. Biodegradability and other environmental issues attract the researchers to search for an alternative for conventional lubricants. Excellent lubrication behavior, renewability, and biodegradability properties of the vegetable oils are an attractive alternative for traditional petroleum-based lubricants. Therefore, some researchers shift their choice towards renewable resources, which is readily biodegradable as well as eco-friendly.

## References

- Adhvaryu A, Sung C, Erhan SZ (2005) Fatty acids and antioxidant effects on grease microstructures. *Ind Crops Prod* 21:285–291. <https://doi.org/10.1016/j.indcrop.2004.03.003>
- Akhtar K, Khalid H, Ul Haq I, Malik A (2016) Improvement in tribological properties of lubricating grease with quartz-enriched rice husk ash. *Tribol Int* 93:58–62. <https://doi.org/10.1016/j.triboint.2015.09.015>
- ASTM D1263-94 (1994) Standard test method for leakage tendencies of automotive wheel bearing greases. ASTM Int. West Conshohocken, PA
- ASTM D1264-16 (2017) Standard test method for determining the water washout characteristics of lubricating greases. ASTM Int. West Conshohocken, PA. <https://doi.org/10.1520/d1264-16.2>
- ASTM D2265-15 (2017) Standard test method for dropping point of lubricating grease over wide temperature range. ASTM Int. West Conshohocken, PA. <https://doi.org/10.1520/d2265-15.2>
- ASTM D2509-14 (2015) Standard test method for measurement of load-carrying capacity of lubricating grease (timken method). ASTM Int. West Conshohocken, PA. <https://doi.org/10.1520/d2509-14.2>
- ASTM D217-02 (2003) standard test methods for cone penetration of lubricating grease. ASTM Int. West Conshohocken, PA
- ASTM D4950-14 (2015) Standard classification and specification for automotive service greases. ASTM Int. West Conshohocken, PA. <https://doi.org/10.1520/d4950-14>
- ASTM D566-16 (2016) Standard test method for dropping point of lubricating grease. ASTM Int. West Conshohocken, PA. <https://doi.org/10.1520/d0566-16.in>
- ASTM D6185-11 (2018) Standard practice for evaluating compatibility of binary mixtures of lubricating greases. ASTM Int. West Conshohocken, PA. <https://doi.org/10.1520/d6185-11r17>
- ASTM D972-16 (2017) Standard test method for evaporation loss of lubricating greases and oils. ASTM Int. West Conshohocken, PA. <https://doi.org/10.1520/d0972-16.2>
- Chang H, Lan CW, Chen CH, Kao MJ, Guo J (2014) Bin: Anti-wear and friction properties of nanoparticles as additives in the lithium grease. *Int J Precis Eng Manuf* 15:2059–2063. <https://doi.org/10.1007/s12541-014-0563-y>
- Chang H, Kao M, Luo J, Lan C (2015) Synthesis and effect of nanogrease on tribological properties. *Int J Precis Eng Manuf* 16:1311–1316. <https://doi.org/10.1007/s12541-015-0171-5>
- Chen J (2010) Tribological properties of polytetrafluoroethylene, nano-titanium dioxide, and nano-silicon dioxide as additives in mixed oil-based titanium complex grease. *Tribol Lett* 38:217–224. <https://doi.org/10.1007/s11249-010-9593-5>
- Chen T, Xia Y, Liu Z, Wang Z (2014) Preparation and tribological properties of attapulgite—bentonite clay base grease. *Ind Lubr Tribol* 66:538–544. <https://doi.org/10.1108/ILT-07-2012-0062>
- Cheng ZL, Qin XX (2014) Study on friction performance of graphene-based semi-solid grease. *Chinese Chem Lett* 25:1305–1307. <https://doi.org/10.1016/j.ccllet.2014.03.010>
- Czarny R (2007) Maciej Paszkowski: The influence of graphite solid additives, MoS<sub>2</sub> and PTFE on changes in shear stress values in lubricating greases. *J Synth Lubr* 24:19–29. <https://doi.org/10.1002/jsl>
- Dai Y, Niu W, Zhang X, Xu H, Dong J (2017) Tribological investigation of layered zirconium phosphate in anhydrous calcium grease. *Lubricants*. 5:22–31. <https://doi.org/10.3390/lubricants5030022>
- Fan X, Xia Y, Wang L, Li W (2014) Multilayer graphene as a lubricating additive in bentone grease. *Tribol Lett* 55:455–464. <https://doi.org/10.1007/s11249-014-0369-1>
- Fernández MB, M, JFS, Tonetto GM, Damiani DE (2009) Hydrogenation of sunflower oil over different palladium supported catalysts : activity and selectivity. *Chem Eng J* 155:941–949. <https://doi.org/10.1016/j.cej.2009.09.037>
- Fox NJ, Stachowiak GW (2007) Vegetable oil-based lubricants—a review of oxidation. *Tribol Int* 40:1035–1046. <https://doi.org/10.1016/j.triboint.2006.10.001>

- Gänsheimer J, Holinski R (1972) A study of solid lubricants in oils and greases under boundary conditions. *Wear* 19:439–449. [https://doi.org/10.1016/0043-1648\(72\)90317-1](https://doi.org/10.1016/0043-1648(72)90317-1)
- García-Zapateiro LA, Franco JM, Valencia C, Delgado MA, Gallegos C (2013) Viscous, thermal and tribological characterization of oleic and ricinoleic acids-derived estolides and their blends with vegetable oils. *J Ind Eng Chem* 19:1289–1298. <https://doi.org/10.1016/j.jiec.2012.12.030>
- García-Zapateiro LA, Valencia C, Franco JM (2014) Formulation of lubricating greases from renewable basestocks and thickener agents: a rheological approach. *Ind Crops Prod* 54:115–121. <https://doi.org/10.1016/j.indcrop.2014.01.020>
- Ge X, Xia Y, Cao Z (2015a) Tribological properties and insulation effect of nanometer TiO<sub>2</sub> and nanometer SiO<sub>2</sub> as additives in grease. *Tribol Int* 92:454–461. <https://doi.org/10.1016/j.triboint.2015.07.031>
- Ge X, Xia Y, Feng X (2015b) Influence of carbon nanotubes on conductive capacity and tribological characteristics of poly (ethylene glycol-ran-propylene glycol) monobutyl ether as base oil of grease. *J Tribol* 138:11801. <https://doi.org/10.1115/1.4031232>
- Ghaednia H, Jackson RL (2013) The effect of nanoparticles on the real area of contact, friction, and wear. *J Tribol* 135:041603–041610. <https://doi.org/10.1115/1.4024297>
- Gonçalves D, Vieira A, Carneiro A, Campos A, Seabra J (2017) Film thickness and friction relationship in grease lubricated rough contacts. *Lubricants*. 5:34. <https://doi.org/10.3390/lubricants5030034>
- Gulzar M, Masjuki HH, Kalam MA, Varman M, Zulkifli N.W.M., Mufti RA, Zahid R (2016) Tribological performance of nanoparticles as lubricating oil additives. *J Nanoparticle Res* 18. <https://doi.org/10.1007/s11051-016-3537-4>
- Gupta RN, Harsha AP (2018) Tribological evaluation of calcium-copper-titanate/ cerium oxide-based nanolubricants in sliding contact
- Gupta RN, Harsha AP, Singh S (2018) Tribological study on rapeseed oil with nano-additives in close contact sliding situation. *Appl Nanosci* 8:567–580. <https://doi.org/10.1007/s13204-018-0670-7>
- He Q, Li A, Guo Y, Liu S, Zhang Y, Kong L (2018) Tribological properties of nanometer cerium oxide as additives in lithium grease. *J Rare Earths* 36:209–214. <https://doi.org/10.1016/j.jre.2017.09.004>
- Holmberg K, Andersson P, Erdemir A (2012) Global energy consumption due to friction in passenger cars. *Tribol Int* 47:221–234. <https://doi.org/10.1016/j.triboint.2011.11.022>
- Holmberg K, Andersson P, Nylund N, Mäkelä K, Erdemir A (2014) Global energy consumption due to friction in trucks and buses. *Tribol Int* 78:94–114. <https://doi.org/10.1016/j.triboint.2014.05.004>
- Honary L, Erwin R (2011) *Biobased lubricants and greases: technology and products*. Wiley
- Hongtao L, Hongmin J, Haiping H, Younes H (2014) Tribological properties of carbon nanotube grease. *Ind Lubr Tribol* 66:579–583. <https://doi.org/10.1108/ILT-08-2012-0071>
- Ji X, Chen Y, Zhao G, Wang X, Liu W (2011) Tribological properties of CaCO<sub>3</sub> nanoparticles as an additive in lithium grease. *Tribol Lett* 41:113–119. <https://doi.org/10.1007/s11249-010-9688-z>
- Kamel BM, Mohamed A, El Sherbiny M, Abed KA (2016) Tribological behaviour of calcium grease containing carbon nanotubes additives. *Ind. Lubr. Tribol.* 68:723–728. <https://doi.org/10.1108/ILT-12-2015-0193>
- Kamel BM, Mohamed A, El Sherbiny M, Abed KA, Abd-Rabou M (2017) Tribological properties of graphene nanosheets as an additive in calcium grease. *J Dispers Sci Technol* 38:1495–1500. <https://doi.org/10.1080/01932691.2016.1257390>
- Kanazawa Y, Sayles RS, Kadiric A (2017) Film formation and friction in grease lubricated rolling-sliding non-conformal contacts. *Tribol Int* 109:505–518. <https://doi.org/10.1016/j.triboint.2017.01.026>
- Kashyap A, Harsha AP (2016) Tribological studies on chemically modified rapeseed oil with CuO and CeO<sub>2</sub> nanoparticles. *Proc Inst Mech Eng Part J J Eng Tribol* 230:1562–1571. <https://doi.org/10.1177/1350650116641328>

- Kobayashi K, Hironaka S, Tanaka A, Umeda K, Iijima S, Yudasaka M, Kasuya D, Suzuki M (2005) Additive effect of carbon nanohorn on grease lubrication properties. *J Japan Pet Inst* 48:121–126. <https://doi.org/10.1627/jpi.48.121>
- Lugt PM (2009) A review on grease lubrication in rolling bearings. *Tribol Trans* 52:470–480. <https://doi.org/10.1080/10402000802687940>
- Mang T, Dresel W (eds) (2007) *Lubricants and lubrication*. WILEY-VCH Verlag GmbH & Co, KGaA
- Melville E (ed) (1984) *NLGI, Lubricating greases guide*. National Lubricating Grease Institute
- Mohamed A, Khattab AA, Osman TAS, Zaki M (2015) Tribological behavior of carbon nanotubes as an additive on lithium grease. *J Tribol* 137:011801–011805. <https://doi.org/10.1155/2013/279090>
- Panchal T, Chauhan D, Thomas M, Patel J (2015) Bio based grease a value added product from renewable resources. *Ind Crops Prod* 63:48–52. <https://doi.org/10.1016/j.indcrop.2014.09.030>
- Panchal TM, Patel A, Chauhan DD, Thomas M, Patel JV (2017) A methodological review on bio-lubricants from vegetable oil based resources. *Renew Sustain Energy Rev* 70:65–70. <https://doi.org/10.1016/j.rser.2016.11.105>
- Peña-Parás L, Taha-Tijerina J, García A, Maldonado D, Nájera A, Cantú P, Ortiz D (2015) Thermal transport and tribological properties of nanogreases for metal-mechanic applications. *Wear* 332–333:1322–1326. <https://doi.org/10.1016/j.wear.2015.01.062>
- Qiang H, Anling L, Yangming Z, Liu S, Yachen G (2017) Experimental study of tribological properties of lithium-based grease with Cu nanoparticle additive. *Tribol Mater Surf Interf* 11:75–82. <https://doi.org/10.1080/17515831.2017.1311560>
- Rawat SS, Harsha AP, Deepak AP (2018) Tribological performance of paraffin grease with silica nanoparticles as an additive. *Appl. Nanosci.* 9:305–315. <https://doi.org/10.1007/s13204-018-0911-9>
- Rawat SS, Harsha AP, Agarwal DP, Kumari S, Khatri OP (2019) Pristine and alkylated MoS<sub>2</sub> Nanosheets for enhancement of tribological performance of paraffin grease under boundary lubrication regime. *J Tribol* 141:072102–072112. <https://doi.org/10.1115/1.4043606>
- Reeves CJ, Siddaiah A, Menezes PL (2017) A review on the science and technology of natural and synthetic biolubricants. *J Bio Tribo Corrosion* 3:11. <https://doi.org/10.1007/s40735-016-0069-5>
- Sahoo RR, Biswas SK (2014) Effect of layered MoS<sub>2</sub> nanoparticles on the frictional behavior and microstructure of lubricating greases. *Tribol Lett* 53:157–171. <https://doi.org/10.1007/s11249-013-0253-4>
- Shen T, Wang D, Yun J, Liu Q, Liu X, Peng Z (2016) Tribological properties and tribochemical analysis of nano-cerium oxide and sulfurized isobutene in titanium complex grease. *Tribol Int* 93:332–346. <https://doi.org/10.1016/j.triboint.2015.09.028>
- Silver HB, Stanley IR (1974) The effect of the thickener on the efficiency of load-carrying additives in greases. *Tribol Int* 7:113–118
- Singh J, Anand G, Kumar D, Tandon N (2016) Graphene based composite grease for elastohydrodynamic lubricated point contact. *IOP Conf Ser Mater Sci Eng* 149:1–9. <https://doi.org/10.1088/1757-899X/149/1/012195>
- Singh J, Kumar D, Tandon N (2017a) Development of nanocomposite grease: microstructure, flow, and tribological studies. *J Tribol* 139:052001. <https://doi.org/10.1115/1.4035775>
- Singh J, Kumar D, Tandon N (2017b) Tribological and vibration studies on newly developed nanocomposite greases under boundary lubrication regime. *J Tribol* 140:1–10. <https://doi.org/10.1115/1.4038100>
- Sumathi S, Chai SP, Mohamed AR (2008) Utilization of oil palm as a source of renewable energy in Malaysia. *Renew Sustain Energy Rev* 12:2404–2421. <https://doi.org/10.1016/j.rser.2007.06.006>
- Wang L, Wang B, Wang X, Liu W (2007) Tribological investigation of CaF<sub>2</sub> nanocrystals as grease additives. *Tribol Int* 40:1179–1185. <https://doi.org/10.1016/j.triboint.2006.12.003>
- Wang L, Zhang M, Wang X, Liu W (2008) The preparation of CeF<sub>3</sub> nanocluster capped with oleic acid by extraction method and application to lithium grease. *Mater Res Bull* 43:2220–2227. <https://doi.org/10.1016/j.materresbull.2007.08.024>



- Wang J, Guo X, He Y, Jiang M, Sun R (2017) Tribological characteristics of graphene as lithium grease additive. *China Pet Process Petrochemical Technol* 19:46–54. <https://doi.org/10.1039/C7RA07252J>
- Wu PR, Kong YC, Ma ZS, Ge T, Feng YM, Liu Z, Cheng ZL (2018) Preparation and tribological properties of novel zinc borate/MoS<sub>2</sub> nanocomposites in grease. *J. Alloys Comp* 740:823–829. <https://doi.org/10.1016/j.jallcom.2018.01.104>
- Yang Y, Yamabe T, Kim B-S, Kim I-S, Enomoto Y (2011) Lubricating characteristic of grease composites with CNT additive. *Tribol Online* 6:247–250. <https://doi.org/10.2474/trol.6.247>
- Zhao G, Zhao Q, Li W, Wang X, Liu W (2013) Tribological properties of nano-calcium borate as lithium grease additive. *Lubr Sci* 26:43–53. <https://doi.org/10.1002/ls.1227>

# Chapter 10

## Lubrication Effectiveness and Sustainability of Solid/Liquid Additives in Automotive Tribology



R. K. Upadhyay

**Abstract** In the automotive industry, losses results from friction and wear processes are huge, and every year almost thirty percent of the economy is consumed due to tribological losses. Recent advancement in technologies now permits the tribologist to design suitable lubrication techniques that were unachievable in the past. Recently, vapor film deposition or adding a thin layer of lubricants with improved physical and chemical properties is enormous. However, the suitability of such type of techniques is still in developing stage. To control the contact mechanism of sliding/rolling elements in the automotive industry, this work reports the importance of solid/liquid particles in lubrication. The friction and wear behavior of nanoparticles based on thin film coating and liquid lubrication technique is studied with traditional lubrication concept of vapor deposition and fluid film lubrication. Both techniques are necessary for designing lubricating film at the nanometer scale to control the surface properties of materials at nano/micro scales. Further, nanoparticles of self-lubricious materials are also used to prepare laboratory grease and are compared with traditional industrial grease. The obtained results are discussed by the intrinsic mechanism of sliding/rolling, theories of friction, wear, and involved parameters in the tribological tests. The potential application of prepared vapor deposition films/nanolubricants is loaded gears, bearings, piston cylinder, etc. The work can also be suitable in other industries where failure occurrence is repeated continuously due to resulting frictional losses.

**Keywords** Lubrication · Tribological effects · Liquid-contact · Vapor deposition · Automotive industry

### 10.1 Introduction

Lubrication is an effective technology to reduce surface fluctuation and provide smooth operation during sliding/rolling contact (Zhu et al. 2019). However, the process is not easy due to the involvement of various factors such as properties of two

---

R. K. Upadhyay (✉)

Mechanical Engineering Department, Indian Institute of Technology Kanpur, Kanpur, India  
e-mail: [medsired@yahoo.co.in](mailto:medsired@yahoo.co.in)

© Springer Nature Singapore Pte Ltd. 2019

J. K. Katiyar et al. (eds.), *Automotive Tribology*, Energy, Environment, and Sustainability,  
[https://doi.org/10.1007/978-981-15-0434-1\\_10](https://doi.org/10.1007/978-981-15-0434-1_10)

183

contact surfaces, environment factors, effective load, and operational speed (Gong et al. 2019; Qin et al. 2019). Among all load and speed are the main influential factors, which determine the performance of components. More than fifty percent of automotive components are made of steel structure and need some lubrication for their proper functioning. Hence, the choice of lubrication method is the most important selection criteria in designing automotive components (Tai et al. 2014).

Based on the working principle, automotive components are provided with liquid or solid lubricants. Solid particles such as graphite, graphene, molybdenum disulfide, and boron nitride are the commonly used solid particles for extreme pressure situation (Miyake 2005; Zhai et al. 2017; Shi and Wu 2018). In solid lubrication, these particles act as a barrier between the contacts because generally these particles are used under boundary lubrication condition. In this case, the exerted load is very high, and the sliding speed is low, which causes a seizure problem. For resolving the seizure problem, extreme pressure grease can be used (Sommer and Haas 2016; Lugt 2016). Grease can also be prepared by solid particle addition for providing support in lubrication mechanism. On the other hand, the need for liquid film arises where operating speed is high and acted load is low. The most important selection criteria are the adequate thickness of film responsible for supporting the film (Cen and Lugt 2019; Jammal et al. 2019; Karakashev et al. 2014). Similar to solid lubrication, this is also achieved in boundary regime with or without any additive in oil medium.

In special cases where chances of heat transfer and local deformation arise it can be provided with vapor deposition, and polymer films (Upadhyay and Kumaraswamidhas 2014, 2015; Upadhyay and Kumar 2019a, b). Both these coatings are highly recommended for their unique properties in reducing friction and wear with the ability to withstand pressure. Nowadays, especially polymer-based nanocomposites are finding its place in a variety of applications (Upadhyay and Kumar 2019a). Generally, they are made of solid/liquid fillers into the epoxy matrix. The only problem of these nanocomposites is their hygroscopic property and the unknown amount of filler quantity that has to be added for a particular application (Upadhyay and Kumar 2019b). Based on the above lubrication methodologies, this chapter provides a detailed tribological investigation of solid/liquid/grease/polymer based lubrication mechanism under the boundary contact condition.

### ***10.1.1 Preparation Method of Lubricants/Vapor Deposition***

Scheme of various lubrication methodologies and their preparation method is presented in Fig. 10.1. In solid lubrication, solid particles are added between the contacts with the help of volatile liquid in order to distribute homogeneously. In liquid lubrication, the major difference is that particles are suspended in an oil medium to provide better lubrication mechanism. Physical vapor deposition (PVD) with sputtering technique is one of the best methods available in the market for application ranging from low to high temperature. Vapor deposition with sputtering is based on dislodging and ejecting the atom from the target to the substrate material in the

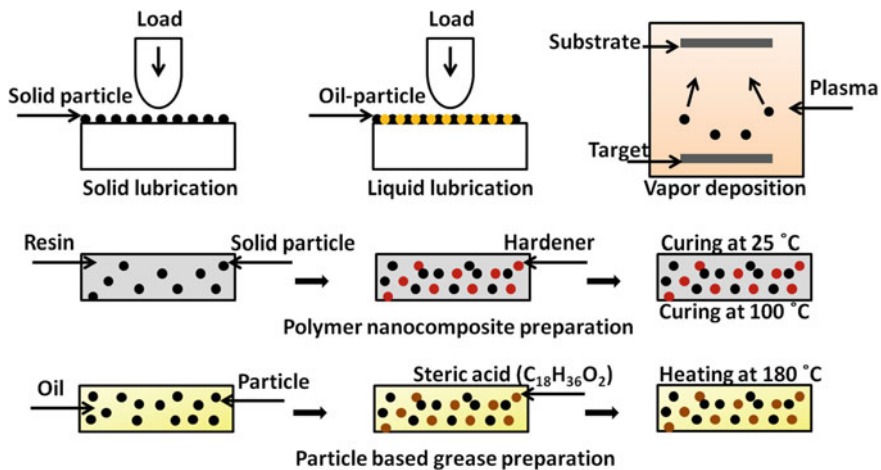


**Fig. 10.1** Various lubrication methodology and preparation method

presence of reactive argon gas. The target material is a type of coating that needs to be provided onto the substrate material. The sputtering process was carried in the presence of high-temperature plasma atmosphere. The dimension of the PVD target was 600 mm height and 125 mm width.

Polymer nanocomposites are prepared by infusing the nano/micro sized solid/liquid particles in the epoxy resin. This type of composites preparation required an extensive stirring process for particles in order to distribute uniformly throughout the matrix. A highly bonded composite is a result of room and temperature curing process. For preparing grease, desired particles are initially suspended in oil medium and provided with ultrasonication at temperature 70 °C. After a while, stearic acid (C<sub>18</sub>H<sub>36</sub>O<sub>2</sub>) was added in the oil suspension and continuously stirred up to 180 °C until it solidifies. This solidification process is known as the saponification reaction. At this stage, the fats are completely absorbed into the liquid soap.

### **10.1.2 Physical Properties of Steel and Ball-on-Disk Test Procedure**

Tool steel (substrate material) and bearing ball SAE 52100 was used in sliding test. The physical properties of both materials are mentioned in Table 10.1. A tribology test was conducted in a room temperature environment under a relative humidity of 60% with  $\pm 2\%$  deviation. The tribology test was performed by ball-on-disk tribometer under 5N load, sliding velocity of 0.41 m/s and rotational speed of thousand revolutions per minute. In a ball-on-disk tribometer, a ball is sliding against the rotating disk utilizing the stepper motor. The friction force is calculated by the deflection of strains gauge system, which is provided adjacent to the ball holder. During sliding,

**Table 10.1** Physical properties and dimensions of substrate and ball material

Material	Hardness (HRC)	Surface roughness $R_a$ ( $\mu\text{m}$ )	Dia (mm)	Thickness (mm)
Tool steel	60	0.40	40	10
SAE 52100	62	3	4	–

ball holder experiences some deflection, which is used in the calculation of friction coefficient. The wear rate was estimated using the Archard's Equation by calculating the wear volume to the applied load and sliding distance.

### 10.1.3 Theory of Sliding Friction and Wear

The friction force is a combined effect of mechanical interactions such as contact asperity deformation, plowing, and adhesion effect. The friction coefficient is the sum of two theories such as adhesion and plowing by hard grit particles (Shaw and Macks 1949). Nevertheless, surface roughness contribution cannot be ignored in friction. Surface roughness determines the deformation of asperities using slip-line plasticity. According to Green (1954), the predicted model of friction values due to asperity deformation are nearby the experimented values. Asperity interlocking and surface roughness during sliding/rolling contact affect the friction force, which signifies the proportionality relation between friction force and surface roughness. Surfaces during boundary contact condition become rough due to the formation of bonding slip, which is caused by the deformation of contact surface by plowing action. In various coating system, the requirement of low friction is achievable by depositing a low shear strength film.

The wear behavior of sliding contact has been earlier explained in terms of the adhesion theory of wear (Holm 1938; Archard 1953). According to the theory, when two sliding surfaces are in contact, wear occurs from the softer surface and sticks to the harder surface by continuous shearing of asperities. A theory presented by Holm (1938) signifies that wear rate is directly proportional to the normal load and inversely proportional to the hardness of the wearing material. Another model was proposed by Archard (1953) and suggests the dependence of wear rate on the normal load and materials hardness. Archard's model describes the proportionality constant, also known as wear coefficient, which is the probability of loose particle formation during the transfer of debris between two sliding surfaces. Wear coefficient of different material can have different values depending on the type of contact. Table 10.2 shows some of the wear coefficient values for different materials.

Adhesion theory of wear is the simplest one, but there are number of criticism have been made. Some of the critical points are:

- The harder surface cannot wear at all. This is a major criticism, which is challenged by the experimental analysis. The theory is later modified by stating that sometimes hard surface contains weak spots and at the same point fracture takes place.

**Table 10.2** Wear coefficient values

Material	Wear coefficient (K)
Mild steel (on mild steel)	$7 \times 10^{-3}$
Copper-beryllium	$3.7 \times 10^{-5}$
Hard tool steel	$1.3 \times 10^{-4}$
Ferritic stainless steel	$1.7 \times 10^{-5}$
Polytetrafluoroethylene	$2.5 \times 10^{-5}$
Polythene	$1.3 \times 10^{-7}$
Poly(methyl methacrylate)	$7 \times 10^{-6}$

- Wear debris only generated through asperities contact. This means that the steady-state wear rate must depend on the surface roughness only, which is criticized through experimental observations.
- Material's plasticity is the maximum work required to generate a wear particle by adhesion. Hence, for better understanding of adhesion phenomena, a wear coefficient factor is introduced.
- Mechanical and structural properties of materials are not linked with the adhesion theory. Under the varied load conditions, mechanical properties depend on the microstructure of test material, which must be included during sliding tests.

From the above criticism and adhesion theory, it is concluded that some of the important properties and parameters have been overlooked, but these properties need to be incorporated during tribological experimental observation.

### 10.1.4 Tribological Investigation

The friction and wear performance of molybdenum disulfide ( $\text{MoS}_2$ ) dispersed in water and oil (paraffin oil) medium with or without dispersants/surfactant is presented in Fig. 10.2. A thin layer of water/oil based solution is provided at the top surface of tool steel. At every fixed duration of time or after every 5-min, the liquid addition process is repeated for continuous lubrication and motion. The friction coefficient and wear rate are high for bare steel surface and dry  $\text{MoS}_2$  nanoparticles due to the absence of any liquid medium. However, as soon as the dispersant (Polyisobutylene succinimides, PIBS) is added the friction values minimize, see Fig. 10.2a. On contrary addition of water has not affected the friction values and attained similar properties like bare surface. This is because of the fact that water is not able to provide lubrication and starts evaporating as soon as the contact zone temperature rises enormously. However, the addition of Sodium dodecyl sulfate (SDS) reduces the friction coefficient by lowering the surface tension and total contact area. Later,  $\text{MoS}_2$  particle based grease is prepared and compared with industrial grease. The

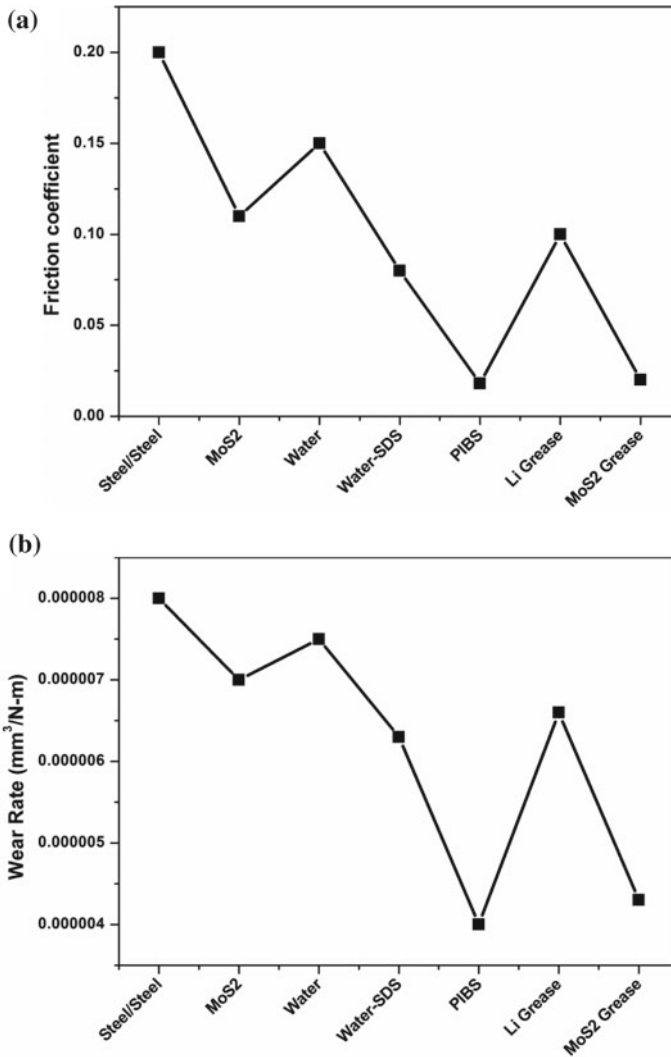


**Fig. 10.2** **a** Friction performance and **b** wear rate of MoS<sub>2</sub> nanoparticles dispersed in a different medium

main purpose of greases is to transmit power, reduce friction and wear, heat dissipation, support load at high pressure, and eliminate vibration and deflections. Industrial grease (lithium based) has provided high friction performance compared to the MoS<sub>2</sub> due to self-lubrication properties of these nanoparticles. Compared to all, the best performance in terms of friction and wear (see Fig. 10.2b) of MoS<sub>2</sub> has been achieved in case of oil-dispersant medium and suggest its use in automotive for intermediate contacts in the form of rolling and sliding.

Oil and water both considered being important lubricants for controlling friction and wear. However, for specific conditions, the functionality of each changes severely. In most of the machine elements oil is used for separating the machine members to avoid contact with each another. This gives minimum or no contact to further control the wear behavior of materials. On the other hand, water cannot be used as an internal lubrication because it can severely attach metal components and triggered the rate of erosion-corrosion. This is why water is only used a coolant during machining or surface finish process.

The friction coefficient and wear rate of vapor deposited single layer, and multilayer molybdenum nitride (MoN, Mo/MoN) films have been investigated under a room temperature environment. As seen in Fig. 10.3, a single layer of coating has been provided high values of friction and wear. On the other hand multilayer of films of molybdenum nitride lowering the friction coefficient by forming a low shear strength films on the surface. This shear film is also responsible for the low values of the wear rate. Molybdenum films possess excellent properties and can be used at temperatures. The friction and wear properties of vapor deposited films completely depend on the nitrogen partial pressure. As the nitrogen partial pressure increases, the resulting tribological losses decreased because of deposited film hardness. Due to high hardness and surface smoothing process, molybdenum nitride produced little wear, and no plowed region was observed for multilayer coatings. The wear behavior of multilayer coatings is better than that of single layer coating.

The hardness of single layer and multilayer coatings were measured by Rockwell hardness tester, see Fig. 10.4. The dark patches nearby the Rockwell indenter reflects under the load. Based on the applied load and pile up process the suitability and hardness of coatings can be identified. Table 10.3 shows some of the mechanical

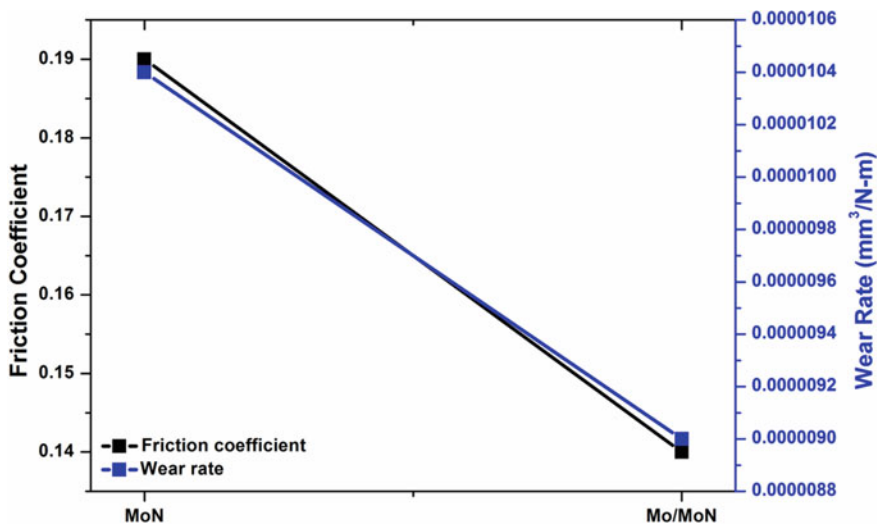
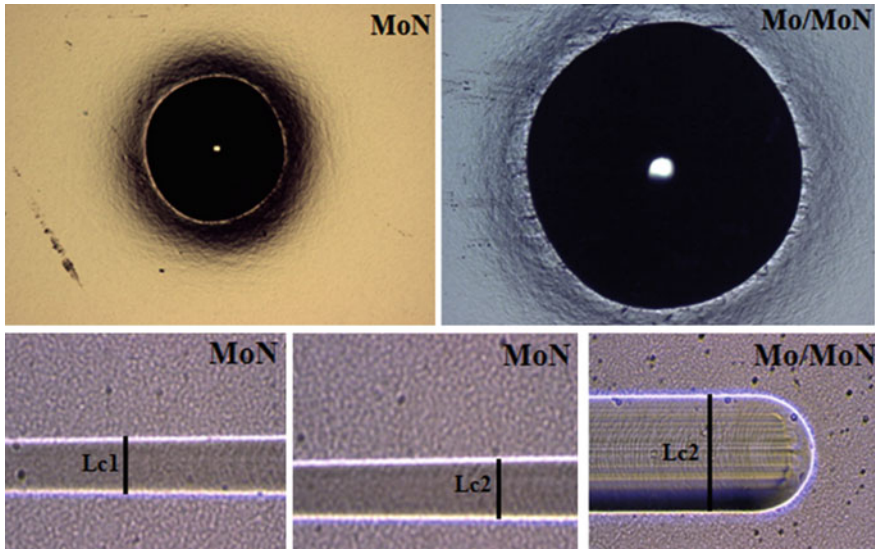


Fig. 10.3 Friction and wear of single/multilayer molybdenum nitride coating





**Fig. 10.4** Rockwell hardness and adhesion measurement of molybdenum single/multilayer coatings

**Table 10.3** Mechanical properties of molybdenum nitride single/multilayer coating

Coating material	Coating type	Hardness (GPa)	Young's modulus (GPa)	H/E ratio	Critical load (N)
Molybdenum	Single layer	38	390	0.097	100+
	Multilayer	48	491	0.097	100+

properties of these coatings. Importantly, coating resistance against the applied load is verified by the plasticity index. The value close to this index ( $\sim 0.1$ ) shows the better behavior of deposited coatings. Scratch adhesion measurement on the surface show only  $Lc_1$  (crack generation) and  $Lc_2$  (crack propagation) region, which signifies the strength of these coatings. Coating spallation can be observed when the scratch adhesion value reached to  $L_s$ , means final delamination.

### 10.1.5 Influencing Wear Parameters

In coating tribology, the wear behavior of two sliding/rolling surfaces is highly depended on the sliding speed, normal load, surface roughness, coating adhesion, coating thickness, the microstructure of sliding material and counterpart material,

elastic modulus, and hardness. All the above effective parameters are summarized in the subsequent sections.

- **Normal Load**

According to the friction theory and Archard wear law, wear volume is directly proportional to the normal load and independent of the geometry and size of contact surfaces. Hence, wear increases with the normal load as the two surfaces tend to slide against each other.

- **Sliding Speed**

Sliding speed is one of the dominant factors that reduce surface strength and results in failure. At very low sliding speed, coating can be worn away due to the developed stick-slip process. A medium range of speed shortens the contact motion and result in low adhesion wear. If the speed increases beyond the prescribed limit, the material wear increases due to brittle fracture. However, the friction coefficient can be lower due to the softening of surface asperities.

- **Substrate Roughness**

The wear rate of the material increases dramatically with an increase in roughness of two sliding/rolling surfaces. However, in some instances, after continuous shearing of these asperities, some film-formation occurs which helps in providing low adhesion between the contacts.

- **Coating Adhesion**

The adhesion strength of coating depends on the bonding mechanism between the atom of the outer surface and internal residual stresses. Coating adhesion can be influenced by several factors, such as temperature, chemical elements of surfaces, a coating method, and the thickness of coating.

- **Coating Thickness**

Coating thickness is an important factor because low thin film shear quickly and worn away due to excessive penetration under varying load. On the other hand, thick coatings may have poor adhesion and induce residual stresses within the coating interface, which degrades coating quality.

- **Microstructure**

The tribological properties of coatings are depended on its microstructure. The microstructure properties mainly depend on the chemical composition of the structure, deposition technique and the deposition parameters like gas pressure, deposition temperature and the substrate bias voltage. In addition, variation in temperature can lead coating surface from crystalline structure to amorphous like solid structures.

- **Hardness and Elastic Modulus Ratio**

Hardness to elastic (H/E) ratio is an important parameter to indicate surface resistance to plastic deformation. Enhancing the H/E ratio can provide a better perspective on tribological performance. The coating hardness must be higher, and the elastic modulus should be kept low for better performance.

- **Elastic Modulus**

Elastic modulus mismatch between coating surface and base substrate surface can lead to failure due to developed residual stresses. Hard and thick coatings have higher elastic modulus than the substrates, and under tensile stresses, coating starts delaminating. Nevertheless, thick coating supports the entire load, and it is independent of substrate elastic modulus. However, for thin coatings, the load is entirely supported by the substrate.

- **Coating Hardness**

High hardness of the coating can result in a low rate of wear. However, if the coating thickness is increased beyond the prescribed limit, it cannot provide good wear resistance. Further, high thickness film induces brittleness in the coating zone and reduces fracture toughness.

- **Substrate Hardness**

The surface fracture of the coating depends on the substrate hardness. Surface fracture of the softer material will be lower compared to the hardest. Hard material prolongs the life of coating for the tribological application. In the present work, tool steel reflects better delamination under adhesion test due to a moderate hardness value.

Above described tribological properties are related to the steel/steel contact. This means a slight difference in the hardness of both materials. Now it is interesting to see the tribological properties of two surfaces having different hardness. In this regard, MoS<sub>2</sub> is infused into a soft polymer, i.e., epoxy resin, and slide against a bearing steel ball. The different concentration (1, 3, 5 wt%) of MoS<sub>2</sub> nanocomposites are prepared, and test for friction and wear behavior. Before that tribological property of pure epoxy were evaluated and found friction coefficient, and wear rate values of 0.4,  $5.5 \times 10^{-7}$  mm<sup>3</sup>/N m, respectively. Figure 10.5a, b show the hardness, friction coefficient and wear rate behavior of MoS<sub>2</sub> nanocomposites filler in epoxy resin. From the friction and wear rate, it is clear that an increase in particle concentration decreases the surface adhesion of composites and provide low values. However, the obtained friction values can be often minimized if the polymer does not have hygroscopic properties. Due to this property, the self-lubrication performance of MoS<sub>2</sub> is affected by its reaction with a humid environment. Filling of vacant asperities triggers the wear mechanism in this scenario. Overall, the surface contact area increased with more filler particles and attained a low wear rate. At starting the wear rate is high, but as soon as the MoS<sub>2</sub> starts providing self-lubrication properties, composite wear rate gets affected.

Another important aspect of these polymer nanocomposites is their contact angle and surface energy. Table 10.4 shows the contact angle and surface energy values

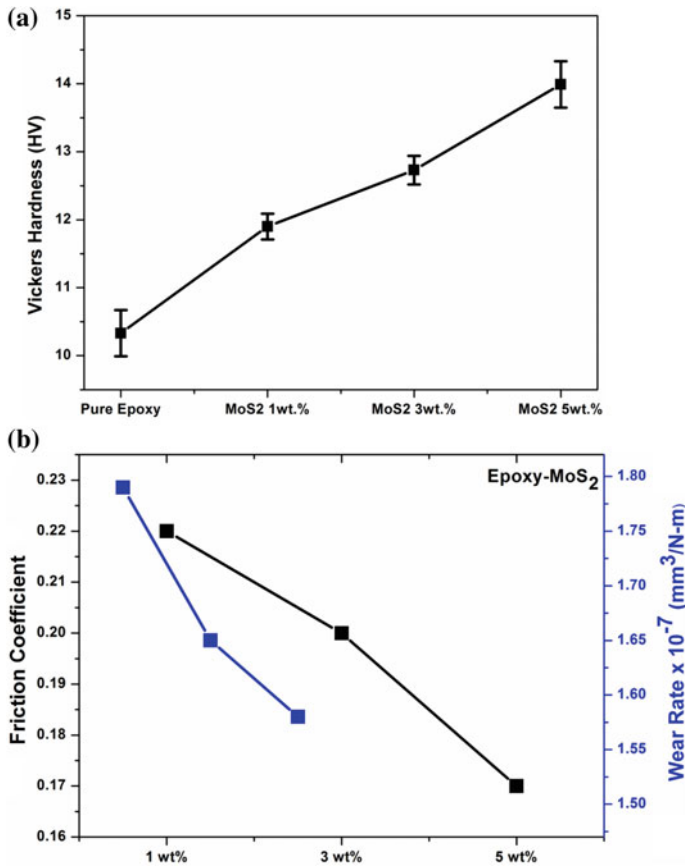


**Fig. 10.5** a Hardness, b friction and wear performance of epoxy-MoS<sub>2</sub> nanocomposites

**Table 10.4** Contact angle and surface energy of epoxy-MoS<sub>2</sub> nanocomposite

Composite	Contact angle (°)	Surface energy (mJ/m <sup>2</sup> )
MoS <sub>2</sub> 1%	50.0	45.30
MoS <sub>2</sub> 3%	45.2	52.56
MoS <sub>2</sub> 5%	41.0	58.23

of epoxy-MoS<sub>2</sub> nanocomposites. With increase in particle concentration, the water contact angle value decreases and surface energy moves towards the high limit. This signifies that nanocomposite should have high adhesion and can result in high friction coefficient and wear rate. However, the observed experimented results are different from the theory. This is because of the fact that MoS<sub>2</sub> has lubrication properties and reduces high contact forces when present in the boundary or any matrix.

Another important aspect is that the utilized volume of water, which is 0.2  $\mu\text{L}$ . Depending on the reactivity of water on the epoxy surface, it spreads on the surface. The contact angle was measured with the help of a Goniometer using distilled water droplet of 0.2  $\mu\text{L}$ . A small volume of liquid in the droplet provides a low effect of gravitational forces and depicts the true physical properties of the equilibrium system (as all the forces are in line contact) (Dimitrakopoulos 2007; Sasges and Ward 1998). Throughout the contact angle measurement, this small droplet retains the spherical shape and contacts with the minimum surface area. Basically, the water molecules are pulled inward by the neighboring molecules on the surface and create internal pressure. This intermolecular attraction is responsible for the contact and is known as surface tension, which maintains the shape of the water molecules on the epoxy surface (Yuan and Lee 2013). If the liquid volume is too large, the droplet reactivity on the epoxy surface increases with high gravitational forces. In this case, the contacting drop on the surface includes additional kinetic energy, which increases the impact force of water molecules. In the presence of high gravitational forces and kinetic energy the shape of water drop changes from spherical to flat, which additionally creates apparent wetting area. This apparent area cannot be used for representing true physical behavior of water and epoxy contact surfaces. Hence, the low volume of the water droplet is used in the experiment to reach the state of equilibrium.

### ***10.1.6 Conclusions and Future Directions***

Lubrication mechanism of particles added in any medium is an important strategy to reduce surface friction and wear. From the study, several conclusions can be drawn in terms of dry, liquid, coating, and composite friction evaluation. Molybdenum disulfide in dry medium provide slight high values of friction and wear due to the requirement of more work to form particles into the lubricant film. In liquid medium, this characteristic is achieved quickly due to developed low shear strength films, which ease sliding between the contact surfaces. Single/multilayer films of  $\text{MoS}_2$  are compatible for high-temperature operation especially in case of tool steels operating under extreme environmental conditions. The critical loading of  $\text{MoS}_2$  film is beyond the critical limit, which also signifies its application. Addition of  $\text{MoS}_2$  into the epoxy resin significantly lowers the wear behavior due to its lubrication mechanism. This is the most demonstrative evidence of two different materials having opposite hardness.

Nanolubricants have found widespread application in the aerospace industry because they are better suited to the more demanding requirements of aerospace than any other materials. The main demanding condition of aerospace applications is that requirement of operation under an extremely wide temperature range. Industrial application of solid/liquid based nanolubricant are bearing, engine oils (automotive, diesel), gas turbine (aircraft), gears (machinery, helicopters), two-cycle engines (scooters). Hence, synthesis and evolution of more specialized materials for nanotribological application is required for future applications. The surface wetting properties are essential, and this needs to be explored in detail with the effect of surfactant

interaction and their role in friction reduction. For coating tribology, more noble and reliable functionally graded materials need to design and develop through a sputtering process where extremely low friction and wear values are of high interest. Another evolution can be done in the area of parallel computing of large-scale simulation. In polymer nanocomposite, still, the exact particle weight concentration needs to be explored for better utilization of available resources economically. Also, various surface characterization techniques such as microstructure studied will be performed to establish the relationship between experimented results and surface properties.

## References

- Archard JF (1953) Contact and rubbing of flat surfaces. *J Appl Phys* 24:981–998
- Cen H, Lugt PM (2019) Film thickness in a grease lubricated ball bearing. *Tribol Int* 134:26–35
- Dimitrakopoulos P (2007) Gravitational effects on the deformation of a droplet adhering to a horizontal solid surface in shear flow. *Phys Fluids* 19(14):122105
- Gong J, Jin Y, Liu Z, Jiang H, Xiao M (2019) Study on influencing factors of lubrication performance of water-lubricated micro-groove bearing. *Tribol Int* 129:390–397
- Green AP (1954) The plastic yielding of metal junctions due to combined shear and pressure. *J Mech Phys Solid* 2:197–211
- Holm R (1938) The friction force over the real area of contacts. *Wiss Veroff Siemens-Werk* 17:38–49
- Jammal N, Rai R, Jha V, Singh BK (2019) The impact of humidity and film thickness on photoemission, optical and morphological properties of CsI thin film photocathodes. *Thin Solid Films* 674:82–90
- Karakashev SI, Stöckelhuber KW, Tsekov R, Phan CM, Heinrich G (2014) Tribology of thin wetting films between bubble and moving solid surface. *Adv Coll Interf Sci* 210:39–46
- Lugt PM (2016) Modern advancements in lubricating grease technology. *Tribol Int* 97:467–477
- Miyake S (2005) Tribology of carbon nitride and boron nitride nanoperiod multilayer films and its application to nanoscale processing. *Thin Solid Films* 493:3160–3169
- Qin W, Wang M, Sun W, Shipway P, Li X (2019) Modeling the effectiveness of oil lubrication in reducing both friction and wear in a fretting contact. *Wear* 426–427:770–777
- Sasges MR, Ward CA (1998) Effect of gravity on contact angle: an experimental investigation. *J Chem Phys* 109:3661–3670
- Shaw MC, Macks EF (1949) *Analysis and lubrication of bearings*. McGraw-Hill, New York
- Shi S-C, Wu J-Y (2018) Deagglomeration and tribological properties of MoS<sub>2</sub>/hydroxypropyl methylcellulose composite thin film. *Surf Coat Technol* 350:1045–1049
- Sommer M, Haas W (2016) A new approach on grease tribology in sealing technology: influence of the thickener particles. *Tribol Int* 103:574–583
- Tai BL, Stephenson DA, Furness RJ, Shih AJ (2014) Minimum quantity lubrication (MQL) in automotive powertrain machining. *Procedia CIRP* 14:523–528
- Upadhyay RK, Kumar A (2019a) Effect of humidity on the synergy of friction and wear properties in ternary epoxy-graphene-MoS<sub>2</sub> composites. *Carbon* 146:717–727
- Upadhyay RK, Kumar A (2019b) Epoxy-graphene-MoS<sub>2</sub> composites with improved tribological behavior under dry sliding contact. *Tribol Int* 130:106–118
- Upadhyay RK, Kumaraswamidhas LA (2014) Surface modification by multilayered W/W<sub>2</sub>N coating. *Surf Eng* 30:475–482
- Upadhyay RK, Kumaraswamidhas LA (2015) Investigation of monolayer-multilayer PVD coating. *Surf Eng* 31:123–133

- Yuan Y, Lee TR (2013) Contact angle and wetting properties. *Surf Sci Techn* 51:3–34
- Zhai W, Srikanth N, Kong LB, Zhou K (2017) Carbon nanomaterials in tribology. *Carbon* 119:150–171
- Zhu S, Cheng J, Qiao Z, Yang J (2019) High temperature solid-lubricating materials: a review. *Tribol Int* 133:206–223

# Chapter 11

## Potential of Bio-lubricants in Automotive Tribology



**Manoj Kumar Pathak, Amit Joshi, K. K. S. Mer, Jitendra K. Katiyar and Vinay Kumar Patel**

**Abstract** Lubricants are used as anti-friction and heat absorbing media and therefore lead to smooth and reliable functions/operations, and therefore reduces the risks of frequent failures and thus enhance the durability/life-cycle of vehicle. At present, due to worldwide concern in protecting the environment from pollution and the increased prices and depletion of reserve crude oil, there has been growing interest to formulate and apply an alternative solution with the research and development in environment-friendly bio-lubricants from natural resources. A bio-lubricant is renewable and sustainable lubricants which is biodegradable, non-toxic, and emits net zero greenhouse gas. This chapter deals the potential of vegetable oil-based bio-lubricant for automotive application. In this chapter, the source, properties, as well as advantages and disadvantages of the bio-lubricant has been detailed. Further, the future prospects and challenges of bio-lubricants as potential alternative of conventional lubricants has been elucidated.

**Keywords** Biolubricant · Automotive application · Tribology · Friction · Wear

### 11.1 Introduction

In recent years, researchers all around the world endeavored to make a product which is environment friendly, durable, reliable and effective for energy utilization in automotive applications (Singh et al. 2019). Innovation in technological resolutions such as introduction of material having light weight, fuels which are harmless, fuel combustion in controlled way, and more efficient gas at exhaust after treatment, are the possible ways to minimize the problems encountered to the environment through industrial machines and vehicles (Gerbig et al. 2004). During the combustion process

---

M. K. Pathak · A. Joshi · K. K. S. Mer · V. K. Patel (✉)  
Department of Mechanical Engineering, Govind Ballabh Pant Institute of Engineering and Technology Ghurdauri, Pauri, Garhwal, Uttarakhand 246194, India  
e-mail: [vinaykrpatel@gmail.com](mailto:vinaykrpatel@gmail.com)

J. K. Katiyar  
Department of Mechanical Engineering, SRM Institute of Science and Technology, Kattankulathur, Tamil Nadu 603203, India

© Springer Nature Singapore Pte Ltd. 2019  
J. K. Katiyar et al. (eds.), *Automotive Tribology*, Energy, Environment, and Sustainability,  
[https://doi.org/10.1007/978-981-15-0434-1\\_11](https://doi.org/10.1007/978-981-15-0434-1_11)



in internal combustion (IC) engine, involvement of high temperature and pressure conditions, result in direct force to the engine components such as pistons, to move it by a certain distance, for achieving the mechanical energy by the transformation of chemical energy (Singer and Williams 1954). In every engineering equipment, the irregularities present in the surface of moving/working components result in the loss of material due to abrasion wear. The possible ways of minimizing the wear in the moving/working components are either by surface properties modification through surface engineering processes or by the application of lubricants (Panchal et al. 2017). At the desired operating conditions, the effective lubrication of moving components of an engine permits them to slide over other components smoothly, for the safe and reliable automobile operation. Reduction of friction and wear during the tribological interaction of automobile components helps in minimizing the energy losses (Mobarak et al. 2014).

The process employed for reducing the wear between the surfaces moving relative to each other is well known as lubrication. The major objectives of lubrication during any application are: (i) to minimize the wear of contacting surfaces moving relative to each other and along with reducing the wear it also helps in preventing the heat loss, (ii) to create the environment which helps surfaces to become corrosion free and oxidation resistant, (iii) to create the environment as an insulator for applications such as transformer applications, (iv) to create the shielding environment for the surfaces against the water, dust and dirt. Heat and wear both the terms are linked to the friction occurred between the moving surfaces and can be minimized up to the significant levels by minimizing the coefficient of friction between the moving surfaces with the application of lubricants found in the solid, liquid and gaseous form. Among all categories of available lubricants, the liquid, solid or semi-solid form of lubricants are most widely used forms in the various applications (Panchal et al. 2017; Ahmed and Nassar 2013; Iqbal 2014).

In an automobile application, at desired operational conditions the effective and efficient lubrication of working/moving parts is the mandatory requirement for safe as well as reliable operation of an automotive vehicle which results in reducing the wear and friction for drive-trains and engines (Singh et al. 2017a, 2019). The lubricants obtained by mineral oils has been extensively used in automotive applications for a very long time. Mineral oils are the byproduct of crude oil and is obtained by the distillation process but the use of mineral oils is limited due to the limited availability of reserves for crude oil. In addition to this, the disposing of mineral oils causes the pollution in the aquatic as well as in the terrestrial ecosystems especially the aquatic system (Ssempebwa and Carpenter 2009). Moreover, the use of mineral oils in engine combustion as a lubricant lead to degradation of environment by emitting the metal traces such as magnesium, phosphorous, zinc, iron nano-particles and calcium (Miller et al. 2007). Furthermore, the current as well as the future prospects of mineral oils in automotive engine applications as a lubricant were analyzed by Tung and McMillan (Tung and McMillan 2004) and they predicted it as bleak for future prospects. Therefore, there is a necessity for identifying the alternative resources to mineral oils which are suitable for use as lubricant in automotive engines (Singh et al. 2019).

The factors such as the limitation on availability of crude oil resources worldwide, the increasing prices of oil, and most importantly the necessity of environment protection against the pollution caused due to the use of lubricating oils focused the attention of researchers towards the development as well as use of alternative lubricants which can protect environment deterioration by replacing lubricating oils (Mobarak et al. 2014; Ruggiero et al. 2017). The certain physico-chemical properties of bio-based lubricant (Bio-lubricant) and their biodegradable properties has shown great potential to use bio-lubricant as an alternative lubricant to mineral oils for automotive application without causing any harm to the environment (Syahir et al. 2017). The bio-lubricant possesses the improved properties such as high flash point, high viscosity index, high lubricity and low evaporative losses in comparison to mineral oils (Asadauskas et al. 1996; Erhan and Asadauskas 2000; Jayadas et al. 2007; Alves et al. 2013; Nagendramma and Kaul 2012). The existence of polar groups and extended fatty-acid chain structure of plant-based oil-lubricant makes them suitable for hydrodynamic and boundary lubrication based automotive sector applications (Jayadas et al. 2007; Alves et al. 2013). The sources of plant-based oil-lubricants are the seeds containing oil and are available in different forms through-out worldwide (Nagendramma and Kaul 2012; Lathi and Mattiasson 2007). As per the available literature, worldwide about 350 distinct crops are identified with oil bearing properties (Mobarak et al. 2014; No 2011; Agarwal 2007). Edible and non-edible are two categories of plant-based oil resources (Mobarak et al. 2014). In the available literature, it is observed that non-edible plant-based oils are preferred to be employed as lubricant in automotive applications specifically in CI engines over the edible plant-based oil resources due to its effect on ecological systems by cultivating crops (Atabani et al. 2013; Adhvaryu et al. 2004). The sources of non-edible plant oils are jojoba, mon-gongo, polanga, neem, castor, *Jatropha curcas*, mahua, karanja, coriander and hingan (Singh and Singh 2010a; Singh et al. 2017b, 2018). In addition to this, the sources of inedible oil include *Sapindus mukorossi*, linseed oil, *Acrocomia aculeata*, nahor oil, *Nicotiana tabacum*, rubber seed oil, *Crambe abyssinica*, *Sapium sebiferum*, and *Euphorbia tirucalli* (Hasni et al. 2017). In available literature, most of the researchers reported use of plant-based oil as an engine fuel, only few researchers reported use of plant-based oils as lubricant in automotive applications (Mobarak et al. 2014).

The main aim of this chapter is to provide specific information to readers, industrialists, policy makers, researchers and engineers who are focused in bio-lubricant based studies in automotive tribology. This study presents the comprehensive review on potential use of bio-lubricants for automotive applications and this review includes the studies from the extremely observed publications and most recent available publications.

## 11.2 Lubrication and Lubricants

Lubrication is the process of imposing the lubricant between the contacting interfaces of moving or working components. Lubrication helps in, reducing the wear, friction, heat loss, oxidation, provides the corrosion prevention environment, provides the insulator environment, and also provides the protection of parts against

moisture, dirt and dust (Panchal et al. 2017; Mobarak et al. 2014). A good lubricant must possess the properties such as its higher oxidation resistant environment, capability of providing corrosion prevention environment, lower value of freezing point, higher value of viscosity index, higher thermal stability, and higher boiling point values (Mobarak et al. 2014). Lubricants can be classified on the basis of physical appearance, resources of base oil and applications.

- i. On the basis of physical appearance, the lubricants can be categorized as solid, semisolid and liquid lubricants: Manmade oils, animal oils, petroleum oils and vegetable oils all comes in the category of liquid lubricants; the solid lubricants are the lubricants which are composed of layers of organic and inorganic compound like cadmium di-sulphide, molybdenum di-sulphide, and graphite; the semisolid lubricants are the lubricants in which the liquid is floated in solid matrix of thickener as well as the additives like grease (Mobarak et al. 2014).
- ii. On the basis of resources of base oil, the lubricants can be categorized as refined oil, natural oil (also known as natural esters) and synthetic oil (also known as synthetic esters): oil extracted from the petroleum as well as crude oil reserves are comes under the category of refined oils like aromatic, naphthenic and paraffinic oils; oil which is the outcome of crop driven as well as the animal driven is comes under the category of natural oils; oil which is the outcome of the end product of reactions as per the requirement comes under the category of synthetic oils and the examples are polyalphaolefines, synthetic esters, diesters, silicones, polyglycols, ionic liquids, perfluoroalkylethers, genetically modified organisms or any other man-made lubricant comprising chemical compounds (Mobarak et al. 2014; Reeves et al. 2017).
- iii. On the basis of applications, the lubricants can be categorized as automotive oils, industrial oils and special oils: oil used in transportation and automobile sector comes under the category of automotive oils like hydraulic as well as brake fluids, gear box oils, transmission oils and engine oils; oil used for industrial purpose comes under the category of industrial oils like hydraulic oils, metal working fluid, compressor oils and machine oils; oil used for specific operation with special purpose comes under the category of special oils like instrumental oils white oils and process oils (Mobarak et al. 2014).

### 11.3 Bio-lubricants

The lubricants which are having the constituents or base which is based on bio-based raw materials like animal fat, vegetable oils or any other environmentally benign hydrocarbons is termed to be bio-lubricant (Reeves et al. 2017). Biodegradability and non-toxicity of bio-lubricants to the human beings and to the other living organisms is mainly due to its base constituents (Salimon et al. 2010). Globally, the demand of bio-lubricants is rising due to its environmentally friendliness factor and the economic factors such as prevention of toxic substances to the environment; depletion of reservoirs of crude oil; hike in the prices of crude oil and the strict regulations

**Table 11.1** Statics of oil-content in some non-edible and edible oil species (Reeves et al. 2017; Usta et al. 2011; Singh and Singh 2010b; Mofijur et al. 2012; Wang et al. 2012; Li et al. 2012; Kumar and Sharma 2011; Sharma and Singh 2010; Karaosmanoglu et al. 1999; Wang et al. 2011)

S. No.	Non-edible species	Oil content (% of volume)	Edible species	Oil content (% of volume)
1.	Moringa	20–36	Coconut	63–65
2.	Linseed	35–45	Corn	48
3.	Mahua	35–50	Olive	45–70
4.	Castor	45–60	Peanut	45–55
5.	Karanja	30–50	Palm	30–60b
6.	Neem	30–50	Rapeseed	38–46
7.	Jatropha	40–60	–	–
8.	Desert date	37–48	–	–
9.	Niger	43–50	–	–

of government from time to time for the operation, use and disposal of petroleum based oils (Deffeyes 2008; Goodstein 2005). In current scenario, the potential of bio-lubricants in automobile sector makes them the best economical alternative to the traditional petroleum-based lubricants.

Production of bio-lubricants is necessary for alternative energy applications due to their numerous worldwide source availability. While looking from country to country the type of feedstock for bio-lubricants may differ due to the different geographical locations. In the literature, it is reported that number of oil-bearing crops are known to be more than 350 among which only peanut oil, cottonseed, rapeseed, safflower, coconut, sunflower, soybean, and palm oils are considered as alternative lubricants which have the potential (Mobarak et al. 2014). Oil content statics of some edible and non-edible seeds are shown in Table 11.1 (Usta et al. 2011; Singh and Singh 2010b; Mofijur et al. 2012; Wang et al. 2012; Li et al. 2012; Kumar and Sharma 2011; Sharma and Singh 2010; Karaosmanoglu et al. 1999; Wang et al. 2011). Oil extracted from non-edible seeds such as karanja, neem and jatropha has received the interest worldwide (Mofijur et al. 2012).

### 11.3.1 Bio-lubricant Properties

Bio-lubricants driven by vegetable oils reveals the suitable properties (Willing 2001). Bio-lubricants possesses various practically preferable capabilities relative to the petroleum driven lubricants (Munoz et al. 2012) or in other words we can say that bio-lubricants possesses many useful and valuable physicochemical properties. Bio-lubricants have high viscosity index, elevated lubricity, high flash point and evaporative conditions which are minimum (Raj and Sahayaraj 2010; Usta et al. 2011; Willing 2001; Asadauskas et al. 1996; Erhan and Perez 2002; Munoz et al. 2012; Das

**Table 11.2** Comparative study of properties of vegetable and mineral oils (Mobarak et al. 2014; Johnson and Miller 2010)

Properties	Vegetable oils	Mineral oils
Viscosity index (VI)	100–200	100
Pour point, 1 °C	–20 to +10	–15
Miscibility with mineral oils	Good	–
Density @20 °C (kg/m <sup>3</sup> )	890–970 (kg/m <sup>3</sup> )	840–920 (kg/m <sup>3</sup> )
Flash point	Higher	Lower
Fire point	Higher	Lower
Hydrolytic stability	Poor	Good
Cold flow behavior	Poor	Good
Oxidation stability	Moderate	Good
Biodegradability (%)	80–100 (%)	10–30 (%)
Sludge forming tendency	Poor	Good
Seal swelling tendency	Slight	Slight
Shear stability	Good	Good
Solubility in water	Non-miscible	Non-miscible
Specific gravity	More	Less

et al. 2012). Overall vegetable oil-based lubricants possess exhibits the superior properties than the mineral oil-based lubricants. Table 11.2 represents the comparative analysis of properties of vegetable oil and mineral oil-based lubricants.

### 11.3.1.1 Viscosity

The most important property of oils is Viscosity which indicates the resistance to the flow. The higher value of viscosity indicates the higher resistance to flow while the lower value indicates the lower resistance to flow. Viscosity of oils directly dependent on pressure, temperature and formation of film (Mobarak et al. 2014).

### 11.3.1.2 Viscosity Index (VI)

VI represents the measure in change of viscosity with the variation of temperature. The higher value of VI represents the lower variation in the temperature while the lower value of VI indicates the higher variation in temperature. This is the most important property of bio-lubricants which ensures bio-lubricant to be more effective at higher temperature ranges by maintaining the thickness of oil film to be thick when compared with the mineral oils. This property of bio-lubricants makes them most suitable lubricants for wide variety of temperature ranges (Mobarak et al. 2014).

### **11.3.1.3 Pour point**

The lowest temperature at which oil start to flow or pours is known to be the pour point of oils. This is one of the most important property of lubricants. The vegetable-based oils are having the low value of pour point while comparing with the mineral oils, which enables bio-lubricants as excellent lubricants for cold start applications (Mobarak et al. 2014).

### **11.3.1.4 Flash Point and Fire Point**

The minimum temperature at which lubricant must be heated before its vaporization is known as the flash point of the lubricant. While mixing of air with lubricant enables it to ignite but not to burn. Fire point is the temperature at which the combustion of lubricant continues. Lubricants volatility and fire resistance properties are identified on the basis of its flash point and fire point. These two factors play vital role during the transportation of lubricants. The bio-lubricants generally have the higher value of flash point in comparison to mineral oils which reduces the risk of fire due to the leaked lubricant and provides the safety on shop floors (Mobarak et al. 2014).

### **11.3.1.5 Cloud Point**

The temperature at which solid dissolves in oil is known as the cloud point. While dropping of the temperature wax is crystallized and became visible. The prevention of filter clogging can be ensured by maintaining the temperature above the cloud point (Mobarak et al. 2014).

### **11.3.1.6 Acid or Neutralization Number**

The amount of base content or acid required by a lubricant for neutralization can be termed as neutralization number or acid number (Mobarak et al. 2014).

### **11.3.1.7 Oxidation Stability**

Ability of lubricant to resist the oxidation forming tendency is known as oxidation stability. With the rise of the temperature oxidation stability of lubricant increases. The noteworthy contributors to oxidation comprise agitation, pressure, contaminants, temperature, metal surfaces and water. The lower value of oxidation stability shows that the oxidation of oil take place rapidly during the use if it is untreated, becomes thick and polymerizes to a plastic-like consistency (Mobarak et al. 2014).

### **11.3.1.8 Rust and Corrosion Prevention**

Chemical reaction between ferrous metals and water is known as rust while the chemical reaction between metals and chemicals is known as corrosion. Bio-lubricants are non-toxic in nature and does not react with ferrous metals, water and chemicals when comparing with the mineral oils (Mobarak et al. 2014).

### **11.3.1.9 Anti-wear Properties**

Vegetable oil-based bio-lubricants indicates the improved anti-wear properties than mineral oils. At low pressure and low speed applications lubricants performs satisfactorily. In case of boundary lubrication, when the oil viscosity is not sufficient to provide the surface contact prevention, the inclusion of additives with anti-wear property provides the defensive film at surfaces on contact to minimize the wear (Mobarak et al. 2014).

### **11.3.1.10 Hydrolytic Stability**

The ability of lubricant to offer the resistance to cleavage or attack of water molecule or vapor of water is known as the hydrostatic stability. This property of a lubricant strongly depends on the synthetic ester and the fatty acid ester structure of bio-based fluids due to the reason that the chemical reaction for these molecules is an equilibrium reaction. In hydrolysis process the bio-based fluids cleave into their acid and alcohol components and influences the ester bond directly. This is known to be hydrolytic splitting process which takes place until the restoration of chemical equilibrium (Totten et al. 2019). Chemical structure is the key factor which influences the hydrostatic stability of an ester. Bio-lubricants have the high degree of hydrostatic stability which are derived from saturated esters with straight chain components in comparison to the branched or unsaturated esters.

## **11.3.2 Biodegradability**

Now a days, the industries as well as the automotive sectors are moving towards the use of green lubricants, which prerequisites the two major properties to be within the bio-lubricants: (i) highly biodegradable and (ii) lower ecotoxicity. The major advantage involved with the use of bio-lubricant is their inherent biodegradable property and the lower toxicity towards the environment. The chemical dissolution process through which the organic materials/substances are broken down with the help of enzymes originated from the living organisms is known as the biodegradation process. In other words, we can say that the bio-lubricants based on raw materials which are renewable and derived from H<sub>2</sub>O and CO<sub>2</sub> via. process of photosynthesis,

**Table 11.3** Biodegradability of some bio-lubricants base stocks (Singh et al. 2019)

Base-stock types	Bio-degradability range (% loss at 21 days)
Non-edible vegetable oils	70–100
Diesters	55–95
Polyethylene glycols	10–75
Polyols	5–95
Aromatic esters	0–90
Alkyl benzenes	5–20
Mineral oils	15–75

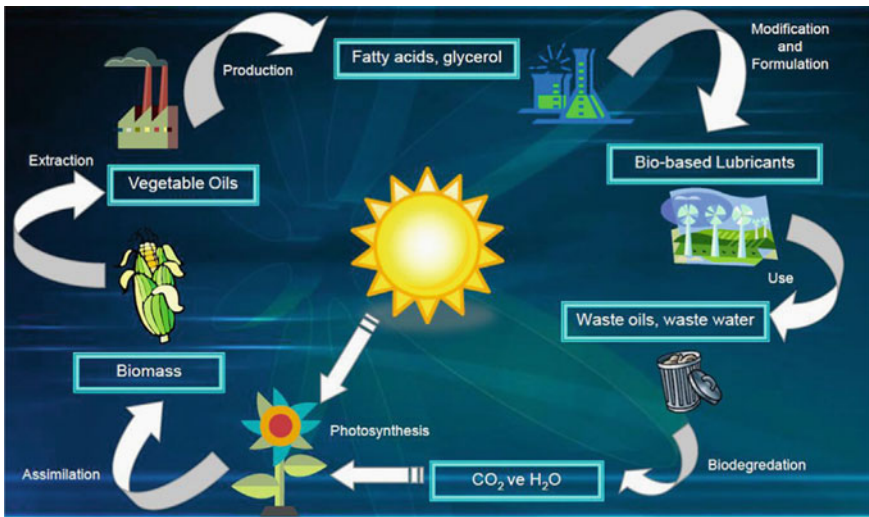


**Fig. 11.1** Life cycle of bio-based lubricants (Mobarak et al. 2014). Copyright (2014) Elsevier Ltd

after the application, at the end returns to environment in the form of  $H_2O$  and  $CO_2$  by the process of biodegradation (Johansson and Lundin 1979). Table 11.3 represents the bio-degradability of some bio-lubricant base stocks (Singh et al. 2019). Figure 11.1 shows the life cycle of the bio-lubricants.

### 11.3.3 Merits and Demerits of Bio-lubricant

Bio-lubricants can be used in their natural form as a lubricant. They have various merits and demerits while considered for industrial, automotive and any other applications.



**Table 11.4** Benefits of bio-lubricants (Mobarak et al. 2014)

Higher viscosity index	Wide range of temperature
Higher boiling temperatures	Lower emissions
Lower volatility	Decreased exhaust emissions
Higher lubricity	Lower friction losses, better fuel economy
Higher flashpoints	Higher safety on shop floor
Higher detergency	Eliminating the requirement of detergent additives
Oil-mist and oil-vapor reduction	Helps in preventing the oil-mist into lungs during breathing
Rapid biodegradation	Reduced toxicological and environmental hazards
Better skin compatibility	High cleanliness and less dermatological at workplace

The merits of bio-lubricants that they have an excellent lubricity while comparing with the mineral oils and they have high viscosity index, high flash point. The properties such as biodegradability, less-toxic nature and renewable nature makes them more attractive for industrial and automotive applications. The increased viscosity also helps in reducing the operational temperature which contributes in saving the energy for automotive applications. The above-mentioned properties make it as the better alternative for industrial and automotive applications as compared to the petroleum-based oils. Benefits of few bio-lubricants are shown in Table 11.4.

The negative side of bio-lubricants is its low oxidation stability which requires the treatment of bio-lubricant before the use for better performance. Bio-lubricants are having the low temperature limitations such as its unpleasant smell, lower compatibility with sealants and paints, filter clogging tendency and flushing propensity due to the low viscosity.

### 11.3.4 *Bio-lubricants in Automotive Tribology*

The best alternative available to the mineral oil-based lubricant is the bio-based lubricants in industrial as well as in the automotive sector due to the excellent inherent qualities of bio-lubricants. The advantages involved with the use of bio-lubricants are their environmentally friendliness property towards the sensitive environments which helps in the preventing the pollution. Now a days, bio-lubricants applications can be seen in the industrial as well as in the automobile sector. The most important applications of bio-lubricants are: automotive oils like engine oils, gear box oils, transmission fluids, brake and hydraulic fluids; industrial oils such as machine oils, hydraulic fluids, metal working fluids, compressor fluids; and special oils like instrumental oils, white oils and process oils. Figure 11.2 shows the major benefits involved with the application of bio-lubricants (Mobarak et al. 2014) whereas

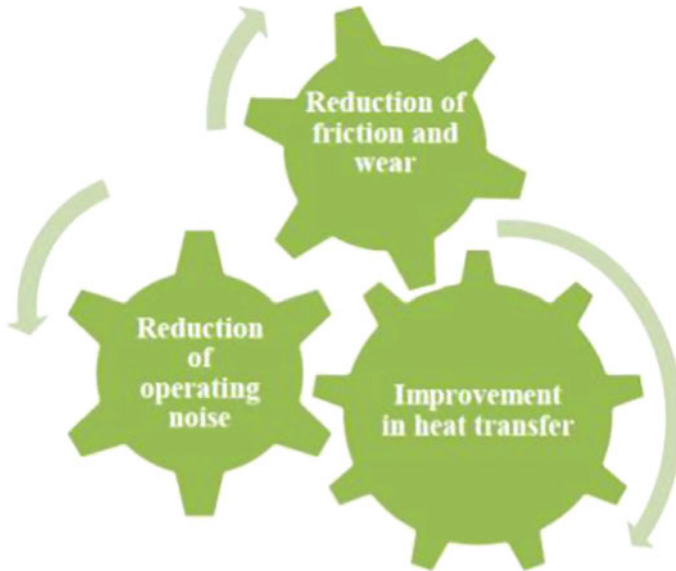


**Fig. 11.2** Major benefits involved with the application of bio-lubricants in an industry (Mobarak et al. 2014). Copyright (2014) Elsevier Ltd

Fig. 11.3 shows the wide areas of application of bio-lubricant in automotive sectors (Mobarak et al. 2014). These oils fruitfully take the place of mineral oils as compressor oils, hydraulic oils, engine oils, aviation oils, metal working oils, insulating oils, general/multi-purpose oils, grease and lubricants for tractors, gears, pump sets generators etc. Table 11.5 shows the work done by various researchers on vegetable oil-based bio-lubricant in different applications.

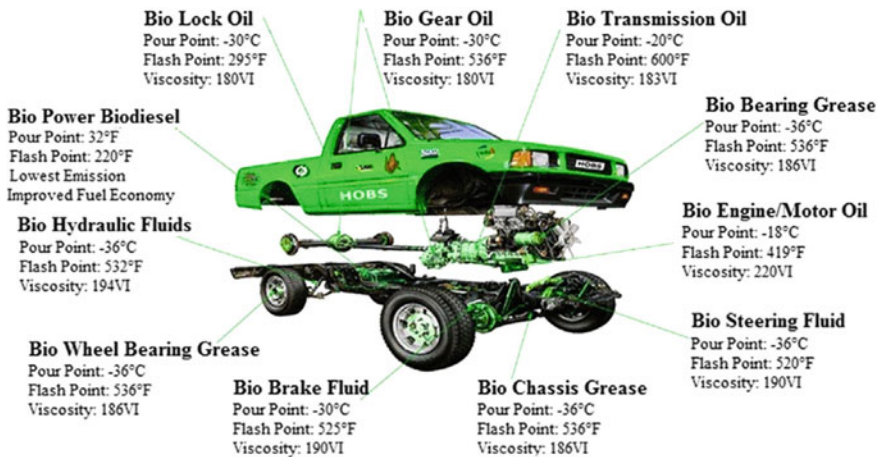


**Fig. 11.3** Requirements of lubrication for a pick-up truck in an automotive sector (Mobarak et al. 2014). Copyright (2014) Elsevier Ltd

**Table 11.5** Previous research summary by researchers on vegetable oil-based bio-lubricant (Singh et al. 2019; Mobarak et al. 2014)

Bio-lubricants	Lubricant taken for reference	Testing method/condition	Result	Reference
Palm oil	SAE20W50	High-frequency reciprocating test rig (ball-on-flat) steel-steel pair contacts	Stronger lubricant film stability Unsaturated hydrocarbon chain reactivity Better anti-corrosion and oxidation properties Lower friction coefficient Low corrosive nature	Haseeb et al. (2010), Lebedevas et al. (2013), Fazal et al. (2011, 2012), Sulek et al. (2010), Anastopoulos et al. (2001), Maleque et al. (2000), Maleque (1997)
Coconut oil	SAE20W50	4-ball tester	Enhanced lubricity properties Higher anti-wear properties Lower friction coefficient	Jayadas et al. (2007)
Waste palm oil	SAE40	4-ball tribo-testing unit with standard method of testing	Viscosity is higher Lower friction coefficient	Kalam et al. (2011)
Vegetable oils (sunflower, mahua, olive, castor, coconut, palm, soybean, karanja, neem, jatropa etc.)	Mineral oils (petroleum based)	Various tribo-testers with standard method of testing	Eco-friendly and cheaper Less expensive Better performance Minimum evaporative losses Enhanced lubricity properties High viscosity and flash point	Singh (2011), Singh et al. (2011, 2014), Singh and Chamoli (2013), Thames and Yu (1999), Suhane et al. (2012), Ting and Chen (2011), Chauhan and Chibber (2013)
Castor oil	Mineral oil (super refined)	4-ball wear testing unit	Antioxidant concentration is higher Low volatility Lower deposit formation tendency Higher viscosity index	Singh et al. (2010)

(continued)

**Table 11.5** (continued)

Bio-lubricants	Lubricant taken for reference	Testing method/condition	Result	Reference
Soybean oil	Mineral oils (petroleum based)	4-ball tribo-testing unit	Eco-friendly and cheaper Non-toxic Enhanced lubricity properties Lower friction coefficient	Asadauskas et al. (1997), Adhvaryu et al. (2005)
TMP ester (palm oil based)	SAE40	High-frequency reciprocating machine	Better wear preventing characteristics in terms of wear-scar diameter and friction coefficient	Erhan et al. (2006)
Palm oil and castor oil	SAE20W40	Pin-on-disc machine	Lower friction coefficient, force of friction and wear Enhanced lubricity properties Lower volatility Eco-friendly, renewable and biodegradable	Zulkifli et al. (2013), Arumugam and Sriram (2012)
Pongamia oil	SAE20W40	Pin-on-disc machine	At all applied loads minimum degradation of lubricant Lower surface wear	Singh et al. (2017b, 2018)
Mongongo oil	SAE20W40	4-ball wear testing unit	Lower deposit forming tendencies Higher viscosity index Lower friction coefficient	Singh et al. (2017b, 2018)
Pongamia oil	SAE20W40	4-stroke, single-cylinder, water-cooled, direct-injection, compression ignition engine	Completely eliminate emission Improved efficiency Frictional losses lower Highest BTE and minimum BSEC at high and medium load conditions	Maleque et al. (1998), Bekal and Bhat (2012)

(continued)

Table 11.5 (continued)

Bio-lubricants	Lubricant taken for reference	Testing method/condition	Result	Reference
Jatropha oil	SAE20W40	Pin-on-disc machine	Lower friction coefficient Chemically modified Lower cumulative weight loss Lower wear loss	Bekal and Bhat (2012)
Rapeseed oil (bio-lubricant)	SAE20W40	High-frequency reciprocating machine	Good performance in terms of friction coefficient and force of friction Better cold flow characteristics Better oxidative stability	Jaina and Suhanea (2013)
Commercial soybean oil	synthetic lubricant	High-frequency reciprocating machine	Viscosity extremely large	Arumugum and Sriram (2013)
Cottonseed oil	SAE 40	Pin-on-disc machine	Biodegradable and eco-friendly Lower friction coefficient Enhanced lubricity properties Low wear at high speeds	Agrawal et al. (2014)

## 11.4 Conclusion

The bio-lubricants based on non-edible oils are biodegradable and eco-friendly. Biodegradability of bio-lubricant makes them most suitable lubricant alternative for the automotive sector applications. Alternative to mineral oil-based lubricants in the form of bio-based lubricants in an automobile sector offers a reasonable solution for obtaining the renewable and environment friendly lubricants with respect to the environmental concern. The non-edible oil-based bio-lubricants are the potential contender for the automotive sector applications. Their inherent characteristics of bio-lubricants such as increased equipment service life, elevated lubricity, high ignition temperature, viscosity, good anti-wear property, high load carrying ability, elevated viscosity index, lower emission of metal trace to atmosphere, higher biodegradability, excellent coefficient of friction and lower evaporation rates makes them better alternative to the mineral-oil based lubricants. But in current scenario, bio-lubricants have not substituted the petroleum-based lubricants completely due to the inappropriate chemical configuration of bio-lubricants, which does not allow them to use in different odd situations. The problems researchers facing in this area is to improve certain characteristics of vegetable oils without damaging the environmentally as well as the tribologically significant properties. Chemical alteration can help to change the chemical configuration of vegetable-oil to make them suitable for automotive sector applications. This area needs to be focused by the researchers to find the solution to the problems associated with non-edible oil-based lubricants to be used as bio-lubricant. This work only explores the potential of bio-lubricants as an alternative to mineral oil-based lubricants in the automotive tribological applications.

## References

- Adhvaryu A, Erhan SZ, Perez JM (2004) Tribological studies of thermally and chemically modified vegetable oils for use as environmentally friendly lubricants. *Wear* 257(3–4):359–367
- Adhvaryu A, Liu Z, Erhan SZ (2005) Synthesis of novel alkoxyated triacylglycerols and their lubricant base oil properties. *Ind Crops Prod* 21(1):113–119
- Agarwal AK (2007) Biofuels (alcohols and biodiesel) applications as fuels for internal combustion engines. *Prog Energy Combust Sci* 33(3):233–271
- Agrawal SM, Lahane S, Patil NG, Brahmankar PK (2014) Experimental investigations into wear characteristics of M2 steel using cotton seed oil. *Proced Eng* 97:4–14
- Ahmed NS, Nassar AM (2013) Lubrication and lubricants. *Tribol Fundam Adv, In tech Open*
- Alves SM, Barros BS, Trajano MF, Ribeiro KSB, Moura E (2013) Tribological behavior of vegetable oil-based lubricants with nanoparticles of oxides in boundary lubrication conditions. *Tribol Int* 65:28–36
- Anastopoulos G, Lois E, Serdari A, Zanicos F, Stournas S, Kalligeros S (2001) Lubrication properties of low-sulfur diesel fuels in the presence of specific types of fatty acid derivatives. *Energy Fuels* 15(1):106–112
- Arumugam S, Sriram G (2012) Effect of bio-lubricant and biodiesel-contaminated lubricant on tribological behavior of cylinder liner–piston ring combination. *Tribol Trans* 55(4):438–445

- Arumugam S, Sriram G (2013) Synthesis and characterisation of rapeseed oil bio-lubricant—its effect on wear and frictional behaviour of piston ring–cylinder liner combination. *Proc Inst Mech Eng Part J: J Eng Tribol* 227(1):3–15
- Asadauskas S, Perez JM, Duda JL (1996) Oxidative stability and antiwear properties of high oleic vegetable oils. *Chem Eng* 52:877–882
- Asadauskas S, Perez JH, Duda JL (1997) Lubrication properties of castor oil—potential basestock for biodegradable lubricants. *Tribol Lubr Technol* 53(12):35
- Atabani AE, Silitonga AS, Ong HC, Mahlia TMI, Masjuki HH, Badruddin IA, Fayaz H (2013) Non-edible vegetable oils: a critical evaluation of oil extraction, fatty acid compositions, biodiesel production, characteristics, engine performance and emissions production. *Renew Sustain Energy Rev* 18:211–245
- Bekal S, Bhat NR (2012) Bio-lubricant as an alternative to mineral oil for a CI engine—an experimental investigation with pongamia oil as a lubricant. *Energy Sourc Part A Recov Util Environ Effect* 34(11):1016–1026
- Chauhan PS, Chhibber VK (2013) Non-edible oil as a source of bio-lubricant for industrial applications: a review. *Int J Eng Sci Innov Technol* 2:299–305
- Das D, Pathak MK, Kumar S, Saini AK, Pant PK (2012) Effect on diesel engine emissions with application of biodiesel fuel. *Int J Res Eng Appl Sci* 2:940–950
- Deffeyes KS (2008) *Hubbert's peak: the impending world oil shortage*, New edn. Princeton University Press, Princeton
- Erhan SZ, Asadauskas S (2000) Lubricant basestocks from vegetable oils. *Ind Crops Prod* 11(2–3):277–282
- Erhan SZ, Perez JM (2002) *Biobased industrial fluids and lubricants*. AOCS Publishing
- Erhan SZ, Sharma BK, Perez JM (2006) Oxidation and low temperature stability of vegetable oil-based lubricants. *Ind Crops Prod* 24(3):292–299
- Fazal MA, Haseeb ASMA, Masjuki HH (2011) Effect of temperature on the corrosion behavior of mild steel upon exposure to palm biodiesel. *Energy* 36(5):3328–3334
- Fazal MA, Haseeb ASMA, Masjuki HH (2012) Degradation of automotive materials in palm biodiesel. *Energy* 40(1):76–83
- Gerbig Y, Ahmed SIU, Gerbig FA, Haefke H (2004) Suitability of vegetable oils as industrial lubricants. *J Synth Lubr* 21(3):177–191
- Goodstein DL (2005) *Out of gas: the end of the age of oil*. WW Norton & Company, New York
- Haseeb ASMA, Sia SY, Fazal MA, Masjuki HH (2010) Effect of temperature on tribological properties of palm biodiesel. *Energy* 35(3):1460–1464
- Hasni K, Ilham Z, Dharma S, Varman M (2017) Optimization of biodiesel production from Brucea javanica seeds oil as novel non-edible feedstock using response surface methodology. *Energy Convers Manag* 149:392–400
- Iqbal M (2014) Tribology: science of lubrication to reduce friction and wear. *Int J Mech Eng Robot Res* 3(3):648
- Jaina AK, Suhanea A (2013) Capability of biolubricants as alternative lubricant in industrial and maintenance applications. *Int J Curr Eng Technol* 3
- Jayadas NH, Nair KB, Ajithkumar G (2007) Tribological evaluation of coconut oil as an environment-friendly lubricant. *Tribol Int* 40(2):350–354
- Johansson LE, Lundin ST (1979) Copper catalysts in the selective hydrogenation of soybean and rapeseed oils: I. The activity of the copper chromite catalyst. *J Am Oil Chem Soc* 56(12):974–980
- Johnson M, Miller M (2010) Eco-friendly fluids for the lubricants industry. *Tribol Lubr Technol* 66(10):28–34
- Kalam MA, Masjuki HH, Varman M, Liaquat AM (2011) Friction and wear characteristics of waste vegetable oil contaminated lubricants. In: *Proceedings of regional tribology conference 2011: RTC2011*. Malaysian Tribology Society, p 47
- Karaosmanoglu F, Tuter M, Gollu E, Yanmaz S, Altintig E (1999) Fuel properties of cottonseed oil. *Energy Sourc* 21(9):821–828

- Kumar A, Sharma S (2011) Potential non-edible oil resources as biodiesel feedstock: an Indian perspective. *Renew Sustain Energy Rev* 15(4):1791–1800
- Lathi PS, Mattiasson B (2007) Green approach for the preparation of biodegradable lubricant base stock from epoxidized vegetable oil. *Appl Catal B* 69(3–4):207–212
- Lebedevas S, Makareviciene V, Sendzikiene E, Zaglinskis J (2013) Oxidation stability of biofuel containing *Camelina sativa* oil methyl esters and its impact on energy and environmental indicators of diesel engine. *Energy Convers Manag* 65:33–40
- Li X, He XY, Li ZL, Wang YD, Wang CY, Shi H, Wang F (2012) Enzymatic production of biodiesel from *Pistacia chinensis* bge seed oil using immobilized lipase. *Fuel* 92(1):89–93
- Maleque M (1997) Investigation of the anti-wear characteristics of palm oil methyl ester using a four-ball tribometer test. *Wear* 206(1):179–186
- Maleque MA, Masjuki HH, Ishak M (1998) Bio-fuel-contaminated lubricant and hardening effects on the friction and wear of AISI 1045 steel. *Tribol Trans* 41(1):155–159
- Maleque MA, Masjuki HH, Haseeb ASMA (2000) Effect of mechanical factors on tribological properties of palm oil methyl ester blended lubricant. *Wear* 239(1):117–125
- Miller AL, Stipe CB, Habjan MC, Ahlstrand GG (2007) Role of lubrication oil in particulate emissions from a hydrogen-powered internal combustion engine. *Environ Sci Technol* 41(19):6828–6835
- Mobarak HM, Mohamad EN, Masjuki HH, Kalam MA, Mahmud KAHA, Habibullah M, Ashraf AM (2014) The prospects of biolubricants as alternatives in automotive applications. *Renew Sustain Energy Rev* 33:34–43
- Mofijur M, Masjuki HH, Kalam MA, Hazrat MA, Liaquat AM, Shahabuddin M, Varman M (2012) Prospects of biodiesel from *Jatropha* in Malaysia. *Renew Sustain Energy Rev* 16(7):5007–5020
- Munoz RAA, Fernandes DM, Santos DQ, Barbosa TGG, Sousa RMF (2012) Biodiesel: production, characterization, metallic corrosion and analytical methods for contaminants. In: *Biodiesel-feedstocks, production and applications*. IntechOpen
- Nagendramma P, Kaul S (2012) Development of ecofriendly/biodegradable lubricants: an overview. *Renew Sustain Energy Rev* 16(1):764–774
- No SY (2011) Inedible vegetable oils and their derivatives for alternative diesel fuels in CI engines: a review. *Renew Sustain Energy Rev* 15(1):131–149
- Panchal TM, Patel A, Chauhan DD, Thomas M, Patel JV (2017) A methodological review on bio-lubricants from vegetable oil based resources. *Renew Sustain Energy Rev* 70:65–70
- Raj FRMS, Sahayaraj JW (2010) A comparative study over alternative fuel (biodiesel) for environmental friendly emission. In: *Recent advances in space technology services and climate change 2010 (RSTS & CC-2010)*, IEEE, pp 80–86
- Reeves CJ, Siddaiah A, Menezes PL (2017) A review on the science and technology of natural and synthetic biolubricants. *J Bio-Tribo Corr* 3(1):11
- Ruggiero A, D’Amato R, Merola M, Valašek P, Müller M (2017) Tribological characterization of vegetal lubricants: comparative experimental investigation on *Jatropha curcas L.* oil, rapeseed methyl ester oil, hydrotreated rapeseed oil. *Tribol Int* 109:529–540
- Salimon J, Salih N, Yousif E (2010) Biolubricants: Raw materials, chemical modifications and environmental benefits. *Eur J Lipid Sci Technol* 112(5):519–530
- Sharma YC, Singh B (2010) An ideal feedstock, kusum (*Schleichera triguga*) for preparation of biodiesel: optimization of parameters. *Fuel* 89(7):1470–1474
- Singer CJ, Williams TI (1954) *A history of technology*, vol 609. Clarendon Press
- Singh AK (2011) Castor oil-based lubricant reduces smoke emission in two-stroke engines. *Ind Crops Prod* 33(2):287–295
- Singh AK, Chamoli A (2013) Composition of biodegradable gear oil. U.S. Patent 8,557,754, issued October 15, 2013
- Singh D, Singh SP (2010a) Low cost production of ester from non edible oil of *Argemone mexicana*. *Biomass Bioenerg* 34(4):545–549



- Singh SP, Singh D (2010b) Biodiesel production through the use of different sources and characterization of oils and their esters as the substitute of diesel: a review. *Renew Sustain Energy Rev* 14(1):200–216
- Singh AK, Pandey NK, Gupta AK (2010) Composition of lubricating oil for two stroke gasoline engine and process for the preparation thereof. U.S. Patent 7,825,077, issued 2 Nov 2010
- Singh AK, Pandey NK, Gupta AK (2011) Composition of hydraulic fluid and process for the preparation thereof. U.S. Patent 8,034,751, issued October 11, 2011
- Singh AK, Pandey NK, Gupta AK (2014) Composition of insulating fluid and process for the preparation thereof. U.S. Patent 8,658,575, issued February 25, 2014
- Singh Y, Farooq A, Raza A, Mahmood MA, Jain S (2017a) Sustainability of a non-edible vegetable oil based bio-lubricant for automotive applications: a review. *Process Saf Environ Prot* 111:701–713
- Singh Y, Singla A, Singh AK (2017b) Tribological characteristics of Mongongo-oil-based biodiesel blended lubricant. *Energy Sourc Part A: Recov Util Environ Effect* 39(3):332–338
- Singh Y, Singla A, Singh AK, Upadhyay AK (2018) Tribological characterization of Pongamia pinnata oil blended bio-lubricant. *Biofuels* 9(4):523–530
- Singh Y, Sharma A, Singla A (2019) Non-edible vegetable oil-based feedstocks capable of bio-lubricant production for automotive sector applications—a review. *Environ Sci Pollut Res* 1–16
- Ssempebwa JC, Carpenter DO (2009) The generation, use and disposal of waste crankcase oil in developing countries: a case for Kampala district, Uganda. *J Hazard Mater* 161(2–3):835–841
- Suhane A, Rehman A, Khaira HK (2012) Potential of non edible vegetable oils as an alternative lubricants in automotive applications. *Int J Eng Res Appl* 2(5):1330–1335
- Sulek MW, Kulczycki A, Malysa A (2010) Assessment of lubricity of compositions of fuel oil with biocomponents derived from rape-seed. *Wear* 268(1–2):104–108
- Syahir AZ, Zulkifli NWM, Masjuki HH, Kalam MA, Alabdulkarem A, Gulzar M, Khuong LS, Harith MH (2017) A review on bio-based lubricants and their applications. *J Clean Prod* 168:997–1016
- Thames SF, Yu H (1999) Cationic UV-cured coatings of epoxide-containing vegetable oils. *Surf Coat Technol* 115(2–3):208–214
- Ting CC, Chen CC (2011) Viscosity and working efficiency analysis of soybean oil based bio-lubricants. *Measurement* 44(8):1337–1341
- Totten GE., Shah RJ, Forester DR (2019) *Fuels and lubricants handbook: technology, properties, performance, and testing*. ASTM International
- Tung SC, McMillan ML (2004) Automotive tribology overview of current advances and challenges for the future. *Tribol Int* 37(7):517–536
- Usta N, Aydoğan B, Con AH, Uğuzdoğan E, Özkal SG (2011) Properties and quality verification of biodiesel produced from tobacco seed oil. *Energy Convers Manag* 52(5):2031–2039
- Wang R, Hanna MA, Zhou WW, Bhadury PS, Chen Q, Song BA, Yang S (2011) Production and selected fuel properties of biodiesel from promising non-edible oils: *Euphorbia lathyris L.*, *Sapium sebiferum L.* and *Jatropha curcas L.* *Bioresour Tech* 102(2):1194–1199
- Wang R, Zhou WW, Hanna MA, Zhang YP, Bhadury PS, Wang Y, Song BA, Yang S (2012) Biodiesel preparation, optimization, and fuel properties from non-edible feedstock. *Datura stramonium L.* *Fuel* 91(1):182–186
- Willing A (2001) Lubricants based on renewable resources—an environmentally compatible alternative to mineral oil products. *Chemosphere* 43(1):89–98
- Zulkifli NWM, Kalam MA, Masjuki HH, Shahabuddin M, Yunus R (2013) Wear prevention characteristics of a palm oil-based TMP (trimethylolpropane) ester as an engine lubricant. *Energy* 54:167–173

**Part IV**  
**Surface Morphologies for Automotive**  
**Applications**

# Chapter 12

## Influence of Surface Texturing on Friction and Wear



**Shubrajit Bhaumik, Chiradeep Ghosh, Basudev Bhattacharya, Viorel Paleu, Rajeev Kumar Naik, Prayag Gopinath, A. Adithya and Ankur Dhanwant**

**Abstract** The chapter highlights the investigations on the friction reduction capability of a pre-determined sized hemispherical dimples of 3 mm diameter, taking into consideration the fact of easy availability of the tool (ball nose end mill) for industrial applications. The dimples were created using CNC milling machines on EN 31 disc. A pin-on-disc tribometer was used to investigate the tribological behavior of the various textured density surface (7.5, 15 and 22.5%) against EN 8 steel under various loading conditions (120, 140, and 160 N) and very harsh lubricating conditions: dry, partial lubrication (lubricant supplied 54 mL dropwise at a flowrate 1 mL/s) and starved lubrication (10 mL lubricant spread over the disc before the experiment). A significant decrease of 12% reduction of coefficient of friction (COF) was observed with 15% texture density under 120 N while the COF increased by 40–60% at texture density of 22.5% and high loads. In dry condition there was no significant change in COF but the specific wear rate decreased by 64.69% in 22.5% texture density. In the present set of experiments carried out at lighter load (120 N), both 7.5 and 15% texture densities exhibited better results as compared to 22.5% texture densities (under partial lubrication). Surface characterizations by optical microscopy revealed that the friction reduction of the dimpled surface was primarily due to the lubricant retaining capability by the dimples which acted as oil reservoirs, but high texture densities intensified the friction.

---

S. Bhaumik (✉) · R. K. Naik · P. Gopinath · A. Adithya · A. Dhanwant  
Tribology and Surface Interaction Research Laboratory, Department of Mechanical Engineering,  
SRM Institute of Science and Technology, Kattankulathur, Chennai 603203, India  
e-mail: [shubrajb@srmist.edu.in](mailto:shubrajb@srmist.edu.in); [shubrajit.research@gmail.com](mailto:shubrajit.research@gmail.com)

C. Ghosh · B. Bhattacharya  
Research and Development, Tata Steel Ltd., Jamshedpur, India

V. Paleu  
Mechanical Engineering, Mechatronics and Robotics Department, Mechanical Engineering  
Faculty, Gheorghe Asachi Technical University of Iasi, 63 D. Mangeron Blvd, Iasi 700050,  
Romania

## 12.1 Introduction

Friction is energy consuming, its reduction being one of the most important tasks continuously aimed by industries. The enterprises which provide the wear and friction reduction solutions always look forward for inexpensive remedies without compromising the performance of the product. Friction reduction by surface texturing is one such methods which is very popular in different industries. Surface textures can be made using various processes, such as chemical etching (Pettersson and Jacobson 2003), laser texturing (Etsion 2005; Kovalchenko et al. 2005; Borghi et al. 2008; Etsion 2004), lithography (Stephens et al. 2002), and pellet pressing (Yan-qing et al. 2009). Zenebe Segu and Hwang (2015) discussed the effect of multi-shaped laser surface texturing on tribological properties of materials. It was found that the multi-shaped dimples gave better results than single shaped dimples. Among the different combinations of circle-ellipse, circle-triangle, and circle-square, the circle-ellipse combination gave the best results under dry and lubricated long sliding conditions. Bhaduri et al. (2017) reported results of tests on the ball-on-disc tribometer with reciprocating sliding motion, presenting the functional response of the textured surfaces with different designs that incorporate arrays of micro-dimples and grooves produced on tungsten carbide blocks by employing laser machining, which were rubbed against stainless steel. It was observed that the micro-arrays and dimples acted as traps for the asperity wear products (third body). Greco et al. (2009) discussed the potential application of vibro-mechanical texturing (VMT) for the generation of dimples on the aluminium and hardened steel on inner cylinder, outer cylinder, and flat end face geometries using a CNC lathe machine. It was found that the VMT method was much more adaptable to the process capabilities, cost effective, and a faster way to create dimples. An error of 1–11% was found on aluminium and 8–9% on hardened steel surface which was attributed to the elastic restoration of the material.

The performance of textured surfaces depends on various factors such as the shape of the textures, arrangement of the textures, materials in contact, load etc. Vilhena et al. (2010) created the surface textures using the LST (Laser Surface Texturing) technique and the tribological tests were conducted for various running parameters. It was found that the tribological behavior of the surface majorly depends upon the dimple depth, or indirectly on aspect ratio (constant diameter), local lubricating conditions, and operating parameter. At more depths and higher sliding speeds the dimpled area has proven to be most beneficial. The most significant result was obtained at a dimple depth of 16.5 microns and 0.45 m/s sliding speeds giving out a COF value as low as 0.006. Olver et al. (2016) prepared specimens of fused silica with small surface modifications in terms of creating small pocket sized micro dimpled geometries and tests were conducted to compare the difference between the textured and the non-textured samples. A reduction of 70% was observed in coefficient of friction (COF) with the textured surfaces. Furthermore, an improvement in film thickness was also observed using textured surfaces. An important result was found that, as the sum of the dimples increased along the length of the stroke, better

frictional and wear properties were observed. It was also inferred that the individual dimple geometry had a very little effect on the properties as long as the overall effect remains positive. Kovalchenko et al. (2011) performed experiments on ball on disc tribometer to determine the effects of surface texturing on the disc surfaces for different oils of various viscosities, combined with different dimple densities with varying depths. The results showed that the increased dimple density caused an increase in wear rates of ball end but a decrease in COF values. The method has been suitably suggested for industrial applications. Yu et al. (2009) studied the effect of different shape dimples on the tribological properties. Different shapes like circles, ellipses, and triangles were made on the surfaces. Each shape was tested in different orientations for several loads and speeds. For example, when the pin slide against the ellipse shape perpendicular to the major axis gave the best results. Triangle is also tested with changing the orientation like sliding towards apex and sliding towards base. Optimized dimple parameters with ellipse shape orientated perpendicular to its major axis gave the best results. After ellipse, circle shape was found to give good results. Etsion and Burstein (1996) developed a model to analyze and compare the contactless seals in lubricated conditions with hemispherical pores. It was investigated if better performances can be achieved with proper selection of dimple size and aspect ratio. They found that the best and optimum dimple size depends on viscosity, contact pressure, and aspect ratio. The hydrodynamic performances were increased at the pore areas on the mechanical seals. Adjemout et al. (2017) studied the influence of real dimple shapes on the performances of the mechanical seals. Numerical solution is used to determine the optimum surface texturing and geometry, the mechanical imperfections being avoided. The real dimple shapes are analyzed and considered within the hydrodynamic lubrication model. The roughness and the bottom surface of the dimples influenced the leakage of oil through the seals. It was also found that enhanced results were obtained if the sides of the triangle were bent towards the center of the dimple. Etsion et al. (1999) developed an analytical model to investigate the performance of the mechanical seals having micro pores on its surfaces, machined using laser surface texturing. Optimization was performed for the spherical shaped pores. It was found that the effect of the pores depth over diameter ratio that is the aspect ratio was very significant. If the hydrostatic forces suppressed the hydrodynamic ones, the performances of the laser textured seals were far better than the conventional mechanical seals. Resendiz et al. (2015) studied the directional friction effects by creating asymmetrically shaped dimpled surfaces on an aluminum work piece using an inclined micro flat end milling tool. When compared with the flat surfaces, the dimpled surfaces resulted in lower friction coefficient values. Also, the asymmetrical textures gave a sliding direction dependent response in terms of measured frictional forces and the coefficient of friction. Jana et al. (2018) studied the frictional behavior and surface properties of tool under textured conditions. Different shapes of texturing were done in tetragonal and hexagonal patterns. Dimple like depressions and S shaped grooves were showing around 40% reduction in coefficient of friction. The tests were conducted in a ring test rig. Other shapes such as circular grooves and spherical dimples when oriented radially towards the sliding load gave better results in coefficient of friction. Shen and Khonsari (2015) tried to develop

and adopt a numerical approximation method to find the most appropriate size of the textures or the dimples which would lead to the highest load bearing capacity of the textured surface. Numerical problems have been solved and then the method is validated and experiments were conducted creating the optimized dimples. The results were then compared with the regular shape dimples. The optimized shape was a chevron shape for unidirectional sliding and trapezoidal shaped dimples for the bi-directional sliding motion. Amini et al. (2016) studied the tribological behaviors of two micro textured surfaces and compared it with that of smooth surface. Pin on disc reciprocating set up is used for testing. Two surfaces that is micro surface textured (MST) and micro furrowed surface (MFS) was tested under load conditions from 20 to 160 N and under boundary lubricated condition. Here both MST and MFT showed better results than the smooth surface. The complex cutting movement is caused by ultrasonic vibrations. The results indicate that proper micro texture by Ultrasonic vibration-assisted milling (UAVM) can improve the load bearing capacity. Li et al. (2014) studied the frictional behavior and wear rates of a textured surface made by laser peen texturing. Texture densities with 5, 13 and 35% are tested by pin-on-disc tribometer and compared with the untextured surface under the load condition from 20 to 400 N. In this case, 13% texture density samples demonstrate better results in friction performance and wear rate. Schneider et al. (2017) studied the influence of aspect ratio, texture pattern, and dimple parameters under mixed lubrication regimes. The texture density was varied from 5 to 30% in different patterns like cubic, hexagonal and random arrangement. The depth to diameter ratio was also varied from 0.1 to 0.2. The lubricant used was POA. Results illustrate that those patterns arranged in hexagonal arrays performed well under the texture density of 10% with aspect ratio of 0.2. Around 80% reduction in friction coefficient was observed in this condition. Varenburg et al. (2002) studied the role of oxide wear debris in fretting wear. The wear rate varies according to the roughness of the material. Here micro dimples act as traps for debris. As the pin is sliding, wear debris gets deposited on the dimples which helps in further reduction in wear rate. They also found that 84% reduction is there due to the dimples acting as pores. Multi dimples with different patterns were created and tribological properties were evaluated and tested to collect data for wear and coefficient of friction values by Tang et al. (2013). The results show that surface texturing is essential and an important method for reducing friction and wear. Amendments in the area fractions and the aspect ratios can significantly improve the tribological characteristics, COF and the wear rates. A significant reduction of 38% in COF and 72% in wear rates were observed under the area fraction of 5% which was increased due to hydrodynamic pressure in the interfacial contacts between the surfaces. Podgornik et al. (2012) investigated the tribological effects of surface texturing under starved, boundary and mixed lubrication regimes. The experiments were conducted with LST technique on pin on disc apparatus and compared the results with varying lubricant viscosity, normal load, sliding speed, dimple/groove size, dimple/groove density, dimple depth and different lubrication regimes. The results show that LST surfaces with lower dimple/groove size and density has less friction under boundary lubricated conditions. Further the largest dimple depth under full

film lubricated conditions gives the lowest friction. Hua et al. (2017) studied the frictional behavior of the contact surfaces lubricated with grease by using disc on ring tribometer. Various parameters like texture density, load, sliding speed and sliding time were varied. The lubrication regime was mixed lubricated regime. The results show that influence of texture density is a significant factor in controlling the tribological properties. Here a texture density of 15% is found to give the best results. Also, the major reason for control of friction is the hydrodynamic effect of the lubricant. Ogawa et al. (2010) investigated the tribological properties of slideways by laser texturing method. Different types of dimples and grooves were made for testing. The dimple width varied from 50  $\mu\text{m}$  to 1 mm. The optimum dimple parameters were found after the test. The textured surface was found to give less friction coefficient as lubricant reservoirs were created inside the dimples. Jahanmir (1985) experimented and observed that the process of wear particle formation is greatly affected by the tangential stresses. Keeping the normal stresses constant and varying the tangential stresses with the COF, it was observed that the wear particles are formed due to deformation of the surface asperities significantly due to plowing and delamination process. It was also concluded that friction modifiers can influence the wear rate and its mechanism. Wear rate can be reduced by reducing the COF value below the threshold limit. Plowing and delamination are one of the causes that influence the wear rate. Under starved lubricating conditions the adhesive wear is predominant. Wang et al. (2017) investigated about the wear and friction performance of three different types of polymer on steel surface using ring on plane device. Texturing of different density values was done on steel surfaces. Polymers of various composition are tested under diverse texture densities and depths. The best results were obtained in dimples with depth of 5  $\mu\text{m}$  rather than dimples with a depth of 10  $\mu\text{m}$ . The wear debris found for non-textured surface were smooth and at higher wear the nature of debris was lumpy and at lower wear rate the nature was like twisted. Zhang et al. (2012) studied and conducted experiments on textured and untextured surfaces of UHMWPE under water lubrication using ring-on-disc tester. The textured surfaces shows a reduction in the COF as much as 66.7–85.7% on different load and speed conditions. The textured UHMWPE with an area density of 29.9%, diameter 50 mm, and depth 15 mm presents a significant effect of wear resistance, being reported as optimized result. It was observed that the micro-scaled surface textures show a greater wear resistance and lower COF values. Chowdhury et al. (2011) investigated the behavior of friction and wear under varying sliding speed, normal load and relative humidity. The experiments were conducted on pin-on-disc tribometer, where disc was made of aluminum and pin was of stainless steel. The results show that as the sliding speed increased, friction decreased and wear rate increased, as aluminum has the property of reacting with air and forming oxides. It forms a layer on the surface reducing metal to metal contact, hence reducing friction. From the above cited works, it can be seen that surface texturing has been used since a long time in various fields to control the friction. The recent work reported by Chen et al. (2019) showed that the load bearing capacity of a separator plate enhanced after texturing. In this case the cylindrical and cuboidal textures performed better than hemispherical textures at low speed. They also reported that the geometrical features of the dimples played a

major role in enhancing the load bearing capacity. A decrease of over 20% wear rate in textured samples made of Ti alloys was reported by Yuan et al. (2019). In another work involving the investigation of tribological properties of Ti alloy reported by Kummel et al. (2019), it was observed that the melt bulges formed around the sides of the channels created using laser were active sites for solid solution of interstitial elements such as oxygen and nitrogen which helped in enhancing the tribological properties of Ti6Al4V.

Thus, it can be seen that surface engineering is an established field in controlling friction and wear and many works have been reported but very few systematic work has been done on dimples created using milling machines. Almost no work has been reported involving extreme harsh conditions of lubrication of dimpled surface. This chapter focuses on the performance of the dimpled surface in highly sparse lubricant condition where very minimal quantity of lubricant with discontinuous flow has been used. Milling machines (vertical) which are very common in any manufacturing unit were used to create the dimples. The cost of creating dimpled surfaces by milling is less expensive and easy to make for any industry. The size of the dimple was also chosen in such a way that the tool necessary for making the dimple is not expensive and easily available in the local market. Thus, the present work will be helpful for process industries in combating wear using dimpled surfaces created by milling process.

## 12.2 Texturing on Tribo Surface Using Milling Operation

A disc of EN 31 steel with 165 mm diameter, thickness 8 mm and hardness 38 HRC was used. Circular dimples were created on the disc surface with a ball end mill cutter in a CNC milling machine (Make: Lakshmi Machine Works, Model: LV45) at a constant feed rate of 120 mm/rev. The dimples on the surface of the specimen were uniformly arranged in a circular orientation as shown in Fig. 12.1. Hua et al. (2017) studied the frictional behavior of the contact surface lubricated with grease by using disc on ring tribometer and reported that the texture density of 15% exhibits least coefficient of friction. Thus, for the present work three dimple densities, namely 7.5, 15 and 22.5% were considered. The design texture density ( $T_d$ ) was calculated using Eq. 12.1 (Hua et al. 2017)

$$T_d = \frac{A_d}{A_s} \times 100\% = \frac{\pi \times D^2}{2 \times \theta(r_1^2 - r_2^2)} \times 100\% \quad (12.1)$$

where

$T_d$  is the texture area ratio (texture density);

$A_d$  is the area of the dimple ( $A_d = \pi D^2/4$ )

$A_s$  is the sector area between the dimple  $A_s = \frac{\theta(r_1^2 - r_2^2)}{2}$

$r_1$  is radius of the bigger sector



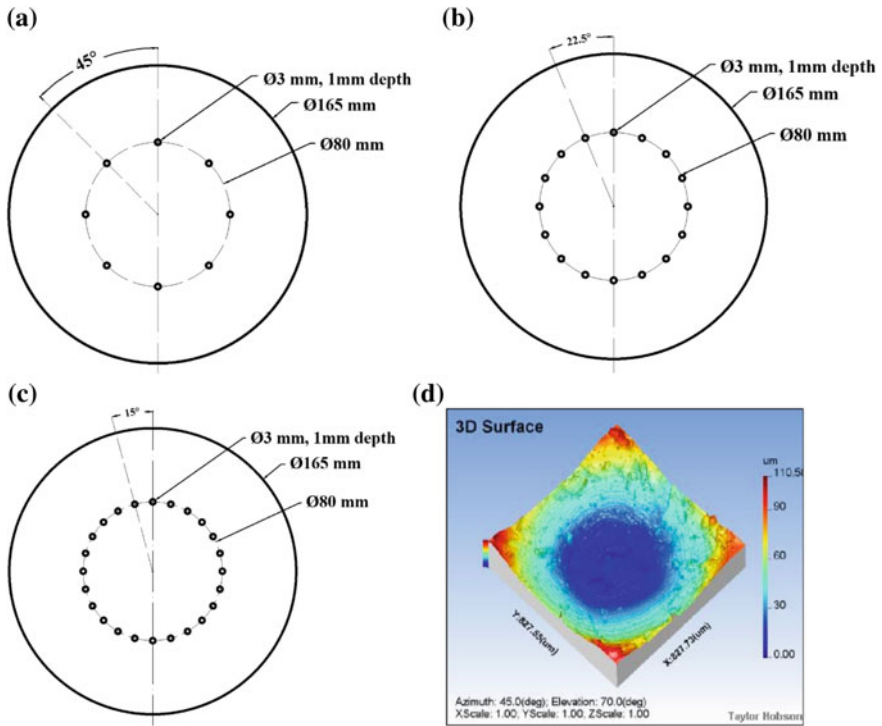


**Fig. 12.1** a 7.5% texture density, b 15% texture density, c 22.5% texture density, d three-dimensional image of dimples

$r_2$  is radius of the smaller sector  
 D is dimple diameter.

The bulges or burrs which formed around the dimple during the machining process were removed by polishing. This reduces the negative effect on the tribological performance of contacting surfaces (Etsion 2004). A cylindrical EN 8 pin (diameter 10 mm, length 30 mm and hardness 31HRC) was used against the EN 31 disc.

In this work circular dimples were developed keeping in mind the following:

- i. Ease of availability of the 3 mm diameter ball nose milling tool in local markets.
- ii. Ellipse and circular dimples exhibited better tribological properties (Yu et al. 2009).
- iii. Textured surfaces with curved bottom were found to show better tribological properties than flat bottom surfaces, sharp angles and straight edges (Qiu et al. 2013).

### 12.3 Investigating the Tribological Properties Using Pin-on-Disc Tribometer

Pin-on-disc tribometer was used to investigate the tribological properties of the textured surface (disc of EN 31). The counter part was the EN 8 pin. SAE 10W30 lubricant was used during the tests and three different loads were considered (120, 140, and 160 N) at a constant speed of 4.2 m/s under the influence of the following lubrication condition:

- i. Dry condition: no lubricant was used.
- ii. Partial lubrication condition: lubricant was supplied between the interface of the pin and disc in a drop wise manner (amount of lubricant used: 54 mL with a flow rate of 1 mL/s).
- iii. Starved lubrication condition: about 10 mL of the SAE 10W30 lubricant was poured over the textured surfaces before the start of the experiment. It was ensured that the lubricant fully covers the disc. The test was started after five minutes ensuring the lubricant to settle in the dimples. No further lubricant was added during the entire duration of the tribo experiment.

Each combination of trials was repeated thrice and an average of the friction coefficient and wear rate has been reported in the work. The experimental parameters are shown in Table 12.1.

The average coefficient of friction for all the experiments are shown in Fig. 12.2a. Here the same chronology is maintained as shown in Table 12.1.

**Dry condition:** From Fig. 12.2a it can be seen that the COF in dry condition is more than the lubricated conditions. When it comes to partial and starved lubrication condition, a decrease in COF is observed. The highest COF is experienced in experiment number 4 (i.e. load 120 N, texture density 22.5% and dry lubrication condition) while the least value is obtained in experiment number 27 (i.e. 120 N, texture density 15% and partial lubrication condition). But in higher loading conditions such as 140 and 160 N performed under partial lubrication the least coefficient of friction is observed in texture density of 7.5%. Figure 12.2b depicts the variations of the wear rates under different testing. It can be seen that the wear rate decreases with the increase in texture density. Same goes with the next 2 sets of intervals (Experiment 5 to Experiment 8; Experiment 9 to Experiment 10). A slight increase in the last experiment (Experiment 8 and Experiment 12) of each set corresponding to the highest texture density in that set.

**Lubricated condition:** Fig. 12.2c shows the trend and variation of wear rates with changes in the experiment conditions which includes changes in loads, lubricating conditions and texture densities. Experiment 13–24 correspond to the starved lubrication under different texture densities and Experiments 25–36 corresponds to the partial lubricating condition. The highest wear rate can be seen in experiment number 36 (160 N, texture density 22.5% and partial lubrication condition) while the least wear rate is observed in experiment number 15 (load 120 N, texture density 15% and starved lubrication condition). In starved lubrication, a decreasing trend for

**Table 12.1** Experimental parameters

Experiment No.	Load (N)	Texture density (%)	Lubrication condition
1	120	0	Dry
2	120	7.5	Dry
3	120	15	Dry
4	120	22.5	Dry
5	140	0	Dry
6	140	7.5	Dry
7	140	15	Dry
8	140	22.5	Dry
9	160	0	Dry
10	160	7.5	Dry
11	160	15	Dry
12	160	22.5	Dry
13	120	0	Starved
14	120	7.5	Starved
15	120	15	Starved
16	120	22.5	Starved
17	140	0	Starved
18	140	7.5	Starved
19	140	15	Starved
20	140	22.5	Starved
21	160	0	Starved
22	160	7.5	Starved
23	160	15	Starved
24	160	22.5	Starved
25	120	0	Partial
26	120	7.5	Partial
27	120	15	Partial
28	120	22.5	Partial
29	140	0	Partial
30	140	7.5	Partial
31	140	15	Partial
32	140	22.5	Partial
33	160	0	Partial
34	160	7.5	Partial
35	160	15	Partial
36	160	22.5	Partial

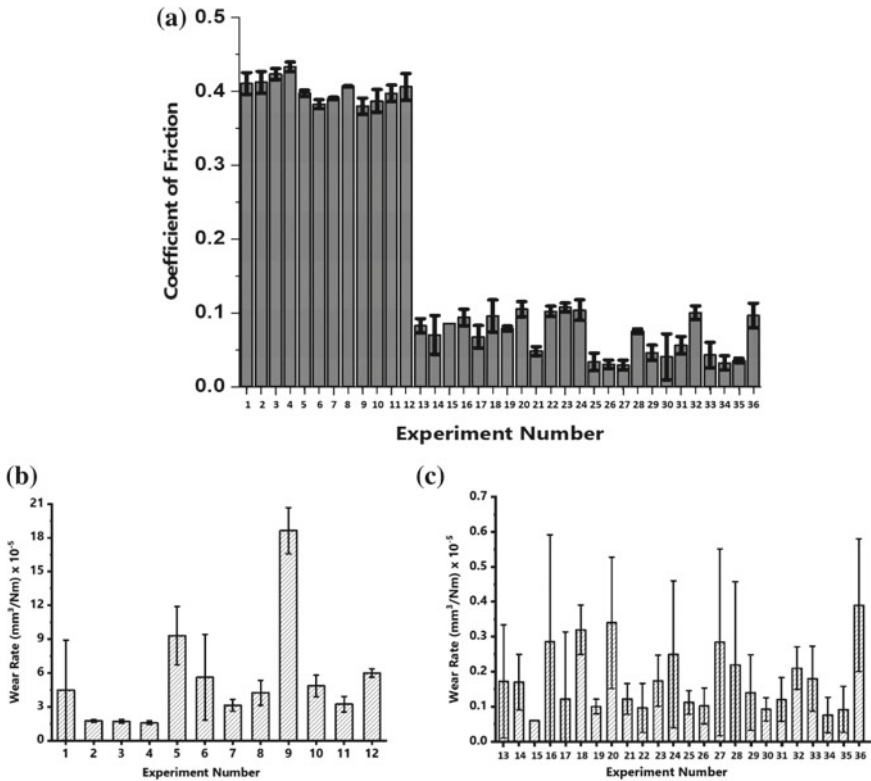


**Fig. 12.2** a Coefficient of friction, b wear rate in dry condition, c wear rate in Lubricated conditions

the first 3 experiments in 1st set (Experiment No. 13–15) and increasing trend for the last 3 experiment in the 3rd set (Experiment No. 22–24) are obtained. This goes for all the intervals (Experiment 29 to Experiment 36). But a nonlinear variation for all experiments in the 2nd set (Experiment No. 17–20) and 7th set (Experiment No. 25–28) is observed. The 4th experiment on each set is always seen to be increasing in each interval similar to dry condition.

From Fig. 12.2, it can be seen that at 140 and 160 N load, the COF and wear rates increased with an increase in texture densities. The lowest COF and wear rate were obtained at 120 N load conditions. The wear rates were high at 140 and 160 N as compared to 120 N of applied load. Figure 12.3 shows the COF and wear rates plotted against texture density at 120 N load conditions performed under various lubricated conditions. A decreasing trend in COF with increasing texture density under partial lubricating regime can be seen in Fig. 12.3a whereas, in starved lubrication the coefficient of friction decreases till 7.5% texture density and then increases. Furthermore, 7.5% texture density exhibited lowest COF (15 and 18% decrease in 0 and 15% texture densities under starved lubricating regime respectively) while in partial lubrication the 15% dimple density have shown beneficiary results as the COF was

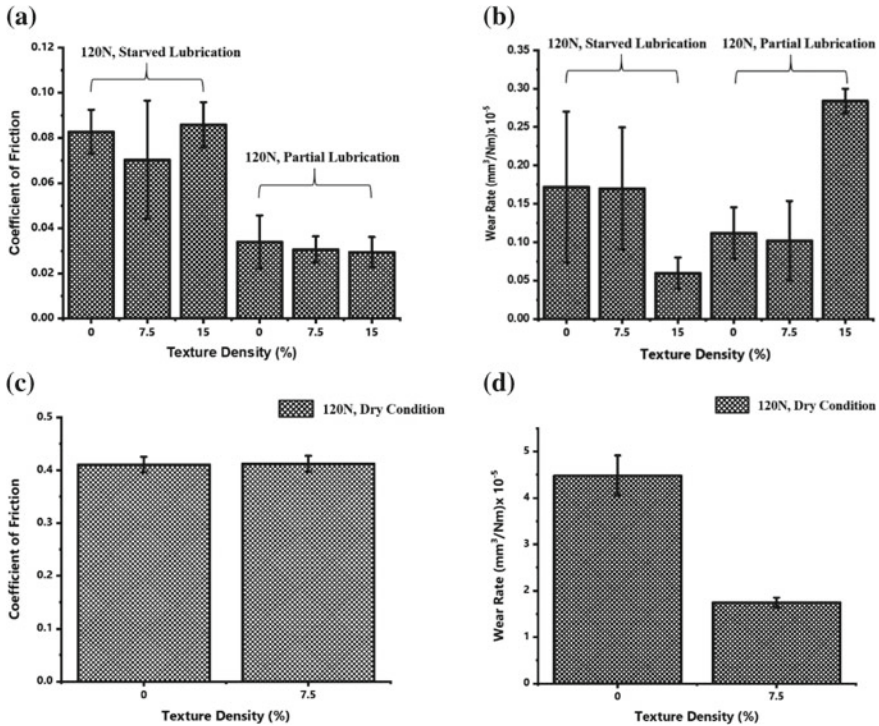
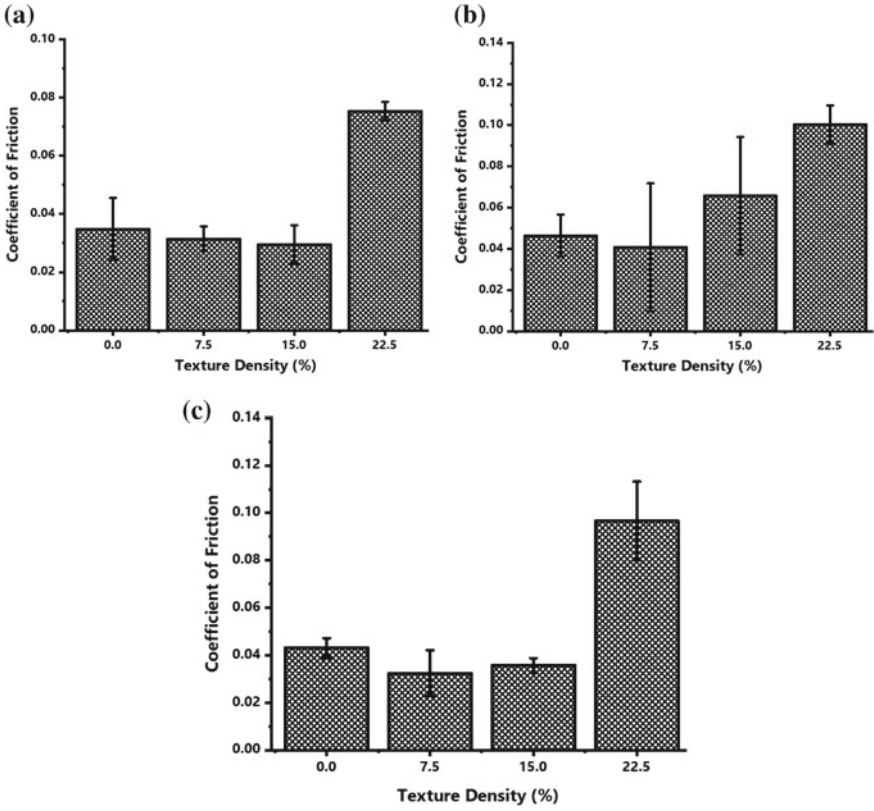


Fig. 12.3 Optimized textured densities in various lubrication conditions

13% less than 0% and 3.6% less than 7.5% texture densities. Thus, a decreasing trend of COF in lubricating conditions indicates the advantage of the presence of dimples on the surface. Figure 12.3b shows the variations between the wear rates and texture density with constant loading conditions and different lubrication regimes (starved and partial lubrication). It can be seen that during starved lubrication condition, there was no significant change in the wear rates at 0 and 7.5% textured density while a significant decrease in wear rate by 64–65% was observed at 15% texture density as compared to the wear rates of 0 and 7.5% texture densities. In partial lubrication, a slight decrease of 9% wear rate was observed at 7.5% as compared to untextured but it increased at 15% texture density. Unlike the COF variations, the least wear rate is found in the texture density of 15% under starved lubrication condition. Figure 12.3c shows the trend of COF with varying texturing density in dry environment and under 120 N loading conditions which exhibited that the COF in non-dimpled and dimpled surface were almost equal, however a significant 61% decrease in wear rate in case of textured surface can be observed as seen in Fig. 12.3d.

From above discussions it can be seen that the COF is less in the case of partial lubrication as compared to dry and starved lubrication conditions. Figure 12.4 shows the COF against texture densities at different load conditions (120, 140 and 160 N) performed under partial lubricated condition. In case of 120 N with partial lubricated



**Fig. 12.4** Frictional trend at various loads in partial lubrication condition, a 120 N, b 140 N, c 160 N

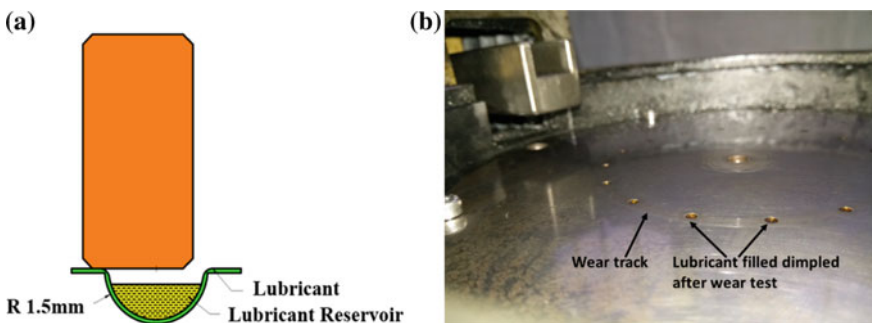
condition (Fig. 12.4a), a gradual decrease in the COF was observed till 15% texture density but there was a 60% decrease in COF at 15% as compared to 22.5% texture density while in 140 and 160 N with partial lubricated conditions (Fig. 12.4b, c), a slight decrease in friction coefficient was observed at a texture density of 7.5% as compared to texture density of 0% and further increasing the texture density the COF increased. It is to be noted that for all loads, an increasing trend of COF was observed with increase in texture density.

## 12.4 Understanding the Mechanisms Involved During Tribo Tests

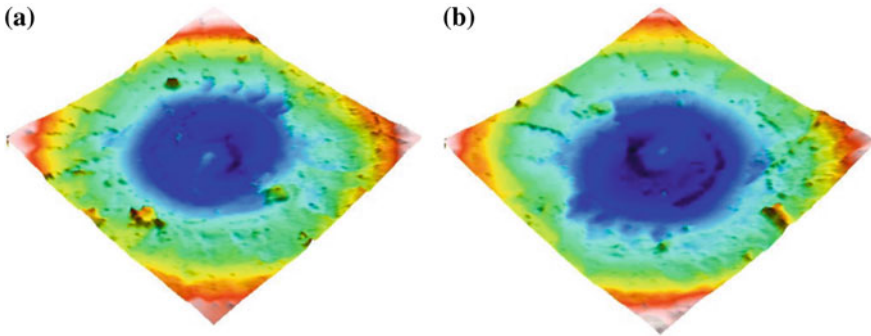
### 12.4.1 Lubricant Reservoirs Leading to Friction Reduction

Figure 12.5 shows the arrangement of the pin and the dimple in a lubricated condition. During the test, the pin surface fully covered the dimple region at an instantaneous moment while sliding. The dimple served as the lubricant reservoir while running in starved lubricating conditions, but in dry sliding condition the dimples behaved as the wear debris storage and prevented the wear debris to affect the overall surface morphology, thus making the surface more wear resistant (Varenberg et al. 2002; Yamakiri et al. 2011). Friction between tribo pairs are less when the lubricating film is thicker than the average surface roughness value or the average height of the asperities but under high loading conditions, the lubricant oozes out of the rubbing track or the frictional zone, leading to the reduction in the film thickness to less than the average asperity height causing greater asperity contacts and ultimately leading to higher frictional force and wear (Bart et al. 2013). In case of textured surfaces, the region where the pin comes in complete contact with the dimple, the thickness of the lubricant film increases due to the presence of lubricant in the dimple. The depth of the dimple helps in retaining the lubricant which in turn increases the thickness of lubricant film leading to an increased hydrodynamic pressure exerted by the lubricant. This results in the increase of load bearing capacity, which ultimately reduces wear (Kovalchenko et al. 2005). It has been reported that increased dimple depths have beneficial effects on the reduction of friction and wear (Ogawa et al. 2010). Furthermore, in hydrodynamic lubricating conditions the effects of surface texturing have also contributed in improving the tribological characteristics (Mo et al. 2017; Qu et al. 2013).

The three-dimensional image of the dimples, shown in Fig. 12.6, clearly depicts that there was no contact between the pin and the base of the dimples, as no major



**Fig. 12.5** **a** Schematic diagram of pin rubbing against the dimple in lubricated conditions, **b** a real time photo of a dimple with entrapped lubricant after the test



**Fig. 12.6** Three-dimensional image of dimple in lubricated condition: **a** before test, **b** after test

deterioration of the surface can be observed, thus indicating the presence of lubricants in the dimples as shown in Fig. 12.6b.

#### ***12.4.2 Presence of Third Bodies in the Dimples (Dry Condition)***

In 120, 140 and 160 N dry condition no significant difference in friction coefficient is observed but the wear rate was less in textured surfaces as compared to the non-textured surface. This may be due to the debris entrapment in the dimples which helped in preventing the direct contact of the tribo pairs and thus reducing the wear (Bhaduri et al. 2017; Varenberg et al. 2002; Fukagai et al. 2019; Yamakiri et al. 2011).

#### ***12.4.3 Increase in COF with the Increase in Load and Texture Density***

As discussed in Sect. 12.3, in partial lubricated conditions COF gradually decreased as the texture density increased, but over 15% the COF increased again. In dry conditions, surface texturing in general will lead to increased friction (Fig. 12.2a), with every dimple acting as obstacle to the sliding motion (Podgornik et al. 2012). The increase in the texture density to 22.5% exhibited an increase in wear rate as compared with texture density of 7.5 and 15%. In the case of 22.5% texture density, the presence of large dimples made the surface less uniform which affected the uniform asperity peaks (Hua et al. 2017) increasing the COF. Furthermore, the heat generated led to localized welding of the small wear debris on the wear track (Elsevier 1987). This continuous welding and accumulation of the wear particles at a high load contributed to an increased frictional property.



At 120 N and partial lubricating conditions, as the texture density was increased the coefficient of friction decreases until texture density of 15%. The dimples acted as a lubricant reservoir and enhance the hydrodynamic action (Ogawa et al. 2010; Yamakiri et al. 2011). Further increasing the texture density to 22.5%, drastic increase in COF was observed. The space between each dimple acted like peaks, which affected the film distribution, thus resulting in higher friction (Hua et al. 2017). Also at higher dimple densities, the surface becomes highly non-linear leading to a turbulent lubricant flow on the surface affecting the shear properties of the interface (Qu et al. 2013). In case of starved lubrication condition as the texture density was increased the COF decreased until texture density of 7.5% and then increased with the increase in texture density. The change of lubrication regime from a partially hydrodynamic condition to very localized boundary conditions resulted in high asperity contacts (Li et al. 2014) during starved lubrication condition which resulted in gradual decrease in film over a period thereby, increasing the COF.

In 140 and 160 N under partial lubricated condition, the COF was less in textured surface as compared to un-textured surface but the increase in COF was similar to that of 120 N, as texture density increased the COF also increased. This is because at higher loads there is always a portion of area coming in contact and as a result, the edge of the dimple perpendicular to sliding direction lead to high stress generation at the edge of dimple (Zhang et al. 2012), thus affecting friction and wear. In 140 N, starved lubricated condition, in un-textured surface the lubricant after certain time drains out and thus, favoring high asperity-asperity contact increase the COF. Furthermore, in case of 7.5% texture density, the number of dimples were less as compared to 15% texture density and hence, more lubricant was retained in 15% texture density as compared to 7.5% texture density. Thus, COF for 7.5% was slightly more than texture density of 15% but further increasing the texture density to 22.5% conducted to augmentation of COF. The increase in COF and wear in high density textured surfaces were primarily due to the ploughing action exhibited by the dimples (Jahanmir 1985). Therefore, the exact number of dimples which is required to control wear and friction also depends on the amount of load applied.

#### ***12.4.4 Understanding the Severity of the Wear on the Counter Surface Against the Textured Surface***

The scanning electron microscope images of the counter body (pin) after the tribo test has been shown in Fig. 12.7 which clearly identifies the severity of the wear during the process. As seen from Fig. 12.7a, b, the surface for dry conditions is more damaged than those of the lubricated condition as seen in Fig. 12.7c (non-textured) and Fig. 12.7d (15% texture density). High abrasive wear can be seen in both cases of dry condition in Fig. 12.7a, b, thus indicating that texturing may not be a good idea in dry condition but as seen in Fig. 12.7c, d, the surfaces are less damaged as compared to Fig. 12.7a, b. Close observation of Fig. 12.7c revealed the formation of grooves in

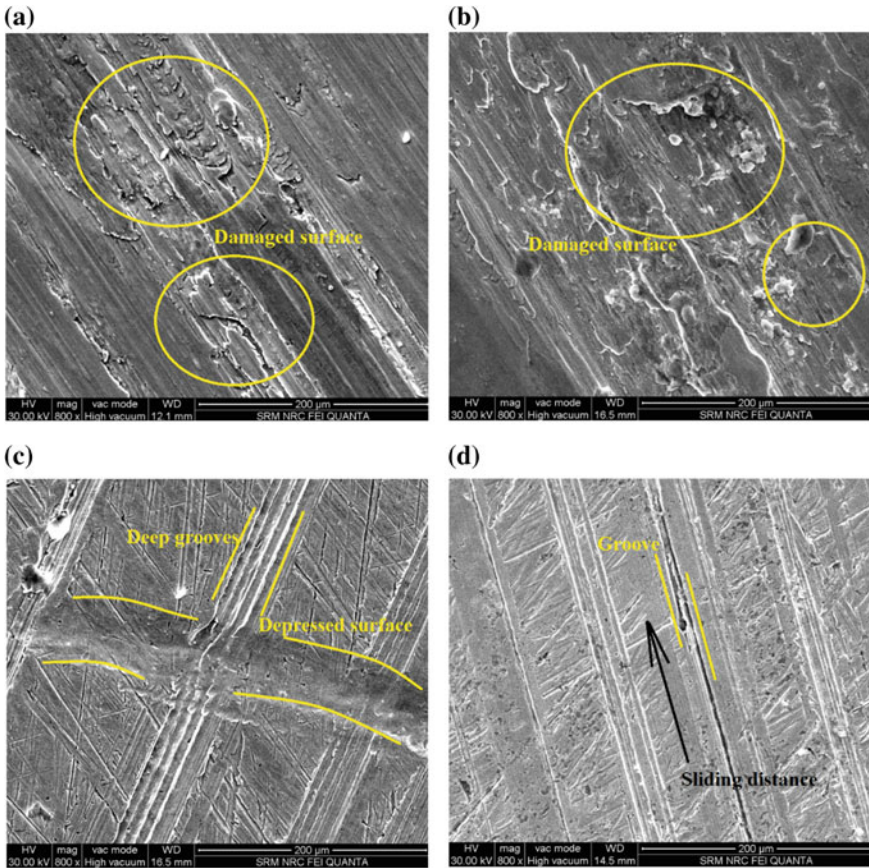


**Fig. 12.7** SEM images of the pin after tribo test with 120 N, **a** dry non dimpled, **b** dry dimpled, **c** lubricated non dimpled, **d** lubricated dimpled (120 N, 15% texture density)

several places and depression were also found as indicated. The formation of such deep grooves and depressed surfaces are due to the film breakage which resulted in high metal to metal contact. Moreover, it is to be noted that the lubrication condition considered for the present work was discontinuous and was supplied in drop wise condition making the situation quite severe, thus the possibility of film breakage is quite certain but looking into Fig. 12.7d (the surface of the pin whose counter body i.e. the disc was having dimples showed almost negligible damage) as compared to those of dry condition and lubricated condition (without dimples, Fig. 12.7c).

## 12.5 Conclusion

The chapter initially discusses the work which was reported by various researchers and then focused on the tribological properties of micro dimpled surfaces. The results showed that texturing may not be effective in dry condition in reducing coefficient of friction but significant decrease in wear rate can be achieved using the correct textured density (in this case 7.5%). The friction and wear reduction capability of textured surfaces primarily depends on the regime of lubrication, applied load and texture densities. However, the creation of micro sized dimples with CNC end mill ball nose cutters is an easy process and is quite capable of reducing the friction under severe conditions. This solution can be adopted by industries as an economical process to control friction and wear.

**Acknowledgements** The authors are grateful for the financial grant received from Tata Steel Jamshedpur, India for carrying out the work. The authors are grateful to Tata Steel for allowing to publish the work.

## References

- Adjemout M, Andrieux A, Bouyer J, Brunetière N, Marcos G, Czerwiec T (2017) Influence of the real dimple shape on the performance of a textured mechanical seal. *Tribol Int* 115:409–416
- Amini S, Hosseinabadi HN, Sajjadi SA (2016) Experimental study on effect of micro textured surfaces generated by ultrasonic vibration assisted face turning on friction and wear performance. *Appl Surf Sci* 390:633–648
- Bart J CJ, Gucciardi E, Cavallaro S (2013) Principles of lubrication. *Biolubricants* 2:10–23
- Bhaduri D, Batal A, Dimov SS, Zhang Z, Dong H, Fallqvist M, M'Saoubi R (2017) On design and tribological behavior of laser textured surfaces. *Proced CIRP* 60:20–25
- Borghi A, Gualtieri E, Marchetto D, Moretti L, Valeri S (2008) Tribological effects of surface texturing on nitriding steel for high-performance engine applications. *Wear* 265:1046–1051
- Chen LY, Li R, Xie F, Wang Y (2019) Load-bearing capacity research in wet clutches with surface texture. *Measurements* 142:96–104
- Chowdhury MA, Khalil MK, Nuruzzaman DM, Rahaman ML (2011) The effect of sliding speed and normal load on friction and wear property of aluminum. *IJMME* 11:45–49
- Elsevier BV (1987) Sliding wear. *Tribol Ser* 6:351–495
- Etsion I (2004) Improving tribological performance of mechanical components by laser surface texturing. *Tribol Lett* 17:733–737
- Etsion I (2005) State of the art in laser surface texturing. *J Tribol* 127:248–253
- Etsion I, Burstein L (1996) A model for mechanical seals with regular micro surface structure. *Tribol T* 39:677–683
- Etsion I, Kligerman Y, Halperin G (1999) Analytical and experimental investigation of laser-textured mechanical seal faces. *Tribol T* 42:511–516
- Fukagai S, Ma L, Lewis R (2019) tribological aspects to optimize traction coefficient during running-in period using surface texture. *Wear*
- Greco A, Raphaelson S, Ehmman K, Wang QJ, Lin C (2009) Surface texturing of tribological interfaces using the vibromechanical texturing method. *J Manuf Sci E-T ASME* 131:061005
- Hua X, Puoza J, Zhang P, Xie X, Yin B (2017) Experimental analysis of grease friction properties on sliding textured surfaces. *Lubricants* 5:42

- Jahanmir S (1985) The relationship of tangential stress to wear particle formation mechanisms. *Wear* 103:233–252
- Jana S, Peter S, Martin F, Martin N, Jana M, Martin K (2018) The influence of the tool surface texture on friction and the surface layers properties of formed component. *Adv Sci Technol Res J* 12:181–193
- Kovalchenko A, Ajayi O, Erdemir A, Fenske G, Etsion I (2005) The effect of laser surface texturing on transitions in lubrication regimes during unidirectional sliding contact. *Tribol Int* 38:219–225
- Kovalchenko A, Ajayi O, Erdemir A, Fenske G (2011) Friction and wear behavior of laser textured surface under lubricated initial point contact. *Wear* 271:1719–1725
- Kummel D, Hamann-Schroer M, Hertzner H, Schneider J (2019) Tribological behavior of nanosecond-laser textured Ti6Al4V. *Wear* 422:261–268
- Li K, Yao Z, Hu Y, Gu W (2014) Friction and wear performance of laser peen textured surface under starved lubrication. *Tribol Int* 77:97–105
- Mo F, Shen C, Zhou J, Khonsari MM (2017) Statistical analysis of surface texture performance with provisions with uncertainty in texture dimensions. *IEEE Access* 5:5388–5398
- Ogawa H, Sasaki S, Korenaga A, Miyake K, Nakano M, Murakami T (2010) Effects of surface texture size on the tribological properties of slideways, proceedings of the institution of mechanical engineers. *J Eng Tribol* 224:885–890
- Pettersson U, Jacobson S (2003) Influence of surface texture on boundary lubricated sliding contacts. *Tribol Int* 36:857–864
- Podgornik B, Vilhena LM, Sedlaček M, Rek Z, Žun I (2012) Effectiveness and design of surface texturing for different lubrication regimes. *Meccanica* 47:1613–1622
- Qiu M, Minson BR, Raeymaekers B (2013) The effect of texture shape on the friction coefficient and stiffness of gas-lubricated parallel slider bearings. *Tribol Int* 67:278–288
- Qu H, Shen Z, Xie Y (2013) Numerical investigation of flow and heat transfer in a dimpled channel among transitional reynolds numbers. *Mathem Prob Eng* 2013:1–10
- Resendiz J, Graham E, Egberts P, Park SS (2015) Directional friction surfaces through asymmetrically shaped dimpled surfaces patterned using inclined flat end milling. *Tribol Int* 91:67–73
- Schneider J, Braun D, Greiner C (2017) Laser textured surfaces for mixed lubrication: influence of aspect ratio. *Textur Area Dimple Arrange Lubric* 5:32
- Shen C, Khonsari MM (2015) Numerical optimization of texture shape for parallel surfaces under unidirectional and bidirectional sliding. *Tribol Int* 82:1–11
- Stephens LS, Siripuram R, Hayden M, McCart B (2002) Deterministic micro asperities on bearings and seals using a modified LIGA process. *Turbo Expo*, 4
- Tang W, Zhou Y, Zhu H, Yang H (2013) The effect of surface texturing on reducing the friction and wear of steel under lubricated sliding contact. *Appl Surf Sci* 273:199–204
- Varenberg M, Halperin G, Etsion I (2002) Different aspects of the role of wear debris in fretting wear. *Wear* 252:902–910
- Vilhena LM, Podgornik B, Vižintin J, Možina J (2010) Influence of texturing parameters and contact conditions on tribological behaviour of laser textured surfaces. *Meccanica* 46:567–575
- Vlădescu S-C, Olver AV, Pegg IG, Reddyhoff T (2016) Combined friction and wear reduction in a reciprocating contact through laser surface texturing. *Wear* 358–359:51–61
- Wang M, Zhang C, Wang X (2017) The wear behavior of textured steel sliding against polymers. *Materials* 10:330
- Yamakiri H, Sasaki S, Kurita T, Kasashima N (2011) Effects of laser surface texturing on friction behavior of silicon nitride under lubrication with water. *Tribol Int* 44:579–584
- Yan-qing W, Gao-feng W, Qing-gong H, Liang F, Shi-rong G (2009) Tribological properties of surface dimple-textured by pellet-pressing. *Proced Earth Planet Sci* 1:1513–1518
- Yu H, Wang X, Zhou F (2009) Geometric shape effects of surface texture on the generation of hydrodynamic pressure between conformal contacting surfaces. *Tribol Lett* 37:123–130
- Yuan S, Lin N, Zhou J, Liu Z, Wang Z, Tian L, Qin L, Zhang H, Wang Z, Tang B, Wu Y (2019) Effect of laser surface texturing (LST) on tribological behavior of double glow plasma surface zirconizing coating on Ti6Al4V alloy. *Surf Coat Technol* 368:97–109

- Zenebe Segu D, Hwang P (2015) Friction control by multi-shape textured surface under pin-on-disc test. *Tribol Int* 91:111–117
- Zhang B, Huang W, Wang X (2012) Biomimetic surface design for ultrahigh molecular weight polyethylene to improve the tribological properties. *Proc Inst Mech Eng J Eng Tribol* 226:705–713

# Chapter 13

## Magneto Rheological Fluid Based Smart Automobile Brake and Clutch Systems



Rakesh Jinaga, Shreedhar Kolekar and T. Jagadeesha

**Abstract** The chapter deals smart fluid i.e. Magneto Rheological fluid which is gaining interest of researcher as the range of application is vast. This book chapter starts with introduction of MR fluid, constituents of MR fluid and detailed study of each constituent. Also, discussing about the present necessity of MR fluid technology we discuss the operational modes of MR fluid. MR devices function basically on three operational modes of MR fluid i.e. flow mode, shear mode and squeeze mode. Every mode possess its own characteristics in high performance application system. Further Mathematical modelling of various rheological parameters and MR fluid is carried out, there after the detailed synthesis process and characterization of MR fluid is discussed. At last overview of MR fluid application is discussed and in detailed progress in MR brakes and clutch system is discussed.

**Keywords** Magneto rheological fluid · Synthesis · MR brake and clutch

### 13.1 Introduction

Magneto rheology is the branch of tribology dealing with response of smart material when they are subjected to external magnetic field. Rabinow (1951) discovered magnetorheological fluid (Rabinow 1951; Hardy 2014). The Magneto Rheological (MR) fluid is the dispersed phase of non-colloidal, magnetically soft and multi-domain particles with particle size ranging from 0.05 to 10  $\mu\text{m}$  in carrier fluid. Under “off state” i.e. nonmagnetic condition the MR fluid appears to be similar to that of carrier fluid with increased viscosity and darker in appearance and exhibits lower shear rate. Under the influence of external magnetic field i.e. “on state” the fluids apparent viscosity changes drastically (106 times) with a reaction time of few milliseconds on application of magnetic field. The fluid recovers viscosity changes completely and reverts back once applied magnetic field is turned off.

---

R. Jinaga (✉) · T. Jagadeesha  
National Institute of Technology Calicut, Kozhikode, Kerala 673601, India  
e-mail: [jagdishsg@itc.ac.in](mailto:jagdishsg@itc.ac.in)

S. Kolekar  
Satara College of Engineering and Management Limb, Satara, Maharashtra 415015, India

© Springer Nature Singapore Pte Ltd. 2019

J. K. Katiyar et al. (eds.), *Automotive Tribology*, Energy, Environment, and Sustainability,  
[https://doi.org/10.1007/978-981-15-0434-1\\_13](https://doi.org/10.1007/978-981-15-0434-1_13)

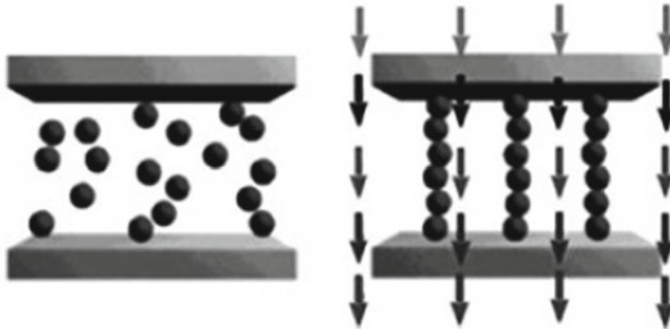


**Fig. 13.1** Schematic representation of magnetic particle under “off state” and “on state” of magnetic field

Under on state condition the particles dispersed in carrier fluid acquire dipole moment this dipole interactions among the particles leads to form chain like structure intern enhancement in apparent viscosity as demonstrated in Fig. 13.1. Once the magnetic field is de-energized the particles loses its dipole moment and again gets disposed in carrier fluid bringing back the viscosity to the original value.

Wide range of metal alloys and ceramic metals have been proposed in order to synthesize MR fluid, the only criteria to fulfill by the magnetic particles is to exhibit low level of coercivity and multi domain magnetic properties. On the other hand, the properties such as particle shape, size, size distribution, density, curvise field and magnetic saturation plays critical role in deciding the characteristics of MR fluid. Not only the magnetizable particle properties plays role in deciding the overall performance, also the carrier fluid, additives for anticorrosion and surfactant properties plays vital role in deciding the re-dispersibility and stability of the synthesized MR fluid.

### ***13.1.1 Constituents of Magneto Rheological Fluid***

The constituent of MR fluid plays critical role in the behavior of fluid under applied magnetic field, hence selection and quantifying the constituent is of great importance. Main constituents of MR fluid are Magnetizable particles or dispersed phase, carrier or base fluid or continuous phase, surfactants and additives.

**Magnetizable particles or dispersed phase.** The magneto rheological fluid also called smart fluid is gaining popularity and researchers are finding various methods and applications to incorporate the MR fluid technology. Under such conditions the magnetic particle present in fluid plays vital role and preferred, the materials high magnetic saturation and low coercivity, which enables the fluid to return to its demagnetized state soon after magnetic field is deactivated in terms of milliseconds.

Highly pure carbonyl iron powder could be preferable magnetic particle selection for most of the particle applications because of its high magnetic saturation and low coercivity. Iron particles synthesized by decomposing iron pentacarbonyl ( $\text{Fe}(\text{CO})_5$ ) (Japka 1988) using CVD method is considered to be opposite of the synthesis via electrolytic or spray atomization process. Since carbonyl iron powder is considered as chemically unadulterated with spherical particle distribution, which is considered as mesoscalar nature, shape anisotropy can be eliminate. The mesoscalar nature ensures multi magnetic domains. Chemical purity level, which is usually greater than 99.7% results lower domain pinning defect. Also, spherical shape of particle helps in reducing magnetic shape anisotropy. Impurities presence in magnetic particle causes magnetic hardness, as a result of confrontation of dislocation motion, resulting in harder magnetic particles. In MR fluid-based applications nonabrasive fluid is preferred. Hence the particle with spherical shape with higher level of purity iron powder is preferred as dispersed media in the continues media for the synthesis of MR fluid.

Attempts have been made to synthesize ferrimagnetic materials like nickel-zinc ferrite and manganese-zinc ferrite with 3  $\mu\text{m}$  particle size. Magnetic saturation for the ceramic ferrites is comparatively lower i.e. 0.4–0.6 T (Fang et al. 2009) hence yield stress value for the fluid drops down. Phule reported that a magnetic flux of 15 kPa results in yield stress of 15 kPa. Hence, carbonyl iron powder is selected as it offers magnetic softness and higher magnetic saturation of 2.1 T at room temperature.

**Dispersed phase, Carrier or Base Fluid or Continuous Phase.** Dispersed phase being the major constituent of the MR fluid is also termed as carrier, base fluid or continuous phase. The properties of the base fluid are prominent under off state condition though the viscosity and appearance are affected by magnetizable particle in MR fluid.

The basic function of carrier fluid is to furnish a nonmagnetic and lower permeability base fluid where in magnetically active particles are dispersed, also the fluid should possess lower permeability to facilitate particle polarization with maximum effectiveness. Thus, magneto rheological effect enhancement. Some of the commonly employed carrier fluids are silicon oils, paraffin oils, mineral oils etc. Silicon oil being the popular carrier fluid followed by hydrocarbon oil. Silicon oil with viscosity of 100 cSt is employed in order to maintain lower “off State” viscosity for the MR fluid synthesis.

The carrier fluid is nonmagnetic fluid in which magnetizable metal particles of micron size are suspended. The carrier fluid possesses inherent damping and lubrication properties. In order to have effective implementation of MR fluid technology, the viscosity of the carrier oil should be as low as possible and should be independent of temperature. The lower viscosity ensures better MR effect i.e. viscosity variation as a function of applied magnetic field dominates the normal viscosity variation (Kolekar 2014a). Presence of dispersed magnetic particles in carrier fluid increases the viscosity of the base oil. Commercially mineral oil, silicon oil and hydrocarbon oil are used as carrier fluid in most of the applications.



**Table 13.1** Properties of carrier oils

Properties	Synthetic oil	Mineral oil	Silicone oil
Viscosity @40 °C	0.1068	0.028	0.1100
Flash point	230	171–185	>300
Fire point	350	260–330	500
Density @25 °C (kg/m <sup>3</sup> )	873–894	825	760
Specific gravity	0.817	0.818–0.95	0.9124
Pour point (°C)	–30 to –50	–25 to 50	50
Cloud point (°C)	–20	–15	–20

In order to enhance MR effect viscosity of synthesized fluid should not be a factor of temperature and also as low as possible, carrier fluid being the major constituent of MR fluid i.e. from 50 to 80% by volume. The generally used carrier fluid are synthetic and mineral oil. In case of mineral oil rate of viscosity change as a function of temperature is high, thus limiting the use of mineral oil as base fluid in low temperature MR applications. The inherent properties of synthetic oils such as high flash point, non-thickening of oil at elevated temperatures, high shear strength, high viscosity index and low friction value (Jinaga et al. 2019). Good temperature stability, oxidation resistant, heat transfer, high flash point and low vapor pressure are the important properties of silicon oil which makes it a best choice for carrier fluid. On other hand difficulty to seal the oil is one of the disadvantages of silicon oil. The change in physical properties of silicon oil over temperature range of –40 to 290 °C is negligible which is evident from flat viscosity versus temperature slope. Various properties of commonly used carrier oils are evaluated in Table 13.1.

Carrier fluid being the major constituent of MR fluid i.e. from 50 to 80% by volume, which contributes to a great extent in defining the rheological properties of MR fluid. The basic function of carrier fluid is to furnish a nonmagnetic and lower permeability medium where in magnetically active particles are dispersed under nonmagnetic condition. The selection of base fluid in MR fluid may vary according to application, working condition and accuracy of the application. In literature, various base fluid has been experimented for the synthesis of MR fluids. silicon oil (López-López et al. 2009), naphtha thickened kerosene and polyvinyl butyl (Guo et al. 2013), light and white grade mineral oil (Chiriac et al. 2009), combination of water, synthetic oil, and organic liquids (Kuzhir et al. 2010) etc. commercially MR fluid which uses silicon oil, hydro carbon oil as base fluid are also available but non economical for a local application.

While selecting carrier oils. The following points to be noted

- (1) Lower viscosity
- (2) Lower density
- (3) Lower freezing point
- (4) Easily available
- (5) Lower cost

- (6) High flash point
- (7) High fire point
- (8) Good thermal stability

**Surfactants and Additives.** The third important constituent of MR fluid being additive and surfactant. The dipole-dipole formation in dispersed magnetic particles is not influenced by addition of surfactant and additives. Hence the use of additives to enhance the magnetic properties of particles dispersed in the fluid. The properties such as

- Reducing the coagulation tendency of particles.
- Reducing the sedimentation of particles over period.
- To enhance re-dispersibility of particles by providing coating.
- To enhance anti oxidation property.

In order to control pH value of water-based MR fluids, liquid additive is used. The generally used Surfactants for the preparation of MR fluid are as follows.

1. White lithium-based grease
2. Soy lecithin
3. Citric acid
4. Tetra methyl ammonium hydroxide
5. Oleic acid

Additives acting as critical composition of MR fluid are used to serve many purposes like reducing the sedimentation of particles over period, reducing the coagulation tendency of particles, enhance anti oxidation property and enhancing the re-dispersibility of particles by providing coating. Sedimentation of magnetisable particles being critical aspect as the MR effect is directly proportional to active floating magnetic particles. The desirable value for sedimentation ratio is zero which is practically impossible hence attempts are made to maintain the sedimentation rate to the possible lowest value.

The high viscous material such as thixo-tropic, grease or other additives is employed to enhance the sedimentation stability. Also, Ferrous oleate or ferrous naphthanate can be employed as a dispersant and the metal soap like sodium stearate or lithium stearate as thixo-tropic additive. The dispersed magnetic particles coated with material such as gaur gum, polystyrene, etc. to ensure non coagulation of CI particles, resulting in no lump formation and finally improved particle density i.e. enhanced sedimentation stability (Viota et al. 2005).

Reduction in sedimentation rate of magnetic particles being critical aspect in quality of synthesized MR fluid. Over the time of application sedimentation rate largely influences characteristics of MR fluid as density of magnetizable particle is higher than that of carrier fluid (Bednarek 2003). Some of the additives supplementing MR fluid to bring down sedimentation rate are surfactants such as silica gel, xanthan gum, carboxylic acids and stearates also thixo-tropic agents. The thixo-tropic network interrupts ultra-low shear rate flow, leading to high viscosity. On the other hand, fluid thins as shear rate value is increased.

The stearates develop a network of inflated strands when deployed in combination of synthetic ester and mineral oil which restricts the motion of particles by entrapping it. Carbon fibers has also been experimented in this regards, presence of these fibers enhances the viscosity value via physical enlargement, also because of shear induced alignment the fluid exhibits shear thinning (Rodríguez-arco et al. 1984; Kim and Choi 2011). In these ways presence of appropriate additive contributes towards suspension of magnetic particles in carrier fluid. By addition of additives and surfactants synthesized MR fluid undergoes minimal properties degradation over the time. Concluding the literature study, considering the application, mode of operation and operating conditions MR fluid should be specially designed. As every application has its own shear rate, yield stress, temperature stability and acceptable sedimentation rate.

### 13.1.2 Operational Mode for Magnetorheological Fluid

The application range of Magneto-rheological fluid being wide engineering applications, the working principle or modes of operations of MR fluid is categorized into three classes (Fang et al. 2009), as shown in Fig. 13.2 “flow mode” is represented where the flow of the fluid is along the constrained surface also normal to that of externally applied magnetic field as demonstrated in Fig. 13.2(i). whereas the “shear mode” is categorized with one of the surface moving with a velocity in one direction along the flow with other surface fixed and the flow is normal to applied magnetic field as demonstrated in Fig. 13.2(ii). Kim et al. (Kim et al. 2012) also the “squeeze mode” quite same as shear mode with a difference of the surface moving with velocity is along the normal to other surface and also parallel to externally applied magnetic field as demonstrated in Fig. 13.2(iii).

The Magneto-Rheological fluid offers solution wide range of engineering application. The development of MR fluid technology is evident in numerous specializations, extending from structural building and automotive to biomedical designing applications. Innumerable Experimental has been reported which distinguish the

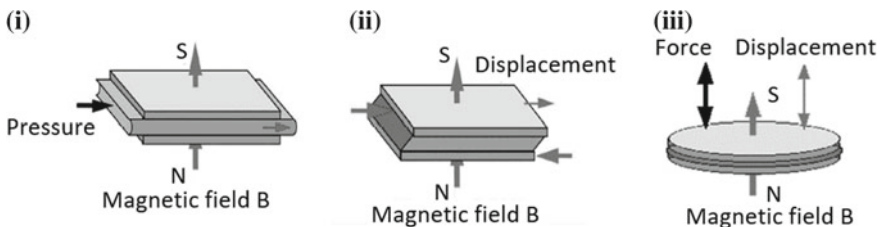


Fig. 13.2 Modes of operation; (i) flow mode, (ii) shear mode, (iii) squeeze mode

advantages or utilizing MR gadgets in different fields (Mazlan et al. 2008). This all-around reported achievement of MR fluids keeps on persuading present and future uses of MR fluid.

Significant achievement of MR fluid gadgets is generally because of progressions in fluid innovation. The present MR fluids are fit for accomplishing yield stresses more than 80 kPa which implies the great scope of fluid dynamic range and controllability. The fluids have additionally showcased enhanced particle stability characteristic. Besides, the strength and life of the fluid have grown with the end goal of commercialization of MR fluid in local market (Guo et al. 2013). Execution of present MR fluid is the result of extraordinary experimentation and study of MR fluid which helps in characterization. There are many numbers of studies and experimentations with works identified with the conduct of MR fluid or the execution of particular MR fluid gadgets (Kuzhir et al. 2010). In various study the information of the execution of the MR gadget goes before an exhaustive comprehension of the conduct, of the fluid functioning in the gadget.

The MR gadgets scheduled for one specific application frequently discovers use in a different MR application where in which the working states of fluid contrast enormously compared to primary designed application. Similar case of this kind “acquired” innovation of numerous uses of Lord Corporation developed Motion Master™ damper. The design of damper, initially proposed for transports specially deployed in trucks, has found its way in prosthetic appendages and structural designing applications (Susan-Resiga et al. 2010). In these various applications, the operational mode of fluid changes considerably. Maybe more outrageous case where in utilization of MR car dampers, designed for automobile essential damping in shocks or impact loading application.

## 13.2 Need for Magneto Rheological Fluid

The modern engineering challenges can be made easy by employing MR fluid technology. The accomplishments of MR technology in various field, ranging from biomedical engineering to structural and automotive engineering challenges (Olabi and Grunwald 2007). The investigations and efforts are count-less identifying the benefits and showing futuristic advantages of employing the technology. Hence the research and experiments are well driven by the amazing effect and results of past finding over implementation of MR technology.

Substantial Achievement of devices working on MR fluid technology is essentially due to development of MR fluid synthesis technology. Present day MR fluid can attain yield stress more than 90 kPa, implying inspiring dynamic range and fluid controllability. Along with impressive yield stress behavior the fluid demonstrates high particle stability. Considering life and durability of the developed fluid that the fluid can be employed commercially (Bica et al. 2013). The high-quality fluid synthesis technology is motivating researchers to develop MR devices in order to resolve given engineering problem. Vast number of studies have been carried out to

identify characteristics of MR fluid also ways to enhance to performance of fluid. In literature we encounter many research works relating to behavior of a specific MR device under magnetic conditions or characterization of MR fluid. In case many MR devices through understanding of MR fluid constituents and its behavior under off and on state of magnetic field is essential (Bica 2007).

Solid matrices in this field also is considered as advantage as the sedimentation of particles reduces to almost zero (Yang et al. 2010; Yu et al. 2015). Also, bounding of MR fluid is not necessary as its leakproof (Liu et al. 2015; Ge et al. 2013). The material of Primary MR based elastomer is viscoelastic and non-magnetic, in which the magnetic particles are distributed uniformly and is processed to a rubber product via curing process (Qin and Brosseau 2012). Out of MR elastomers the soft magnetic particle based elastomers are widely used for its high permeability, low coercivity, high magnetic saturation and low magnetic remanence (Tian et al. 2011; Zhu et al. 2018; Qi et al. 2018).

Hence the higher permeability and magnetic saturation leads to stronger inter interactions, finally leading to stronger aggregations and chain structures (Tian et al. 2011; López-López et al. 2008). Interaction rate between the particles largely on particles shape and size. Also, the particle interaction because of enhanced field intensity can result in larger particle aggregates. Natural rubber being common material matrix for MR elastomers (Yu et al. 2015; Hajalilou et al. 2016; Wu et al. 2017). Polyisobutylene rubber (Kim and Choi 2011), polyurethane (PU) (Yu et al. 2015; Gong et al. 2013), and silicon rubber (Puente-Córdova et al. 2018).

The devices employing MR fluid designed for specific application usually satisfies the necessary conditions to fit in alternative application where in working condition are varied completely from primary application.

## 13.3 Mathematical Modelling

### 13.3.1 Magnetic Properties of Suspended Particles

In addition to magnetic behavior of isolated magnetic particles, static magnetic property of the MR fluid characterized by M-H and B-H hysteresis finds its importance. Hypothetical model for fluid and device working on MR fluid requires magnetization as input value (Park et al. 2001). The magnetic properties will aid in forecasting MR response on application of external magnetic field by current supplied to device. The induction value of MR fluid subjected to various field is quantified by different methods, such as Alternating Gradient Magnetometer, Vibrating Sample Magnetometer and other induction measuring techniques.

At a given lower magnetic field value, the dipole moment developed magnetically in particles suspended in MR fluid is given by (Japka 1988)

$$m = 4\pi\mu_0R^3\beta H \quad (13.1)$$

$$\beta = \frac{\mu_p - \mu_f}{\mu_p + 2\mu_f} \quad (13.2)$$

where  $R$ , is magnetic particle radius and  $\mu_f$  and  $\mu_p$  are the relative permeability of the fluid and the particle, respectively (Burda et al. 2005).

At higher field values where magnetization of the particle reaches its saturation value, the magnitude value for moment becomes independent of applied field value and is given by

$$m = \frac{4}{3}\pi\mu_0R^3M_s \quad (13.3)$$

where  $\mu_0M_s$  is magnetic saturation.

The magnetic saturation of fluid,  $\mu_0M_f$  is connected to the magnetic saturation of bulk magnetic solid,  $\mu_0M_s$ , through volume fraction  $\Phi$  of the solid present

$$\mu_0M_f = \Phi\mu_0M_s \quad (13.4)$$

Ginder and Phulé reported two kind of fluid demonstrating static magnetic properties employing personalized hysteresis graph. The fluid with 36 percent volume fraction of Fe particles,  $\mu_0M_f$  was recorded 0.75 T and for 35 vol% fraction it read approximately 0.14 T. Bulk magnetic saturation for ferrite it is 0.4 T and for Fe is 2.1 T.

### 13.3.2 Viscous Incompressible Flow with Pressure Gradient

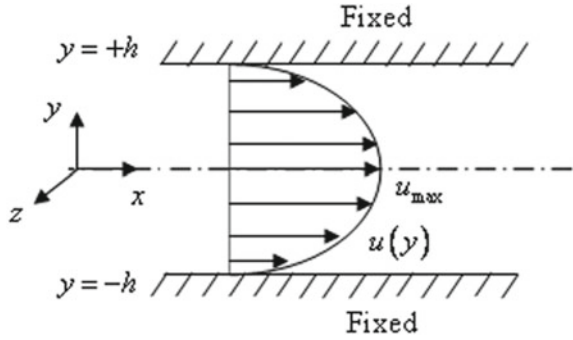
Before discussing the mathematical modelling of the Magneto Rheological fluids lets understand the flow behaviour of a Newtonian fluid long pair of parallel plate through pressure gradient (Cho et al. 2004). The parallel plate flow can be closely correlated to flow as fluid flow in a damping application as fluid flows through the perforations of the piston. The flow between parallel plates with pressure gradient is also called as Poiseuille Flow.

Consider an incompressible, laminar viscous two-dimensional flow along the two parallel plates separated by a distance of  $2h$  as shown in Fig. 13.3 where, plates are fixed however the pressure fluctuates along x-axis. It is accepted that the plates are too wide and long so the flow is basically axial i.e. ( $u \neq 0, v = w = 0$ ). Utilizing continuity equation, it prompts a similar end that  $u = u(y)$ . Additionally,  $v = w = 0$  and gravity is dismissed, the momentum equations in the axis is deduced as;

We have Navier Stroke equation as

$$\rho \left\{ \frac{\partial u}{\partial t} + u \frac{\partial u}{\partial x} + v \frac{\partial u}{\partial y} + w \frac{\partial u}{\partial z} \right\} = \rho g_x - \frac{\partial p}{\partial x} + \mu \left\{ \frac{\partial^2 u}{\partial x^2} + \frac{\partial^2 u}{\partial y^2} + \frac{\partial^2 u}{\partial z^2} \right\} \quad (13.5)$$

**Fig. 13.3** Viscous incompressible flow along parallel plates



We have,

Y Momentum  $\frac{\partial p}{\partial y} = 0$ , z momentum  $\frac{\partial p}{\partial z} = 0$ ;  $p = p(x)$ .

$$\text{X-momentum } \mu \frac{\partial^2 u}{\partial y^2} = \frac{\partial p}{\partial x} = \frac{dp}{dx} \tag{13.6}$$

In the x momentum equation, it might be noticed that the left-hand side contains the variation with  $u_y$  whereas the right-hand side demonstrates the variation with  $p_x$ . It must prompt a same constant else they would not be independent to each other. Since flow needs to conquer the wall shear stress and pressure must decrease toward flow direction, the constant must be negative value. This kind of pressure driven flow is called as Poiseuille flow which is especially basic in the water driven frameworks, brakes in automotive and so on. The last type of equation got for a pressure gradient flow along two fixed parallel plates is given by.

$$\mu \frac{\partial^2 u}{\partial y^2} = \frac{dp}{dx} = \text{Constant} < 0 \tag{13.7}$$

By double integrating Eq. 13.7 the solution can be obtained as

$$u = \frac{1}{\mu} \left( \frac{dp}{dx} \right) \left( \frac{y^2}{2} \right) + c_1 y + c_2 \tag{13.8}$$

The constants are determined by no-slip condition

$$\text{At } y = +h; \quad u = 0 \Rightarrow c_1 = 0 \quad \text{and} \quad c_2 = -\frac{dp}{dx} \left( \frac{h^2}{2\mu} \right) \tag{13.9}$$

The general solution is obtained by substituting and solving as

$$u = \frac{1}{\mu} - \left( \frac{dp}{dx} \right) \left( \frac{h^2}{2\mu} \right) \left( 1 - \frac{y^2}{h^2} \right) \tag{13.10}$$

The flow demonstrated by the equation follows Poiseuille parabola at constant curvature also maximum velocity  $u_{\max}$  along centerline  $y = 0$

$$u_{\max} = \frac{1}{\mu} - \left(\frac{dp}{dx}\right) \left(\frac{h^2}{2\mu}\right) \quad (13.11)$$

Volume flow rate  $q$  flowing between the parallel plates per unit depth is given by

$$q = \int_{-h}^h \left(\frac{1}{2\mu}\right) \left(\frac{dp}{dx}\right) (h^2 - y^2) dy = \frac{2h^3}{3\mu} \left(\frac{dp}{dx}\right) \quad (13.12)$$

The pressure-drop between two point  $\Delta p$  at a distance  $l$  along  $x$  direction, then

$$q = \frac{2h^3}{3\mu} \left(\frac{\Delta p}{l}\right) \quad (13.13)$$

Average velocity is expressed as

$$u_{avg} = \frac{q}{2h} = \frac{h^2}{3\mu} \left(\frac{\Delta p}{l}\right) = \frac{3}{2} u_{\max} \quad (13.14)$$

The shear stress obtained from Newtonian fluid is given by

$$\begin{aligned} \tau_w &= \mu \left( \frac{\partial u}{\partial y} + \frac{\partial v}{\partial x} \right)_{y=\pm h} = \mu \frac{\partial}{\partial y} \left[ \left( -\frac{dp}{dx} \right) \left( \frac{h^2}{2\mu} \right) \left( 1 - \frac{y^2}{h^2} \right) \right]_{y=\pm h} \\ \tau_w &= \pm \left( \frac{dp}{dx} \right) h = \pm \frac{2\mu u_{\max}}{h} \end{aligned} \quad (13.15)$$

The above equation represents shear stress for parallel plate pressure influenced Newtonian fluid flow. Now let us try modeling and analysis of MR fluids.

### 13.3.3 Magneto Rheological Fluid Models

Magneto Rheological (MR) fluid modeling plays a very critical role in synthesis of MR fluid and the applications working on these fluids, as many properties and factors are responsible for the behaviour. Under so many variables governing the behaviour of the fluid it becomes very important to model and analyse a mathematical model which can simulate and predict the performance of the magneto rheological fluid (Chin et al. 2001).

The following study deals with two model for operation of the MR fluid, the first model describes visco-plastic behavior using two mathematical model, also



using Navier-Stokes equations a quasi-steady state model for MR fluids through fixed parallel plate. The development of this equation can be used to validate latter experimental results.

**Visco Plastic Model.** The model which is usually used to elaborate field-dependent characteristic of the MR fluid is Bingham-plastic model. The Bingham model is expressed as

$$\tau = \pm\tau_0 + \mu\gamma \tag{13.16}$$

where  $\tau_0$ —yield stress,  $\gamma$ —shear rate and  $\mu$ —viscosity.

The fluid starts flowing at a point where the yield stress is overcome by shear stress i.e. for  $\tau < \tau_0 \Rightarrow \gamma = 0$ . In Fig. 13.4 displays the Bingham-plastic model, which effectively represents the behavior of magnetic field dependent yield stress.

The other model which can replace the Bingham model with almost same is Herschel Bulkley model which deals with post yield shear thinning characteristic of MR fluid. Herschel Bulkley model is expressed as (Noroozi et al. 2013)

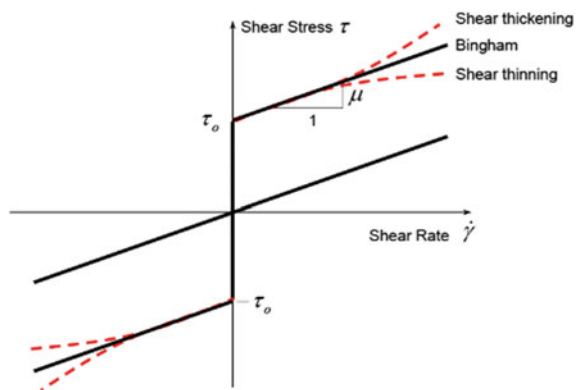
$$T = \pm\tau_0 + K|\dot{\mu}|^{\frac{1}{m}} \tag{13.17}$$

where  $m$  and  $K$  are fluid characteristics.

Shear thinning of the fluid when  $m$  takes the value greater than unity whereas the when  $m$  takes the value less than unity the equation represents shear thickening, also for the value  $m$  equals unity the equation reduces to Bingham-plastic model.

The Bingham and Herschel-Bulkley models have been utilized in number of models used to portray the conduct of particular MR fluid applications. Numerous such models are gotten from the work done by Phillips. A few experimental studies have stretched out Phillip’s work to axisymmetric damper models (Sawalkar et al. 2015; Kuzhir et al. 2003). As a rule, the gap size is very small in contrast with the annulus diameter, the axisymmetric problem is deduced to the parallel plate

**Fig. 13.4** Visco-plastic models often used to describe MR fluids



approximation (Sawalkar et al. 2015). It has been demonstrated that the most of the errors between the parallel plate approximation and axisymmetric model is under 5% (Kuzhir et al. 2003). The effortlessness of the parallel plate model and the small error legitimizes its utilization in 20 most-damper models. Besides, MR fluid parallel flow forms the reason for modeling of MR fluid device working in shear mode or valve mode.

**Quasi-Steady Parallel Flow of MR Fluid.** The essential material science of fluid flow can be explained by the conditions of momentum and mass conservation. The equation of movement for a Newtonian, incompressible i.e. constant density and single-phase fluid can be composed as Eq. 13.5.

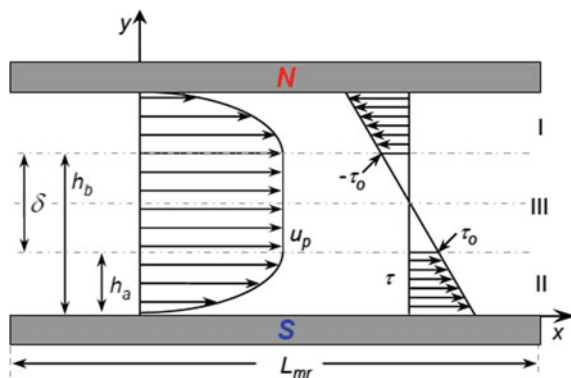
MR fluid comprise of three essential elements, in particular, carrier fluid or base fluid, magnetic particles and additive or stabilizer to improve the dispersion of the magnetic particles in the carrier fluid for better execution of the fluid when exposed to given application. In any case, MR fluids without an applied magnetic field acts like that of a Newtonian fluid, when the fluid is exposed to an applied magnetic field leads to yield stress development and the fluid behaves as a Bingham fluid which can be expressed by the relation (Gabriel and Laun 2009)

$$\tau = \pm\tau_0 + \mu \frac{du}{dy} \tag{13.18}$$

where  $\tau_0$ —the yield stress field dependent,  $\mu$ —the viscosity, and  $du/dy$ —the shear rate.

Figure 13.5 demonstrates quasi steady flow of MR fluid through constrained parallel plates. Note that this flow behaviour is regularly used to describe the fluid course through a MR valve. The flow response shown in Fig. 13.5 can be distinguished into three particular sections. Review that the beginning of flow does not happen until the point when the yield stress has been surpassed. In this manner, the flow with in the channel can be distinguished into three distinct sections. In section I and II, where the shear rate is extensive, the fluid flows much like the Newtonian flow. Whereas

**Fig. 13.5** MR fluid flow through fixed parallel plates



in area III, be that as it may, the fluid is moving as a strong or fitting through the channel. In this area, the yield stress  $\tau_0$ , has not been surpassed and subsequently the fluid isn't being sheared.

With a specific end goal to decide an articulation for the pressure drop caused by the flow characteristic as shown in Fig. 13.5. The technique illustrated starts with the Navier-Stokes equation (Chin et al. 2001). By implementing boundary conditions on both the shear rate and velocity, in terms of the channel geometry the velocity profile is calculated. A moment balance of fluid results in plug geometry and takes into consideration in decrease of the velocity profile. At last, a cubic articulation for the pressure gradient is found from the mean velocity and flow rate. The cubical equation solution is expressed in closed form.

The reduced form can be written as

$$\rho \left( \frac{\partial u}{\partial t} + u \frac{\partial u}{\partial x} \right) = \rho g_x - \frac{\partial p}{\partial x} + \mu \frac{\partial^2 u}{\partial y^2} \quad (13.19)$$

Considering horizontal and developed flow, momentum equation is written as

$$\frac{\partial^2 u}{\partial y^2} = \frac{1}{\mu} \frac{dp}{dx} \quad (13.20)$$

Integration the above equation and applying the boundary conditions

$$\frac{du}{dy}(h_a) = 0 \quad 0 \leq y \leq h_a \quad (13.21)$$

$$\frac{du}{dy} = 0 \quad h_a \leq y \leq h_b \quad (13.22)$$

$$\frac{du}{dy}(h_b) = 0 \quad h_b \leq y \leq h \quad (13.23)$$

Hence, we have equations for shear rate. Also the shear rates for region I and II are expressed using Eqs. 13.21 and 13.23 as

$$\frac{du}{dy} = \frac{1}{\mu} \frac{dp}{dx} (y - h_a) \quad 0 \leq y \leq h_a \quad (13.24)$$

$$\frac{du}{dy} = \frac{1}{\mu} \frac{dp}{dx} (y - h_b) \quad h_b \leq y \leq h \quad (13.25)$$

Whereas the shear rate, velocity in various sections can be determined by integrating again against  $y$  and applying the following boundary conditions

$$u(0) = 0 \quad 0 \leq y \leq h_a \quad (13.26)$$

$$u = u_p \quad h_a \leq y \leq h_b \tag{13.27}$$

$$u(h) = 0 \quad h_b \leq y \leq h \tag{13.28}$$

Using Eqs. 13.26 and 13.28, the velocity profile in the regions I and II are determined in terms of the plug geometry as

$$u = \frac{1}{2\mu} \frac{dp}{dx} y(y - 2h_a) \quad 0 \leq y \leq h_a \tag{13.29}$$

$$u = \frac{1}{2\mu} \frac{dp}{dx} [(y^2 - h^2) - 2h_b(y - h)] \quad h_b \leq y \leq h \tag{13.30}$$

**Plug Geometry.** To determine velocity profile completely the unknowns  $u_p$ ,  $h_a$  and  $h_b$  has to be determined. Using either of the equations i.e. 13.29 or 13.30, the plug velocity can be determined using the conditions  $uI(h_a) = u_p$  or  $uII(h_b) = u_p$ . Assessing the velocity profile in region I at  $y = h_a$ , we have the expression given for the plug velocity as (Walikar et al. 2015)

$$u_p = -\frac{h_a^2}{2\mu} \frac{dp}{dx} \tag{13.31}$$

To obtain the expression for plug thickness  $\delta = h_b - h_a$ , is calculated by applying equilibrium condition on the plug. Considering fluid element as shown in Fig. 13.6. The forces acting on fluid element are the shear forces and the pressure gradient.

Force balance over fluid element shown in Fig. 13.6 hence,

$$\Delta p dy dz = -2\tau_0 dx dz \tag{13.32}$$

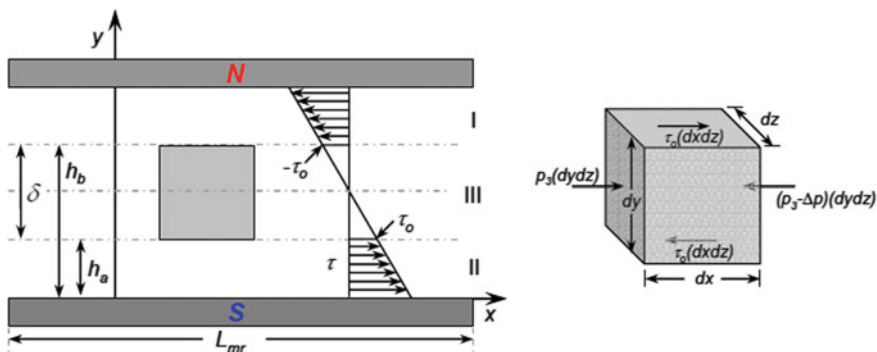


Fig. 13.6 Force balance over fluid element in plug selection

The clockwise rotation of element is due to shear stress is expressed as positive (Bednarek 2003). Also, in terms of the plug section, Eq. 13.32 can be expressed as

$$\frac{dp}{dx} \delta = -2\tau_0 \quad (13.33)$$

The plug thickness is then

$$\frac{dp}{dx} \delta = h_b - h_a = -\frac{2\tau_0}{dp/dx} \quad (13.34)$$

The velocity profile being symmetry we have  $h_b = h - h_a$  and thus from Eq. 13.34 we estimate the values as

$$h_a = \frac{h}{2} + \frac{\tau_0}{dp/dx} \quad (13.35)$$

$$h_b = \frac{h}{2} - \frac{\tau_0}{dp/dx} \quad (13.36)$$

In terms of  $\tau_0$  and  $h$  the velocity profiles can be rewritten as

$$u = \frac{1}{2\mu} \frac{dp}{dx} y(y-h) - \frac{\tau_0}{\mu} y \quad 0 \leq y \leq h_a \quad (13.37)$$

$$u = \frac{1}{2\mu} \frac{dp}{dx} y(y-h) + \frac{\tau_0}{\mu} (y-h) \quad h_b \leq y \leq h \quad (13.38)$$

Similarly, the plug velocity can be written as

$$u_p = -\frac{1}{8\mu} \frac{dp}{dx} h^2 - \frac{\tau_0}{2\mu} \left\{ h + \frac{\tau_0}{dp/dx} \right\} \quad (13.39)$$

By integrating the velocity profile along thickness of channel mean velocity can be written as

$$u_m = \frac{1}{h} \int_0^h u dy = \frac{1}{h} \left[ \int_0^{h_a} u dy + \int_{h_a}^{h_b} u dy + \int_{h_b}^h u dy \right] \quad (13.40)$$

Substituting the expression for  $h_a$  from Eq. 13.33, we have

$$u_m = -\frac{1}{12\mu} \frac{dp}{dx} h^2 - \frac{h\tau_0}{4\mu} + \frac{1}{3\mu h} \frac{\tau_0^3}{(dp/dx)^2} \quad (13.41)$$

Also, it can be seen that for  $\tau_0 = 0$ , Eq. 13.41 deduces the mean velocity for the Newtonian flow. Also, by knowing  $\tau_0$  and  $u_m$ , the above equation can be written in

third order equation for pressure gradient.

$$\left(\frac{dp}{dx}\right)^3 + \left(\frac{12u_m\mu}{h^2} + \frac{3\tau_0}{h}\right)\left(\frac{dp}{dx}\right)^2 - \frac{4\tau_0^3}{h^3} = 0 \quad (13.42)$$

Again for  $\tau_0 = 0$ , Eq. 13.39 follows Newtonian flow

$$\frac{dp}{dx} = -\frac{12u_m\mu}{h^2} \quad (13.43)$$

Also considering opposite sides where flow does not occur because of plug formation of width  $h$ . When  $\delta = h$ , Eq. 13.43 we can be expressed as critical pressure drop

$$\frac{dp}{dx_c} = -\frac{2\tau_0}{h} \quad (13.44)$$

Which is the lowest pressure gradient which can still propagate flow along parallel plates. Hence, in order to have a flow along parallel plates the following condition must be satisfied:

$$\frac{dp}{dx} \geq \frac{dp}{dx_c} \quad (13.45)$$

**Pressure Gradient Solution.** For solving Eq. 13.45 for pressure gradient, we must normalize with respect to Newtonian flow (Omidbeygi and Hashemabadi 2013)

$$\left(\frac{dp/dx}{dp/dx_N}\right)^3 - \left(1 + \frac{3\tau_0 h}{12u_m\mu}\right)\left(\frac{dp/dx}{dp/dx_N}\right)^2 + 4\left(\frac{\tau_0 h}{12u_m\mu}\right)^3 = 0 \quad (13.46)$$

Also, the two non-dimensional parameters (Bednarek 2003)

$$\mathcal{P} = -\frac{dp}{dx} \frac{h^2}{12u_m\mu} \quad (13.47)$$

$$\mathcal{T} = \frac{\tau_0 h}{12u_m\mu} \quad (13.48)$$

Equation 13.43 reduces to the form presented by Phillips (Bednarek 2003).

$$\mathcal{P}^3 - (1 + 3\mathcal{T})\mathcal{P}^2 + 4\mathcal{T}^3 = 0 \quad (13.49)$$

The above equation can be written as

$$\mathcal{P}^3 + a\mathcal{P}^2 + b = 0 \quad (13.50)$$

where  $a = -(1 + 3T)$  and  $b = 4T^3$

Substituting and solving Eq. 13.50 we have

$$m = \frac{1}{3}(1 + 3T)^2 \quad (13.51)$$

$$\theta = \cos^{-1} \left\{ \frac{54T^3}{(1 + 3T)^{5/2}} \right\} \quad (13.52)$$

$$g = -\frac{2}{3}(1 + 3T) \quad (13.53)$$

From the transformation, we find the solution for  $\mathcal{P}$

$$\mathcal{P}(T) = \frac{2}{3}(1 + 3T) \left\{ \cos \left( \frac{1}{3} \cos^{-1} \left( 1 - \frac{54T^3}{(1 + 3T)^{5/2}} \right) \right) + \frac{1}{2} \right\} \quad (13.54)$$

The solution for the non-dimensional pressure gradient,  $\mathcal{P}$  is expressed by Eq. 13.54 in terms of the non-dimensional yield stress,  $T$ . Also, along the solution, an equation for pressure drop in the flow channel can be written in terms of the channel geometry as

$$\Delta P_\tau = \frac{12\mathcal{P}u_m\mu}{h^2} L_{mr} \quad (13.55)$$

Equation 13.55 represents pressure drop developed in the MR fluid flowing along two fixed plate. The pressure drop is responsible for the controllability of the MR fluid flow.

## 13.4 Magneto Rheological Fluid

Magneto rheological fluid being the hope of future technologies in various fields of engineering applications. The fluid which is acting as control system for devices working on MR fluid. As the properties of fluid plays critical role in overall functioning of MR system, the constituents and the mode of synthesis are of great importance. Also, the behavioral study of the synthesized fluid under applied magnetic field enables us to predict behavior of MR fluid-based systems (Hajalilou et al. 2016; Walikar et al. 2015). The sedimentation rate of magnetic particles in fluid being deciding criteria for accuracy, consistency and life of MR fluid, it is important to study sedimentation rate of fluid.

### 13.4.1 Synthesis and Characterization

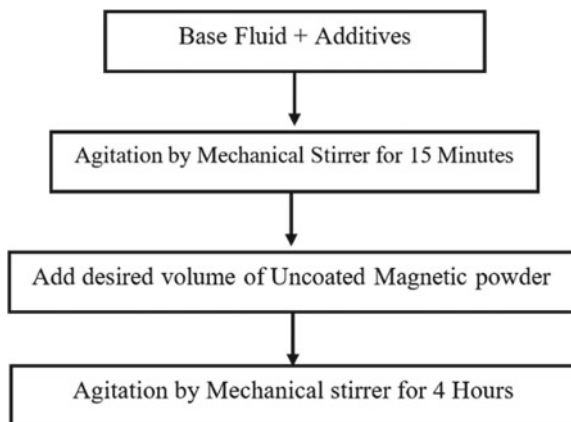
Synthesis of MR fluids is basically a process of mixing the constituent thoroughly using any mechanical agitation process before starting the synthesis process one should know the quantities of all constituents of MR fluid. In order to prepare MR fluid, one should know appropriate amount of additives, which can be combination of antioxidant, anti-wear, antirust, anticorrosion, and friction modifier to help in improving the characteristics of synthesized MR fluid (Kamble and Kolekar (2015), Kamble et al. (2015), Kolekar (2014b), Kolekar et al. (2014) Gong et al. 2013; Puente-Córdova et al. 2018; Park et al. 2001; Burda et al. 2005). To the measured quantity of base oil this additive combination is added and thoroughly mixed for 20 min using stirrer. The magnetic metal particles of known quantity are added to the mixture so as to disperse the particles thoroughly in the fluid. The obtained homogenized mixture is stirred using mechanical stirrer at 1000 rpm for duration of 24 h to obtain homogeneously dispersed MR fluid. Flow chart representing the process incorporated in synthesis is shown in Fig. 13.7.

Characterization plays very critical role in determining the field of application of MR fluid various plots detailing properties of MR fluid could be plotted using magneto rheometer, Parallel plate rheometer standard gap of 1 mm is used separating the parallel plate. The electric coils are incorporated to generate magnetic flux lines which are normal to parallel plates (Zhang et al. 2010). The MR attachment is so designed to generate continuously varying magnetic field, which is applied parallel to sample,

Experimentation is carried out by maintaining constant temperature of 25 °C for each sample, also the shear rate is kept constant for 5 s till measured shear stress value reaches steady state, the rpm is maintained constant so is to obtain consistency in measurement (Zhang et al. 2010).

The following tests can be carried out

**Fig. 13.7** Flow chart for synthesis route





- (1) Shear rate, Shear stress, viscosity and strain using Magneto rheometer
  - (i) Rheological properties under controlled shear rate  
Shear stress versus shear rate, Shear viscosity versus Shear rate, Shear Viscosity versus shear stress, under different magnetic field conditions
  - (ii) Oscillatory Shear Test (Dynamic Test)
    - (a) Amplitude sweep results at different magnetic field
      - (i) Loss modulus versus Strain
      - (ii) Storage Modulus versus Strain
    - (b) Frequency sweep results at different magnetic field
      - (i) Loss modulus versus Strain
      - (ii) Storage Modulus versus Strain
- (2) Yield stress measurement under different magnetic field conditions  
Yield stress versus Magnetic field strength.

### 13.5 Sedimentation Test

Sedimentation is the affinity of the particles in a colloidal solution to come to rest at the bottom after they are scattered in a fluid. This is the result of Brownian movement within the fluid in response to the forces acting over the particles. The cause of forces may gravitational force, magnetic field or centrifugal forces. The rate of sedimentation, in the MR Fluid is measured by ignoring the magnetic force on the MR Fluid particle (Sherje 2016). Also, the characteristic difference in density of carrier fluid and iron particle leads to particle sedimentation, resulting in upper clarified volume designated as supernatant fluid above the mud line (Tan et al. 2010). The mud lines form the boundary in between supernatant fluid and turbid part in colloidal solution so developed. The observations are recorded followed by visual observing the position change in the sedimentation in MR fluid sample.

The setup employed for the observation and data collection is shown in Fig. 13.8. The setup consists of a clear graduated test-tube and a graduated ruler to record the level of supernatant fluid. The level of supernatant fluid increases and the turbid part decreases as time elapses.

Sedimentation levels are recorded after visual inspection during daytime in order to have a clear observation made to record the turbid part and height of supernatant of MR fluid. Synthesized fluid is filled in glass test-tube up to 10 cm and allowed to rest for few hours at vertical position. Using stopwatch and ruler the supernatant fluid height ( $H_s$ ) is measured after a fixed interval of time lapse.

Sedimentation ratio is the ratio of the supernatant fluid height to test height of the MR fluid taken for observation and is expressed as (Fang et al. 2009)

$$S_R = \frac{H_s}{H_T} \times 100\%$$

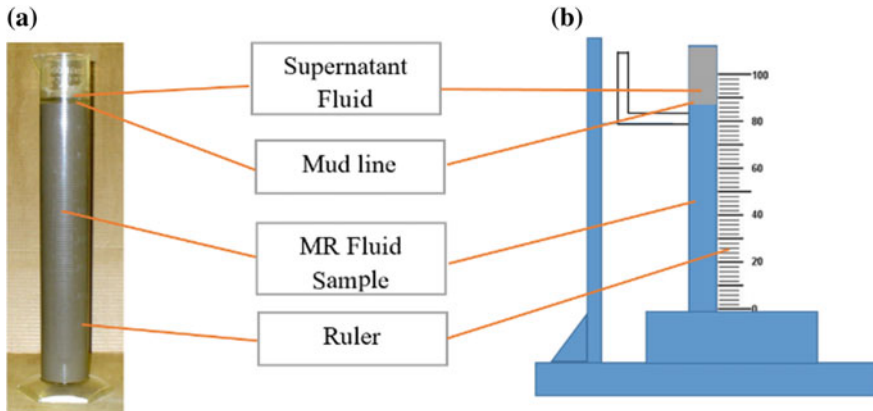


**Fig. 13.8** **a** Measurement of sedimentation and **b** pictorial clarification used for determination of sedimentation-ratio

where,  $S_R$  is the sedimentation ratio,

$H_T$  is total height of fluid taken in test-tube for observation

$H_s$  is the height of supernatant fluid.

## 13.6 Applications of MR Fluid

Potential utilizations of MR fluids are in gadgets which require brisk, reversible change and persistent in rheological properties (Wang and Gordaninejad 2006). Magneto rheological gadgets have picked up an awesome enthusiasm amid the most recent decades, since a magneto rheological fluid puts mechanical gadgets in coordination with an electronic framework, subsequently empowering persistent assurance of mechanical attributes of the device. A portion of these gadgets which use magneto rheological fluids are another age of clutches, brakes and dampers (Fang et al. 2009). Magneto rheological dampers particularly as shock absorber are the most utilized gadgets of this kind. Power steering pumps, control valves, artificial joints, alternators, engine mounts, chemical sensing, sound propagation applications and others are a portion of these precedents. Medication conveyance and tumor treatment strategies in solution are some cutting edge uses of magnetic suspensions.

In a generally thorough examination, Bica et al. Examined the potential utilizations of magneto rheological dampers. They distinguished vital variables influencing the execution of MR fluids in an application (Susan-Resiga et al. 2010; Bica et al. 2013). In another examination, Wang and Meng assessed different attributes and utilizations of magneto rheological fluids. Their study demonstrated that the three primary issues against across the board utilization of MR fluid innovation in numerous advanced gadgets are their non-settling ability, durability and the cost factor (Bin Cheng et al.

2009; Wang and Meng 1948). Having no case to cover every one of the applications, the followings quickly talk about probably the most vital uses of magneto rheological fluids. Kciuk and Turczyn contemplated fundamental properties of MR fluid and their broad applications in different ventures. In another investigation (Kciuk and Turczyn 2009; Kciuk and Turczyn 2006), Olabi and Grunwald contemplated properties of magneto rheological fluids and additionally their applications (Mazlan et al. 2008; Olabi and Grunwald 2007).

As indicated by their overview, promising highlights of MR fluids innovation like quick response, basic interface between electrical power input and mechanical power yield and furthermore exact control capacity, settle on them the following innovation decision for some applications (Iglesias et al. 2012).

MR fluid can be synthesized rendering to a specific engineering application due to large variation of process and design parameters. Major area of application for MR fluid application are MR brakes, MR clutch MR dampers, MR journal bearing, MR surface finishing (Kciuk and Turczyn 2009; Kumbhar et al. 2015).

### 13.6.1 Magneto-Rheological Brake and Clutch System

Two modes of operation are employed in designing of MR fluid brake and clutch system namely flow and shear mode (Park et al. 2009). In the brake system design the core is deployed to rotate and casing is stationary, whereas in clutch system inverse technic is employed. Magnetic field intensity which is intern controlled by input current is the governing factor for torque levels in brake and clutch system (Wang and Meng 1948). Hence, precise controlling of stopping torque and torque transmission is achieved by effective MR fluid devices.

A generalized MR braking and clutch system is shown in Fig. 13.9, the MR breaking and clutch system comprising of housing and core separated by narrow gap for MR fluid, which have relative rotational motion during operation deploying

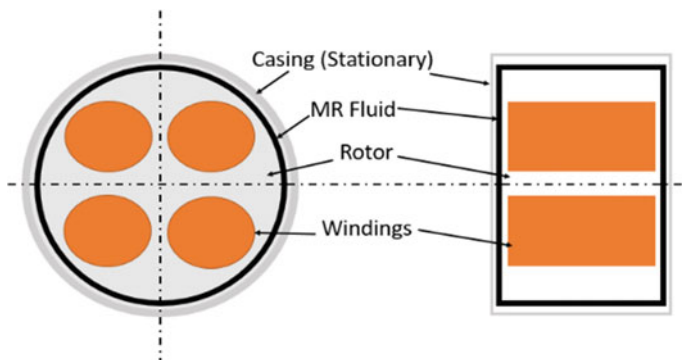


Fig. 13.9 Schematic representation of magneto rheological braking system



**Fig. 13.10** Fabricated prototype MR fluid brake measurement system

flow and shear mode. The disk is designed to have relative rotational motion within MR fluid which is filled up in the narrow slit between stator and rotor (Kciuk and Turczyn 2006). The rotor rotates along the fluid imparting very low resistance to the rotor, as the magnetic field is activated increases the viscosity intern increasing yield stress due to shear resisting rotation and hence braking or clutching phenomenon is achieved (Kumbhar et al. 2015). Literature shows studies that braking effect can be achieved with in 65 ms which make the system a quick and reliable (Ashtiani et al. 2015). The system for investigating the torque developed by MR fluid-based braking system is shown in Fig. 13.10.

In the year 2013, the designs of MR brake and clutches ca be categorized into four types namely multi-plate, multi-disc, multi-pole and multi-gap. The design of these systems being simple fabrication of MR system is easy as it includes only coil and the disc (Bica et al. 2013). In year 2014, modification in the MR brake was proposed by Nguyen, wherein the casing design was changed in order to optimize magnetic field lines. This modified design can be called as initial breakthrough in innovative design of MR fluid devices with respect to casing material and optimization. The designed system resulted same level of torque value as that of conventional, whereas the manufacturing cost was brought down drastically.

In year 2015, new model for MR brake was developed by Nguyen with provision of interchangeable structure of magnetic and electric coils. This was achieved by placing electric coils outside of housing. In the year 2016, combination of MR fluid and permanent magnetic was employed in the design proposed by Yu. The results so obtained showed that performance of system in torque controlling was enhanced, wherein practical application of the system was difficult because of large casing and magnet size. Moreover, maintenance of each component in the assembly was not easy.

In the year 2017, new method for MR clutch system was proposed by Rizzo in which a permanent magnet was deployed in order to control magnetic field lines of the MR clutch system. The position of magnet was varied in order to vary torque magnitude. Under nonmagnetic conditions, the position of magnet was maintained

to not to connect to MR fluid region with the help of spring. Under the influence of applied magnetic field, part of permanent magnet is moved to MR fluid region again via spring. Thus, the rotational motion of connected MR fluid devices can be controlled effectively. The unique One feature of this design is at the same level of applied magnetic field the torque value can be increased resulting in prevention of block up phenomenon where in motion of MR fluid is not occurring (Li et al. 2017). During year 2018, there was no major design configuration for MR clutch and brake systems were proposed. Though, research on bringing down the Magnetic saturation of magnetic materials has been experimented with various combinations.

## 13.7 Classification of MR Fluid Based Braking System

The special characteristics of MR fluid such as high dynamic range, better stability control and low sensitivity towards foreign impure particles makes it best suitable for MR brake and clutch application. Considering the various characteristics of MR fluid various combination of rotary brakes and its geometry is developed, these MR brake systems are classified basically into five types (Avraam et al. 2010). Major variation in these different types of braking systems are the physical properties such as rotor shape and fluid gap between rotor and stator.

Basic types of MR braking systems are:

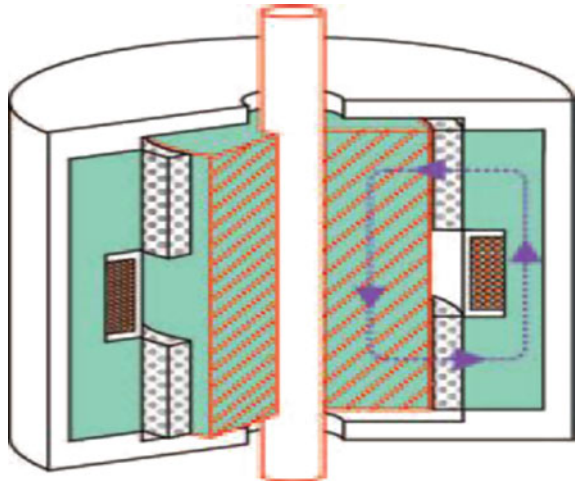
- a. Drum type.
- b. Inverted drum type.
- c. T-shaped type.
- d. Disk type.
- e. Multiple disk type (Avraam et al. 2010).

The classification widely depends on mode of operation and physical appearance of braking system. The characteristics such as weight, design complexity, manufacturing cost, braking torque required, material type, etc. are the factors considered for distinguish MR braking system.

### 13.7.1 Drum Brake

One of the easiest design of a MR braking system could be drum type braking system. Figure 13.11 demonstrates the alignment of this type braking system, the system consists of a cylindrical rotor. In this system the applied magnetic field is in radial direction (Avraam et al. 2010; Imaduddin et al. 2013). Stator of system, which is stationary during the functioning of braking system is in cylindrical shape and usually made of nonmagnetic material. The interior of braking system consist of cylindrical rotor mounted over a shaft, which is intern connected to driving system for brake (Avraam et al. 2010).

**Fig. 13.11** Drum rotor MR braking system



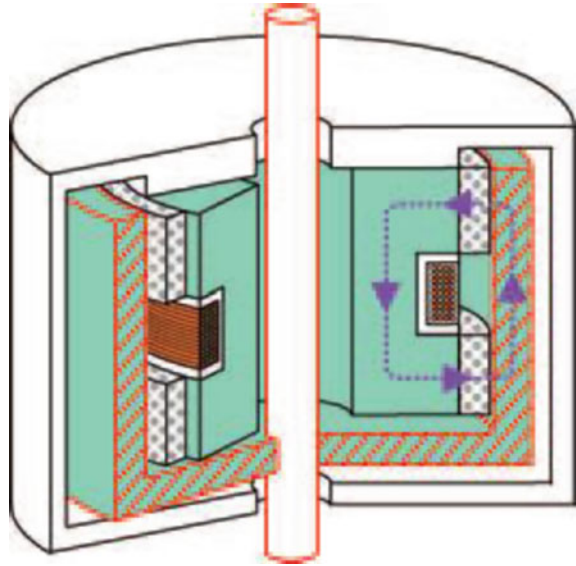
A small gap between the rotor and stator of braking system is maintained which is filled up with MR fluid. As the braking torque is produced by the MR fluid which is the function of current input to system. The positioning of stator and rotor is taken care with the help of housing. The magnetic coil which is responsible for the generation of magnetic field is placed between rotor and housing. Usually the gap between rotor and stator is maintained considerably small (Avraam et al. 2010; Jolly et al. 1999). Hence in order to achieve greater torque value one should maintain gap as small as possible.

### 13.7.2 *Inverted Drum Brake*

Modified version of drum type MR fluid braking system is inverted drum type. Figure 13.12 displays arrangement of various components in the system. The inertia of this system is considerably high because of large rotor size. Apart from minor changes such as arrangement of rotor and design, basic operation of the system remains similar to drum type brake system (Avraam et al. 2010).

The rotor of the system is inverted and is mounted over the shaft at the ends. The rotor is not completely mounted as in drum type braking system. The design of this system being more compact because of hollow arrangements. Magnetic coil is embedded inside the core. The complications related to hollow arrangement, compact design and embedded arrangements adds up to the manufacturing cost and intern overall cost of the system (Avraam et al. 2010).

**Fig. 13.12** Inverted drum rotor MR braking system

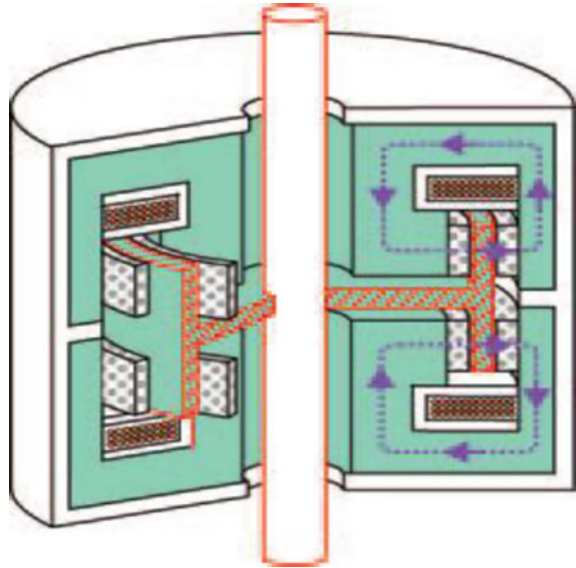


### 13.7.3 T-Shaped Rotor Brake

The improved version of the MR braking system with respect to performance is T Shape rotor braking system, the cross section of rotor of the system is in the shape of T. the actuating system comprises of magnetic coil, core and MR fluid. The gap between rotor and stator is divided into two parts as displayed in Fig. 13.13. The design of this braking system deals with increasing the radial gap by incorporating two smaller magnetic circuit. In this system the shaft is equipped with a locking mechanism in order to connect the rotor, and stator being outside of braking system (Avraam et al. 2010). The two magnetic circuit generates two different magnetic field on both the side of core. To achieve maximum torque value in T shaped braking system rotor is usually made of soft iron, screwed and glued to central portion. The magnetic coil is wounded over plastic support in order to rectify eddy current under operation (Avraam et al. 2010). The coils are covered using soft iron magnetic core, with optimized design to for achieving low weight of braking system and uniform distribution of magnetic field.

Manufacturing of T shaped braking system being compact is quite difficult in manufacturing (Avraam et al. 2010; Güth et al. 2011). The performance of braking system encourages its use over others braking systems, on other hand at some instance the undesired vibrations are developed in the system.

**Fig. 13.13** T-shaped rotor MR braking system



### 13.7.4 Disk Type Brake

Disk type braking system is the widely used MR braking design. The braking system consist of disk as rotor which is mounted over driving shaft. Stator of the system surrounds the rotor assembly as demonstrated in Fig. 13.14. The gap is filled with MR fluid between rotor and stator (Avraam et al. 2010; Jun et al. 2005; Smith et al. 2007). Magnetic flux generated by the magnetic circuit acts perpendicular to the rotor

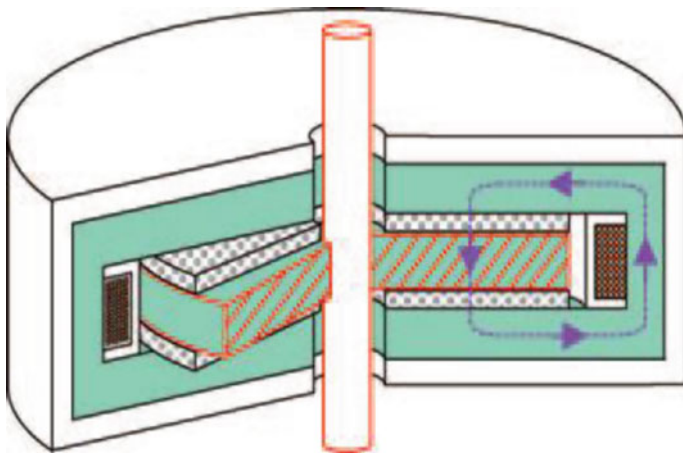


**Fig. 13.14** Disk rotor MR braking system



of the system which is a thick solid disc. Magnetic coil in the system are placed in vertical direction between the rotor and the stator, as demonstrated in Fig. 13.14.

Like that of drum rotor MR braking system, this system needs to enhance the effective area in order to bring up the performance of braking system. The working principle of the disc rotor MR braking system is based on friction under active magnetic field condition (Avraam et al. 2010; Tian et al. 2003). Increasing effective surface area, torque value and stability of system along shear is improved.

### 13.7.5 Multiple Disk Brake

In multiple disk MR braking system is the improved design of disk type rotor braking system multiple disc are assembled one over other to form central core of braking system. The rotor of the braking system can be either single piece with slots for stator or multiple disk combination with MR fluid between disks. This arrangement of the multiple disks is mounted centrally over the shaft with locking arrangement. Stator of the system is placed outside the rotor system maintaining minimal gap as demonstrated in Fig. 13.15, the gap between stator and rotor is filled with MR fluid and the vertical positioning of magnetic coil, similar to that of disk type rotor braking system. (Avraam et al. 2010). The concentric arrangement of rotor disk makes design compact and enhances the structural design.

In this type of braking system, the design has compact structure with restricted space. This system primarily finds its application in automobiles with requirement of high braking torque i.e. greater than 50 N m (Avraam et al. 2010).

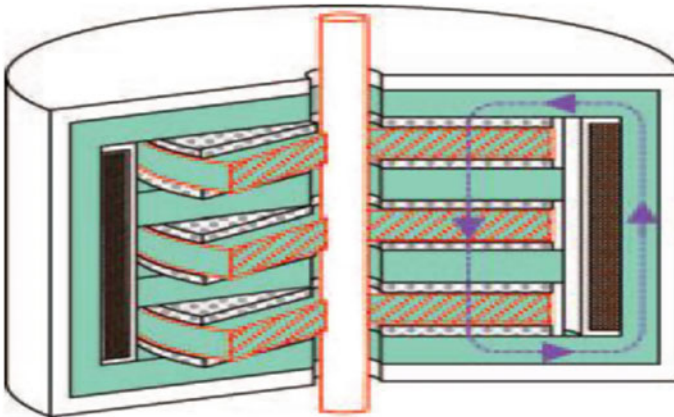


**Fig. 13.15** Disk MR brake

## 13.8 Summary

The implementation of smart systems in the applications of Engineering have revolutionized the development. MR fluid being one of its kind, the development dates back to 1949 by Jacob Rabinow. Since then the development of fluid, characterization, optimization of magnetic parameters, applications and optimizing operational characteristics of MR fluid-based device. This chapter focuses on the development of MR fluid along the timeline also considering its applications, focusing on the performance dependence over particle size/shape, additive and carrier fluid. Also, various additives employed for enhancing rheological characteristics of magnetic field-dependent solid and matrices based MR materials.

Mathematical model has been explained considering various parameters, further the detailed methodology for the synthesis of MR fluid is explained. The characteristics of MR fluid being critical aspects in performance of MR based devices, various tests considered to evaluate fluid has been discussed along with sedimentation test in order to evaluate sedimentation ratio. Sedimentation being one of greatest hurdles for a good MR fluid understanding the phenomenon and its measurement helps in reducing its effect resulting in a stable MR fluid.

MR brake and clutches find wide application in any mechanical system, an attempt is made to explain basic working principle of MR brake and clutch. Also, output measurement of MR based devices in terms of torque in case of brake and clutch is demonstrated by the assembled prototype as shown in Fig. 13.10. At the end of chapter various types of MR brakes employed is demonstrated with exploded view of each braking system.

## References

- Ashtiani M, Hashemabadi SH, Ghaffari A (2015) A review on the magnetorheological fluid preparation and stabilization. *J Magn Magn Mater* 374:711–715
- Avraam M, Horodincă M, Romanescu I, Preumont A (2010) Computer controlled rotational MR-brake for wrist rehabilitation device. *J Intell Mater Syst Struct* 21(15):1543–1557
- Bednarek S (2003) Non-linearity and hysteresis of Hall effect in magnetorheological suspensions with conducting carrier. *J Magn Magn Mater* 264(2–3):251–257
- Bica D et al (2007) Sterically stabilized water based magnetic fluids: synthesis, structure and properties. *J Magn Magn Mater* 311(1):17–21
- Bica I, Liu YD, Choi HJ (2013) Physical characteristics of magnetorheological suspensions and their applications. *J Ind Eng Chem* 19(2):394–406
- Bin Cheng H, Wang JM, Zhang QJ, Wereley NM (2009) Preparation of composite magnetic particles and aqueous magnetorheological fluids. *Smart Mater Struct* 18(8)
- Burda C, Chen X, Narayanan R, El-Sayed MA (2005) Chemistry and properties of nanocrystals of different shapes. *Chem Rev* 105(4)
- Chin BD, Park JH, Kwon MH, Park OO (2001) Rheological properties and dispersion stability of magnetorheological (MR) suspensions. *Rheol Acta* 40(3):211–219
- Chiriac H, Stoian G, Lostun M (2009) Magnetorheological fluids based on amorphous magnetic microparticles. *J Phys Conf Ser* 149:012045

- Cho MS, Lim ST, Jang IB, Choi HJ, Jhon MS (2004) Encapsulation of spherical iron-particle with PMMA and its magnetorheological particles. *IEEE Trans Magn* 40(4 II):3036–3038
- Fang FF, Choi HJ, Jhon MS (2009) Magnetorheology of soft magnetic carbonyl iron suspension with single-walled carbon nanotube additive and its yield stress scaling function. *Colloids Surf A Physicochem Eng Asp* 351(1–3):46–51
- Gabriel C, Laun HM (2009) Combined slit and plate-plate magnetorheometry of a magnetorheological fluid (MRF) and parameterization using the Casson model. *Rheol Acta* 48(7):755–768
- Ge L, Gong X, Fan Y, Xuan S (2013) Preparation and mechanical properties of the magnetorheological elastomer based on natural rubber/rosin glycerin hybrid matrix. *Smart Mater Struct* 22(11)
- Gong Q, Wu J, Gong X, Fan Y, Xia H (2013) Smart polyurethane foam with magnetic field controlled modulus and anisotropic compression property. *RSC Adv* 3(10):3241–3248
- Guo C, Zhou L, Lv J (2013) Effects of expandable graphite and modified ammonium polyphosphate on the flame-retardant and mechanical properties of wood flour-polypropylene composites. *Polym Polym Compos* 21(7):449–456
- Güth D, Cording D, Maas J (2011) MRF based clutch with integrated electrical drive. In: International conference on advanced intelligent mechatronics, AIM, pp 493–498
- Hajjalilou A, Mazlan SA, Shila ST (2016) Magnetic carbonyl iron suspension with Ni-Zn ferrite additive and its magnetorheological properties. *Mater Lett* 181(1–3):196–199
- Hardy EJR (2014) The magnetic fluid clutch. *J Inst Electr Eng* 1952(1):33–34
- Iglesias GR, López-López MT, Durán JDG, González-Caballero F, Delgado AV (2012) Dynamic characterization of extremely bidisperse magnetorheological fluids. *J Colloid Interface Sci* 377(1):153–159
- Imaduddin F, Mazlan SA, Zamzuri H (2013) A design and modelling review of rotary magnetorheological damper. *Mater Des* 51(April):575–591
- Japka JE (1988) Microstructure and properties of carbonyl iron powder. *JOM* 40(8):18–21
- Jinaga R, Thimmaiah J, Kolekar S, Choi S-B (2019) Design, fabrication and testing of a magnetorheologic fluid braking system for machine tool application. *SN Appl Sci* 1(4):1–12
- Jolly MR, Bender JW, Carlson JD (1999) Properties and applications of commercial magnetorheological fluids. *J Intell Mater Syst Struct* 10(1):5–13
- Jun JB, Uhm SY, Ryu JH, Do Suh K (2005) Synthesis and characterization of monodisperse magnetic composite particles for magnetorheological fluid materials. *Colloids Surf A Physicochem Eng Asp* 260(1–3):157–164
- Kamble VG, Kolekar S (2015) Analysis of rheological properties of MR fluid based on variation in concentration of iron particles. *Am J Nanotechnol* 5(2):12–16
- Kamble VG, Kolekar S, Madivalar C (2015) Preparation of magnetorheological fluids using different carriers and detailed study on their properties. *Am J Nanotechnol* 6(1):7–15
- Kciuk M, Turczyn R (2006) Properties and application of magnetorheological fluids. *J Achiev Mater Manuf Eng* 18(1):127–130
- Kciuk M, Turczyn R (2009) Magnetorheological characterisation of carbonyl iron based suspension. *J Achiev Mater Manuf Eng* 33(2):135–141
- Kim JE, Choi HJ (2011) Magnetic carbonyl iron particle dispersed in viscoelastic fluid and its magnetorheological property. *IEEE Trans Magn* 47(10):3173–3176
- Kim MS, Liu YD, Park BJ, You CY, Choi HJ (2012) Carbonyl iron particles dispersed in a polymer solution and their rheological characteristics under applied magnetic field. *J Ind Eng Chem* 18(2):664–667
- Kolekar S (2014a) Vibration analysis of simply supported magneto rheological fluid sandwich beam. *Appl Mech Mater* 612:23–28
- Kolekar S (2014b) Preparation of magnetorheological fluid and study on its rheological properties. *Int J Nanosci* 13(02):1450009
- Kolekar S, Kurahatti RV, Kamble PPKV, Reddy N (2014) Preparation of a silicon oil based magneto rheological fluid and an experimental study of its rheological properties using a plate and cone type rheometer. *J ISSS* 3(2):23–26

- Kumbhar BK, Patil SR, Sawant SM (2015) Synthesis and characterization of magneto-rheological (MR) fluids for MR brake application. *Eng Sci Technol Int J* 18(3):432–438
- Kuzhir P, Bossis G, Bashtovoi V, Volkova O (2003) Flow of magnetorheological fluid through porous media. *Eur J Mech B/Fluids* 22(4):331–343
- Kuzhir P, Lopez-lopez M, Bossis G, Kuzhir P, Lopez-lopez M, Bossis G (2010) Magnetorheology of fiber suspensions. II. Theory to cite this version: HAL Id: hal-00439872, vol 53, no 1
- Li L, Li S, Mu J, Sun H, Wei J, Liu N (2017) Preparation of magnetorheological fluids. *Int J Sci* 4(9):106–109
- Liu J, Wang X, Tang X, Hong R, Wang Y, Feng W (2015) Preparation and characterization of carbonyl iron/strontium hexaferrite magnetorheological fluids. *Particology* 22:134–144
- López-López MT, Zugaldia A, Gómez-Ramírez A, González-Caballero F, Durán JDG (2008) Effect of particle aggregation on the magnetic and magnetorheological properties of magnetic suspensions. *J Rheol (N Y N Y)* 52(4):901
- López-López MT, Kuzhir P, Bossis G (2009) Magnetorheology of fiber suspensions. I. Experimental. *J Rheol (N Y N Y)* 53(1):115–126
- Mazlan SA, Ekreem NB, Olabi AG (2008) An investigation of the behaviour of magnetorheological fluids in compression mode. *J Mater Process Technol* 201(1–3):780–785
- Noroozi S, Tavangar S, Hashemabadi SH (2013) CFD simulation of wall impingement of tear shape viscoplastic drops utilizing openfoam. *Appl Rheol* 23(5)
- Olabi AG, Grunwald A (2007) Design and application of magneto-rheological fluid. *Mater Des* 28(10):2658–2664
- Omidbeygi F, Hashemabadi SH (2013) Exact solution and CFD simulation of magnetorheological fluid purely tangential flow within an eccentric annulus. *Int J Mech Sci* 75:26–33
- Park JH, Chin BD, Park OO (2001) Rheological properties and stabilization of magnetorheological fluids in a water-in-oil emulsion. *J Colloid Interface Sci* 240(1):349–354
- Park BJ, Song KH, Choi HJ (2009) Magnetic carbonyl iron nanoparticle based magnetorheological suspension and its characteristics. *Mater Lett* 63(15):1350–1352
- Puente-Córdova JG, Reyes-Melo ME, Palacios-Pineda LM, Martínez-Perales IA, Martínez-Romero O, Elías-Zúñiga A (2018) Fabrication and characterization of isotropic and anisotropic magnetorheological elastomers, based on silicone rubber and carbonyl iron microparticles. *Polymers (Basel)* 10(12)
- Qi S, Yu M, Fu J, Zhu M, Xie Y, Li W (2018) An EPDM/MVQ polymer blend based magnetorheological elastomer with good thermostability and mechanical performance. *Soft Matter* 14(42):8521–8528
- Qin F, Brosseau C (2012) A review and analysis of microwave absorption in polymer composites filled with carbonaceous particles. *J Appl Phys* 111(6)
- Rabinow J (1951) Magnetic fluid torque and force transmitting device. US Patent Specification 2575360
- Rodríguez-arco L, Gómez-ramírez A, Durán JDG, López-lópez MT (1984) New perspectives for magnetic fluid-based devices using novel ionic liquids as carriers
- Sawalkar VR, More CS, Patil PTB (2015) Preparation and testing of magneto rheological fluid. *Int J Tech Res App* 3(2):237–240
- Sherje NP (2016) Preparation and characterization of magnetorheological fluid for damper in automobile suspension. *Int J Mech Eng Tech* 7(4):75–84
- Smith AL, Ulicny JC, Kennedy LC (2007) Magnetorheological fluid fan drive for trucks. *J Intell Mater Syst Struct* 18(12):1131–1136
- Susan-Resiga D, Bica D, Vékás L (2010) Flow behaviour of extremely bidisperse magnetizable fluids. *J Magn Magn Mater* 322(20):3166–3172
- Tan L, Pu H, Jin M, Chang Z, Wan D, Yin J (2010) Iron nanoparticles encapsulated in poly(AAm-co-MAA) microgels for magnetorheological fluids. *Colloids Surf A Physicochem Eng Asp* 360(1–3):137–141
- Tian Y, Zou Q, Meng Y, Wen S (2003) Tensile behavior of electrorheological fluids under direct current electric fields. *J Appl Phys* 94(10):6939–6944

- Tian TF, Li WH, Alici G, Du H, Deng YM (2011) Microstructure and magnetorheology of graphite-based MR elastomers. *Rheol Acta* 50(9–10):825–836
- Viota JL, De Vicente J, Durán JDG, Delgado AV (2005) Stabilization of magnetorheological suspensions by polyacrylic acid polymers. *J Colloid Interface Sci* 284(2):527–541
- Walikar CA, Kolekar S, Hanumantharaya R, Raju K (2015) A study on vibration characteristics of engine oil based magnetorheological fluid sandwich beam. *J Mech Eng Autom* 5(3B):84–88
- Wang X, Gordaninejad F (2006) Study of magnetorheological fluids at high shear rates. *Rheol Acta* 45(6):899–908
- Wang J, Meng G (1948) Magnetorheological uid devices: principles, characteristics and applications in mechanical engineering. *Current* 215:165–175
- Wu C, Zhang Q, Song Y, Zheng Q (2017) Microrheology of magnetorheological silicone elastomers during curing process under the presence of magnetic field. *AIP Adv* 7(9)
- Yang Z, Peng H, Wang W, Liu T (2010) Crystallization behavior of poly( $\epsilon$ -caprolactone)/layered double hydroxide nanocomposites. *J Appl Polym Sci* 116(5):2658–2667
- Yu M, Qi S, Fu J, Yang PA, Zhu M (2015) Preparation and characterization of a novel magnetorheological elastomer based on polyurethane/epoxy resin IPNs matrix. *Smart Mater Struct* 24(4):1–9
- Zhang X, Li W, Gong X (2010) Thixotropy of MR shear-thickening fluids. *Smart Mater Struct* 19(12):2–8
- Zhu M, Yu M, Qi S, Fu J (2018) Investigations on response time of magnetorheological elastomer under compression mode. *Smart Mater Struct* 27(5)

# Chapter 14

## Shot Peening Effects on Abrasive Wear Behavior of Medium Carbon Steel



Neeraj Kumar and Jayant Singh

**Abstract** Effect of shot peening on high stress abrasive wear behavior of medium carbon steel (AISI 6150 steel) at varying applied load and abrasive size has been studied. The shot peening leads to sub-surface work hardening and surface denting. The extent of work hardening and denting increases with increase in shot peening intensity. The experiments are performed on shot peening machine under two conditions of applied load, abrasive size and shot peening intensity as 7 N, 90  $\mu\text{m}$  and 0.486 mm Almen “A” and 1 N, 30  $\mu\text{m}$  and 0.117 mm Almen “A”, respectively. The wear rate decreases by 20–30% due to shot peening to a level of 0.117 mm Almen “A” from the un-peened state. Further increase in peening intensity does not lead to any significant improvement in wear resistance. The wear rate decreases with increase in sliding distance due to work hardening and degradation of abrasive media.

**Keywords** Shot peening · Wear · Work hardening

### 14.1 Introduction

Medium carbon steels are widely used as agricultural implements especially for soil engaging components. These components are subjected to severe abrasive conditions which resulting in greater extent of wears. As a result, the life of component becomes considerably less (one to two season). This becomes more problematic, as no standard composition or heat treatment or procedures is followed for manufacturing these components. Thus, it is expected, that selection of suitable composition, heat treatment schedule and manufacturing procedure would be very important for considerations in manufacturing of such components. The uses of medium carbon manganese steels include shafts, couplings, crankshafts, axles, gears and forgings. Steels in the range 0.40–0.60% C are also used for rails, railway wheels, and rail axles.

---

N. Kumar · J. Singh (✉)

Mechanical and Automation Engineering Department, Dr. Akhilesh Das Gupta Institute of Technology and Management, New Delhi 110053, India  
e-mail: [singhjayant11@gmail.com](mailto:singhjayant11@gmail.com)

© Springer Nature Singapore Pte Ltd. 2019

J. K. Katiyar et al. (eds.), *Automotive Tribology*, Energy, Environment, and Sustainability, [https://doi.org/10.1007/978-981-15-0434-1\\_14](https://doi.org/10.1007/978-981-15-0434-1_14)

269

Shot peening is another method in which the surface is work hardened with the peening action of shots on the specimen surface. Shot peening does not alter the microstructure significantly. It just create some amount of residual compressive stress on the surface and vis-à-vis surface gets work hardened due to generation of higher dislocation density. The surface characteristics of the shot peened materials primarily depends on the shot peening intensity, which again depends on shot size, type of shots, impact of shots and amount of shots. Because of generation of compressive stress on the surface, the component should have higher fatigue life.

A Shot peening process is a procedure in which spherical shots made of glass or metal is impacted on the surface of a metallic part. As the shot strikes the surface of the metallic portion it results in a slight depression due to the radial stretching and plastic flow of the metal at the surface of the contact. Thereby, shot peening method results in increase in the fatigue strength of the parts. If used judiciously it can give a part with improved performance most economically. Attempts have been made to explore the possibility of shot peening on agricultural components to improve their performance. Buckley, reported that the abrasive wear was related to their relative hardness (Buckley 1971). In general abrasive wear behaviour of materials is proportional to the load applied to the surface in contact, and the sliding distance but inversely proportional to hardness. Raval and Kaushal reported that the abrasive wear of under grinding wheel reduced after hard facing (Raval and Kaushal 1990). They described various wears possible in agriculture machinery. Out of these, abrasive wear as most dominating.

Khrushchov and Babichev found that wear resistance of steels was proportional to hardness (Khrushchov and Babichev 1962). Richardson said that the increase in surface hardness and its effect on microstructure make the material superior abrasion resistant (Richardson 1967). Modi et al., studied the abrasive wear behaviour of high carbon steel (Modi et al. 2003). They observed that wear rate was a strong function of inter lamellar spacing. They also found that wear rate remained practically unchanged by the abrasive size up to 25  $\mu\text{m}$ . Rautaray, in his Ph.D. thesis on “fatigue and wear characterization on shot peened rotavator blade materials” reported that fatigue life of shot peened specimens exhibited much longer lifetime than the unpeened specimens. He also reported an optimum shot peening intensities for the optimum range of fatigue life of specimens (Rautaray 1997). Similarly, the study further reveals that at optimum range of the peening intensity the wear resistance was maximum. Saxena and Sharma (Saxena and Sharma 2001), in their article “Wear of shot peened thresher peg” reported the economical benefits acquired through shot peening over bulk hardening in low carbon steel (EN-8). They reported a higher ratio of relative wear resistance to relative cost ratio (1.77) in bulk harden shot peened compare to bulk harden low carbon steel. Saxena in his Ph.D. thesis on “Metallurgy and process development for thresher peg” investigated the effect of bulk hardening of medium carbon, medium carbon-low alloy steel and high carbon steel for thresher peg (Saxena and Sharma 2001). Foley, reported that the cutting points of the soil working components of agriculture machineries are subjected to both abrasive wear and impact loadings (Foley and McLees 1986).

Friction and wear are not the intrinsic material properties. They are dependent on both the properties of materials and the working conditions. Widely varied wearing conditions cause wear of materials by various mechanisms (Pürçek et al. 2002; Lee et al. 1987). Small changes of load, speed, frictional temperature or along with the microstructures, properties of materials cause significant variations in the wear of contacting surfaces (Blau 2005).

There is in our hands now, the physical ability to produce mechanical pre-stressing of parts by several means, at established cost, and often with the background experience that indicates the benefits to be gained. The one most important drawback is our inability to measure accurately the depth, intensity and distribution of the cold-worked effect (dimples) on the production part without destructive examination.

Shot peening is a cold working method in which the surface of a part is blasted with small spherical media called shot (Champaigne 2001; Meguid et al. 1999). Each piece of shot striking the metallic surface acts as a tiny peening hammer, producing to the surface a small depression or dimple (Diepart 1994; Saritas et al. 1999). The dimples are formed due to yielding of surface fibers in tension. The dimples are hemispherical cold-worked material which are highly stressed in compression, and are formed below the surface. The fibers restore the surface to its original shape as shown in Fig. 14.1. The overlapping depressions try to develop an even layer with residual compressive stresses.

It is well established that cracks initiation and propagation is delayed in a compressive stressed zone (Cary 1981). The fatigue and stress corrosion failures emerge at the surface of a part, compressive stresses induced by shot peening provide significant resistance to fatigue and thus, enhance the life of the parts. On comparing the compressive residual stresses at or under the surface with the material being peened, it is at least greater than half the yield strength (Waisman and Phillips 1952). The surface hardness of the material results into increase of cold working effect due to shot peening (Gao 2011).

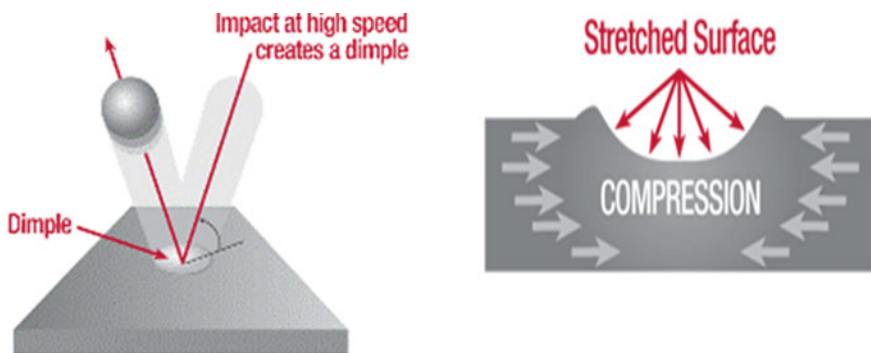


**Fig. 14.1** Impact of shot creating dimple on the surface with the cold worked material highly stressed in compression



The present work is a part of larger work. The work deals with the detailed study of the different shot-peening intensities on the steel samples for varying load, sliding distance and abrasive size. These parameters influence the wear rate and wear resistance of the samples, which have been studied in detail.

## 14.2 Experimental Details

### 14.2.1 Specimen Preparation for Shot Peening

Specimens for shot peening (45 mm × 45 mm × 4.5 mm) were prepared from medium carbon steel plates and polished according to standard metallographic techniques up to 400 μm abrasive size. The chemical composition, physical properties and mechanical properties of the investigated steels is shown in tables below. Both the surfaces are made parallel and polished. Chemical composition of the as received materials used in the present study were evaluated using Sparkmet at RRL, Bhopal. Chemical composition of AISI 6150 steel is Table 14.1.

### 14.2.2 Shot Peening

The samples are shot peened at Central Institute of Agricultural Engineers (CIAE), Bhopal, using the shot peening machine, model: *PB-150120*.

Figure 14.2, clearly indicates the positions of nozzle assembly and the lightening arrangement inside the working chamber. Position of nozzle height from the working surface i.e., standoff height can be changed as shown clearly, by just loosening and tightening of few bolts at the assembly. Figure 14.2b, shows the front panel of the machine, which incorporates all the controls. Window over the two large holes, from where the positions of the samples while shot peening can be controlled, is there to see the condition of the samples during the shot peening operation.

**Table 14.1** Chemical composition of AISI 6150 steel

S. No.	Component	wt% of AISI 6150 steel
1	C	0.53
2	Cr	0.98
3	Mn	0.8
4	P	0.035
5	S	0.04
6	Si	0.23
7	V	0.15
8	Fe	97.235

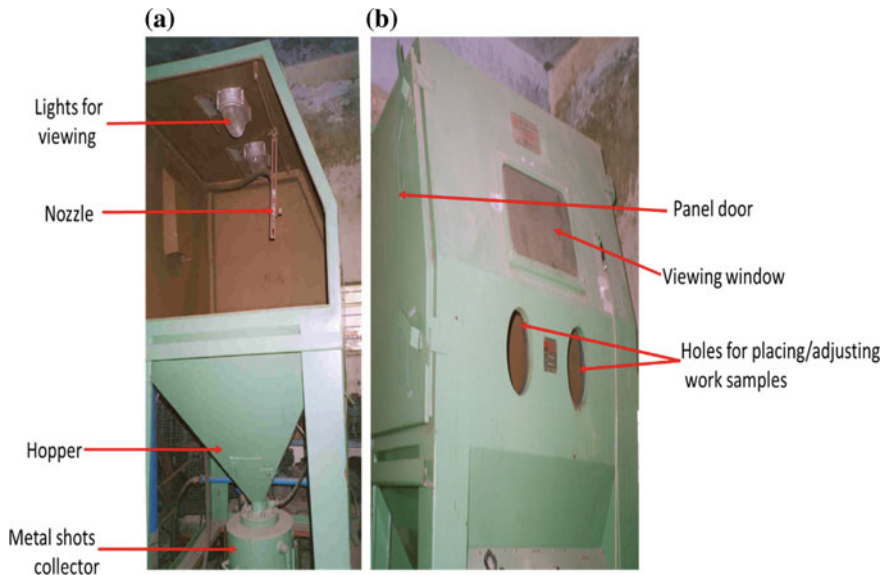


**Fig. 14.2** Photographic view of shot peening machine—**a** side view and **b** front view

**14.2.2.1 Shot Peening Machine Specifications**

The specifications of machine are shown below. The abrasive storage capacity is 42 L. The electrical specifications are 3-phase, 415 V AC, 50 Hz, 2.5 A. The dust collector includes fan motor of 1.5 HP and with the capacity of 22.6 m<sup>3</sup>/min. The dimensions for blast host size and blast nozzle orifice are 19 mm and 6 mm, respectively. The other parameters are mentioned in Tables 14.2, 14.3, 14.4, 14.5 and 14.6.

Shot peening at 6 kg/cm<sup>2</sup> (0.589 MPa), for 10 s gives the shot peening intensity value of 0.117 mm Almen “A” and at 60 s, the shot peening intensity which we get is

**Table 14.2** Overall dimensions

Specifications	Dimensions (mm)
Height (D)	2170
Width (E)	1665
Depth (P)	2730

**Table 14.3** Opening specifications

Specifications	Dimensions (mm)
Width (G)	1100
Height (H <sub>1</sub> )	290
Height (H <sub>2</sub> )	800

**Table 14.4** Working chamber size

Specifications	Dimensions (mm)
Height (A)	900
Width (B)	1500
Depth (C)	1200

**Table 14.5** Shot peening parameters

S. No.	Peening parameter	Critical value
1	Peening pressure (MPa)	0.589
2	Peening nozzle diameter (mm)	6.00
3	Shot size (mm)	0.825
4	Shot hardness (HRC)	45
5	Standoff height (mm)	154.00
6	Average mass flow rate (t/h)	0.400
7	Angle of peening (°)	90
8	Almen strip used	Almen "A"
9	Surface coverage (%)	98–100

**Table 14.6** Peening time and intensity

S. No.	Peening time (s)	Peening intensity (mm ALMEN "A")
1	10	0.117
2	60	0.486

0.486 mm Almen "A". Working pressure for all the experiments is kept at 6 kg/cm<sup>2</sup> (0.589 MPa).

### 14.2.3 Abrasive Wear Test

Anyone while investigating friction and wear of metals is faced with a large number of variables to control. One of the first choices to make is the selection of a suitable wear testing machine. It has become axiomatic that the best wear test is one that closely approximates the actual conditions encountered in service. However, here high stress abrasive wear tests are done using SUGA (NUSI, JAPAN) abrasion testing machine. Schematic view of the machine is shown in Fig. 14.3.

Two body abrasive wear tests were conducted on 45 × 45 × 4.5 mm<sup>3</sup> size specimens using Suga Abrasive Tester (Model: NUSI, Japan). A schematic diagram of the test apparatus is shown in Fig. 14.3. The equipment consisted of a stage with a locking arrangement for holding the specimens in position against a 50 mm diameter,

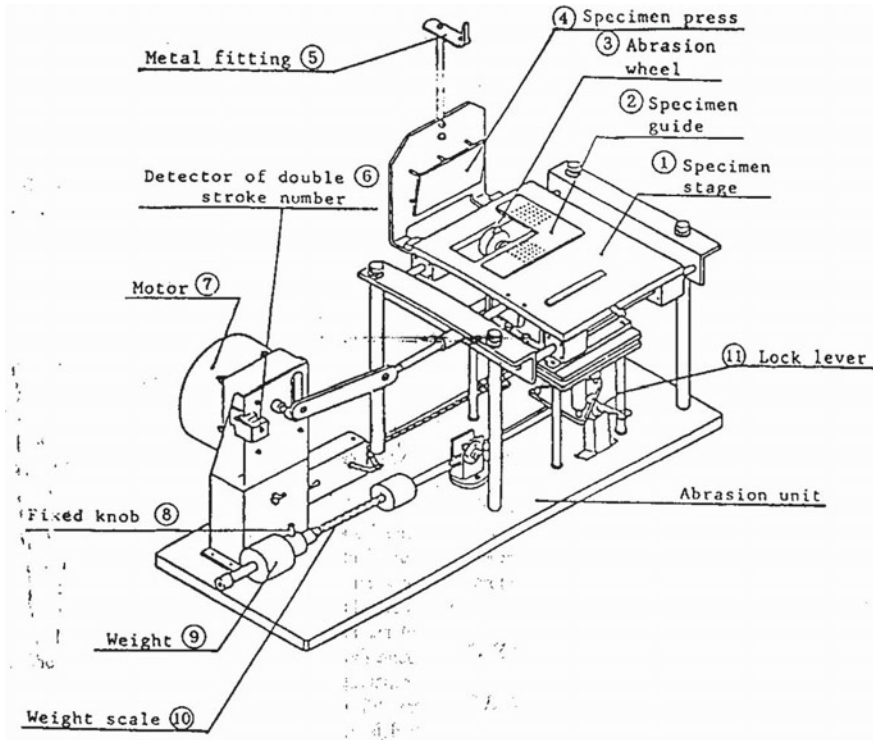


Fig. 14.3 Two body abrasive wear testing machine

12 mm thick metallic disc. Emery paper embedded with silicon carbide particle was cut into sizes and fixed on a wheel with the help of double sided tape to serve as the abrasive medium. The locking arrangement was used to fix the specimen with the abrasive medium. The stage was attached with a motor; the latter imparted to and fro motion to the specimens along with facilities to display the stage. The equipment was attached with facilities to display the number of strokes. It also had an end buzzer to signal the finishing of test. Cantilever mechanism was used to apply load on the specimen. Under the reciprocating motion, the specimen was subjected against abrasive medium. After completion of each stroke, with the corresponding sliding distance of 0.0675 m, the emery paper changes its position which enables the exposure of fresh abrasive to the specimen on each stroke. Weight loss of the specimen was measured after each 400 strokes (each cycle consists of one forward and one backward movement of the sample over the wheel and each revolution of wheel corresponds to 27 m linear distance).

Prior to and after each test, the samples were washed and cleaned with acetone and weighed (up to the accuracy of 0.01 mg using Mettler microbalance). The wear rate was estimated from the weight loss measurement and expressed in the terms of volume loss per unit sliding distance i.e. in  $\text{m}^3/\text{m}$ .

Wear rate ( $W_r$ ) is calculated using the following formula:

$$W_r = (W_i - W_f)/(\rho.D)$$

where,  $W_i$  is the initial weight of specimen before the start of each test,  $W_f$  is the final weight of specimen after the completion of wear test,  $\rho$  is the density of the test specimen material and  $D$  is the sliding distance (i.e., 27 m, 54 m, 81 m and 108 m after 400 strokes, 800 strokes, 1200 strokes and 1600 strokes respectively). For each experiment, values after the 1600 strokes were taken for the calculation and analysis purposes.

#### ***14.2.4 Micro-hardness Measurements***

The subsurface of peened samples were polished, using standard metallographic practices i.e. wheel grinding, polishing in emery papers (110, 210, 310 and 410 grade sizes) and finally cloth polishing was done. The polished samples were etched with Nital reagent.

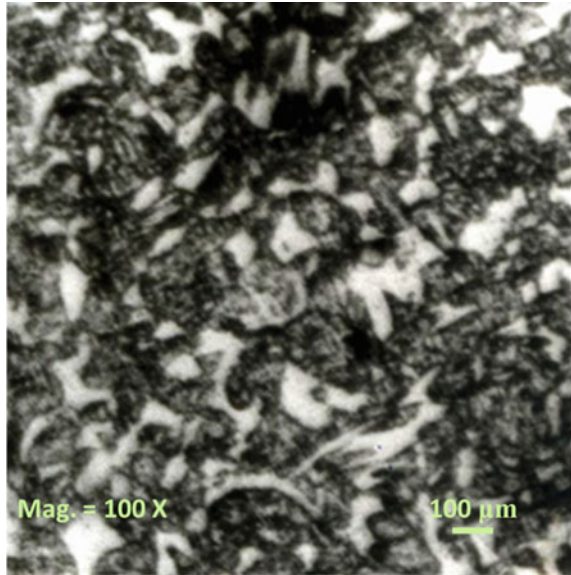
Micro-hardness was measured using Vickers's hardness tester of LEICA make and model VMHT 30A. Load was kept at 25 gf and dwell time kept at 15 s for all measurements. Micro-hardness was taken on the polished surface from peening surface towards the center.

### **14.3 Results and Discussion**

#### ***14.3.1 Materials and Microstructure***

The investigated material is received in the form of plates of 8 mm thickness. It contains around 0.53-wt% carbon. Accordingly it should give ferrite-pearlitic structures, where pearlitic colonies are surrounded by network of ferrite, and the steel is in annealed condition. The volume fraction of ferrite and pearlite would be approximately 30% and 70% respectively. When the steel is in normalized condition, the eutectic point shift towards lower carbon content and thus the steel should exhibit around 80–85% pearlite. The investigated steel exhibits near pearlitic structure confirming that the steel plates received are in normalized condition. The typical microstructure of AISI 6150 steel is shown in Fig. 14.4.

**Fig. 14.4** Microstructure of AISI 6150 steel



### 14.3.2 Microstructure After Shot Peening

Typical microstructures of shot peened samples are shown in Fig. 14.5a, b for AISI 6150 steel for 0.117 mm Almen “A” and 0.486 mm Almen “A” intensities, respectively. These figures clearly indicate formation of dimples on the peened surface

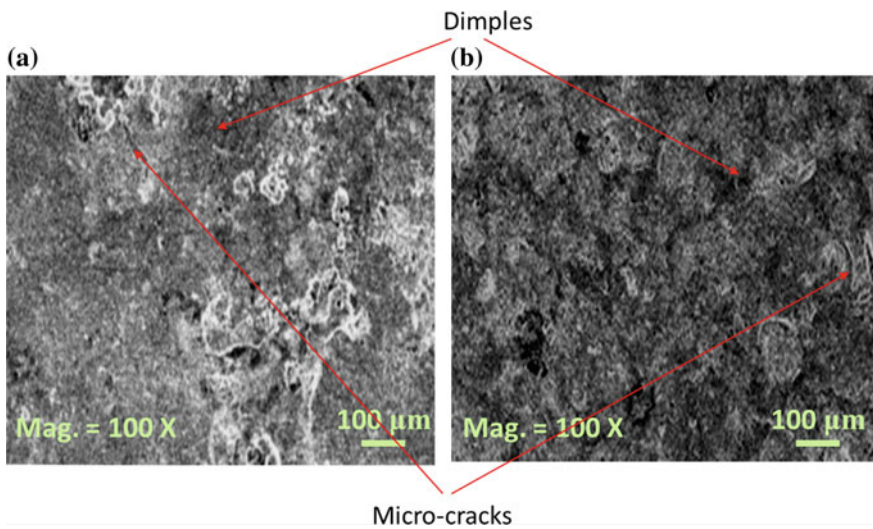


**Fig. 14.5** AISI 6150 steel samples **a** 0.117 mm Almen “A” and **b** 0.486 mm Almen “A”

and the size of dimple increases with increase in peening intensity. It is further evident from these microstructures that dimple density also increases with increase in peening intensity. At higher intensity micro-cracks are also observed.

### 14.3.3 Micro Hardness

The variation of the micro-hardness as a function of distance from peening surface is shown in Fig. 14.6 for AISI 6150 steel. It is evident from the figure that average hardness values decreases with increase in distance from the peened surface and reaching to a constant value representing the bulk micro-hardness of the materials. Higher hardness values in the peened surface indicates work-hardening due to peening and development of compressive stresses on the specimen surface (Maawad et al. 2012).

For AISI 6150 steel at high peening intensity (0.486 mm Almen “A”), micro-hardness at the interface i.e.  $MH_i$  is 250 VHN, bulk value i.e.  $MH_b$  is 150 VHN and at low peening intensity (0.117 mm Almen “A”), micro-hardness at the interface i.e.  $MH_i$  is 200 VHN and bulk value is 150 VHN respectively. So the residual stress for AISI 6150 steel at high peening intensity (0.486 mm Almen “A”) is 140 MPa and at low peening intensity (0.117 mm Almen “A”), the residual stress is 70 MPa. The depth of peening is around 350  $\mu\text{m}$  for high intensity and 300  $\mu\text{m}$  for low intensity (Table 14.7).

The residual stress was calculated using the following relationship (Ray and Mondal 1991):

$$\sigma_r = \{(MH_i - MH_b) \times 10\} / 7.1 \tag{14.1}$$

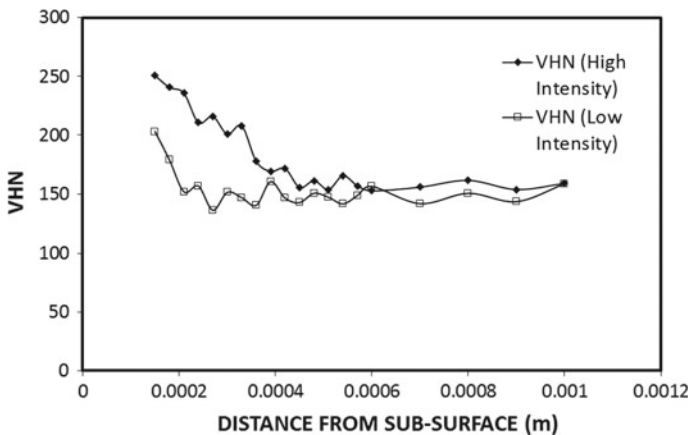


Fig. 14.6 Micro-hardness variation for AISI 6150 steel

**Table 14.7** Residual stresses at different peening intensities

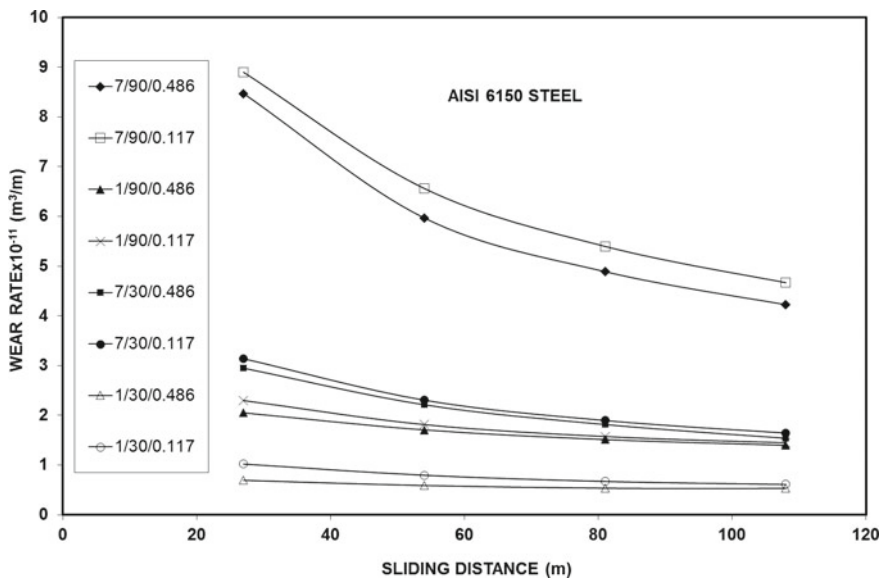
S. No.	Shot peening intensity (mm Almen "A")	Residual stress ( $\sigma_r$ ) for AISI 6150 steel (MPa)
1	0.117	70
2	0.486	140

### 14.3.4 Wear Behaviour

Wear rate of a material is a function of several parameters such as applied load, abrasive size, sliding speed, hardness of the material, temperature and environmental conditions. In present study, high stress abrasive wear behaviour of medium carbon steels has been investigated. In this study the wear rate is considered as the response variable. This response variable has been examined as a function of applied load, abrasive size and shot peening intensity.

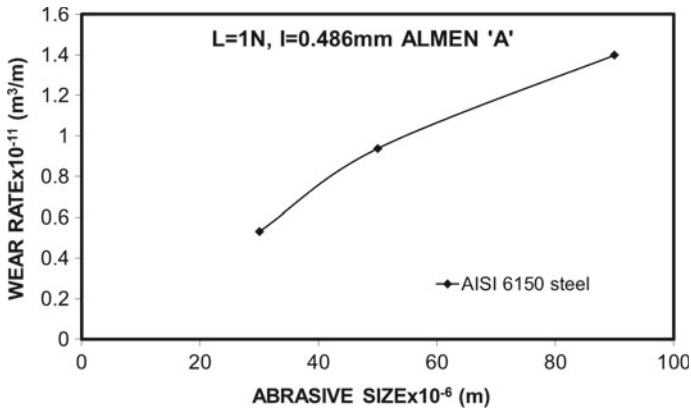
#### 14.3.4.1 Effect of Sliding Distance on Wear Rate

Figure 14.7, represents variation of wear rate with sliding distance under varying applied loads, abrasive sizes and shot peening intensities, for AISI 6150 steel. It is evident from this figure that the wear rate increases with increase in applied load and



**Fig. 14.7** Effect of sliding distance on wear rate for AISI 6150 steel. The legend represents load (N)/abrasive size ( $\mu\text{m}$ )/shot peening intensity (mm Almen "A")





**Fig. 14.8** Effect of abrasive size on wear rate

abrasive size but decreases with increase in shot peening intensity. The wear rate in general decreases with increase in sliding distance and approaching to a stable value. The extent of reduction in wear rate with sliding distance is most prominent at higher applied load and coarser abrasive size.

The decrease in wear rate with sliding distance is attributed to: Modi et al. (2003) Work hardening of the surface, blunting of abrasives, capping of the abrasives, clogging between the abrasive particles and attrition of the abrasive particles.

#### 14.3.4.2 Effect of Abrasive Size on Wear Rate

The variation of wear rate of the shot peened steels at an applied load of 1 N and an intensity of 0.486 mm Almen "A", as a function of abrasive size, is reported in Fig. 14.8. It is evident from the figure that the wear rate increases with increase in abrasive size.

The increase in wear rate with abrasive size is primarily attributed to deeper and wider groove formation during abrasion. The wear mechanism at finer abrasive size dominated by ploughing and rubbing type of wear, whereas at coarser abrasive size, the dominating wear mechanisms were micro-cutting associated with micro-cracking. It is interesting to note that with increase in abrasive size the number of abrasives per unit area decreases, as a result the load shared by individual abrasives increases. This should lead to deeper penetration of the abrasive to the specimen surface and resulting in deeper and wider abrasive grooves.

#### 14.3.4.3 Wear Resistance

The wear resistance of the material is defined as:

$$\text{Wear Resistance} = 1/\text{Wear Rate} \tag{14.2}$$

The corresponding wear rate with the type of peening intensity is demonstrated in Fig. 14.9. The wear rate is considered for unpeened, low and high peened surfaces.

Figure 14.10 also demonstrate that the wear resistance increases with increase in peening intensity. Increase in wear resistance with peening intensity attributed to the fact of surface work hardening and generation of compressive stress field on the specimen surface. The work hardening increases the surface hardness of the specimens whereas the compressive stress reduces the tendency of micro cracking during abrasive wear.

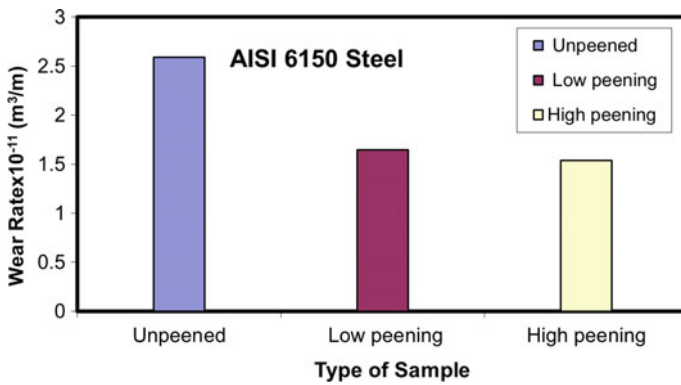


**Fig. 14.9** Wear rate of AISI 6150 steel. Where, Unpeened means virgin sample, low peening means peened with 0.117 mm Almen intensity and high peening means peened with 0.486 mm Almen intensity

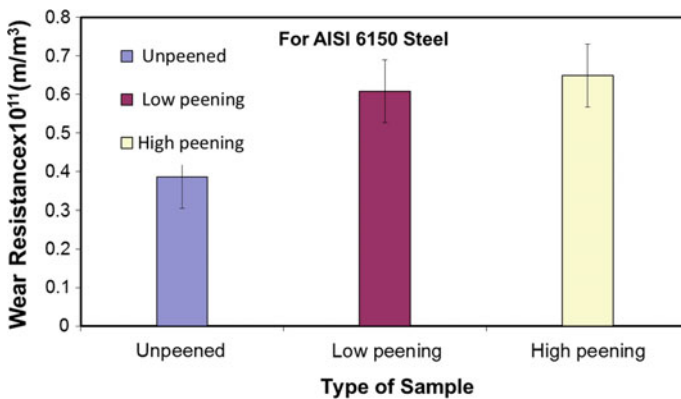


**Fig. 14.10** Wear resistance of AISI 6150 steel at the load of 1 N with the sliding distance of 0.0675 m

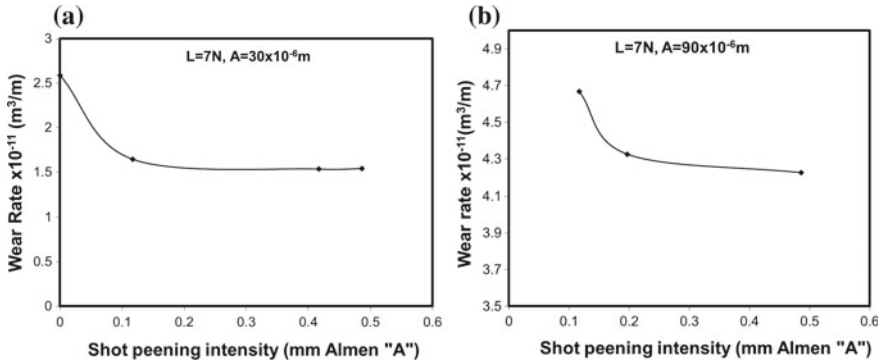


Fig. 14.11 Effect of shot peening intensity on wear rate with the sliding distance of 0.0675 m

**14.3.4.4 Effect of Shot Peening Intensity on Wear Rate**

The wear rate of the material at an applied load of 7 N and abrasive size of 30 μm, for AISI 6150 steel as a function of peening intensity is shown in Fig. 14.11. It is evident from this figure that the wear rate decreases drastically when the material is subjected to peening intensity of 0.117 mm Almen “A”, from the virgin state. Further increase in peening intensity leads to only marginal decrease in wear rate.

**14.3.4.5 Worn Surface Analysis**

There exhibits continuous as well as discontinuous wear grooves. In some regions the dimples generated due to shot peening are observed, which signifies that the wear is taking place due to removal of materials from the boundary of the dimples and finally the dimples are getting removed. This also signifies that the contact area of the peened sample also plays important role in the abrasive wear of the specimen. Initially, there is a possibility of greater degree of interlocking between abrasives and the dimpled region of the shot peened specimen, which causes greater extent of material removal at the initial stage. Sharp regions of the dimples also subjected to higher stress fields during testing and this also responsible for greater degree of material removal. As time progresses the surface becomes smoother and the abrasives also degraded and thus, the contact due to interlocking decreases, which in due course leads to less material removal at later stage.

At higher load and higher abrasive size there is also possibility of surface cracking as shown in Fig. 14.12, which leads to more fragmentation of material on the wear surface. Under the same applied load but at higher peening intensity (0.486 mm Almen “A”), the wear surface looks to be slightly different indicating more dimples as compared to that observed in earlier figures at low intensity. It strongly recommends that the wear is taking place through progressive removal of dimples and finally reaches to a smoother surface. Thus, deeper dimples and greater work hardening

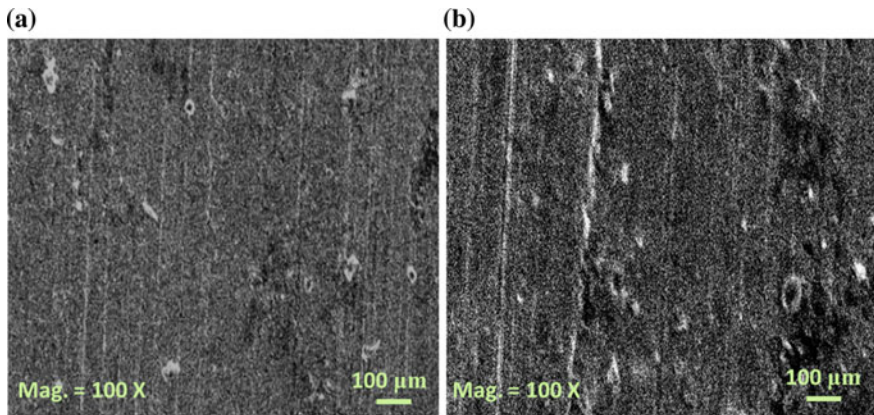


**Fig. 14.12** SEM micrographs of the worn surfaces of **a** lower higher load and lower abrasive size and **b** higher load and higher abrasive size

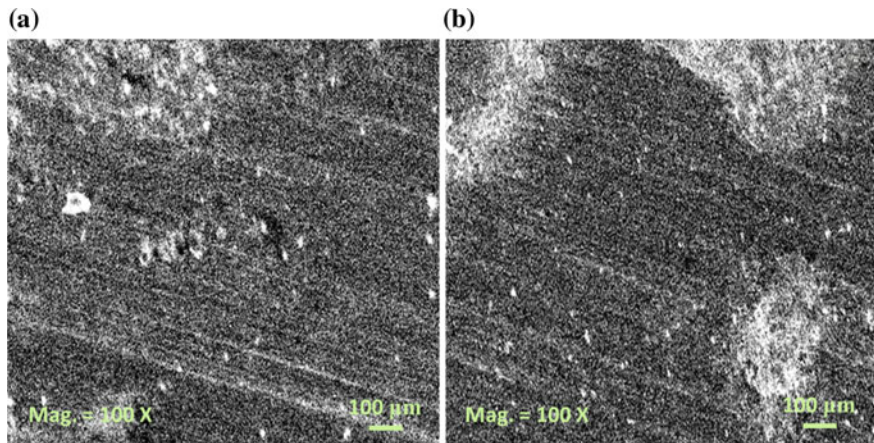


**Fig. 14.13** SEM micrographs of worn surfaces of **a** low peened and **b** high peened surface

effects gets nullified by the surface cracking (Fig. 14.13). So at considerably higher peening intensity level only marginal improvement in wear resistance is noted.

## 14.4 Conclusion

The outcome of the present work can be summarized in following points:

- The wear rate decreases by 20–30% due to shot peening to a level of 0.117 mm Almen “A” from the un-peened state. Further, increase in shot peening intensity does not results into significant improvement in wear resistance.

- Wear rate increases with increase in applied load and abrasive size.
- The combined effect of applied load and abrasive size on the wear rate is quite significant.
- The wear rate decreases with increase in sliding distance due to work hardening and degradation of abrasive media.
- The shot peening leads to sub-surface work hardening and surface denting. The extent of work hardening and denting increases with increase in shot peening intensity.
- The converted residual stress from micro hardness values demonstrate that the residual stress in the shot peened steel is of the order of 70–160 MPa depending on peening intensity.

**Acknowledgements** The authors are thankful to Central Institute of Agricultural Engineers (CIAE), Bhopal for performing the shot peening experiments on the samples.

## References

- Blau PJ (2005) On the nature of running-in. *Tribol Int* 38:1007–1012
- Buckley DH (1971) Friction, wear, and lubrication in vacuum. National Aeronautics and Space Administration, Washington, D.C.
- Cary PE (1981) History of shot peening. In: 1st international conference on shot peening, Paris, France, pp 23–28
- Champaigne J (2001) Shot peening overview, Electronics Inc. 1428 W. 6TH Street Mishawaka, IN 46544
- Diepart CP (1994) Modelling of shot peening residual stresses-practical applications. In: Materials science forum, vol 163. Trans Tech Publications, pp 457–464
- Foley AG, McLees VA (1986) A comparison of the wear of ceramic tipped and conventional precision seed drill coulters. *J Agric Eng Res* 35:97–113
- Gao YK (2011) Improvement of fatigue property in 7050–T7451 aluminum alloy by laser peening and shot peening. *Mater Sci Eng, A* 528:3823–3828
- Khrushchov MM, Babichev MA (1962) Research on wear of metals. National Engineering Laboratory
- Lee PP, Savaskan T, Laufer E (1987) Wear resistance and microstructure of Zn–Al–Si and Zn–Al–Cu alloys. *Wear* 117:79–89
- Maawad E, Sano Y, Wagner L, Brokmeier HG, Genzel C (2012) Investigation of laser shock peening effects on residual stress state and fatigue performance of titanium alloys. *Mater Sci Eng, A* 536:82–91
- Meguid SA, Shagal G, Stranart JC, Daly J (1999) Three-dimensional dynamic finite element analysis of shot-peening induced residual stresses. *Finite Elem Anal Des* 31:179–191
- Modi OP, Mondal DP, Prasad BK, Singh M, Khaira HK (2003) Abrasive wear behaviour of a high carbon steel: effects of microstructure and experimental parameters and correlation with mechanical properties. *Mater Sci Eng, A* 343:235–242
- Pürçek G, Savaşkan T, Küçükömeroğlu T, Murphy S (2002) Dry sliding friction and wear properties of zinc-based alloys. *Wear* 252:894–901
- Rautaray SK (1997) Fatigue and wear characterization on shot peened rotavator blade materials
- Raval AH, Kaushal OP (1990) Wear and tear of hard-surfaced cultivator shovel. *AMA, Agric Mech Asia Afr Latin Am* 21:46–48

- Ray KK, Mondal D (1991) The effect of interlamellar spacing on strength of pearlite in annealed eutectoid and hypoeutectoid plain carbon steels. *Acta Metall Mater* 39:2201–2208
- Richardson RCD (1967) The wear of metallic materials by soil—practical phenomena. *J Agric Eng Res* 12:22–39
- Saritas S, Dogan C, Varol R (1999) Improvement of fatigue properties of PM steels by shot peening. *Powder Metall* 42:126–130
- Saxena AC, Sharma MC (2001) Wear of shot peened thresher pegs. In: Shot peening and blast cleaning, Proceeding of international conference on shot peening and blast cleaning, MACT, Bhopal, India, pp 281–287
- Waisman IL, Phillips A (1952) Simplified measurement of residual stresses. In: Proceedings of the society experimental stress analysis, p 11

# Chapter 15

## Tribological Performance of Surface Textured Automotive Components: A Review



Nilesh D. Hingawe and Skylab P. Bhore

**Abstract** Presently, worldwide research is focused on energy efficiency to meet the requirement of greenhouse gas emission and economic reasons. The substantial amount of energy is consumed mainly in industrial, transportation and power generation sectors. The leading source of energy consumption is friction. Friction causes wear of the machine components and their replacement. Therefore, to minimize energy consumption the friction reduction is a foremost objective. Potential mechanisms for the reduction of friction are modified lubricants, coatings, and surface texture. In comparison with other mechanisms, surface texturing is a feasible, promising and well-established technique to improve the tribological performance of machine components for more than two decades. Surface texture decreases an area of contact, act as a reservoir and improves hydrodynamic effect in dry, mixed and hydrodynamic lubrication regime respectively. All of this contributes to reducing the friction coefficient. In addition to this, the surface texture improves the load capacity, dynamic stability and noise intensity of the bearings. It develops additional hydrodynamic effect and minimizing fluid leakage in oil and gas seals. Also, in automobile components such as piston rings, cylinder liner and wet clutch, the texture geometry is considered to be micro-pocket. Lubricant retained in the micro-pocket can be released to surrounding areas of texture to improve the tribological performance. This article outlines the recent advancement in texture design for different automotive components, their mechanisms, key findings and future roadmap. Also, the challenges in the fabrication of surface texture for automotive components are discussed in detail.

**Keywords** Surface texture · Lubrication regimes · Friction and wear · Micro-pocket

---

N. D. Hingawe (✉) · S. P. Bhore  
Department of Mechanical Engineering, Motilal Nehru National Institute of Technology  
Allahabad, Prayagraj, Uttar Pradesh 211004, India  
e-mail: [nileshhingwe@yahoo.in](mailto:nileshhingwe@yahoo.in)

© Springer Nature Singapore Pte Ltd. 2019  
J. K. Katiyar et al. (eds.), *Automotive Tribology*, Energy, Environment, and Sustainability,  
[https://doi.org/10.1007/978-981-15-0434-1\\_15](https://doi.org/10.1007/978-981-15-0434-1_15)

## 15.1 Introduction

The growing global population, societal needs, and enlargement in automotive (industrial and transportation) sectors are increasing the energy demand rapidly. In addition, limited oil resource, and environmental pollution are nowadays serious issues. At present, about one-third of the global energy resource is consuming to overcome the friction (Holmberg and Erdemir 2017). Especially in automotive engines, approximately 50–60% frictional loss comes from piston ring-cylinder system (Zhan and Yang 2014). This causes millions of tons of CO<sub>2</sub> emission per year (Braun et al. 2014). Additionally, friction causes wear and tear which leads to failure of the automotive components. Reducing friction in the automotive system can therefore improve the life of components, energy consumption, fuel efficiency, and hence gas emission.

In general, two surfaces in relative motion cause friction. It is desirable in generalized applications such as holding an object, walking on the floor, applying brakes, etc. However, in automotive components such as bearings, piston-cylinder arrangement, etc. friction is undesirable. As friction is associated with wear and lubrication, tribology plays an important role. Tribology is basically a science evolving friction, wear, and lubrication. To improve the tribological performance of automotive components the majority of research consisting of modification in (1) lubrication, and (2) surface engineering as follows (Blau and Qu 2004):

### 1. Lubrication

- Lubricants
- Lubricant filtration and supply

### 2. Surface engineering

- Surface treatment: Coating
- Surface topography: Surface texturing.

However, the modification in surface engineering specifically surface topography is found to be the most effective and reasonable technique. Surface topography includes surface texturing on the surface. The intentional creation of well defined identical features on the surface is called surface texturing. Surface texture on the surface is not a new concept to improve the tribological characteristics. In 1966, Hamilton et al. (1966) have proposed that surface micro-irregularities can reduce the friction between parallel surfaces. But in the following three decades the little attention was paid by the researchers on the textured surface. The new momentum was gained by Etsion's group in 1996. Since then extensive research on surface texturing is going on. At present, it is a well-established and promising technique to improve the tribological performance of automotive components such as bearings, seals, piston ring, wet clutch, cylinder liner, etc. Adopting surface texture on these components can improve the load carrying capacity, fluid film stiffness, friction, wear, leakage, and noise intensity.



In recent times few review articles on the advancement of surface texture in bearings (Gropper et al. 2016; Wang 2014), piston-cylinder systems and mechanical seals (Ahmed et al. 2016) have been published. The theoretical modeling of these components has been summarized by Etsion (2013). Etsion (2005) reviewed the effect of surface texture on bearing sliders under different lubrication condition. Whereas Shamsul Baharin et al. (2016) have presented the mechanism of surface texture to improve the tribological characteristics at different lubrication regimes. In addition to this, advancement in the fabrication of surface texture is nowadays a hot topic of research (Ibatan et al. 2015; Gachot et al. 2017; Coblas et al. 2015). While special attention is paid on laser surface texturing technique (Arslan et al. 2016; Patel et al. 2018). However, the influence of texture design parameters on the tribological performance of automotive components has not been discussed in detail so far. It is therefore essential to summarize the texture behavior in automotive components that affects energy consumption and environmental pollution. With this consideration, in the present review article, the influence of texture design parameters on the tribological performance of automotive components is presented. The recent advancement in texture design is mainly discussed. Moreover, modern texture fabrication techniques (both conventional and non-conventional), and their pros and cons are discussed. Also, key findings and future roadmap to improve the tribological performance of automotive components is presented.

## 15.2 Texture Design

Designing of surface texture is an essential part of surface topography. Extensive research work on texture design characteristics is carried out. Still, there is no fixed rule for the selection of texture shape under the given operating condition for a particular application. Though surface texturing has the potential to improve the tribological characteristics, it may show an adverse effect if designed wrong. Therefore, a clear understanding of texture design is necessary. Here, the texture design is majorly classified based on geometrical characteristics and positional features as shown in Fig. 15.1.

### 15.2.1 Texture Geometry

Texture geometrical characteristics such as shape (top profile and bottom profile), and parameters are discussed in detailed as follows:

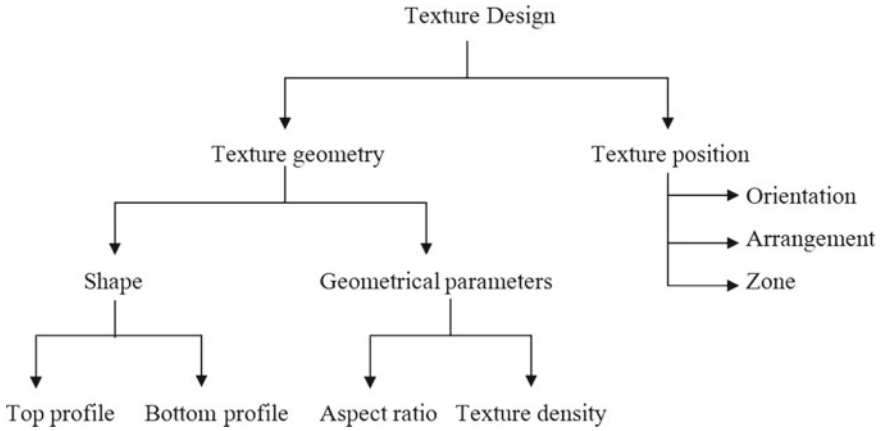
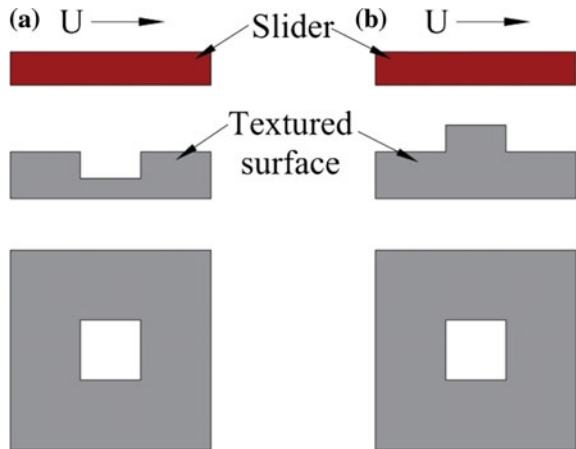


**Fig. 15.1** Texture design features

**15.2.1.1 Texture Shape**

Both negative (recessed) and positive (protruded) texture shapes can be generated as shown in Fig. 15.2. While negative texture is majorly accepted due to advantages in terms of lubrication and ease of manufacturing. Under hydrodynamic lubrication, the negative texture shape is better for friction reduction. But from a leakage point of view, the positive texture showed good results (Siripuram and Stephens 2004). Texture shape is characterized by its top and bottom profile.

**Fig. 15.2** Textured parallel slider **a** negative texture **b** positive texture



### Top Profile

An extensive research work has been conducted on standard texture profiles. Siripuram and Stephens (2004) considered the standard texture profiles viz. circle, square, diamond (square-oriented), hexagonal, and triangular for studying the effect of geometry on the hydrodynamic lubrication. They found that the friction coefficient is insensitive to these texture profiles.

However, Yu et al. (2010, 2011) investigated that elliptical texture profile gives better performance than square and circular profile for friction reduction. The commonly used texture top profiles are shown in Fig. 15.3.

Motivated by triangular profile, Uddin and Liu (2016) have observed that star like (series of triangular spikes around the center) texture profile performs better than standard top profiles both in terms of film pressure and friction coefficient. Under mixed lubrication condition, Ren et al. (2007) developed a numerical model for non-standard texture profiles: triangular grooves, sinusoidal waves, fishbone with grooves, fishbone with dimples, and honeycombs. The short grooves and sinusoidal waves showed the strongest load carrying capacity. Galda et al. (2009) have investigated the tribological performance of newly developed texture profiles viz. short drop, and a long drop. They found that spherical and long drop shapes are superior to short drop profile. For the maximization of load capacity and minimization of friction coefficient in grease lubricated textured bearing, Yu et al. (2016) have

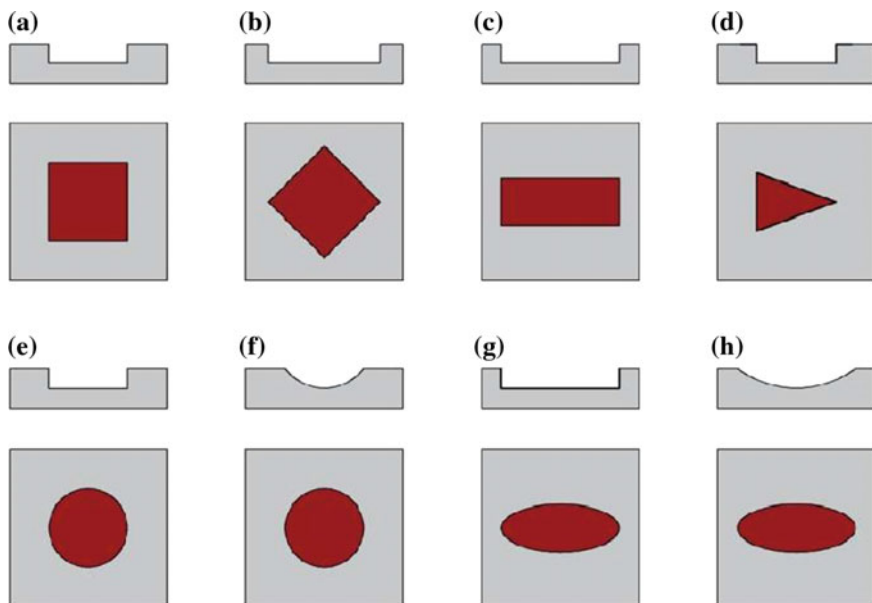


**Fig. 15.3** Standard textured profiles **a** square **b** diamond **c** rectangle **d** triangle **e** cylinder **f** sphere **g** elliptical **h** ellipsoidal

found that triangular profile performs better than the sphere, spheroid, and T shaped grooved profile. In micro-turbine bearings, Bompos et al. (2012) adopted the egg-shaped texture profile. In comparison with smooth bearing a substantial improvement in hydrodynamic characteristics was observed for textured bearing. For the gas lubricated parallel slider, Qiu et al. (2012, 2013) have found that texture shape with a round edge (sphere, ellipsoidal and circle) performs better than straight-edged profiles (triangle and chevron) to improve the hydrodynamic pressure, friction coefficient, and bearing stiffness. From the above discussion, it is observed that modified (non-standard) texture profiles have better tribological characteristics than predefined simple geometries.

To further improve the results, the texture profile needs to be optimum. Rahmani et al. (2010a), Rahmani and Rahnejat (2018) have optimized the standard texture profiles: square, rectangle and isosceles triangle using an analytical approach for maximization of load capacity and minimization of friction coefficient. For the maximization of load capacity, Fesanghary and Khonsari (2012) have optimized the hydrodynamic film in sectorial-shape thrust bearing using sequential quadratic programming technique. The optimally designed bearing showed more than 100% increase in load capacity than the conventional bearing. Fesanghary and Khonsari (2013) developed the optimization model for grooved texture. The obtained “heart-like” texture profile was validated experimentally. Shen and Khonsari (2015) have presented the numerical optimization of texture top profile using sequential quadratic programming (SQP) for maximization of load capacity. Under unidirectional and bidirectional sliding, the optimum texture profiles were obtained as chevron-type and trapezoid-like respectively. Also, Zhang et al. (2017) have optimized the irregular texture shape for minimum friction coefficient and maximum load capacity using a genetic algorithm (GA) optimization technique. The optimized fusiform texture profile showed a better result than elliptical and circular profiles. Wang et al. (2018a) presented the numerical optimization of chevron-shaped grooved texture to maximize the load capacity of thrust bearing using hybrid (GA-SQP) technique. Experimentally they confirmed that optimum chevron-shaped grooved texture reduces the friction coefficient and temperature rise of the specimen. For gas mechanical seals, Wang et al. (2018b) have modified the spiral grooved texture using multi-objective optimization. The optimized grooved profile showed better result than conventional spiral grooved texture. From the above literature, it is confirmed that the optimized non-standard texture profiles performs better than simple profiles.

### Bottom Profile

Texture bottom profile also significantly influences the tribological characteristics. The commonly used texture bottom profiles are flat, curved, and asymmetric wedge (see Fig. 15.4). With the cavitation effect, Nanbu et al. (2008) have analyzed the influence of wedge-shaped texture bottom profiles on the hydrodynamic characteristics. They found that texture bottom profile strongly influences the pressure distribution and film thickness. Shen and Khonsari (2013) have observed that cavitation occurs

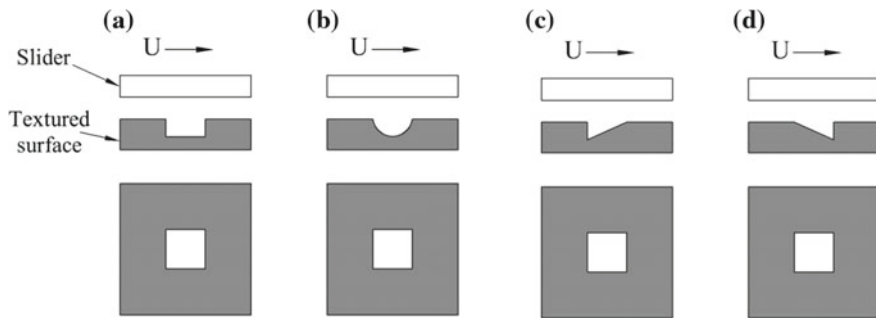


**Fig. 15.4** Commonly used texture bottom profiles **a** flat **b** curved **c** convergent wedge **d** divergent wedge

in the divergent region of the texture, this leads to an asymmetric distribution of pressure. For this mechanism, the load capacity generated by the rectangular bottom profile is larger than the triangular (oblique and isosceles) bottom profiles. Wang et al. (2018c) compared the four different bottom profiles of grooved texture. They observed that the location of cavitation region, the volume fraction of vapor phase and the shape of vortex are influenced by the bottom shape of the groove texture in thrust bearing.

Meng et al. (2015) have observed that the flat (rectangle) and curved (spherical) bottom profile are the most commonly used texture bottom profile to improve the tribological characteristics. For taking the advantages of both rectangle and spherical profiles, they combined these profiles to form the structure characterized by two-layer pores defined as compound texture. In which, first and second layers are rectangle and spherical, respectively. Compound texture showed improved load carrying capacity and friction coefficient than smooth and simple (rectangle) textured hydrodynamic journal bearing due to its twice hydrodynamic effect. Further, they developed the compound groove textures that reduce the acoustic power level of the journal bearing than that of smooth and simple grooved bearings (Meng and Zhang 2018).

Without a cavitation effect, Han et al. (2011) have found that divergence and convergence clearance in the symmetrical texture bottom profile is balanced. However, an asymmetrical bottom profile showed more potential to enhance hydrodynamic characteristics. Similarly, Schuh and Ewoldt (2016) investigated that asymmetric bottom profile generates the normal force, and reduces the shear stress and friction coefficient. Further, Lee et al. (2017) have obtained the significant improvement in hydrodynamic performance with arbitrarily shaped texture bottom profile. Adopting an optimization approach, Lin et al. (2017) have optimized the arbitrary texture bottom profile using sequential linear programming (SQL) for increasing normal force and decreasing friction force. Wang et al. (2017) used the hybrid (GA-SQP) optimization technique for the grooved bottom profile. The optimized profile showed better load capacity than common profiles such as micro wedge and step.

From the above discussion, it is observed that asymmetrical bottom profiles perform better than symmetrical bottom profiles. For top profile also it is confirmed

that the modified profile is preferable over simple profiles. However, the simultaneous modification of both top and bottom profile using the optimization technique can appreciably improve the result is still lagging. This approach can be adopted in different machine components including automotive components.

**15.2.1.2 Texture Parameter**

The surface texture has a certain size along the length, width, and depth. But it is essential to form parameters that include all geometrical aspect of the texture. For this, the non-dimensional parameters: texture density and the aspect ratio are widely used in the literature. These texture parameters are sensitive to tribological characteristics in most automotive components (Gropper et al. 2016).

**Aspect Ratio**

Aspect ratio is defined as the ratio of texture depth ( $h_b$ ) and the characteristics length ( $l$ ) (see Fig. 15.5).

$$\text{Aspect ratio, } Ar = \frac{h_b}{l} \tag{15.1}$$

Aspect ratio is described by (i) varying the texture depth and keeping length constant and (ii) varying texture length and keeping depth constant. The former way to define the aspect ratio is directly related to depth, and hence more popular. In some literatures, the aspect ratio is also named as depth ratio.

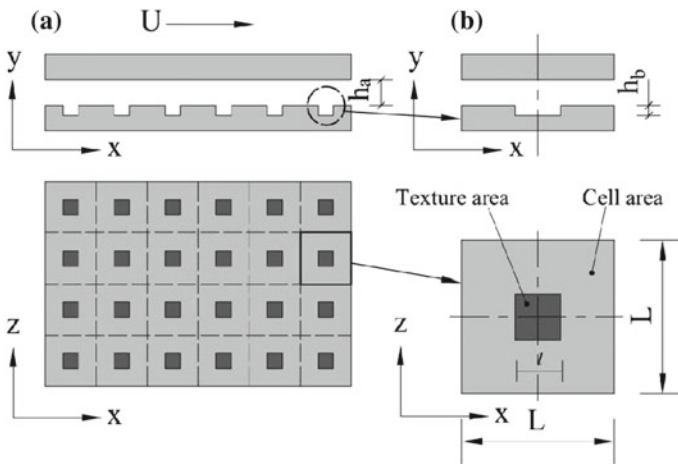


**Fig. 15.5** a Textured parallel slider and b square textured unit cell

## Texture Density

Texture density is defined as the ratio of texture area ( $l^2$ ) and the cell area ( $L^2$ ) as shown in Fig. 15.5.

$$\text{Texture density, } T_d = \frac{l^2}{L^2} \quad (15.2)$$

For entire surface, the texture density is expressed as the N times texture area to the total surface area (see Fig. 15.5a). In some literature texture density is also known to be area ratio.

### 15.2.2 Texture Position

Although texture shape and its geometrical characteristics influence the tribological characteristics, the texture distribution pattern influences the result. This is because the volume and position of lubricating oil accumulate generates the hydrodynamic effect.

#### 15.2.2.1 Texture Orientation

Texture shape can be oriented at different angles along the direction of motion. Yu et al. (2010) have investigated that elliptical texture perpendicular to the direction of sliding gives a better result for friction reduction than oriented along the direction of sliding. However, Ismail and Sarangi (2013) considered both positive and negative textures for elliptical and triangular profiles. They found that the angular orientation of negative texture is uncertain on hydrodynamic performance. But the positive textures: 60° triangular orientation, and 90° elliptical orientation showed better performance parameters than other orientations. In textured gas seals, Bai et al. (2010) have investigated the influence of elliptical texture orientation on hydrodynamic characteristics such as load capacity and slide leakage. They investigated that texture oriented at 0° and 90° in the direction of flow has less leakage, but the hydrodynamic effect is not significant. However, at 40°–70°, the significant improvement in load capacity is obtained. But leakage is also found to be high.

#### 15.2.2.2 Texture Arrangement

In most of the surface texture analysis as discussed above, the linear texture arrangement has been adopted. In journal bearing, Lu et al. (2014) have modified the conventional texture arrangement to the phyllotactic patterned. Experimentally they found

20–30% less frictional coefficient than the conventional linear textured arrangement. Braun et al. (2014) have investigated the tribological behavior of sliding pairs with spherical textures arranged in a hexagonal pattern in the mixed lubrication regime of the pin-on-disk experiment resulted in decreasing friction coefficient. Also, Schneider et al. (2017) examined the different texture arrangements viz. hexagonal, cubical and random for friction reduction. In comparison with plane surface, 82% friction reduction occurred in a hexagonal arrangement. For cubical and random arrangement, respectively 50 and 48% reduction in friction coefficient than plane surface was achieved.

### 15.2.2.3 Texture Zone

Surface texturing on the entire bearing surface does not necessarily improve the hydrodynamic characteristics. Surface texture may show adverse results if designed wrong. Kango et al. (2012) have observed that surface texture at different locations of the bearing surface helps in enhancing bearing the bearing performance. Brizmer and Kligerman (2012) have investigated that texturing on the entire surface is meaningless for both short and infinite long oil lubricated bearings. Kango et al. (2014) have found that surface texture (both dimple and groove) in the converging zone of the bearing is a preferable arrangement. At variable process parameters such as eccentricity ratio, clearance, journal speed and oil viscosity, Shinde and Pawar (2017a) found that grooved texture in  $90^{\circ}$ – $180^{\circ}$  zone gives maximum load capacity. However, the minimum frictional torque is achieved at  $90^{\circ}$ – $360^{\circ}$  texture zone. But for multi-objective optimization, textured zone  $90^{\circ}$ – $175^{\circ}$  showed appropriate result (Shinde and Pawar 2017b). Similarly, Zhang et al. (2018a) have done optimization of texture position in the convergent zone of the journal bearing. The optimized semi-elliptical shaped texture arrangement showed better bearing load and friction coefficient than half-textured and plane surfaces. They also optimized the texture position numerically in bearing sliders for maximization of load capacity and minimization of friction coefficient. Experimentally they verified that optimized texture position shows best performance than plane, fully textured, and conventionally partial textured surfaces (Zhang et al. 2018b). Contrarily, Tala-Ighil et al. (2011) have investigated that surface texturing in the divergent zone ( $185^{\circ}$ – $230^{\circ}$ ) improves the bearing performance. Further, they observed found that texture arrangement is sensitive to journal speed (Tala-Ighil and Fillon 2015). At lower operating speed,  $0^{\circ}$ – $180^{\circ}$  textured position showed best result. Upon further increasing the speed,  $185^{\circ}$ – $230^{\circ}$  texture zone obtained best performance. Also in piston ring, partial texturing shows better results than full texturing Kligerman et al. (2005). Etison and Sher (2009) have found that partial laser texture (symmetrical type) has obtained about 4% reductions in fuel consumption. However, it is found to be insignificant for the effect of exhaust gas. Also, noticeable difference in engine oil temperature and crank case pressure is observed than plane surface.

From the above discussion, it is clear that texture shape, geometrical parameters, position, zone, etc. have significant influence on tribological characteristics. But the



detailed analysis by considering every parameter is time-consuming. Also, it is difficult to predict the exact behavior of texture design parameters on output responses. However, response surface methodology has the potential to address this issue. A large number of parameters can be considered in a single design model for different output responses. This approach can significantly reduce the computation time and experimental cost. Fu and Untaroiu (2017) have investigated the tribological performance of surface textured thrust bearing using a design of experiment followed by multi-objective optimization for optimal partially texture geometry with an elliptical dimple. The output responses aimed to maximize the load capacity and minimize the friction torque. The geometrical characteristics such as length of major and minor axes, dimple depth, radial and circumferential space between two dimples, and the radial and circumferential extent were parameterized and analyzed using response surface methodology based central composite design of experiment technique. Using this, the proper combinations of parameter were obtained. Further, they (Fu and Untaroiu 2018) compare the rectangle and elliptical texture using a design of experiment. Using the parametric study, a model was developed. Based on this, they found that elliptical textures have more potential to improve tribological characteristics than rectangular texture.

### 15.3 Surface Texturing in Automotive Components

Surface texture has significant influence on tribological performance of automotive components. In fluid film bearings, surface texture increases the film thickness. The increase in film thickness at the convergent zone generates additional hydrodynamic pressure to further separate the surfaces. This resulted in increasing load capacity and decreasing local shear stress and hence friction (Gropper et al. 2016). Surface texture on one of the mating faces in circumferential gas seal generates considerable hydrodynamic effect which maintains the small clearance between shaft and seal ring. This prevents the rubbing and hence decreases in friction and wear (Kligerman and Etsion 2008). To improve the lubricant quantity in automobile components such as piston rings and wet clutch, the texture geometry is act as micro-pocket. Lubricant retained in the micro-pocket can be released at surrounding areas of texture to improve the tribological performance (Kligerman et al. 2005; Yagi et al. 2015). Adopting surface texture on the rake face of the cutting tool decreases the tool–chip contact area. Also, the debris trapped in the texture and reduction of stiction at the tool–chip interface takes place. This result in a decrease in friction, wear and hence lesser heat generated in the cutting tool (Jesudass Thomas and Kalaichelvan 2018). In case of an artificial implant, adopting surface texture decrease surface contact under boundary lubrication and acts as a lubricant reservoir in elasto-hydrodynamic lubrication (Ghosh and Abanteriba 2016). Surface texture has widespread applications in automotive components such as piston ring, cylinder liner, clutches etc. as discussed in detail as follows.

### 15.3.1 *Cylinder Liner*

A cylinder liner serves as the inner wall of cylinder to be fitted into an engine block. It forms sliding surface for the piston ring while retaining lubricant within. The main function of cylinder liner is to control the friction loss between piston ring and cylinder liner, wear of piston ring and cylinder liner, consumption of lubricant, emission of gases and fuel efficiency. To improve this, one of the feasible and possible techniques is to modify topography of cylinder liner by honing scratches/grooves. Dimkovski et al. (2012) have optimized the cylinder liner surface finish for base honing pressure and plateau honing time. But, axial scratches occurred due to abrasive wear are undesirable. Also, they studied on undesirable scratches on the liner which increases the oil consumption and gas emission (Dimkovski et al. 2011). However, Guo et al. (2013) have investigated that the lubrication performance of the cylinder liner is sensitive to surface texture. Grabon et al. (2017) have considered different surface textures were of cylinder liner. They found that increasing honing angle of cylinder liner causes higher frictional resistance. However, at lower honing angle the reduction of liner height was significant. Kim et al. (2018) have found that valley generated by honing functions is undesirable for the formation of dynamic pressure on interacting surfaces. The different mark of plateau honing was compared for friction and wear with those of randomly ground surfaces. They found that deep-grooved honing marks produce larger amounts of wear than shallow-grooved honing. From the tests with the deep-grooved honing marks, it was found that the severe interactions due to asperity contacts and the formation of relatively thin films produced larger amounts of wear volumes than the test with the shallow-grooved ones.

### 15.3.2 *Wet Clutch*

In automatic transmission of automobile wet clutches are used. In wet clutch, paper-based friction materials are used as sliding member. It requires high and stable friction at variable speed, wear resistant and heat resistant. To achieve this, researchers have worked on material characteristics or modifications of paper-based wet clutch such as optimization of material composition, different additives in the automatic transmission of fluid and pore characteristics of the paper (Kitahara and Matsumoto 1994; Matsumoto 1996; Kugimiya 2000). However, limited work has been done on surface modification of paper to improve the tribological characteristics. Yagi et al. (2015) formed microscale texture in the form of microgrooves at variable depth and pitch on the paper-based friction material using laser surface texturing. At low temperature and low surface pressure conditions, the dynamic friction coefficient was improved due to microgroove. Also, they found that the dynamic friction coefficient is depends upon depth and pitch of the microgrooves. It can be controlled by properly designing of microgroove pattern. However, adopting microgrooves was found to be insignificant to improve static friction coefficient.

### ***15.3.3 Piston Ring***

Piston ring is the major source of engine friction. Reducing friction occurred by piston ring is an effective way to decrease fuel consumption and hence exhaust gas emission. To improve the tribological characteristics of the piston ring by adopting surface texture is largely studied by Etsion and co-authors (Arslan et al. 2016; Ronen et al. 2001; Ryk et al. 2002). They found that laser surface texturing is feasible and most promising technique to improve the tribological characteristics of the piston ring. Kligerman et al. (2005) developed the analytical model for partial laser surface textured piston ring for friction reduction. This is verified experimentally by Ryk et al. (2005). For symmetrical type partial laser texture, Etsion and Sher (2009) have found that approximately 4% reduction in fuel consumption is obtained than smooth surface. However, the effect on exhaust gas is found to be insignificant. Ahmed et al. (2016) reviews the effect of texture geometrical parameters on piston ring. They found that (i) aspect ratio is the most significant parameter to improve the tribological characteristics of piston ring (ii) for better performance maximum possible texture density should be selected. (iii) Under starved lubrication condition higher texture depth shows detrimental results. Also, optimum texture depth is depends on the operating conditions. (iv) Partial texturing shows better result for friction reduction than full texturing. Recently, Bifeng et al. (2018) have proposed a novel texturing scheme on piston ring by modifying barrel-shaped ring scheme in the form of variable texture depth. They found that average friction power for novel texture pattern is 10.04% lesser than normal texturing. While, in comparison with barrel shape, it has obtained 16.85% lesser average friction power.

### ***15.3.4 Engine Bearings***

The plane and textured hydrodynamic journal bearing as shown in Fig. 15.6 is well established. Although, limited research is carried out on engine bearings with texture effect. Surface texture adopted in engine bearings can decrease the friction coefficient, noise intensity, fuel consumption and increase in load carrying capacity. This ultimately reduces energy consumption to cause a decrease in fuel consumption and engine emissions (Ligier and Noel 2015).

In modern times, surface texture analysis of tires in automobiles can be studied to control the friction for safe driving at various road conditions. Furthermore, surface texture can also be adopted in automotive components such as piston pin, cam and follower, brake to improve the performance.

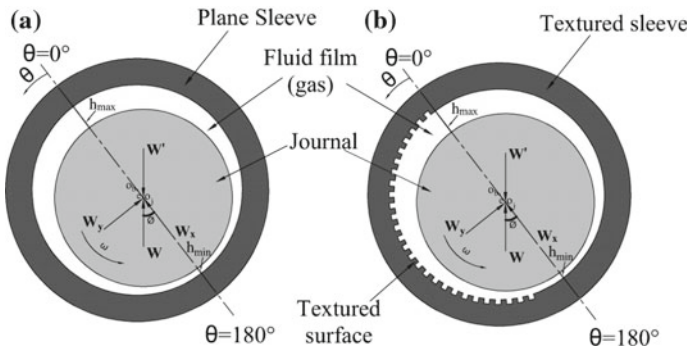


**Fig. 15.6** Hydrodynamic lubricated **a** plane bearing and **b** textured bearing

## 15.4 Texture Fabrication Techniques

Texture quality is largely affected by fabricating technique (Ibatan et al. 2015). Surface textures can be fabricated by several conventional and non-conventional machining processes (Ahmed et al. 2016). It is therefore essential to have a detailed discussion on each fabricating technique along with pros and cons.

The conventional machining processes such as vibro-rolling and abrasive machining can be used to create grooves (Rahmani et al. 2010b). While embossing technique is capable of generating surface texture on plastically deformable materials (Pettersson and Jacobson 2006). But this technique is not suitable for hard and brittle materials. Jesudass Thomas and Kalaichelvan (2018) fabricated the surface texture on the rake face of a single point cutting tool using surface indentation techniques viz. Rockwell hardness tester, Vickers hardness tester, and diamond dresser. They found that surface texturing using Vickers hardness tester has obtained better tribological performance than other techniques. Also, standard texture profiles can be generated using micro-grinding process. It is a simple, productive and inexpensive technique to create surface texture on the surface (Stepien 2008). Moreover, Cannon and King (2009) fabricated the surface-texture using micro-casting which is a relatively new technique. This technique can create holes of about 10–100  $\mu\text{m}$  diameter and aspect ratio of 2:1. A vibromechanical texturing technique which is based on single point turning process can produce surface texture. In the conventional turning process, the controlled motion of cutting tool along the  $X$ -axis (rotation about spindle axis) and  $Y$ -axis (across the length of the workpiece) can generate continuous spiral grooves along the circumference of the workpiece. Adopting controlled motion (tunable oscillation of the tool path) along the  $Z$ -axis, a variety of texture sizes can be machined. This method is cost-effective, produces less surface damage, and is very precise (Greco et al. 2009). To investigate the influence of texture bottom profile in thrust bearing, Schuh and Ewoldt (2016) developed the asymmetric-depth-profile angled along the normal surface. The asymmetric depth was achieved by tilting the workpiece with respect to the end mill axis of rotation. Overall it is observed that surface texture using conventional/traditional machining techniques are easier to fabricate. However, its accuracy is affected.

Presently, non-conventional machining processes are most widely used to fabricate surface texture. Wakuda et al. (2003) have considered abrasive jet machining to fabricate the micro-texture. The textured surface showed an improved friction coefficient. However, the bottom profile was affected. Different forms of etching can also generate texture on the surface. Lu and Khonsari (2007) generated cylindrical and elliptical texture shapes on the surface of the journal bearing using chemical etching. The process includes imprinting of the pattern followed by etching. The texture depth was controlled by etching time. Although etching is flexible to generate complex texture geometries, it is a time-consuming process. Moreover, the profile features of the texture such as round shape cannot be controlled. The other etching techniques such as reactive ion etching, UV lithography, photo-etching, physical vapour deposition and UV photo-lithography can also produce a variety of texture shapes (Rahmani et al. 2010b). In electrochemical machining (ECM) process, the material removal is taking place by electrolysis process. ECM generates a very smooth surface without heat affected layer with higher efficiency and at low cost. These advantages attract the researchers to fabricate surface texture using this technique. Lu et al. (2014) developed the phyllotactic patterned surface texture on hydrodynamic lubricated bearing surface using ECM. In comparison with conventional linear textured arrangement the significant improvement in friction reduction (about 20–30%) was obtained. Using ultrasonic machining (USM), different texture shapes such as circle, rectangle, and spherical texture shapes can be produced with high accuracy. Shin et al. (2015) have created the surface texture on bearing steel surface using USM. They found that the reduction in friction coefficient is taken place at appropriate density and depth. But this technique is limited to brittle material and it is not cost effective. Electric discharge machining (EDM) is based on the mechanism: melting and vaporization of the material. Using this technique the complex texture geometry with smooth surface finish can be achieved with no mechanical stress on the workpiece (Pal and Choudhury 2016). However, the material removal rate is low and heat affected zone influences the tribological performance. Yamaguchi et al. (2016) developed the whirling electrical discharge texturing (WEDT) to create microtextures on the inner surface of a cylinder using single-pulse discharge. They confirmed that it is an effective technique to reduce the friction coefficient. Moreover, they found that based on lubrication condition, the optimal texture-area ratio exists. These techniques can be employed for surface texturing but laser surface texturing (LST) is the most efficient technique (Ahmed et al. 2016). LST is a promising technique based on its flexibility and speed (Arslan et al. 2016). It is clean to the environment and provides excellent control of texture size. Earlier, LST was unable to produce complex texture geometry. To achieve this goal, the direct laser interference patterning technique is employed which use multiple laser beam interference. However, burrs or bulges are created after machining is a limitation of this process.

## 15.5 Concluding Remarks

In the present research review first the texture design is presented in details for automotive components. Then fabrication techniques for automotive components are discussed in details. It is concluded that,

- Texture design parameters have a significant influence on the tribological performance of automotive components.
- To improve the tribological performance, the parametric analysis of texture design parameter should be carried out for qualitative analysis. This significantly reduces the computation time and cost of the experiment without sacrificing the accuracy.
- Optimized texture parameters perform better than simple/standard texture shapes to improve the tribological characteristics of automotive components. However, the optimum process parameters depend on operating conditions and specific application.
- In the automotive system, majority of the research is focused on adopting surface texture on piston-ring cylinder. It is essential to investigate the tribological performance of surface textured crank case bearings, wet clutch, piston pin, cam and follower and tires,
- The conventional machining processes are cheaper and easier to generate the texture. But they are less accurate and it is very difficult to produce complex texture. While a variety of non-conventional texturing techniques can easily generate complex texture geometries with accuracy. Especially laser surface texturing is most famous, widely used and it provides excellent control on texture size.

## References

- Ahmed A, Masjuki HH, Varman M, Kalam MA, Habibullah M, Al Mahmud KAH (2016) An overview of geometrical parameters of surface texturing for piston/cylinder assembly and mechanical seals. *Meccanica* 51(1):9–23
- Arslan A, Masjuki HH, Kalam MA, Varman M, Mufti RA, Mosarof MH, Khuong LS, Quazi MM (2016) Surface texture manufacturing techniques and tribological effect of surface texturing on cutting tool performance: a review. *Crit Rev Solid State Mater Sci* 41(6):447–481
- Bai S, Peng X, Li Y, Sheng S (2010) A hydrodynamic laser surface-textured gas mechanical face seal. *Tribol Lett* 38(2):187–194
- Bifeng Y, Dashu G, Shao S, Bo X, Hekun J (2018) Research on the profile design of surface texture in piston ring of internal combustion engine. *J Tribol* 140(6):061701
- Blau PJ, Qu J (2004) Laser surface texturing of lubricated ceramic parts. FY 2004 progress report on heavy vehicle propulsion materials, pp 123–128. URL: [http://www1.eere.energy.gov/vehiclesandfuels/pdfs/hv\\_propulsion\\_04/4k\\_blaulaser.pdf](http://www1.eere.energy.gov/vehiclesandfuels/pdfs/hv_propulsion_04/4k_blaulaser.pdf)
- Bompos DA, Nikolakopoulos PG, Papadopoulos CI (2012) A tribological study of partial-arc bearings with egg-shaped texture for microturbine applications. In: *Proceedings of ASME Turbo Expo 2012, Copenhagen, Denmark*
- Braun D, Greiner C, Schneider J, Gumbsch P (2014) Efficiency of laser surface texturing in the reduction of friction under mixed lubrication. *Tribol Int* 77:142–147

- Brizmer V, Kligerman Y (2012) A laser surface textured journal bearing. *J Tribol* 134(3):031702
- Cannon AH, King WP (2009) Casting metal microstructures from a flexible and reusable mold. *J Micromech Microeng* 19(9):095016
- Coblas DG, Fatu A, Maoui A, Hajjam M (2015) Manufacturing textured surfaces: state of art and recent developments. *Proc Inst Mech Eng Part J J Eng Tribol* 229(1):3–29
- Dimkovski Z, Anderberg C, Ohlsson R, Rosén BG (2011) Characterisation of worn cylinder liner surfaces by segmentation of honing and wear scratches. *Wear* 271(3–4):548–552
- Dimkovski Z, Cabanettes F, Löfgren H, Anderberg C, Ohlsson R, Rosén BG (2012) Optimization of cylinder liner surface finish by slide honing. *Proc Inst Mech Eng Part B J Eng Manuf* 226(4):575–584
- Etsion I (2005) State of the art in laser surface texturing. *J Tribol* 127:248–253
- Etsion I (2013) Modeling of surface texturing in hydrodynamic lubrication. *Friction* 1(3):195–209
- Etsion I, Sher E (2009) Improving fuel efficiency with laser surface textured piston rings. *Tribol Int* 42(4):542–547
- Fesanghary M, Khonsari MM (2012) Topological and shape optimization of thrust bearings for enhanced load-carrying capacity. *Tribol Int* 53:12–21
- Fesanghary M, Khonsari MM (2013) On the optimum groove shapes for load-carrying capacity enhancement in parallel flat surface bearings: theory and experiment. *Tribol Int* 67:254–262
- Fu G, Untaroiu A (2017) An optimum design approach for textured thrust bearing with elliptical-shape dimples using computational fluid dynamics and design of experiments including cavitation. *J Eng Gas Turbines Power* 139(9):092502
- Fu G, Untaroiu A (2018) The influence of surface patterning on the thermal properties of textured thrust bearings. *J Tribol* 140(6):061706
- Gachot C, Rosenkranz A, Hsu SM, Costa HL (2017) A critical assessment of surface texturing for friction and wear improvement. *Wear* 372:21–41
- Galda L, Pawlus P, Sep J (2009) Dimples shape and distribution effect on characteristics of Stribeck curve. *Tribol Int* 42(10):1505–1512
- Ghosh S, Abanteriba S (2016) Status of surface modification techniques for artificial hip implants. *Sci Technol Adv Mater* 17(1):715–735
- Grabon W, Pawlus P, Wos S, Koszela W, Wieczorowski M (2017) Effects of honed cylinder liner surface texture on tribological properties of piston ring-liner assembly in short time tests. *Tribol Int* 113:137–148
- Greco A, Raphaelson S, Ehmann K, Wang QJ, Lin C (2009) Surface texturing of tribological interfaces using the vibromechanical texturing method. *J Manuf Sci Eng* 131(6):061005
- Gropper D, Wang L, Harvey TJ (2016) Hydrodynamic lubrication of textured surfaces: a review of modeling techniques and key findings. *Tribol Int* 94:509–529
- Guo Z, Yuan C, Liu P, Peng Z, Yan X (2013) Study on influence of cylinder liner surface texture on lubrication performance for cylinder liner–piston ring components. *Tribol Lett* 51(1):9–23
- Hamilton DB, Walowit JA, Allen CM (1966) A theory of lubrication by microirregularities. *J Basic Eng Trans ASME* 88(1):177–185
- Han J, Fang L, Sun J (2011) Hydrodynamic lubrication of surfaces with asymmetric microdimple. *Tribol Trans* 54:607–615
- Holmberg K, Erdemir A (2017) Influence of tribology on global energy consumption, costs and emissions. *Friction* 5:263–284
- Ibatan T, Uddin MS, Chowdhury MA (2015) Recent development on surface texturing in enhancing tribological performance of bearing sliders. *Surf Coat Technol* 272:102–120
- Ismail S, Sarangi M (2013) Influence of texture orientation on the hydrodynamic lubrication. In: 1st International and 16th national conference on machines and mechanisms IIT Roorkee, India, Dec, pp 18–20
- Jesudass Thomas S, Kalaichelvan K (2018) Comparative study of the effect of surface texturing on cutting tool in dry cutting. *Mater Manuf Process* 33(6):683–694
- Kango S, Singh D, Sharma RK (2012) Numerical investigation on the influence of surface texture on the performance of hydrodynamic journal bearing. *Meccanica* 47(2):469–482

- Kango S, Sharma RK, Pandey RK (2014) Comparative analysis of textured and grooved hydrodynamic journal bearing. *Proc Inst Mech Eng Part J J Eng Tribol* 228(1):82–95
- Kim ES, Kim SM, Lee YZ (2018) The effect of plateau honing on the friction and wear of cylinder liners. *Wear* 400:207–212
- Kitahara S, Matsumoto T (1994) The present and future trends of wet friction materials. *Jpn J Tribol* 39:1020–1025
- Kligerman Y, Etsion I (2008) Analysis of the hydrodynamic effects in a surface textured circumferential gas seal. *Tribol Trans* 3:472–478
- Kligerman Y, Etsion I, Shinkarenko A (2005) A improving tribological performance of piston rings by partial surface texturing. *J Tribol* 127:632–638
- Kugimiya T (2000) Effect of additives of ATF and components of friction material for AT on  $\mu$ - $v$  characteristics. *Jpn J Tribol* 45:387–395
- Lee YH, Schuh JK, Ewoldt RH, Allison JT (2017) Enhancing full-film lubrication performance via arbitrary surface texture design. *J Mech Des* 139:053401–1
- Ligier JL, Noel B (2015) Friction reduction and reliability for engines bearings. *Lubricants* 3:569–596
- Lin C, Lee YH, Schuh JK, Ewoldt RH, Allison JT (2017) Efficient optimal surface texture design using linearization. *World congress of structural and multidisciplinary optimization, Braunschweig, Germany*, pp 633–647
- Lu X, Khonsari MM (2007) An experimental investigation of dimple effect on the stribeck curve of journal bearings. *Tribol Lett* 27(2):169
- Lu Y, Liu Y, Wang J, Liu H (2014) Experimental investigation into friction performance of dimples journal bearing with phyllotactic pattern. *Tribol Lett* 55(2):271–278
- Matsumoto T (1996) Influence of paper based friction material porosity on the practical performance of a wet clutch. *Jpn J Tribol* 41:816–821
- Meng FM, Zhang W (2018) Effects of compound groove texture on noise of journal bearing. *J Tribol* 140(3):031703
- Meng FM, Zhang L, Liu Y (2015) Effect of compound dimple on tribological performances of journal bearing. *Tribol Int* 91:99–110
- Nanbu T, Ren N, Yasuda Y, Zhu D, Wang QJ (2008) Micro-textures in concentrated conformal-contact lubrication: effects of texture bottom shape and surface relative motion. *Tribol Lett* 29(3):241–252
- Pal VK, Choudhury SK (2016) Fabrication of texturing tool to produce array of square holes for EDM by abrasive water jet machining. *Int J Adv Manuf Technol* 85(9–12):2061–2071
- Patel D, Jain VK, Ramkumar J (2018) Micro texturing on metallic surfaces: state of the art. *Proc Inst Mech Eng Part B J Eng Manuf* 232(6):941–964
- Pettersson U, Jacobson S (2006) Tribological texturing of steel surfaces with a novel diamond embossing tool technique. *Tribol Int* 39(7):695–700
- Qiu M, Delic A, Raeymaekers B (2012) The effect of texture shape on the load-carrying capacity of gas-lubricated parallel slider bearings. *Tribol Lett* 48(3):315–327
- Qiu M, Minson B, Raeymaekers B (2013) The effect of texture shape on the friction coefficient and stiffness of gas-lubricated parallel slider bearings. *Tribol Int* 67:278–288
- Rahmani R, Rahnejat H (2018) Enhanced performance of optimized partially textured load bearing surfaces. *Tribol Int* 117:272–282
- Rahmani R, Mirzaee I, Shirvani A, Shirvani, H (2010a) An analytical approach for analysis and optimization of slider bearings with infinite width parallel textures. *Tribol Int* 43(8):1551–1565
- Rahmani R, Shirvani A, Shirvani H (2010b) Optimised textured surfaces with application in piston-ring/cylinder liner contact. *Woodhead Publishing*, pp 470–517
- Ren N, Nanbu T, Yasuda Y, Zhu D, Wang Q (2007) Micro textures in concentrated-conformal-contact lubrication: effect of distribution patterns. *Tribol Lett* 28(3):275–285
- Ronen A, Etsion I, Kligerman Y (2001) Friction reducing surface texturing in reciprocating automotive components. *Tribol Trans* 44(3):359–366



- Ryk G, Kligerman Y, Etsion I (2002) Experimental investigation of laser surface texturing for reciprocating automotive components. *Tribol Trans* 45(4):444–449
- Ryk G, Kligerman Y, Etsion I, Shinkarenko A (2005) Experimental investigation of partial laser surface texturing for piston rings friction reduction. *Tribol Trans* 48:583–588
- Schneider J, Braun D, Greiner C (2017) Laser textured surfaces for mixed lubrication: influence of aspect ratio, textured area and dimple arrangement. *Lubricants* 5(3):32
- Schuh JK, Ewoltdt RH (2016) Asymmetric surface textures decrease friction with Newtonian fluids in full film lubricated sliding contact. *Tribol Int* 97:490–498
- Shamsul Baharin AF, Ghazali MJ, A Wahab J (2016) Laser surface texturing and its contribution to friction and wear reduction: a brief review. *Ind Lubr Tribol* 68(1):57–66
- Shen C, Khonsari MM (2013) Effect of dimple's internal structure on hydrodynamic lubrication. *Tribol Lett* 52(3):415–430
- Shen C, Khonsari MM (2015) Numerical optimization of texture shape for parallel surfaces under unidirectional and bidirectional sliding. *Tribol Int* 82:1–11
- Shin M, Kwon S, Chung S, Kwon S, Park J, Kim J, Choi W (2015) Characteristic of friction on texturing bearing steel with ultrasonic hole machine 31(1):21–27
- Shinde AB, Pawar PM (2017a) Effect of partial grooving on the performance of hydrodynamic journal bearing. *Ind Lubr Tribol* 69(4):574–584
- Shinde AB, Pawar PM (2017b) Multi-objective optimization of surface textured journal bearing by Taguchi based Grey relational analysis. *Tribol Int* 114:349–357
- Siripuram RB, Stephens LS (2004) Effect of deterministic asperity geometry on hydrodynamic lubrication. *J Tribol* 126:527–534
- Stepien P (2008) Mechanism of grinding wheel surface reproduction in regular surface texture generation. *Surf Eng* 24(3):219–225
- Tala-Ighil N, Fillon M (2015) A numerical investigation of both thermal and texturing surface effects on the journal bearings static characteristics. *Tribol Int* 90:228–239
- Tala-Ighil N, Fillon M, Maspeyrot P (2011) Effect of textured area on the performances of a hydrodynamic journal bearing. *Tribol Int* 44(3):211–219
- Uddin MS, Liu YW (2016) Design and optimization of a new geometric texture shape for the enhancement of hydrodynamic lubrication performance of parallel slider surfaces. *Biosurf Biotribol* 2(2):59–69
- Wakuda M, Yamauchi Y, Kanzaki S, Yasuda Y (2003) Effect of surface texturing on friction reduction between ceramic and steel materials under lubricated sliding contact. *Wear* 254(3–4):356–363
- Wang L (2014) Use of structured surfaces for friction and wear control on bearing surfaces. *Surf Topogr Metrol Prop* 2(4):043001
- Wang W, He Y, Zhao J, Li Y, Luo J (2017) Numerical optimization of the groove texture bottom profile for thrust bearings. *Tribol Int* 109:69–77
- Wang W, He Y, Zhao J, Mao J, Hu Y, Luo J (2018a) Optimization of groove texture profile to improve hydrodynamic lubrication performance: theory and experiments. *Friction* 1–12
- Wang X, Shi L, Huang W, Wang X (2018b) A multi-objective optimization approach on spiral grooves for gas mechanical seals. *J Tribol* 140(4):041701
- Wang W, He Y, Li Y, Wei B, Hu Y, Luo J (2018c) Investigation on inner flow field characteristics of groove textures in fully lubricated thrust bearings. *Ind Lubr Tribol* 70(4):754–763
- Yagi S, Katayama N, Hasegawa H, Matsushita H, Okhihara S, Kusumoto T, Tsuboi A (2015) Effect of microscale texture on the tribological behavior of paper-based friction materials for a wet clutch. *Tribol Online* 10:390–396
- Yamaguchi K, Takada Y, Tsukuda Y, Ota M, Egashira K, Morita T (2016) Friction characteristics of textured surface created by electrical discharge machining under lubrication. *Procedia CIRP* 42:662–667
- Yu H, Wang X, Zhou F (2010) Geometric shape effects of surface texture on the generation of hydrodynamic pressure between conformal contacting surfaces. *Tribol Lett* 37(2):123–130
- Yu H, Deng H, Huang W, Wang X (2011) The effect of dimple shapes on friction of parallel surfaces. *Proc Inst Mech Eng Part J J Eng Tribol* 225(8):693–703

- Yu R, Li P, Chen W (2016) Study of grease lubricated journal bearing with partial surface texture. *Ind Lubr Tribol* 68(2):149–157
- Zhan J, Yang M (2014) Investigation on the application of YAG laser texturing technology to the cylinder wall of auto engine. *Ind Lubr Tribol* 66(3):387–392
- Zhang H, Dong GN, Hua M, Chin KS (2017) Improvement of tribological behaviors by optimizing concave texture shape under reciprocating sliding motion. *J Tribol* 139(1):011701
- Zhang H, Hafezi M, Dong G, Liu Y (2018a) A design of coverage area for textured surface of sliding journal bearing based on Genetic Algorithm. *J Tribol* 140(6):061702
- Zhang H, Liu Y, Hua M, Zhang DY, Qin LG, Dong GN (2018b) An optimization research on the coverage of micro-textures arranged on bearing sliders. *Tribol Int* 128:231–239

# Chapter 16

## Applications of Tribology on Engine Performance



Sangeeta Das  and Shubhajit Das 

**Abstract** The improvement of engine efficiency has been of utmost necessity for automobile industries in order to control the increasing climate change and greenhouse emissions. Hence, the fuel efficiency may be increased by minimizing the energy losses from the engine. In spite of wide applications of reciprocating internal combustion (IC) engines in most of the ground and sea transport vehicles and electrical power generations, they have several shortcomings. The IC engines possess low thermal and mechanical efficiencies due to increased loss of fuel energy as heat and friction. They also release a substantial amount of particulate and NO<sub>x</sub> (nitrogen oxide) emissions that gives rise to greenhouse effect. Amongst the various approaches of improving engine efficiency, the tribologists and lubrication engineers focused mainly on reduced engine friction as a vital and economic method. The achievement of efficient lubrication of moving engine components with least or no unfavorable effect on the environment is important to lessen friction and wear. The improvements in different tribological engine components and additives may lead to reduced fuel consumption, exhaust emissions and maintenance along with increased engine power outputs and durability. The tribological performance of an engine can be improved by employing materials of superior tribological properties for manufacturing different mechanical parts, improved surface coatings as well as developed lubrication technologies. This chapter presents the details of various components of reciprocating IC engines as well as the lubricants used and the remedial measures to reduce the engine wear and friction.

**Keywords** Internal combustion engine · Tribology · Engine efficiency

---

S. Das (✉)

Department of Mechanical Engineering, Girijananda Chowdhury Institute of Management and Technology, Guwahati, Assam 781017, India  
e-mail: [sangeeta\\_me@gimt-guwahati.ac.in](mailto:sangeeta_me@gimt-guwahati.ac.in)

S. Das

Department of Mechanical Engineering, National Institute of Technology, Yupia, Arunachal Pradesh 791112, India

© Springer Nature Singapore Pte Ltd. 2019

J. K. Katiyar et al. (eds.), *Automotive Tribology*, Energy, Environment, and Sustainability, [https://doi.org/10.1007/978-981-15-0434-1\\_16](https://doi.org/10.1007/978-981-15-0434-1_16)

307

## 16.1 Introduction

In today's world, the automotive engine technology is mainly governed by two factors, viz. environmental safety and consumer gratification (Nakada 1994). Hence, the development in the field of automobile industry takes place based on the compatibility between efficient energy use, safety measures and environmental impacts. Due to increased environmental and safety issues, there exists various strict standards for fuel efficiency, emissions, safety and durability. However, the ever-increasing consumer demands on greater trustworthiness, reduced maintenance, better comfort and reduced fuel consumption leads to the developments of newer technologies for better fuel economy that satisfies both consumer and environmental issues.

The fuel efficiency can be increased and the amount of fuel required to drive a vehicle can be decreased by minimizing the energy losses from the vehicle. The engine performance is optimized by improving its tribological performance to improve fuel efficiency as most of the energy is lost from the engine itself. The different tribological engine components involving interacting surfaces are bearings, pistons, transmissions, clutches, gears, wiper blades, tyres and electrical contacts. Moreover, good lubrication between moving and interacting parts of an engine helps in improving the performance of an internal combustion (IC) engine. Recently, nano lubricants are an emerging technology in the field of automotive lubricants. The lubricants must be able to resist high temperatures, and be stable under engine conditions. There is a requirement of new tribo-materials for automotive components that runs at higher temperatures and pressures. Furthermore, the tribological behavior of existing materials for various tribo-components can be improved by means of surface coating.

## 16.2 Automotive Tribology and Its Importance

The major power units in most petrol and diesel engines are the reciprocating IC engines because of its extreme reliability and versatility characteristics. In spite of this, it has several drawbacks that may influence the national and international economies. The drawbacks are low thermal and mechanical efficiencies of the IC engines due to loss of a significant fraction of the energy of fuel as heat (Taylor 1998). As a result, a large amount of fuel needs to be consumed to overcome the losses that lead to the emission of enormous harmful particulates, nitrous oxide and hydrocarbon and can cause greenhouse effect. The mechanical losses are mainly due to the frictional losses between the piston rings and the cylinder liner assembly. The most of the chemical energy of the fuel gets converted into thermal energy and then to mechanical energy in the cylinder and piston assembly of the IC engine (Kumar et al. 2018). A little wear of material from the moving parts in IC engines can decrease the performance or even entire breakdown of the engine. The consumption of 12–13 MBBL/day of oil by nearly 250 million of vehicles on US road is lost in overcoming engine friction (~10%) and friction in the driveline (~5%). Thus,

the petroleum consumption can be reduced from 150,000 to 200,000 BBL/day by reducing the engine and driveline friction by 10% (Fenske 2014). Hence, the concepts of tribology need to be developed to lessen the coefficient of friction (COF) and wear at the interfaces of various moving components of an IC engine.

The theories of tribology can be used to deal with a minor problem that may arise at the level of structural integrity of the moving parts of an IC engine. Otherwise, the consequences of the damage of the moving components itself may lead to the entire failure of the engine. A significant development in tribology leads to systematic design and performance analysis based on the stress-strain study of the various moving components of an IC engine. At present, the engine components are not required to be lubricated with oil or grease very often and that has been possible due to the proper understanding of the working of the tribological components and their design analysis. It is achievable due to the better understanding of the effect of viscosity and the mechanism of generation of effective lubricant film thickness between the moving contacts. The tribology can be successfully applied to each and every engineering component in moving contact and hence can be used for enhancing the performance of engines. The benefits of improved tribological performance includes low fuel intake, high engine output, reduced harmful exhaust emissions and maintenance to design highly durable and reliable engines.

### 16.3 Components of IC Engine Subjected to Friction and Wear

The stringent government regulations for fuel emission and economy have motivated the need for engine friction mechanism research aiming for higher efficiency, reliability and performance. An engine's mechanical efficiency is directly compromised by frictional losses, since power is wasted to overcome friction within the engine. Thus, it is important to reduce the engine friction which will lead to increase the fuel economy. The IC engine manufacturers encounter complex design considerations due to change in engine components temperature. During operation, the engine components become relatively hot due to friction and combustion of gases within the cylinders. The lubrication conditions also change due to change in oil viscosity. In an IC engine, out of all the energy losses, frictional loss alone is in the range of 4–15% (Kumar et al. 2019). A large amount of fuel energy is wasted in the form of heat losses. The mechanisms that cause mechanical loss in engines include piston-crank mechanism, piston ring-cylinder-liner fuel pump and other auxiliary assemblies. The numerous parts of the IC engine rely mainly on the interaction of their surfaces to function. These includes many tribological components such as bearings, pistons, clutches, gears, transmissions, wiper blades, tires and electrical contacts. The losses contributed by different engine components are shown in Fig. 16.1.

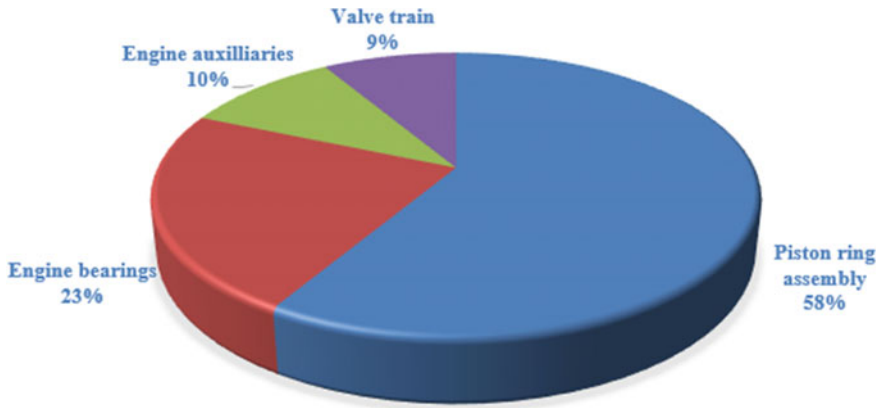


**Fig. 16.1** Approximate quantities of losses in different engine components

### 16.3.1 Piston Rings

One of the important elements in the IC engine are the piston rings. The sliding surfaces between the piston rings and the cylinder liners may be among the most complex tribological phenomena in the IC engines. It is even more severe with an increase of the engine power. The piston assembly comprises sliding between the cylinder walls and the reciprocating piston and also sliding between the piston pin and the piston bore. The friction between the piston rings and the cylinder liners significantly contribute to the mechanical power losses of the engine. Sliding between piston ring and cylinder wall is often said to be the largest contributor to frictional energy losses (Rosenberg 1981; Wong and Tung 2016). It is also the contact where the wear problem called scuffing sometimes occur in the marine low speed, two-stroke engines. A piston ring acts as a dynamic seal as it slides against the wall of the cylinder bore. The main function of the piston rings is to facilitate smooth running of the reciprocating parts. It aids to prevent the escape of the combustion gases into the crankcase from the combustion chamber. It also prevents leakage of the lubricating oil into the combustion chamber from the crankcase. To keep friction and wear low, the seal is normally lubricated. The lubrication should be controlled such that excessive oil does not remain on the walls as it leads to high oil consumption due to evaporation and combustion. Also, there is transfer of heat by the rings from the piston to the liners which stabilizes the piston in the cylinder bore. Loss of energy to friction between piston ring and cylinder liner constitutes 20–40% of total mechanical losses and is regarded as the greatest mechanical loss (Cakir and Akcay 2011).

Friction is important in terms of engine efficiency and fuel economy. The kinetic energy that is lost due to friction is mainly converted into heat that is conducted away. It also results in vibration and emission of sound, both leading to dissipation of energy. Some of the energy is converted within the material surfaces and wear debris by plastic deformation, material intermixing and tribo-chemical reactions. In

an IC engine, the sliding velocity, load and viscosity are dynamic and change rapidly. Other parameters like piston ring shape, surface topography, oil availability, ignition timing, secondary motions of the piston and piston rings and properties of the surface layers affect the mode of friction level. The strongest wear of the cylinder liners takes place on top of the piston ring, where the chemical, thermal, erosive, abrasive and adhesive conditions are the severest. At low cylinder surface temperatures, the tribo-chemical wear of the cylinder liner increases drastically due to increase in Sulphur content of the fuel. There are five forms of wear that occur in IC engine components namely abrasion, adhesion, fatigue, corrosion and lubrication breakdown. Abrasion, adhesion and fatigue involve mechanical damaging of surfaces. The wear rate in the piston ring/cylinder wall is generally in the range of nm/hour, which is comparatively very low (Shakhvorostov et al. 2006; Scherge et al. 2006; Dienwiebel et al. 2007). If hard particles get into the lubricating oil, abrasion can lead to high wear rates.

Adhesion is that part of the wear leading to material being moved around rather than removed. Adhesion is also part of scuffing failure, although the scuffing procedure is more complex than only adhesion. Tribo-chemical wear or corrosion is also important especially in the marine engine running on heavy fuel oil, which has a high sulphur content leading to high levels of sulphuric acid in the combustion chamber. Decreasing the friction in the piston assembly is an important way of improving the mechanical efficiency. A 10% reduction in mechanical losses can reduce fuel consumption by 1.5–2.5% (Andersson 1991; Mishra et al. 2009). With increase in the engine power, the tribology of the sliding surfaces of piston rings and cylinder shows extremely complicate phenomena. Due to dynamic operating conditions in IC engines, changes occur in the lubrication regime depending on the position of the piston in the cylinder. When the piston changes direction, at dead center, the friction coefficient increases due to zero piston speed. The hydraulic lubrication regime changes to mixed lubrication or limit lubrication regime. Cold starting, speed changes, sudden loads are some of the factors which cause changes to the lubrication regime in IC engines (Taylor 1993; Priest and Taylor 2000). It is always preferred to have a hydrodynamic oil film at the interface between the rings and the liners as the performance, durability and exhaust emissions are greatly affected by it.

Wear of the cylinder liner is caused to a great extent by the action of the piston rings. A higher friction coefficient in IC engines also increases loss of material due to wear of component surfaces. The wear of piston rings and cylinder liner increases due to three body abrasive wear caused by the presence of small amount of solid particles in the lubricating oil, which are added by component wear, ambient air dust particles and contaminants from the oil sump or combustion chamber. A good lubricating property of fuel plays an important role in reducing wear and friction losses. Strong adhesive forces between the piston rings and liner occur due to inadequate lubrication, leading to high frictional losses and metal scuffing, resulting in high wear. Apart from sliding wear, piston ring surfaces degrade due to blow by of hot gases from the high temperature combustion chamber, which carry soot along with them. Improving the lubricating properties of the fuel will reduce the mechanical friction losses within the fuel pump.

### 16.3.2 *Journal Bearings*

Engine bearing performance is affected mainly by mechanical configuration and hydrodynamics of the oil film. In plain journal bearing, the hard shaft rotating in a soft bearing shell are separated by a lubricant. The journal bearings mainly operate in pure hydrodynamic lubrication regime for increased life span. But then, in present automobile industry, there is a necessity of fuel consumption and emissions due to restrictions by legislation and customer satisfaction. Studies suggest the journal bearings must be operated in the transition between pure hydrodynamic lubrication and mixed lubrication regime to reduce friction coefficient. However, this may lead to wear and durability problems due to metal-metal contact. Thus, efficient journal bearings can be designed using simulation approach that can describe complex behavior of mixed elasto-hydrodynamic lubrication for a wide range of operating conditions (Sander et al. 2016). Journal bearings including those of the connecting rods, camshaft and crankshaft are affected by dust particles. The hard contaminant particles, which get into the clearance between the journal and the bearings, are pressed by the harder surface into softer surface leading to abrasive wear. The particle size has a major effect on the wear of the engine bearings. The most severe wear in the bearing is caused by particles with sizes in the range from 10 to 35  $\mu\text{m}$ . The bearing location affects the wear rate in connecting rod bearings. A reduction in the sliding surface area of the crankshaft or connecting rod bearings or increasing bearing clearance will reduce engine friction. However, these methods increase the possibility of wear, seizure or knocking in the bearings.

In recent trends, the engine downsizing leads to smaller engines and its components that results in higher stresses on the components and the lubricated contacts. For example, the big-end bearing of the connection rod has to withstand specific loads above 100 MPa that may expect to increase in future. As a result, the lubrication gap in journal bearing decreases below 1  $\mu\text{m}$  that may cause metal to metal contact. With the increasing use of start-stop cycle, the bearing wear accelerates as the bearing has to overcome the boundary and mixed lubrication regime at the starting of the engine before a hydrodynamic film has formed (Sander et al. 2016). The prediction techniques used in engine bearing has been improved in recent years due to augmented computing power and precise methods that directly benefits the designer. Due to this, more realistic bearing conditions can be considered and better bearing performance prediction is possible. The use of computer aids in presenting data in an improved way for good interpretation of the results (Martin 1983). The journal bearing design approaches to reduce power loss and increase load carrying capacity include artificial texturing, axial and circumferential grooves and bushing specific shapes (e.g. three-lobe bearings) (Bompos and Nikolakopoulos 2016). Ghorbanian et al. (2011) studied a problem of complex hydrodynamic modeling of journal bearings in IC engines along with an optimization process described by numerous variables and constraints that are to be parallelly modified and satisfied.



A ratio of bearing length  $L$  and bearing internal diameter  $D$  in the range of 0.4–0.6 is normally preferred for dynamically loaded bearings. This is because any value below this range will cause excessive loss of lubricants from the ends of the bearings. On the other hand, any value above this range may result in alignment problem that may lead to edge loading. With high value of diametral clearance, there occurs a reduction in load carrying capacity, oil whirl, excessive damage due to cavitation erosion, etc. In contrast to this, a low diametral clearance value restricts the quantity of oil flow in the bearing that increases the lubricant temperature and reduces its viscosity that in turn reduces the film thickness. In actual practice, it is impossible to achieve an ideal single clearance value due to inevitable limitations in manufacturing processes. Hence, the engine bearing must be designed for maximum and minimum values of clearance (Hirani et al. 1999). In practice, impairment of a bearing may often be the outcome of several mechanisms operating concurrently. The related literature and real-world experience show that the plain bearing damages are mainly triggered by wear, either as a direct cause or as a result of various anomalies in design, manufacture, assembly, operation and maintenance of the engine and bearings. The wear is a very complex process originated by the act of different mechanisms, and can be established by different wear types which are often related: adhesive wear, abrasive wear, surface fatigue wear, erosive wear, cavitation wear, fretting wear, oxidative wear and corrosive wear (Vencl and Rac 2014).

### ***16.3.3 Valve Train***

The operating conditions of modern engine valve trains are becoming severe due to design alterations driven by different parameters like increased fuel economy, environmental policies and higher output. The valves damage during operation due to abrasive wear of the seat face and the stem, stem corrosion, damage of the seat face caused by products of combustion, damage of the seat face caused by blobby exhaust gases and burning, bursting of the seat face, and breakage of the valve head or the stem. These types of damage arise due to physicochemical interactions of the working medium at high temperature. They are also the result of mechanical stresses caused by the occurrence of excessive temperature gradients (Siczek 2016). In conventional engine design, the cam and follower slide over each other under the boundary lubrication condition. At low camshaft speed, valve train friction can contribute significantly to overall engine friction. To reduce the cam and follower wear, roller followers were used instead of slipper type of followers in some of the production engines. Valve train design with the roller follower type is now becoming popular in order to reduce friction in valve trains where the friction is reduced by half. The performance of roller follower valve train is subjected to rotational efficiency of rollers that is mainly governed by oil film thickness. The best way to reduce the friction at cam/tappet interface is to replace the conventional flat faced tappet with roller followers (Khurram et al. 2019). In a valve train, the valve spring load can be decreased by reducing the mass of the reciprocating part. Reducing the spring

load reduces friction because of the lower surface pressure between the cam and the follower. In direct acting valve train, poor lubrication results in asperity contact which leads to higher frictional heating of material surfaces resulting in polish wear and scuffing of the tribological components (Dyson and Naylor 1960). The performance of the valve train is also affected due to temperature rise in cam contact area. The rolling motion of roller in the roller follower valve train ensures better lubrication which results in reduced friction force and wear (Chiu 1992; Ji and Taylor 1998).

A valve train system consisting of various contacting parts with interactions governed by different phenomena. Thus, requirement for a relevant prediction is an integrated model of the inertial dynamics (usually expressed in Lagrangian or Newton–Euler formulation), tribology (governed by Reynolds equation), contact mechanics, surface characteristics and physical chemistry of the lubricant. This method is commonly referred to as multi-physics. From tribological point of view, one type of solution includes the solution of Reynold's equation that includes accurate prediction of dynamic behavior of the mechanism. The correct application of this approach has proven to be very accurate although any simulation is time consuming and requires advance computer programming skills. In the second approach, the behavior of the tribological concurrences is predicted using extrapolated oil film thickness formulae. This include equations obtained through regression of numerical studies that correlates the applied load, entrainment velocity, lubricant viscosity and mechanical properties of contact surfaces for different contact geometries and oil film thickness. In spite of various limitations due to simplifying assumptions, such formulae are relatively easy to use that gives relatively accurate and quick results (Teodorescu 2010).

The total valve train energy loss is the sum of the friction energy consumed by all its individual components. A typical valve train system consists of cam, tappet, pushrod, rocker-arm, valve and spring. The major losses occurring in the valve train shown in Fig. 16.2 includes losses between cam and tappet (1), between the tappet and its bore (3), in the rocker arm bearing (5), between the valve stem and the valve guide (7) and in the camshaft bearings. The friction forces at the two ends of the push rod (2, 4) and the friction between the valve stem top and the rocker arm end (6) are much lower than in the other components. They appear as a residual term in the overall balance of frictional losses (Teodorescu 2010).

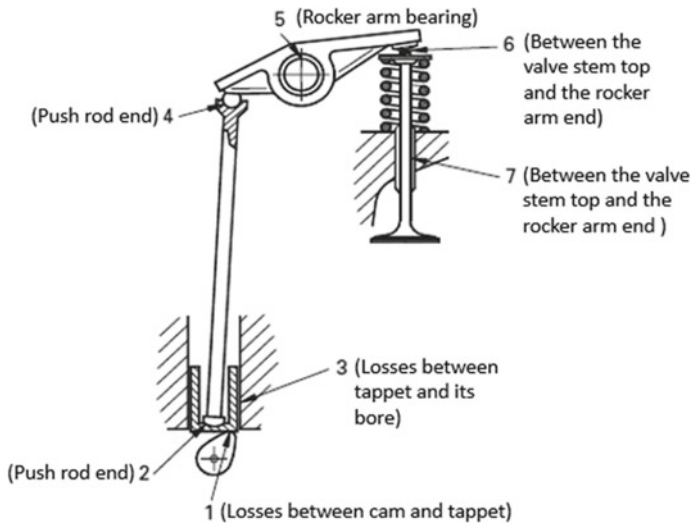


**Fig. 16.2** Schematic of the push rod valve train and the major components of the friction losses (Teodorescu 2010)

## 16.4 Tribological Improvements of IC Engine

The improvement in automobile industry is mainly focused to satisfy customer's needs like better fuel economy and strict regulations of government for environment security. This can be achieved through the knowledge of tribology that can be applied to control frictional losses, wear and fuel consumption. Tribological study can be adopted to develop new engine oils with low or no sulphur, phosphorus and ash content for reduction of harmful emissions or to develop new surface materials with less or no dependence on sulphur and phosphorus containing oils (Komvopoulos et al. 2003). A small improvement in engine efficiency, emission level and durability make a vehicle more reliable having major effect on world economy and environment in the long run in future (Taylor 1998). Improved tribological performance can be achieved in three ways: enhancing the tribological properties of the materials used for the mechanical parts; coating surfaces to improve tribological behavior; or developing lubricants that improve tribological behavior. In order to achieve low fuel consumption and high engine reliability in automobile industry, the tribology study can be successfully implemented in reducing engine friction and engine size, hybridization and developing new engine combustion methods.

### 16.4.1 Engine Friction Reduction

The friction in the engine components can be reduced by various methods that may cause serious tribology related problems. These problems need to be addressed before applying the methods to engine design to reduce engine friction (Nakada 1994). The methods of friction reduction along with their problems are shown in Table 16.1. The three most important methods to reduce friction and wear in an engine are (i) mechanical design of micro geometries and major components like power cylinder, bearings and valve trains, (ii) surface and material engineering and coatings and (iii) lubricant and additive technologies (Wong and Tung 2016).

#### Component materials and system design

The automotive design is directly or indirectly related to value engineering. The main motive of a designer in designing any moving part of an IC engine is to meet the required functions (components life, noise and vibration, oil consumption, weight, etc.) simultaneously minimizing its cost. A component with improved performance might be adopted instead of its higher manufacturing cost. Besides these, the additional requirement of an engine design engineer is engine's reliability. In earlier days, tribological failure was a common problem. However, in modern automotive industry, there is no scope for poor reliability as consumer's expectations are considerably increasing (Adam's 2010). The various technological developments in automobile industries requires innovative system designs for the tribo-components to function well under more severe conditions. There is a necessity of development of new materials for different tribo-components that can be operated at high temperature, pressure and velocity (Enomoto and Yamamoto 1998). The knowledge of applied tribology is essential for design engineers to continuously improve a product as well as to critically assess supplier designs in automobile industry. Tribology can be applied to the design process at the very beginning by using improved design tools and methods. Design guides and computer programs are the main tribological design tools to calculate the parameters affecting performance of various components. Design

**Table 16.1** Friction reduction methods and their related problems (Nakada 1994)

Components	Methods of friction reduction	Problems
Piston	Reduction of weight and sliding surface, surface treatment on piston skirt	Increased oil consumption, wear, seizure, slap noise; low reliability
Piston ring	Surface treatment and reduction in tension	Increase in oil consumption and decrease in reliability
Valve train bearing (crank and connecting rod)	Reduction of weight and sliding surface	Increased oil consumption, wear, seizure, slap noise; poor reliability
Engine oil	Low viscous oil with additives	Increased wear and seizure

guides aid in setting limits on physical dimensions, materials, stress levels etc. that are required in designing a component. Computer methods like finite element analysis can be successfully applied to the distortion and stresses of various components such as cylinder block and connecting rod (Willermet 1989).

From the viewpoint of materials, most of the primary structures in IC engine are made of easily available metallic elements like iron and aluminum (Becker 2004). Conventionally, an engine cylinder block subjected to maximum friction loss is made up of heavy cast iron. In order to reduce weight in automobiles, most of the metal structures are replaced by cheaper and corrosion resistant polymer components (Friedrich 2018). In recent days, an aluminum alloy engine block with or without cast iron cylinder liner insert is popularly used for passenger cars (Enomoto and Yamamoto 1998). Aluminum alloy 390 having high silicon content are used to manufacture cylinder blocks due to their good wear resistant property in spite of poor machinability. One of the major tribo-components that contribute to engine friction is piston skirt to cylinder block interface. The clearance between the piston and the engine block should be small enough to reduce vibration and noise. On the other hand, there should be adequate clearance between the two to prevent seizure. The advantage of using cast aluminum as a piston material is light weight to reduce engine vibration and high thermal conductivity to prevent piston overheating. In contrast, the high thermal expansion coefficient of aluminum makes the piston cylinder arrangement too loose at low temperature that had appropriate clearance at operating temperature. Hence, aluminum alloy containing copper and nickel is used that possesses low thermal expansion coefficient than pure aluminum but higher than cast iron. At present, the upper compression rings are made up of either nitrided stainless steel or molybdenum coated cast iron as they are subjected to severe wear in comparison to lower rings (Becker 2004). The advantage of using Cr–N ion plating having low friction coefficient ( $\sim 0.01 - 0.015$ ) is that the wear of the top piston ring is reduced by 90% and that of cylinder bore is reduced by 15% in comparison to conventional Cr plated ring (Enomoto and Yamamoto 1998).

The cylinder heads that are generally made of cast aluminum cannot withstand the high temperature and loads at the valve seating area. This can be resolved by inserting a valve seat, made up of steel containing one or more element like cobalt, chromium, vanadium etc. and medium to high carbon (0.5–3 wt%), into the cylinder head. Generally, the cam shafts are made of gray cast iron with induction or flame hardened cam lobes and the lifter surface is made of hardened cast iron or hardened steel. Also, powder metal for cam lobes and ceramics for lifter surface can be a viable alternative. The journal bearing and the shaft should simultaneously be hard and soft for better embeddability of small particles to remove them from coming into contact (Becker 2004). The problem of seizure in bearing due to wear and reduced oil thickness can be overcome by improving the topography of the plated surface and dispersion of fine hard particles in a plated layer. The wear resistance of bearing can be considerably improved by dispersing  $\text{Si}_3\text{N}_4$  fine powder in Pb–Sn–In composite electro-plating and Co hard powder in Cu–Sn–Pb alloy (Enomoto and Yamamoto 1998).

## Surface engineering

The recent trends in IC engine include the improvement in surface structures with suitable coatings instead of earlier trend of using monolithic materials to minimize frictional losses. The friction between the sliding pairs can be significantly reduced by surface texturing such as dimple, groove and mesh pattern textures. The different surface texturing techniques are mechanical milling or shot blasting, photolithography, etching, laser beam processing, pellet pressing etc. (Yan-qing et al. 2009). Initially, the concept of lubrication mechanism is nothing but providing reserved oil in different surface textures. Hence, the inside of the cylinders of combustion engines was designed with cross-hatch pattern by honing process for not less than 60 years. The micro-irregularities help in achieving improved hydrodynamic pressure that increases the load carrying capacity of the surfaces (Yan et al. 2010). Yu et al. (2011) studied the effect of dimples of different shapes, viz. circle, square and ellipse, on the tribological performance of surface texture and found that the elliptical dimples showed the best friction reduction effect.

Studies revealed that a large amount of heat generated in the combustion chamber of IC engine is absorbed by piston and the walls of the combustion chamber that reduces its performance. This situation can be overcome by using thermal barrier coating that reduces the heat loss which in turn helps in burning the un-burnt gases to reduce pollution in exhaust gases (Dhomne and Mahalle 2018). Titanium alloys can be a competent light weight material for automotive applications due to its high strength, low density and excellent corrosion resistance. But at high temperatures, the engine components are subjected to oxidation, creep and thermal fatigue. Especially, the engine valves frequently strike the seat inserts, at hot environment of combustion gases  $\sim 500^\circ\text{C}$ , that are subjected to short distance sliding contact leading to localized wear. The development of tribolayer is expected to reduce the intensity of wear. The weight of Ti alloy valves is 45% less than the stainless steel valves that increases the engine speed and reduces vibration and noise. Instead of great importance of Ti alloy such as Ti-6Al-4V in automobile industry, it is subjected to oxidational wear at low sliding speed and metallic wear at high sliding speed. Hence, various surface engineering methods like physical vapour deposition of Ti alloy coating, chemical vapour deposition of carbon based polycrystalline diamond coating, ion implantation with nitrogen and oxygen and thermal oxidation. Amongst these techniques, the thermal oxidation method can be implemented at a lower cost for mass production (Lou and Alpas 2019). Some of the hard antiwear coatings are diamond-like carbon (DLC), boron nitride (BN), silicon carbide (SiC), titanium nitride (TiN), tungsten carbide (WC), etc. (Zhmud 2011). Mutafov et al. (2014) observed that tungsten doped DLC coating on laboratory samples and valve lifter possess good adhesion and hardness nearly 15 GPa. The coating showed excellent wear resistance in pin-on-disc and engine testing due to the formation of thin solid tribolayer of 2–4 nm on the coating surface.

### Lubrication and additive technology

The engine lubricants are basically used to make the engine more durable, to improve fuel economy and to reduce emission level. In order to increase engine's durability, the lubricant must prevent wear through hydrodynamic lubrication or by using anti-wear additives and inhibit corrosion formed by oil degradation or its contamination by combustion gases and unburnt fuel (Howard 2014). The introduction of nanoparticles to engine oils improves the tribological behavior of IC engine due to rolling, mending and polishing effect and formation of protective film as shown in Fig. 16.3. The spherical nano particles act as rollers for the two sliding surfaces as well interacts with the friction surfaces to form a protective film between them. Also, the nanoparticles form physical tribo-film by depositing on the friction surfaces to reduce mass loss and reduce the roughness of the rubbing surfaces by their abrasiveness property (Ali and Xianjun 2015). Darminesh et al. (2017) reviewed the present status of biodegradable nanolubricant possessing improved properties. Several surface-active anti-wear additives like zinc dialkyldithiophosphate (ZDDP), antiscuff phosphorus and sulphur improves the friction and wear behavior due to chemical reactions with the surfaces forming cohesive anti wear tribochemical films. The regeneracy and stability of a tribofilm at high loads and temperatures are the key factors in determining its efficiency and persistence (Komvopoulos 2003).

In addition, the lubricant must possess low viscosity to minimize power loss due to viscous drag and hence increase efficiency. Tormos et al. (2017) made a comparative fuel consumption test of low viscosity engine oil (LVEO) on an urban compressed natural gas buses fleet and tribometers. They found reduced fuel consumption in fleet test and reduced friction in tribometers due to the application of LVEO. The fuel economy can be improved by using friction modifier additives that are long molecules with polar head groups that attach to the metal surface to make the surface more slippery in boundary lubrication. The engine efficiency can be increased by better handling of oxidation and contaminants with lubricants to maintain a viscosity profile which provides the required film strength for protection. The use of

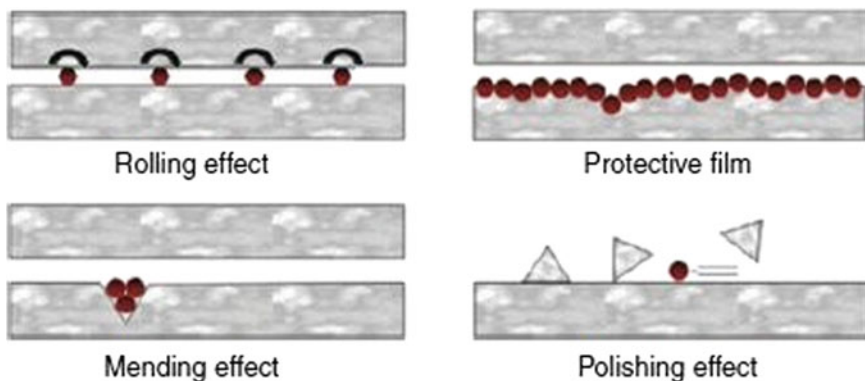


Fig. 16.3 Mechanism of lubrication of nanolubricants (Ali and Xianjun 2015)

anti-oxidant additives in lubricants can reduce oxidation and dispersants within the additives reduce contamination. Engine's good emission performance is possible due to lubricant's ability to prevent wear and deposits along with several after treatment methods, viz. particulate filters, NO<sub>x</sub> adsorbers and selective catalytic reduction (SCR) systems (Howard 2014).

### 16.4.2 Hybridization and Engine Downsizing

Engine downsizing means employing smaller engines in a vehicle that provides the same power as that of larger engines using recent technologies. It involves the reduction of engine size by reducing the number of cylinders and the displacement. It is one of the viable methods to improve fuel economy and combustion by reducing friction and automobile weight. In spite of having advantageous properties, engine downsizing can have certain drawbacks like poor acceleration, lowered maximum speed and smaller internal space. Nozawa et al. (1994) performed a numerical simulation to assess the consequences of engine downsizing on the frictional losses and fuel ingestion of automobiles by making use of simplified models for friction and combustion. They observed an improvement in fuel economy and an existence of optimal engine displacement due to engine downsizing.

Engines are said to be downsized when they possess high load levels. Hence, downsized engine possesses high power density and/or high full load mean pressures and specific full load torque. The engine power density  $P_e/V_H$  is given by (Golloch and Merker 2005):

$$\frac{P_e}{V_H} = i.n.P_{me} = 2\pi.n.\frac{M}{V_H} \quad (16.1)$$

where  $V_H$  is the piston displacement,  $n$  is the engine speed,  $P_{me}$  is the engine's effective pressure,  $i$  is the number of cycles per crankshaft rotation and  $M$  is the torque. The power density can be increased by increasing  $n$  or  $P_{me}$ . Engines use high load concepts through effective charging systems and other measures to show high mean effective pressures and specific powers (Golloch and Merker 2005). The engine downsizing process involves increased performance by using turbochargers, superchargers and twin charging. These methods alone cannot have high efficiencies and can be coupled with new techniques, viz. direct fuel injection (DI), advanced exhaust gas recirculation (EGR) and variable valve timing (VVT). Turbocharging is used to provide the required amount of air in the combustion chamber to burn additional fuel for efficient and clean combustion. A hybrid turbocharger is used to obtain high electrical efficiency due to absence of mechanical linkage between the turbine and the compressor. The hybrid turbocharger consists of a series of hybrid setup where compressor speed and power are independent from turbine speed and power that improves turbine and compressor efficiency. The supercharger compresses air to increase its pressure and density with the help of mechanical power of the



engine. Twin charger is an amalgamation of an exhaust-driven turbocharger and an engine-driven supercharger that work together to give maximum work output. Downsizing will be a great boon for petrol and diesel engines in future containing just two cylinders and lower displacement that provides the required torque and power and reduces the amount of pollutants (Patil et al. 2017).

The emergence of various innovative vehicle technologies like electric vehicles (EVs), hybrid electric vehicles (HEVs) and fuel cell vehicles (FCVs) leads to the improvement of fuel economy and reduced emissions. So far, the HEVs are the most cost-effective feasible choice as they use smaller battery pack and are similar to conventional vehicles. The different automobile industries are developing solutions to the standardization of electric systems to the extent that the hybridization factors, viz. bus voltage, motor size and the relative size of the motor to IC engine, are concerned. Lukic and Emadi (2004) showed that hybridization improves fuel economy and vehicle performance up to a critical optimum point. Beyond that, the performance did not improve satisfactorily on increasing the capacity of electric propulsion system. Besides, there was a considerable benefit of fuel economy when fitted with small electric motors. Katrašnik (2007) proposed combined simulation and analytical approach to accurately determine the energy distribution and losses in the individual components of the hybrid powertrain. They showed that the utmost necessity to enhance fuel economy by hybridization and downsizing involves the determination of optimum hybridization factor.

### ***16.4.3 New Combustion Concepts***

The present scenario of engine combustion and its related emissions is very complex that leads to rigorous research in the field of new combustion concepts. There is no significant distinction associated with gasoline and diesel fuel use in SI and CI engine respectively, homogeneous or non-homogeneous and stoichiometric or lean mixtures. The new combustion concept in traditional stoichiometric homogeneous SI engine for better fuel economy includes lean burn combustion and stratified gasoline combustion. In lean burn combustion, a homogeneous mixture of low air-fuel ratio is used to improve fuel efficiency. However, the after-treatment process becomes complicated as the conventional three-way catalyst cannot reduce  $\text{NO}_x$  with excess oxygen. In stratified gasoline combustion, the stratification of cylinder charge is done with high pressure in-cylinder injection of the fuel that prepares a near stoichiometric mix in the vicinity of the spark plug (Payri et al. 2014).

The efficient diesel engines having the problems of harmful emission can be improved using high pressure injection, lower compression ratio through advanced valve timing, lean burning and advanced after treatment techniques and renewable energy sources. Direct use of biofuels or biogas as a fuel, along with use of hydrogen fuel, synthetic fuel and electricity for electric vehicles produced from wind, hydro or wave energy can reduce the emissions to a large extent (Olander 2018). The  $\text{NO}_x$  and particulates are in a trade-off position in diesel engines. The  $\text{NO}_x$  can be

reduced by lowering the combustion temperature using techniques like EGR, timing retard, low swirl, pilot injection etc. Whereas, particulate matter can be reduced by air-fuel mixture using high pressure fuel injection, low sulphur fuel, HC reduction and a decrease in lubrication oil consumption (Odajima 1994). Igartua et al. (2011) developed a new generation lubricating oil for two-stroke engines that is compatible with Bioethanol E85 having the properties like low friction, good wear and scuffing protection, no residual ash, low carbon soot or existence of deposits. Penchaliah et al. (2011) examined the effect of four contaminants viz. soot, oxidation, moisture and sulphuric acid, and observed that they reduce the conductivity of oil. The sulphuric acid and soot influenced the wear rate in the form of abrasion and polishing wear whereas sulphuric acid and moisture produced corrosive wear. On the other hand, all contaminants and their levels increased the coefficient of friction.

## 16.5 Summary

The review shows the contribution of different components of IC engine to the total frictional losses and the minimization of these losses through various techniques. In order to increase the efficiency and durability and to reduce emissions of IC engine, it is important to design the major frictional components based on the knowledge of tribology. The importance of improved lubrication, surface profiles and surface finish has been focused. The automobile engineers, material engineers and tribologists must work together to eliminate the difficulties of engine tribology.

Despite the threats of strict pollution legislation, globalization and variable fuel quality, the IC engine will continue as a title role in the next decades with significant improvement in technologies. Technologies that are already available in the market includes stop-start, EGR and VVT systems, advanced after-treatment systems to deal with lean combustion. Some emerging technologies may include low temperature combustion concept and modified operating cycles. The widely used efficiency enhancing technologies in current automotive engines is engine downsizing due to which engines are able to increase their rated power. Different boosting technologies are being investigated so as to decrease turbo-lag and to broaden turbocharger operation range, limited by surge and overspeed. Some of the active fields of research may involve accurate engine control in system integration level, management of subsystem requirements, operational limits and their interaction, providing a systematic calibration procedure and adapting the control system to variations in the environment and to engine ageing.

## References

- Adams DR (2010) Tribological considerations in internal combustion engines. In: Tribology and dynamics of engine and powertrain, pp 251–283
- Ali MKA, Xianjun H (2015) Improving the tribological behavior of internal combustion engines via the addition of nanoparticles to engine oils. *Nanotechnol Rev* 4(4). <https://doi.org/10.1515/ntrev-2015-0031>
- Andersson BS (1991) Company perspectives in vehicle tribology-Volvo. In: 17th Leeds-Lyon symposium on tribology—vehicle tribology, vol 18, pp 503–506
- Becker EP (2004) Trends in tribological materials and engine technology. *Tribol Int* 37:569–575
- Bompos DA, Nikolakopoulos PG (2016) Tribological design of a multistep journal bearing. *Simul Model Pract Theory* 68:18–32
- Cakir M, Akcay IH (2011) An investigation on correlation between engine performance and piston ring-cylinder friction in internal combustion engines. *J Tech Sci* 16(2)
- Chiu Y (1992) Lubrication and slippage in roller finger follower systems in engine valve trains. *Tribol Trans* 35(2):261–268
- Darminesh SP, Sidik NAC, Najafi G, Mamat R, Ken TL, Asako Y (2017) Recent development on biodegradable nanolubricant: a review. *Int Commun Heat Mass Transfer* 86:159–165. <https://doi.org/10.1016/j.icheatmasstransfer.2017.0>
- Dienwiebel M, Pohlmann K, Scherge M (2007) Origins of the wear resistance of AlSi cylinder bore surfaces studies by surface analytical tools. *Tribol Int* 40:1597–1602
- Dhomne S, Mahalle AM (2018) Thermal barrier coating materials for SI engine. *J Mater Res Technol*. <https://doi.org/10.1016/j.jmrt.2018.08.002>
- Dyson A, Naylor H (1960) Application of the flash temperature concept to cam and tappet wear problems. *Proc Inst Mech Eng Autom Div* 14(1):255–280
- Enomoto Y, Yamamoto T (1998) New materials in automotive tribology. *Tribol Lett* 5(1):13–24
- Fenske G (2014) Engine friction reduction technologies. Argonne National Laboratory. [https://www.energy.gov/sites/prod/files/2014/07/f17/ft012\\_fenske\\_2014\\_p.pdf](https://www.energy.gov/sites/prod/files/2014/07/f17/ft012_fenske_2014_p.pdf). Accessed on 03/05/2019
- Friedrich K (2018) Polymer composites for tribological applications. *Adv Ind Eng Polym Res*. <https://doi.org/10.1016/j.aiepr.2018.05.001>
- Ghorbanian J, Ahmadi M, Soltani R (2011) Design predictive tool and optimization of journal bearing using neural network model and multi-objective genetic algorithm. *Sci Iranica B* 18(5):1095–1105
- Golloch R, Merker GP (2005) Internal combustion engine downsizing. *MTZ Worldwide* 66(2):20–22. <https://doi.org/10.1007/bf03227737>
- Hirani H, Athre K, Biswas S (1999) Comprehensive design methodology for an engine journal bearing. *Proc Inst Mech Eng Part J* 214:401–412
- Howard K (2014) Advanced engine oils to improve the performance of modern internal combustion engines. In: Alternative fuels and advanced vehicle technologies for improved environmental performance, pp 138–164. <https://doi.org/10.1533/9780857097422.1.138>
- Igartua A, Nevshupa R, Fernandez X, Conte M, Zabala R, Bernaola J, Zabala P, Luther R, Rausch J (2011) Alternative eco-friendly lubes for clean two-stroke engines. *Tribol Int* 44(6):727–736. <https://doi.org/10.1016/j.triboint.2010.01.019>
- Ji F, Taylor C (1998) A tribological study of roller follower valve trains. Part 1: a theoretical study with a numerical lubrication model considering possible sliding. *Tribology series*, vol 34, pp 489–499
- Katrašnik T (2007) Hybridization of powertrain and downsizing of IC engine—a way to reduce fuel consumption and pollutant emissions—part 1. *Energy Convers Manage* 48(5):1411–1423. <https://doi.org/10.1016/j.enconman.2006.12.004>
- Khurram M, Mufti RA, Bhutta MU, Afzal N, Abdullah MU, ur Rahman S, ur Rehman S, Zahid R, Mahmood K, Ashfaq M, Umar M (2019) Roller sliding in engine valve train: effect of oil film thickness considering lubricant composition. *Tribol Int*. <https://doi.org/10.1016/j.triboint.2019.06.022>

- Komvopoulos K (2003) Adhesion and friction forces in microelectromechanical systems: mechanisms, measurement, surface modification techniques, and adhesion theory. *J Adhes Sci Technol* 17:477–517
- Komvopoulos K, Do V, Yamaguchi ES, Ryason PR (2003) Effect of sulfur- and phosphorus-containing additives and metal deactivator on the tribological properties of boundary-lubricated steel surfaces. *Tribol Trans* 46(3):315–325
- Kumar V, Sinha SK, Agarwal AK (2018) Tribological studies of an internal combustion engine. Energy, environment, and sustainability, pp 237–253. [https://doi.org/10.1007/978-981-13-3275-3\\_12](https://doi.org/10.1007/978-981-13-3275-3_12)
- Kumar V, Sinha SK, Agarwal AK (2019) Wear evaluation of engine piston rings coated with dual layer hard and soft coatings. *J Tribol* 141:1–10
- Lou M, Alpas AT (2019) High temperature wear mechanisms in thermally oxidized titanium alloys for engine valve applications. *Wear* 426–427:443–453
- Lukic SM, Emadi A (2004) Effects of drivetrain hybridization on fuel economy and dynamic performance of parallel hybrid electric vehicles. *IEEE Trans Veh Technol* 53(2):385–389. <https://doi.org/10.1109/tvt.2004.823525>
- Martin FA (1983) Developments in engine bearing design. *Tribol Int* 16(3):147–164
- Mishra PC, Rahnejat H, King PD (2009) Tribology of the ring-bore conjunction subject to a mixed regime of lubrication. *Proc Inst Mech Eng C J Mech Eng Sci* 223(4):987–998
- Mutafov P, Lanigan J, Neville A, Cavaleiro A, Polcar T (2014) DLC-W coatings tested in combustion engine—frictional and wear analysis. *Surf Coat Technol* 260:284–289
- Nakada M (1994) Trends in engine technology and tribology. *Tribol Int* 27(1):3–8
- Nozawa R, Morita Y, Shimizu M (1994) Effects of engine downsizing on friction losses and fuel economy. *Tribol Int* 27(1):31–37. [https://doi.org/10.1016/0301-679x\(94\)90060-4](https://doi.org/10.1016/0301-679x(94)90060-4)
- Odajima M (1994) Trends in diesel exhaust gas control and engineers' expectations from tribology. *Tribol Int* 27(1):9–15. [https://doi.org/10.1016/0301-679x\(94\)90057-4](https://doi.org/10.1016/0301-679x(94)90057-4)
- Olander P (2018) Tribology for greener combustion engines. Scuffing in marine engines and a lubricating boric acid fuel additive. <https://uu.diva-portal.org/smash/get/diva2:1161025/FULLTEXT01.pdf>. Accessed on 29/05/2019
- Patil C, Varade S, Wadkar S (2017) A review of engine downsizing and its effects. *Int J Curr Eng Technol*. <https://inpressco.com/wp-content/uploads/2017/06/Paper75319-324.pdf>. Accessed on 28/05/19
- Payri F, Luján J, Guardiola C, Pla B (2014) A challenging future for the IC engine: new technologies and the control role. *Oil Gas Sci Technol Rev d'IFP Energies Nouvelles* 70(1):15–30. <https://doi.org/10.2516/ogst/2014002>
- Penchaliah R, Harvey TJ, Wood RJK, Nelson K, Powrie HEG (2011) The effects of diesel contaminants on tribological performance on sliding steel on steel contacts. *Proc Inst Mech Eng Part J J Eng Tribol* 225(8):779–797. <https://doi.org/10.1177/1350650111409825>
- Priest M, Taylor C (2000) Automobile engine tribology—approaching the surface. *Wear* 241(2):193–203. [https://doi.org/10.1016/s0043-1648\(00\)00375-6](https://doi.org/10.1016/s0043-1648(00)00375-6)
- Rosenberg RC (1981) General friction considerations for engine design. SAE paper 821576, pp 59–70
- Sander DE, Allmaier H, Priebisch HH (2016) Friction and wear in automotive journal bearings operating in today's severe conditions. In: *Advances in tribology*, pp 143–172. <https://cdn.intechopen.com/pdfs/51522.pdf>. Accessed on 19/06/2019
- Scherge M, Martin JM, Pohlmann K (2006) Characterization of wear debris of systems operated under low wear-rate conditions. *Wear* 260:458–461
- Shakhvorostov D, Pohlmann M, Scherge M (2006) Structure and mechanical properties of tribologically induced nanolayers. *Wear* 260:433–437
- Siczek KJ (2016) Valve train tribology. In: *Tribological processes in the valve train systems with lightweight valves*, pp 85–180
- Taylor CM (1993) Lubrication regimes and the internal combustion engine. *Engine tribology*, pp 75–87. [https://doi.org/10.1016/s0167-8922\(08\)70008-7](https://doi.org/10.1016/s0167-8922(08)70008-7)

- Taylor CM (1998) Automobile engine tribology—design considerations for efficiency and durability. *Wear* 221:1–8
- Teodorescu M (2010) A multi-scale approach to analysis of valve train systems. In: *Tribology and dynamics of engine and powertrain*, pp 567–587. <https://doi.org/10.1533/9781845699932.2.567>
- Tormos B, Ramírez L, Johansson J, Björling M, Larsson R (2017) Fuel consumption and friction benefits of low viscosity engine oils for heavy duty applications. *Tribol Int* 110:23–34. <https://doi.org/10.1016/j.triboint.2017.02.007>
- Venci A, Rac A (2014) Diesel engine crankshaft journal bearings failures colon Case study. *Eng Fail Anal* 44:217–228
- Willermet PA (1989) Tribological design—the automotive industry. *Tribology series*, pp 33–39. [https://doi.org/10.1016/s0167-8922\(08\)70178-0](https://doi.org/10.1016/s0167-8922(08)70178-0)
- Wong VW, Tung SC (2016) Overview of automotive engine friction and reduction trends—effects of surface, material, and lubricant-additive technologies. *Friction* 4(1):1–28
- Yan-qing W, Gao-feng W, Qing-gong H, Liang F, Shi-rong G (2009) Tribological properties of surface dimple-textured by pellet-pressing. *Procedia Earth Planet Sci* 1:1513–1518
- Yan D, Qu N, Li H, Wang X (2010) Significance of dimple parameters on the friction of sliding surfaces investigated by orthogonal experiments. *Tribol Trans* 53(5):703–712
- Yu H, Deng H, Huang W, Wang X (2011) The effect of dimple shapes on friction of parallel surfaces. *Proc Inst Mech Eng Part J J Eng Tribol* 225(8):693–703
- Zhmod B (2011) Developing energy efficient lubricants for auto applications. *Tribology and Lubrication Technology*, pp 42–49. [www.stle.org](http://www.stle.org). Accessed on 25/05/19

# Chapter 17

## Asbestos Free Braking Pads by Using Organic Fiber Based Reinforced Composites for Automotive Industries



**Sandeep Kumar, Brijesh Gangil, K. K. S. Mer, Don Biswas and Vinay Kumar Patel**

**Abstract** This book chapter focuses on the development in replacement of first generation brake materials (asbestos) by organic fiber based polymer composites. This replacement is necessary as the asbestos brake pads causes hazardous effects to the human being and environment. Many researchers report the several organic alternatives for asbestos in different journals. In this chapter, some of the best performed and eco-friendly compositions for brake materials are discussed. The uses of organic fibers and fillers such as flax, basalt, coconut, palm kernel shell, periwinkle shell, and pineapple leaf etc. are studied as an alternative to the asbestos based materials for braking pads. Different combinations of organic fibers with different binders like phenolic resin, polyester, and epoxy etc. are also studied and its influence on the behavior of brake pads is reviewed. Moreover, wear and friction coefficient are the two significant factors to be considered for suitability of any friction materials for braking pad application. Moreover, the influential rules and mechanism of braking conditions like pressure, velocity, and temperature on the friction and wear behaviors of organic reinforcing friction materials are summarized.

**Keywords** Brake pad · Organic fiber · Binders · Polymer composite · Material properties

---

S. Kumar · B. Gangil

Department of Mechanical Engineering, S.O.E.T., H.N.B. Garhwal University Srinagar, Garhwal, Uttarakhand 246174, India

K. K. S. Mer · V. K. Patel (✉)

Mechanical Engineering Department, Govind Ballabh Pant Institute of Engineering and Technology, Pauri, Garhwal 246194, India  
e-mail: [vinaykrpatel@gmail.com](mailto:vinaykrpatel@gmail.com)

D. Biswas

University Science Instrumentation Centre, H.N.B. Garhwal University Srinagar, Garhwal 246174, India

© Springer Nature Singapore Pte Ltd. 2019

J. K. Katiyar et al. (eds.), *Automotive Tribology*, Energy, Environment, and Sustainability, [https://doi.org/10.1007/978-981-15-0434-1\\_17](https://doi.org/10.1007/978-981-15-0434-1_17)

327

## 17.1 Introduction

In automotive vehicle system, brake is highly essential part so as to slow down or to completely stop the vehicle. This stoppable process has been done by the creation of friction between rotating disc and brake pads (conversion of kinetic energy of the vehicle into heat energy). Therefore, the brake pads should have some properties such as resistant to wear, withstand the high temperature, and quickly absorb the heat energy. Also, the brake pad materials must have capability to maintain a high friction coefficient (FC) with the brake disc and it should not be broken down like that of the FC with the brake disc, which is compromised at higher temperature. Generally, brake pads are manufactured by following constituents; reinforcing fibers, fillers, binders, and friction additives. These constituents are mixed properly with various weight proportion and brake pads are obtained by using several manufacturing techniques. The constituents play the following roles: reinforcing fibers enable the mechanical strength to the friction material; binders maintain the structural integrity under thermal and mechanical stresses; fillers improve its manufacturability; friction additives like abrasives provide enhancement in friction coefficient and lubricants develop the friction coefficient at higher temperature. Earlier generation of composites used in modern brake pad materials are based on health hazardous asbestos reinforcement because of its good chemical and physical properties. It is used in friction lining, brake coupling, and brake pads; however, asbestos causes health risk and carcinogenic effects on human health (Fu et al. 2012). Hence, in recent year asbestos free reinforcement such as glass, Kevlar, carbon, and organic fibers have been extensively used as replacement of asbestos (Liew and Nirmal 2013). Among all the non-asbestos reinforcement, organic fibres reinforced friction materials are now emerging as new and low cost friction material in the brake pads development. Even though these fibres have good friction and mechanical properties, there are some major disadvantages like susceptibility to friction-induced noise and poor affinity with polymer matrix. However, because of their eco-friendly nature, excellent mechanical properties, and economical benefit, these fibers are recently gaining interest in the field of automotive industry (Keskin 2011). The researchers established that the natural fibers had positive influence on the mechanical and wear properties of fiber reinforced polymer composites (Kumar et al. 2016, 2017a, b, 2019a; Venketeshwaran and Perumal 2010; Patel et al. 2018). Kumar et al. (2018) prepared the composite samples with the combination of bast-leaf natural fibers in epoxy composites and revealed that the wear behaviour of epoxy composites improved by the addition of natural fiber. In other observation, effect of various inorganic microfillers such as  $\text{CaCO}_3$ ,  $\text{Al}_2\text{O}_3$ , and  $\text{TiO}_2$  on physico-mechanical properties of *Luffa cylindrica*/polyester composites was studied by Patel and Dhanola (2016). The specimen prepared with 5 wt%  $\text{TiO}_2$  microfillers in luffa fiber reinforced polymer composite exhibited smallest specific wear rate among all filled/unfilled polymer composites. The different natural fibers such as sisal, *Grewia optiva*, *Bauhinia-vahlii*, and hemp etc. in polymer composite exhibited similar improvement in wear property of fiber reinforced composites (Kumar et al. 2017a, b, 2019b, c; Patel and Rawat 2017).

Pujari and Srikan (2019) observed that the palm kernel (50% volume fraction) reinforced phenolic composites had efficiently improved the wear resistance behaviour of the composites. In other investigation, Unaldi and Kus (2017) observed that the porosity, hardness and wear rate characteristics of the brake pad materials were greatly affected by the weight proportion of phenolic matrix and *Miscanthus* in the mixture. There are four possible mechanisms of failure modes of braking in automobiles: (i) thermal instability, (ii) wear mechanism, (iii) chemical changes, and (iv) micro-cracks.

The aim of the present chapter is to review the properties and preparation of different alternative materials (organic) as suitable alternative of asbestos brake pads. Braking pads made up with organic fibers and fillers like banana peel, kernel shell, and palm waste etc. are summarized. Also, the different binders such as phenolic resin and epoxy resin are also discussed and its influence on the performance of brake pads is presented.

## 17.2 Literature Review

### 17.2.1 *Organic Fiber as Reinforcing Material for Braking Pads*

Recently, eco-friendliness, economic point of view, and governmental regulation in the use of organic reinforcing fibers the asbestos, which produces carcinogenic effects, has received growing interest in the brake pads system in automotive industries. Xin et al. (2007) prepared brake pad material using organic fiber such as sisal for its eco-friendly nature with phenolic as resin and revealed that the 3:4 proportions of phenolic/sisal delivered the superior value of friction and wear properties. Moreover, in comparisons of asbestos and mineral/steel fiber, sisal fiber reinforced friction material attained good FC at different friction temperature. The waste of banana (peels) are found as a suitable replacement of asbestos and phenolic resin wherein it was found out that the 30 wt% of carbonized banana peel exhibited better wear properties (Idris et al. 2015). Ikpambese et al. (2016) produced environmental friendly non-asbestos brake pads by using kernel fiber with epoxy resin binder and it was revealed that the composition of 10 wt% palm kernel waste, 40 wt% epoxy, 15 wt% calcium carbonate, and 29 wt% graphite gave the optimum properties. The results indicates that the palm kernel fibers can be a possible replacement of asbestos embedded brake pads production. The enhancement of wear resistance properties can be done by using 3 wt% of cotton fibers, so the brake pads embedded with cotton fiber reinforcement is another option to asbestos free braking system. Ma et al. (2013) focused on the impact of bamboo fiber on friction performance of brake pad material. They examined the specimen reinforced with bamboo fibers of 3, 6, 9 and 12 wt% and revealed that the FC of 12 wt% bamboo reinforced friction material



(BRFC) decreased with increasing temperature. The optimum value of friction coefficient and wear properties were attained at 3 wt% of BRFC. In other investigation, Ma et al. (2014) investigated the influence of wool fibers on tribological behavior of friction material. They prepared sample with 0, 3, and 4 wt% of wool fiber in friction material and found out that the superior results were attained at 3 wt% of wool content. Moreover, impact strength increased and hardness decreased with increase in the wool content in friction material. A natural cotton flower fiber known as *Areva javanica* is a possible alternate of asbestos in braking system and the authors revealed that the developed brake pad obtained a hardness of HRS 91, density of 2.01 g/cm<sup>3</sup>, and Loss on ignition 21.68%, respectively. These values were approximately similar to acrylic fiber reinforced brake pad (Ahmed et al. 2018).

### **17.2.2 Organic Filler as Reinforcing Material for Braking Pads**

The industrial wastes particles such as fly ash and bagasse ash; Fly ash is the by-product of coal and it is obtained from combustion of coal in power generation industries, whereas bagasse ash is obtained from combustion of bagasse in sugarcane factories. These materials attained higher value of hardness and are positively used as abrasives in order to reduce and control the wear rate in brake pads (Boz and Kurt 2007). Choosri et al. (2018) suggested that the 4 wt% of subordinate abrasive (fly ash and bagasse ash) delivered optimized overall properties of friction material and showed a possible use as secondary abrasives in the phenolic composites for environmental friendly brake pads. Hazelnut, walnut, and apricot shells are extensively used as filler reinforcement in various polymeric materials (Ibhadode and Dagwa 2008; Gürü et al. 2006, 2008; Çöpür et al. 2007). These natural fillers hold higher lignin as compared to organic fibers, therefore the thermal decomposition of nut shells leads to formation of higher amount of char due to its high lignin composition. This leads to a positive impact on increasing wear resistance properties (Sutikno et al. 2010). Abutu et al. (2018) studied the asbestos free braking pads and the material included seashell (52%) as reinforcement, epoxy matrix (35%) as binder, aluminum (8%) as abrasive, and graphite (5%) as friction modifier in manufacturing a braking pad. They observed that the 24.26 and 55.23% of curing time had the noteworthy impact on friction coefficient and wear rate respectively in the development of braking pads. Yawas et al. (2016) focused on the periwinkle shell as alternative for asbestos in braking pads. They revealed that the 1251 m size of periwinkle particle with 35 wt% resin was obtained favorable with that of commercial brake pads in automotive industry. In other investigation on periwinkle shell, the authors developed the factorial design and revealed that the enhancement in wear resistance depended on the sliding speed, normal load, and temperature (Amaren et al. 2013).

## 17.3 Experimental Procedure

Organic fiber/filler in raw form cannot be directly used as reinforcement for brake pad application. So some mechanical and chemical modifications are necessary before using them in brake pad fabrication. Here are certain modifications are presented for organic fiber/filler based upon the literature survey.

### 17.3.1 *Seashell*

Seashells were collected and suspended in a solution of caustic soda for few hours and cleaned by using dried cloths. After that, seashells were washed with water and dried in hot air oven at a temperature of 150 °C. The dried seashell was grinded into powder form using a pestle and mortar and was thereafter sieved using sieve size <125 μm aperture (Abutu et al. 2018).

### 17.3.2 *Periwinkle Shell*

The periwinkle shell was sun dried followed by oven dried (150 °C for five hours). After the moisture was completely removed, it was transferred into Denver cone crusher and reduced into the size of 3–4 mm. Further, this shell was charged into roll crusher to reduce the size in the range of 1–2 mm. Then the periwinkle shell was ball milled for two hours and then the Periwinkle shell sieve sizes of  $\leq 125$  μm apertures were mixed with 35 wt% of phenolic resin (Amaren et al. 2013).

### 17.3.3 *Palm Kernel Fiber*

Palm kernel fibers, first suspended in a solution of caustic soda for a day to remove the residue of red oil left after extraction and then washed with water to eliminate the caustic soda and sun dried for one week. The dried fiber was converted into powder form by applying a hammer mill and then sieved using sieve size of greater than or equal to 100 μm aperture (Ikpambese et al. 2016).

### 17.3.4 *Banana Peels*

The sun dried banana peels was converted into powder form by using a ball mill with the rotation of 250 rpm and further, it was converted into banana peel ash by



**Fig. 17.1** The images of raw seashell (a), Periwinkle shell (b), Palm kernel fiber (c), banana peel un-carbonized (d), and Banana peel carbonized (e)

applying the powder in a graphite crucible and fired in electric resistance furnace at temperature of 1200 °C (Idris et al. 2015).

### 17.3.5 *Sisal Fibers*

Sisal fibers was first dipped into sodium hydroxide solution-ammonia base liquor with consistence of 10 wt% and then applied for brake composites (Ma et al. 2014). The formulation of brake pad by Lapinous fibers (Singh and Patnaik 2015) and basalt fiber (Singha 2012) can be done without any chemical treatment. The images of raw organic fiber/filler used in brake pads is depicted in Fig. 17.1.

## 17.4 Preparation and Characterization of the Brake Pad Composites

After the mechanical and chemical treatment, the final product is prepared with the ingredients of binder, filler, and frictional additives etc. in different formulations. Some of the formulations and the characterizations of brake pad based on organic fibers and organic filler are discussed below.

## 17.4.1 Organic Fibers

### 17.4.1.1 Palm Kernel Fiber

Ikpambese et al. (2016) reinforced the Palm kernel fiber into brake material sample as depicted in Fig. 17.2. Each raw material was mixed by using a blender to obtain a homogeneous mixture. Then, the mixtures were compacted by pressing at 100 kN load for two minutes at room temperature. Further the brake pads were cured at 250 °C for 90 min. The mechanical, physical, and morphological properties were investigated. In the prepared brake pad containing 10 wt% palm waste, 40% epoxy resin, 6 wt%  $Al_2O_3$ , 15 wt% calcium, and 29 wt% graphite gave better brake properties among all the fabricated specimens. Pujari and Srikiran (2019) developed an asbestos free brake pad by using palm kernel as a fiber with phenolic resin as a binder. They varied the palm kernel fiber content from 10 to 50 wt% with an interval of 10 wt% with inclusion of Nile rose (0–15 wt%), and wheat (0–10 wt%). They revealed that at 350 rpm (50 wt%), 450 rpm (10 wt%), and 550 rpm (10 wt%) exhibited better wear resistance property and therefore it can be concluded that palm kernel fiber can replace asbestos in reinforcing friction material.

### 17.4.1.2 Banana Peel Fiber

Idris et al. (2015) fabricated the brake pad by varying the phenolic resin (5–30 wt%) at an interval of 5 wt% in the banana peels particles. The authors prepared two types of samples by using the un-carbonized and carbonized banana peels particles. To achieve a homogeneous mixture, the formulation was properly mixed in mixer and

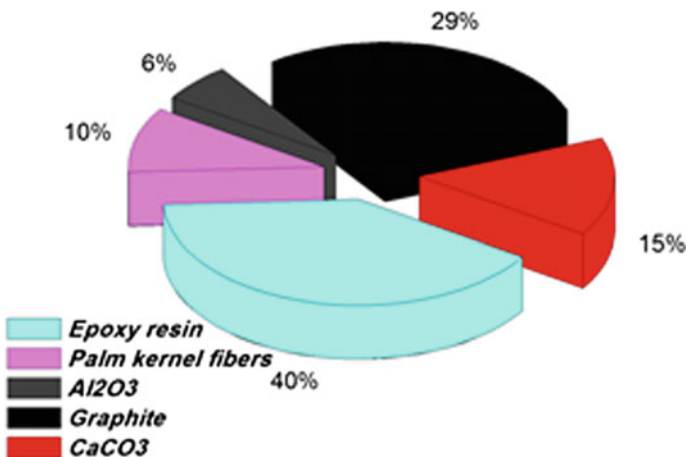


Fig. 17.2 Constituents of the brake pad composites using palm kernel fiber

**Table 17.1** Comparisons of properties of asbestos based/pineapple leaf based brake pad (Swamidoss and Prashanth 2015)

Properties	Brake pad (asbestos)	Pineapple leaf fiber based brake pad
Compressive Strength (N/mm <sup>2</sup> )	111	107.25
Average wear (mg/m)	3.85	4.09
Brinell hardness (HB)	101	100.88
Thickness swell in Water (%)	0.30	2.75

applied the hot press at temperature of 150 °C under  $9.81 \times 10^7$  pressure for 2 min. Further, the brake pad sample was cured in oven for 8 h. This work focused on physical, mechanical, wear, and morphological behavior of the new brake pad and observed that the properties such as compressive strength, hardness, and specific gravity increased with increase in the filler content. Bashir et al. (2015) fabricated brake pad sample with 13 ingredients with incorporation of banana peel and phenolic resin as binder. During the experiment, the phenolic resin and banana peel were varied and remaining eleven constituents were fixed. The friction and wear property of newly fabricated brake pad was evaluated by using reciprocating friction monitor. They revealed that the coefficient of friction was increased at elevated temperature and the wear characteristic indicated that binding ability of phenolic based brake pad can be effectively increased by the addition of banana peel powder.

#### 17.4.1.3 Pineapple Leaf

Swamidoss and Prashanth (2015) fabricated four different combinations (such as S1, S2, and S3) and prepared by varying pineapple fibre weight percent from 10, 20, and 30 wt% along with binder. The combination of pineapple leaf fibre with epoxy resin is applied into mould and kept dried in a hot platen temperature of 140 °C for 2 min. After removing the brake pad from hot platen, the brake pad was cured in oven at 120 °C of temperature for 8 h. The comparison of properties of commercial and pineapple leaf based brake pads is shown in Table 17.1 and the results show that the natural fiber like pineapple leaf fiber can effectively replace the asbestos brake pad which is harmful to human health.

#### 17.4.1.4 Bamboo and Coconut Fiber

Sutikno et al. (2018) fabricated three composition of Bamboo fiber/coconut fiber reinforced brake pad material which consisted of (i) 29% bamboo/coconut, 40% epoxy, 20% Al<sub>2</sub>O<sub>3</sub>, and 11% MgO (ii) 29% bamboo/coconut, 40% epoxy, 25%

Al<sub>2</sub>O<sub>3</sub>, and 6% MgO; (iii) 29% bamboo/coconut, 40% epoxy, 30% Al<sub>2</sub>O<sub>3</sub>, and 1% MgO. They revealed that bamboo/coconut fiber reinforced brake pad had the hardness of 37.14 HRB/44.10 HRB, temperature resistance 251.53 °C/250.56 °C, wear rate 0.0323 mm<sup>3</sup>/N mm/0.242 mm<sup>3</sup>/N mm, and FC 0.454/0.46. The hardness of both fabricated composites had lower value than commercial brake pad whereas FC and wear rate were similar to commercial one. The mixture of bamboo, aluminum powder, and glass fiber in polyester matrix gave higher hardness (14.47 BHN) as compared to existing brake pad (13.7 BHN) (Purboputro et al. 2018). Thus, the coconut fiber can be used as reinforcing material for brake pads application especially for small and medium vehicle (Pinca-Bretotean et al. 2018).

Crăciun et al. (2016) investigated the hardness and density properties of brake pad product manufactured with coconut fiber as an alternative filler material. The fiber content was used with different weight percentages 0–15 wt% and phenolic resin was used as binder. The specimens were prepared by using powder metallurgy technique. Results showed that the highest hardness attained at 5 wt% fiber content and coconut fibers had emerged as a potential reinforcing agent for automotive braking system components. Abutu et al. (2019) developed a non-asbestos brake pad by using coconut shell as filler material and epoxy resin as binder. They prepared a brake pad with different percentage of constituents; 35% binder, 58% coconut shell, 8% abrasive, and friction modifier with 5%. The comparison of mechanical and wear properties of commercial brake pad and coconut shell reinforced brake pad revealed that the coconut reinforced exhibited better tensile, hardness and wear properties whereas commercial brake pad revealed better bending, compressive, and impact strength.

#### 17.4.1.5 Flax and Basalt Fiber

Ilanko and Vijayaraghavan (2016) prepared three combinations of brake pad materials by using basalt, flax, and their hybrid as reinforcing agent in phenolic. The ingredients used in this investigation are shown in Fig. 17.3. All these constituents were blended by mechanical stirrer for 2 min. After that, the mixture was poured into a cast iron die and a vertical load (10 MPa) was applied at 180 °C in diffusion bonding machine for 10 min. Further, post treatment was applied in an oven for 4 h at 180 °C. They revealed that wear rate of basalt fiber reinforced material was decreased with increase in the sliding velocity which was attributed to the wear debris of basalt fiber acting as protective barrier. Atmika et al (2016) focused on the wear behavior of an automotive brake pad with basalt powder. The three combinations of constituents with and without sodium hydroxide treatment were: 30%/70%, 60%/40%, and 80%/20%. The result showed that the wear rate of the composites was increased by 18.75% with 5% sodium hydroxide and proposed the basalt fiber as substitute of asbestos because of its environmental friendly nature. The FC of composites was found to be stabilized by reinforcing 5.6 vol% of flax fiber and also the wear resistance at higher temperature (Fu et al. 2012).

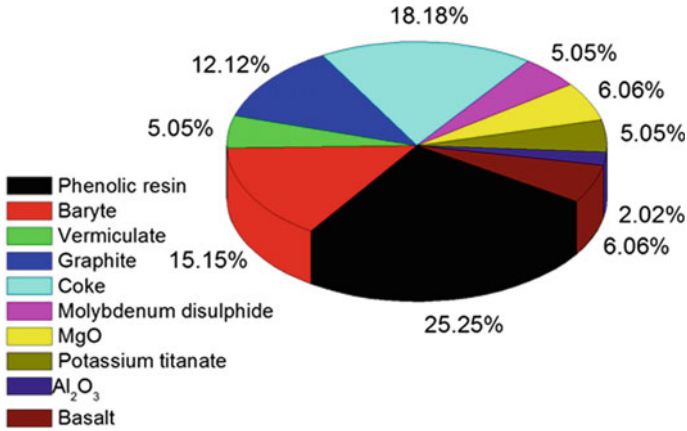


Fig. 17.3 Ingredients of the brake pads using basalt fiber

### 17.4.2 Organic Fillers

#### 17.4.2.1 Cocoa Beans Shell Filler

Olabisi et al. (2016) formulated a brake pad by cocoa beans shell as shown in Fig. 17.4a, b. The test specimens were fabricated by powder metallurgy method. All ingredients were mixed properly into a container for 15 min to obtain a homogeneous mixture. The epoxy and homogeneous mixture paste was poured into the mould cavity and allowed to cure. Then, they were left in adverse environment for

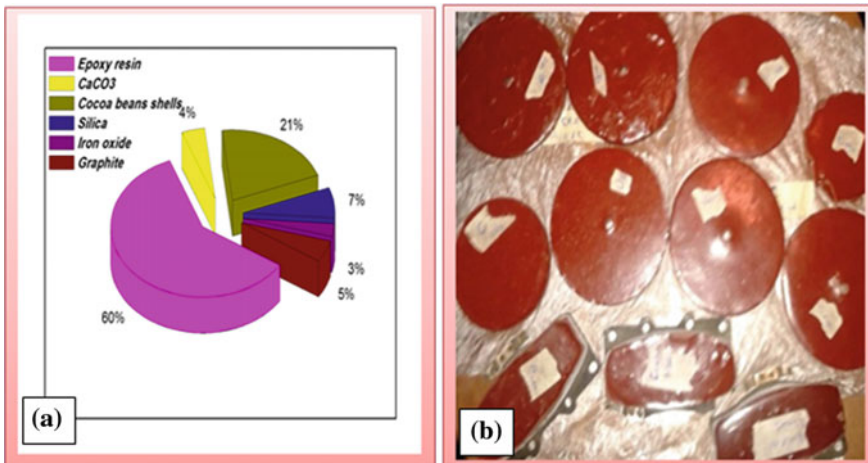


Fig. 17.4 The ingredients (a) and brake pads sample (b) using Cocoa beans shells (Olabisi et al. 2016)

21 days in order to allow them to obtain full strength before carrying out mechanical test. They prepared three samples of brake pads in their investigation by three different weight percentages (21, 26, and 21%). The results showed that newly developed specimens had a density of 1.01 and 1.37 g/cm<sup>3</sup> while the commercial brake pad (CBP) density was 3.36 g/cm<sup>3</sup>; the oil absorption was between 0.28 and 0.74% while the CBP were 0.033%; the wear rate under dry sand abrasion test was 0.72 and 3.93 (g/m) and the CBP wear rate was 0.19 g/min; and the hardness was between 10.67 and 12.27 while the CBP was 2.53. The evaluated properties were lower than CBP due to its higher wear rate, but it was preferable to be used as substitute for CBP because of its eco-friendly nature and less health hazard as compared to the asbestos brake pad.

#### 17.4.2.2 Periwinkle Shell Filler

Amaren et al. (2013) fabricated the phenolic based specimens with different particle sizes of 125, 250, 355, 500, and 710 μm. They investigated the wear characteristic of automotive brake pad material with periwinkle shell. The result showed that wear rate increased with increase in the speed and load with the optimum result obtained at 125 μm periwinkle size, thus, the smaller size periwinkle shell performed better as filler material in phenolic resin and can be effectively used as a replacement of asbestos in braking system especially for brake pads.

#### 17.4.2.3 Hazelnut and Walnut Shell Filler

Öktem et al. (2015) fabricated a new composites brake pad by using hazelnut/walnut shell as a filler material and phenolic as a binder. They analyzed the mechanical and physical properties of the developed brake pad. It was observed that the 3.5 wt%/7 wt% of hazelnut and walnut imparted optimum value of hardness and studies showed that the hazelnut and walnut shell based composite brake pad was eco-friendly and therefore proposed this composition as an alternative of asbestos in braking system component. Akıncioğlu et al. (2018) carried out the physico-mechanical and wear properties of hazelnut and boron oxide reinforced eco-friendly brake pad material. The composition of friction material consisted of the hazelnut was (7 wt%) and boron oxides (6 wt%). Physio-mechanical and wear tests were conducted to evaluate the properties (density, hardness, water absorption, shear testing, and friction-wear test) of the material. The results showed that the hardness, water absorption, compressibility ratio, and coefficient of friction of boron oxide and hazelnut incorporation material were higher than the commercial brake pad. The properties of eco-brake pads using different organic fibers/filler and asbestos brake pads is illustrated in Table 17.2.



**Table 17.2** Comparisons of properties of different organic filler/fiber based brake pad with commercial used brake pad

Types of brake pad	Wear rate (mg/m)	Specific gravity (g/cm <sup>3</sup> )	Thickness swells in SEA oil	Compressive strength (N/mm <sup>2</sup> )	Hardness values	Tensile strength (MPa)	Thermal conductivity (W/mK)
Asbestos based	3.800	1.890	0.30%	110	101	7.0	0.539
Cocoa beans (Olabisi et al. 2016)	3.934	1.010	0.28%	23.2	120.3 MPa	16.88	0.239–0.338
Hazelnut (Öktem et al. 2015)	–	–	0.60%	–	92 (shore D)	–	1.202
Periwinkle shell (Amaren et al. 2013)	–	1.01	0.37%	147	116.7 HRB	–	–
Banana peel Carbonized (Idris et al. 2015)	4.67	1.2	1.12%	–	71.6 HRB	61.20	–
Palm kernel fiber (Ikpambese et al. 2016)	3.98	2.1	$0.26 \times 10^{-7}$ m <sup>3</sup> /s	–	10 HRB	–	–

## 17.5 Friction, Wear Behavior, and Mechanisms of Organic Fiber Reinforced Brake Friction Materials

It is well known the friction and wear properties of friction materials are strongly influenced by braking and surrounding conditions (Eriksson et al. 2001). Furthermore, it was observed that friction and wear behavior of brake friction material depend on the factors of (i) material characteristics such as chemical, physical, and mechanical properties of brake pad materials etc. (ii) braking conditions like initial braking speed, temperature rise in braking, and breaking pressure. (iii) Surrounding conditions such as humidity, temperature, and airflow etc. (iv) Structural parameters like size, contact modality, and shape etc. Among all these conditions, the braking condition is considered as the most valuable external factor and various researchers focused their studies on these influential factors of braking pressure, initial temperature, and braking speed (Krenkel and Berndt 2005). Therefore, the impact of these factors on the friction and wear behavior of organic friction material are discussed in this context.

In general, the friction coefficient increases with the increase in the temperature and after attaining a certain temperature, the FC suddenly falls off whereas wear rate increases with increase in the temperature. Yun et al. (2011) focused the research on the influence of temperature on the friction and wear behavior of organic brake friction composites with silica particle as abrasive and revealed that the friction and wear behaviors of fabricated material had similar impact laws with temperature. The enhancement in FC was reported with the increase in the temperature initially but decrement started when the temperature reached to 300 °C. However, the wear rate kept increasing with increase in temperature, which proved that the wear of friction material was more at a higher temperature. In other investigation, Ma et al. (2013) focused on the impact of temperature on the friction and wear behavior of bamboo fiber reinforced friction material and observed that friction coefficient of bamboo friction material decreased with increase in the temperature and detected that the friction coefficient had some variation at the temperature of 250 °C. The braking pressure affects the friction and wear through the deformation and size of actual contact area (according to modern tribology). Kumar and Bijwe (2014) studied the friction and wear behavior of non-asbestos-organic brake under different braking pressures. The results showed that the FC increased first and then fell off with the increasing braking pressure. Öztürk et al. (2013) examined the effect of speed, temperature, and load on friction and wear behavior of brake friction material. The effects of speed and temperature on friction coefficient and wear rate is depicted in Figs. 17.5a, b and 17.6a, b. They revealed that the FC of material decreased with increase in the sliding speed whereas the wear rate increased with increase in the speed. Further, the optimum value of FC was attained at 300 °C and then decreased above this temperature. They observed that at higher temperature the friction property was intensely affected by softening and thermal degradation of the resin.

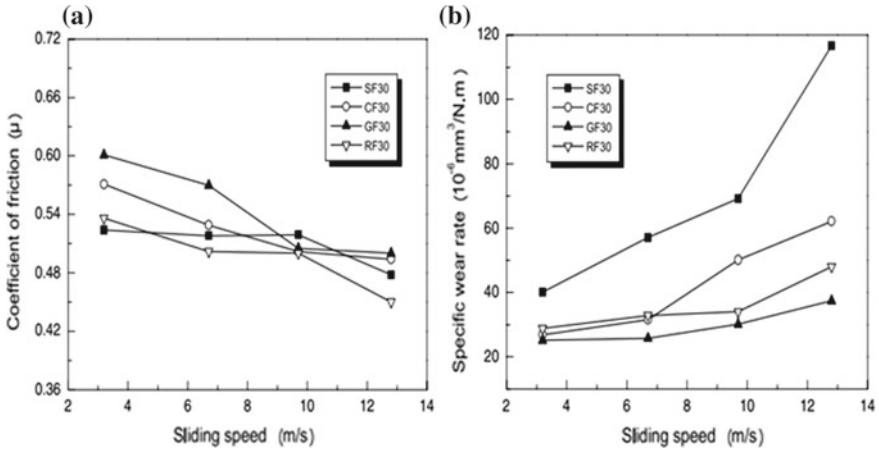


Fig. 17.5 a and b Influence of sliding speed on FC and wear rate of friction brake pad material. Copyright (2013) Taylor & Francis

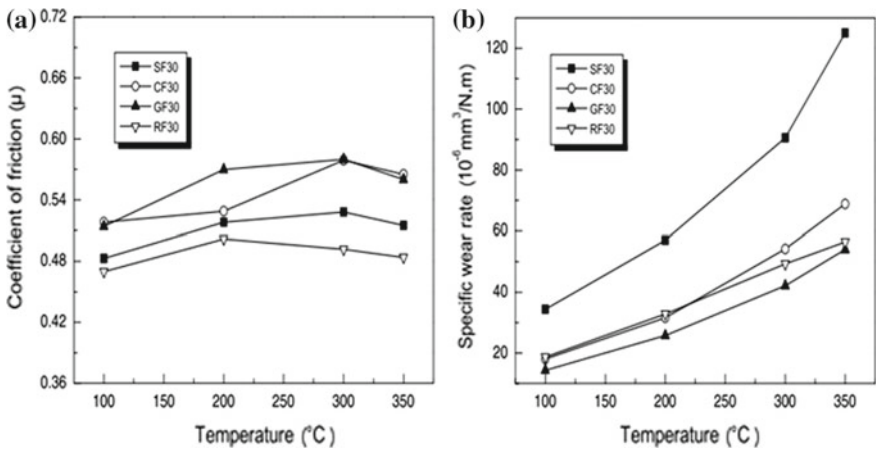


Fig. 17.6 a and b Influence of temperature on FC and wear rate of friction brake pad material. Copyright (2013) Taylor & Francis

### 17.6 Current Challenges and Future Research Direction in Brake Pad Composites

The replacement of asbestos with non-hazardous materials in the production of brake pad is receiving serious attention in the laboratory and lots of work have been done, but these works have not been translated into commercial purpose. Thus, the design of the organic fiber based friction material with other ingredients needs to be considered carefully as it is found that the asbestos free brake pads have many challenges.

From this review it is observed that the organic fiber based brake pads have low thermal stability as compared to commercial one, but due to much less toxicity and environmental point of view non-asbestos brake pads have much better performance. Again, it becomes essential to utilize these combination of organic fiber/filler material in different ratios to further study their influence on physico-mechanical and tribological behaviour of brake pads.

## 17.7 Conclusion

In this review, the application of non-hazardous (organic fiber/filler) reinforcement material as possible substitute for asbestos has been focused. The physico-mechanical and tribological properties of these brake pads compared favorably with the presently used brake pad. The organic fiber might be efficiently used as a substitute for asbestos in brake pad fabrication when suitable with some other constituents to fit a better performance of brake pad. Further, regarding their low thermal stability, they should be wisely considered.

## References

- Abutu J, Lawal SA, Ndaliman MB, Lafia-Araga RA, Adedipe O, Choudhury IA (2018) Effects of process parameters on the properties of brake pad developed from seashell as reinforcement material using grey relational analysis. *Eng Sci Technol Int J* 21:787–797
- Abutu J, Lawal SA, Ndaliman MB, Lafia-Araga RA, Adedipe O, Choudhury IA (2019) Production and characterization of brake pad developed from coconut shell reinforcement material using central composite design. *SN Appl Sci* 1:82
- Ahmed MJ, Balaji MS, Saravanakumar SS, Sanjay MR, Senthamaraiannan P (2018) Characterization of *Areva javanica* fiber—a possible replacement for synthetic acrylic fiber in the disc brake pad. *J Ind Text*. <https://doi.org/10.1177/1528083718779446>
- Akincioğlu G, Öktem H, Uygur I, Akincioğlu S (2018) Determination of friction-wear performance and properties of eco-friendly brake pads reinforced with hazelnut shell and boron dusts. *Arab J Sci Eng* 43:4727–4737
- Amaren SG, Yawas DS, Aku SY (2013) Effect of periwinkles shell particle size on the wear behavior of asbestos free brake pad. *Results Phys* 3:109–114
- Atmika KA, Setiadi WN, Parwata MD (2016) Wear behavior of basalt powder reinforced phenolic resin matrix composites brake lining pads. In: *International conference on mechanics, materials and structural engineering (ICMMSE 2016)*. Atlantis Press
- Bashir M, Saleem SS, Bashir O (2015) Friction and wear behavior of disc brake pad material using banana peel powder. *Int J Res Eng Technol* 4:650–659
- Boz M, Kurt A (2007) The effect of  $Al_2O_3$  on the friction performance of automotive brake friction materials. *Tribol Int* 40:1161–1169
- Choosri S, Sombatsompop N, Wimolmala E, Thongsang S (2018) Potential use of fly ash and bagasse ash as secondary abrasives in phenolic composites for eco-friendly brake pads applications. *Proc Inst Mech Eng Part D* 0954407018772240
- Çöpür Y, Güler C, Akgül M, Taşcıoğlu C (2007) Some chemical properties of hazelnut husk and its suitability for particleboard production. *Build Sci* 42:2568–2572

- Crăciun AL, Heput T, Bretotean CP (2016) Formulation of materials with natural fiber for brake system components. *Ann Fac Eng Hunedoara Int J Eng* 14(3)
- Eriksson M, Lord J, Jacobson S (2001) Wear and contact conditions of brake pads: dynamical in situ studies of pad on glass. *Wear* 24:272–278
- Fu Z, Suo B, Yun R, Lu Y, Wang H, Qi S, Matejka V (2012) Development of eco-friendly brake friction composites containing flax fibers. *J Reinf Plast Compos* 31:681–689
- Gürü M, Tekeli S, Bilici I (2006) Manufacturing of urea–formaldehyde-based composite particle board from almond shell. *Mater Des* 27:1148–1151
- Gürü M, Atar M, Yıldırım R (2008) Production of polymer matrix composite particleboard from walnut shell and improvement of its requirements. *Mater Des* 29:284–287
- Ibbadode AOA, Dagwa IM (2008) Development of asbestos-free friction lining material from palm kernel shell. *J Braz Soc Mech Sci Eng* 30:166–173
- Idris UD, Aigbodion VS, Abubakar II, Nwoye CI (2015) Eco-friendly asbestos free brake-pad: using banana peels. *J King Saud Univ Eng Sci* 27:185–192
- Ikpambese KK, Gundu DT, Tuleun LT (2016) Evaluation of palm kernel fibers (PKFs) for production of asbestos-free automotive brake pads. *J King Saud Univ Eng Sci* 28:110–118
- Ilanko AK, Vijayaraghavan S (2016) Wear behavior of asbestos-free eco-friendly composites for automobile brake materials. *Friction* 4:144–152
- Keskin A (2011) Investigation of using natural zeolite in brake pad. *Sci Res Essays* 6:4893–4904
- Krenkel W, Berndt F (2005) C/C–SiC composites for space applications and advanced friction systems. *Mater Sci Eng A* 412:177–181
- Kumar M, Bijwe J (2014) Influence of different types of binder in non-asbestos-organic brake lining materials: a case study on inertia brake dynamometer. *Proc Inst Mech Eng Part J* 228:584–592
- Kumar S, Gangil B, Patel VK (2016) Physico-mechanical and tribological properties of *Grewia optiva* fiber/bio-particulates hybrid polymer composites. In: AIP conference proceedings, vol 1728, pp 020384
- Kumar S, Kumar Y, Gangil B, Patel VK (2017a) Effect of agro-waste and bio-particulate filler on mechanical and wear properties of sisal fiber reinforced polymer composites. *Mater Today Proc* 4:10144–10147
- Kumar S, Mer KKS, Parsad L, Patel VK (2017b) A review on surface modification of bast fiber as reinforcement in polymer composites. *Int J Mater Sci Appl* 6:77–82
- Kumar S, Patel VK, Mer KKS et al (2018) Influence of woven bast-leaf hybrid fiber on the physico-mechanical and sliding wear performance of epoxy based polymer composites. *Mater Res Express* 5:105705
- Kumar S, Patel VK, Mer KKS, Gangil B, Singh T, Fekete G (2019a) Himalayan natural fiber-reinforced epoxy composites: effect of *Grewia optiva/Bauhinia Vahlia* fibers on physico-mechanical and dry sliding wear behavior. *J Nat Fibers*. <https://doi.org/10.1080/15440478.2019.1612814>
- Kumar S, Mer KKS, Gangil B, Patel VK (2019b) Synergy of rice-husk filler on physico-mechanical and tribological properties of hybrid *Bauhinia-vahlia*/sisal fiber reinforced epoxy composites. *J Mater Res Technol* 8:2070–2082
- Kumar S, Prasad L, Kumar S, Patel VK (2019c) Physico-mechanical and Taguchi-designed sliding wear properties of Himalayan agave fiber reinforced polyester composite. *J Mater Res Technol*. <https://doi.org/10.1016/j.jmrt.2019.06.004>
- Kumar S, Prasad L, Kumar S, Patel VK (2019d) Physico-mechanical and Taguchi-designed sliding wear properties of Himalayan agave fiber reinforced polyester composite. *J Mater Res Technol* 8:3662–3671. <https://doi.org/10.1016/j.jmrt.2019.06.004>
- Liew KW, Nirmal U (2013) Frictional performance evaluation of newly designed brake pad materials. *Mater Des* 48:25–33
- Ma Y, Shen S, Tong J, Ye W, Yang Y, Zhou J (2013) Effects of bamboo fibers on friction performance of friction materials. *J Thermoplast Compos Mater* 26:845–859
- Ma Y, Liu Y, Gao Z, Lin F, Yang Y, Ye W, Tong J (2014) Effects of wool fibers on tribological behavior of friction materials. *J Thermoplast Compos Mater* 27:867–880

- Öktem H, Uygur İ, Akıncioğlu G, Kır D, Karakaş H (2015) Evaluation of non-asbestos high performance brake pads produced with organic dusts. In: METAL2015 24th international conference on metallurgy and materials, Brno, Czech Republic, EU, pp 3–5
- Olabisi AI, Adam AN, Okechukwu OM (2016) Development and assessment of composite brake pad using pulverized cocoa beans shells filler. *Int J Mater Sci Appl* 5:66–78
- Öztürk B, Arslan F, Öztürk S (2013) Effects of different kinds of fibers on mechanical and tribological properties of brake friction materials. *Tribol Trans* 56:536–545
- Patel VK, Dhanola A (2016) Influence of  $\text{CaCO}_3$ ,  $\text{Al}_2\text{O}_3$ , and  $\text{TiO}_2$  microfillers on physico-mechanical properties of Luffa cylindrica/polyester composites. *Eng Sci Technol Int J* 19:676–683
- Patel VK, Rawat N (2017) Physico-mechanical properties of sustainable Sagwan-teak wood flour/polyester composites with/without gum rosin. *Sustain Mater Technol* 13:1–8
- Patel VK, Chauhan S, Katiyar J (2018) Physico-mechanical and wear properties of novel sustainable sour weed fiber reinforced polyester composites. *Mater Res Express* 5:045310
- Pinca-Bretotean C, Josan A, Birtok-Băneasă C (2018) Laboratory testing of brake pads made of organic materials intended for small and medium vehicles. In: IOP conference series: materials science and engineering, vol 393, p 012029
- Pujari S, Srikanth S (2019) Experimental investigations on wear properties of Palm kernel reinforced composites for brake pad applications. *Def Technol* 15:295–299
- Purboputro PI, Hendrawan MA, Hariyanto A (2018) Use of bamboo fiber as a brake pad lining material and the influence of its portion on hardness and durability. In: IOP conference series: materials science and engineering, vol 403, no 1
- Singh T, Patnaik A (2015) Performance assessment of lapinus–aramid based brake pad hybrid phenolic composites in friction braking. *Arch Civ Mech Eng* 15:151–161
- Singha K (2012) A short review on basalt fiber. *Int J Text Sci* 1:19–28
- Sutikno M, Marwoto P, Rustad S (2010) The mechanical properties of carbonized coconut char powder-based friction materials. *Carbon* 48:3616–3620
- Sutikno M, Pramujati B, Safitri SD, Razitania A (2018) Characteristics of natural fiber reinforced composite for brake pads material. In: AIP conference proceedings, vol 1983, p 050009
- Swamidoss VF, Prashanth (2015) Fabrication and characterization of brake pad using pineapple leaf fiber (PALF). *Int J Res Comput Appl Rob* 3:107–111
- Unaldi M, Kus R (2017) The effect of the brake pad components to the some physical properties of the ecological brake pad samples. In: IOP conference series: materials science and engineering, vol 191, p 012032
- Venkateshwaran N, Ayyasamy Elayaperumal (2010) Banana fiber reinforced polymer composites—a review. *J Reinf Plast Compos* 29:2387–2396
- Xin X, Xu CG, Qing LF (2007) Friction properties of sisal fibre reinforced resin brake composites. *Wear* 262:736–741
- Yawas DS, Aku SY, Amaren SG (2016) Morphology and properties of periwinkle shell asbestos-free brake pad. *J King Saud Univ Eng Sci* 28:103–109
- Yun R, Martynková SG, Lu Y (2011) Performance and evaluation of non-asbestos organic brake friction composites with  $\text{SiC}$  particles as an abrasive. *J Compos Mater* 45:1585–1593